2010-08-11

Influence of Relative Compaction on Passive Resistance of Abutments with Mechanically Stabilized Earth (MSE) Wingwalls

Alec N. Strassburg
Brigham Young University - Provo

Influence of Relative Compaction on Passive Resistance of Abutments with Mechanically Stabilized Earth (MSE) Wingwalls

Alec N. Strassburg

A thesis submitted to the faculty of

Brigham Young University

in partial fulfillment of the requirements for the degree of

Master of Science

Kyle M. Rollins, Chair
Travis M. Gerber
Fernando S. Fonseca

Department of Civil and Environmental Engineering

Brigham Young University

December 2010

ABSTRACT

Influence of Relative Compaction on Passive Resistance of Abutments

with Mechanically Stabilized Earth (MSE) Wingwalls

Alec N. Strassburg

Department of Civil and Environmental Engineering

Master of Science

Large scale static lateral load tests were completed on a pile cap with wingwalls under several different sand backfill configurations: no backfill, loosely compacted unconfined, loosely compacted slip plane wall confined, loosely compacted MSE wingwall confined, and densely compacted MSE wingwall confined. The relative compaction of the backfill was varied during each test to observe the change in passive resistance provided by the backfill. The wall types were varied to observe the force placed on the walls and the wall displacement as a result of the laterally loaded pile cap and backfill relative compaction. Passive force-displacement curves were generated from each test.

It was found that the densely compacted material provided a much greater passive resistance than the loosely compacted material by 43% (251 kips) when confined by MSE walls. The outward displacement of the MSE walls decreased noticeably for the dense MSE test relative to the loose MSE test. Backfill cracking and heave severity also increased as the relative compaction level of the backfill increased. As the maximum passive force was reached, the reinforcement reached their peak pullout resistance.

Correlations were developed between the passive pressure acting on the pile cap and the pressure measured on the MSE wingwalls as a function of distance from the pile cap for both loose and dense backfills. The pressure measured on the wingwalls was approximately 3 to 9% of the pressure acting on the pile cap. As the distance from the pile cap increased, the pressure ratio decreased. This result helps predict the capacity of the wingwalls in abutment design and the amount of allowable wall deflection before pullout of the backfill reinforcement occurs. Three methods were used to model the measured passive force-displacement curves of each test. Overall, the computed curves were in good agreement with the measured curves. However, the triaxial soil friction angle needed to be increased to the plane strain friction angle to accurately model both the loose and dense sand MSE and slip plane wall confined tests. The plane strain friction angle was found to be between 9 to 17% greater than the triaxial friction angle.

Keywords: passive force, MSE walls, abutments, pile caps, lateral resistance

ACKNOWLEDGEMENTS

I wish to acknowledge and show appreciation to my graduate committee chair and adviser, Dr. Kyle M. Rollins. He has guided me through completing this research and supported me in all my efforts as a graduate student. I also wish to thank my other graduate committee members, Dr. Travis M. Gerber and Dr. Fernando S. Fonseca. Their insights and expertise were much appreciated. Fellow students Nathan Bingham, Joshua Pruett, and Richard Christensen contributed significantly to the work and research completed, with other staff and students participated in the testing completed at the airport. I appreciate their contributions.

Also, I want to thank my family, especially, my wife, Lorie, for their love and support throughout my graduate studies. Without my wife's faith, persistence, and hard work, I would not have been able to push through my schooling.

This research was supported by the California, Montana, New York, Oregon, and Utah Departments of Transportation through a Federal Highway Administration (FHWA) pooled-fund arrangement under Contract Number 069148 "Dynamic Passive Pressure on Abutments and Pile Caps," the National Science Foundation (NSF) under Award Number CMS-0421312, and the George E. Brown, Jr. Network for Earthquake Engineering Simulation (NEES) which operates under NSF Award Number CMS-0402490. This support was greatly appreciated. The Utah Dept. of Transportation served as the lead agency for the pooled-fund study with Daniel Hsiao as the project manager.

The opinions, interpretations and recommendations in this report are those of the author and do not necessarily reflect those of the sponsors.

TABLE OF CONTENTS

LIST OF TABLES

LIST OF FIGURES

1 INTRODUCTION

1.1 Background

Pile groups are often connected to a pile cap in the foundation design of bridge and building structures to provide increased lateral stability and moment resistance for loadings resulting from earthquakes or strong wind. The lateral stability of this type of foundation is derived from the interaction of the piles and the soil below the pile cap, and the passive resistance generated between the pile cap and the surrounding backfill material. As a pile cap is loaded laterally, a passive soil pressure develops in response to counteract the lateral load placed on the pile cap. Theories, such as Rankine, Coulomb, and log spiral, have been developed to assist in predicting the maximum passive pressure that soil adjacent to a pile cap can resist under static loadings.

While the theories mentioned above are useful in estimating the ultimate passive resistance of a backfill material, how the soil passive pressure develops as a function of foundation deflection is not as well defined. This information is useful, however, when the pile cap or abutment movement necessary to develop the full passive resistance cannot be tolerated, or in displacement-based design approaches, such as performance-based design, a more widely used method in seismic design.

Currently, a limited amount of research has been conducted to determine the passive force-foundation displacement relationship. Rollins and Cole (2006), Rollins and Sparks (2002), Mokwa and Duncan (2001), Romstad et al. (1996), and a few others have conducted large scale tests to help define the relationship. These large scale tests have led to the development of simple linear elastic and non-linear (ie., hyperbolic) models to predict how the soil passive force develops as a function of foundation deflection.

These tests and models are significant, but previously, only one other study has considered the load-deflection relationship in conjunction with the use of mechanically stabilized earth (MSE) wingwalls to truncate the backfill behind the pile cap or abutment. When MSE wingwalls are utilized in this way, the effective width of the backfill is reduced, also reducing the passive resistance on the pile cap. However, the reinforcement implemented, tends to increase the passive resistance. As a result, current bridge abutment designs utilizing MSE wingwalls may not appropriately consider MSE use in the development of load-displacement relationships, which can result in inaccurate predictions of the maximum passive resistance provided by the backfill.

1.2 Research Objectives

The research presented herein was conducted to accomplish the following objectives:

1. Develop typical passive force-displacement curves for abutments with MSE wingwalls.
2. Determine the appropriateness of using plane strain strength parameters in computing ultimate passive force for abutments with MSE wingwalls.

3. Evaluate the effect of backfill compaction on passive force-displacement results for abutments with identical MSE wingwall and reinforcement configurations.

1.3 Scope of Research

The research conducted was focused on the effects of backfill relative compaction on the development of appropriate passive load-deflection curves for a laterally loaded pile cap with a sand backfill confined by MSE wingwalls or side isolation paneling. A series of 10 large scale field tests with varying backfill conditions and wall setups were completed to accomplish this task. The field tests consisted of two unconfined (3D) tests where no walls were implemented, two slip plane (2D) tests where plywood walls were used to create plane strain-like conditions, three MSE tests where various MSE wingwall configurations were utilized, and finally, three no backfill tests to develop a baseline force-deflection reading for the pile cap and pile group.

During each test, equipment was used to monitor and record the conditions of the pile cap and piles, walls, and backfill. Information regarding the pile cap and reinforcing mat loads, soil pressure, wall, cap, and backfill displacements, backfill and reinforcing strain, and backfill heave and cracking were collected. The data was analyzed and reduced to develop the material presented herein. Only data from the loose sand unconfined (3D), loose sand slip plane (2D), loose sand MSE, and first dense sand MSE tests will be fully presented in this thesis. Some results from the remaining field tests are shown in the results comparison chapter of this thesis while a complete set of the results of the additional tests can be found in Bingham (2010).

2 LITERATURE REVIEW

The following information is presented as a discussion of information pertaining to the thesis topic of the effects of backfill relative compaction on developing passive force-abutment displacement curves for backfills confined by MSE wingwalls. The first section summarizes the different methods for predicting the passive load-displacement relationship for soils surrounding abutments or pile caps. The second and third sections describe information regarding plane strain soil conditions and MSE wall design that was utilized in the design and evaluation of the field tests conducted in this study.

2.1 Methods of Predicting Passive Earth Pressure as a Function of Deflection

Caltrans Seismic Design Approach

The Caltrans Seismic Design method for predicting the ultimate passive pressure placed on a laterally loaded abutment as a function of abutment deflection was developed from research conducted by Maroney (1995) and Romstad et al. (1996) on large scale abutments and later adopted by Caltrans in the *Caltrans Seismic Design Criteria* Manual (2004). The research, conducted at the University of California at Davis, CA, was based on a linear elastic assumption for the backfill material, which was a densely compacted silty loam. Two generalized values were developed from the testing: an initial stiffness (K_i) value for the embankment fill of approximately 20 kip/in./ft (11.5 kN/mm/m) and a maximum passive pressure of 5.0 ksf (239

kPa) based on a uniform pressure distribution. The stiffness and pressure values were not intended for use with loosely compacted materials.

The following equations, Equations 2.1 and 2.2, were developed from the large scale testing to calculate the load-deflection relationship:

$$K_{abut} = \begin{cases} K_i * w * \dfrac{h}{5.5} & \text{(US Units)} \\ K_i * w * \dfrac{h}{1.7} & \text{(SI Units)} \end{cases} \quad \textbf{(2.1)}$$

$$P_{max} = \begin{cases} A_{abut} * 5.0 \text{ ksf} * \dfrac{h}{5.5} & \text{(US Units)} \\ A_{abut} * 239 \text{ kPa} * \dfrac{h}{1.7} & \text{(SI Units)} \end{cases} \quad \textbf{(2.2)}$$

where

K_{abut} = stiffness of the backfill material, kip/in. (kN/mm)

w = width of the abutment, ft (m)

h = height of the abutment, ft (m)

A_{abut} = area of the abutment, ft^2 (m^2)

P_{max} = ultimate passive force, kips (kN).

The h/5.5 (h/1.7) term in Equations 2.1 and 2.2 is an abutment height proportionality term since the height of the abutment used in the original testing was 5.5 ft (1.7 m). One important note with these equations is the inability to adjust for the backfill properties; only the abutment dimensions are considered. As a result, the load-deflection relationship appears like that shown in Figure 2.1.

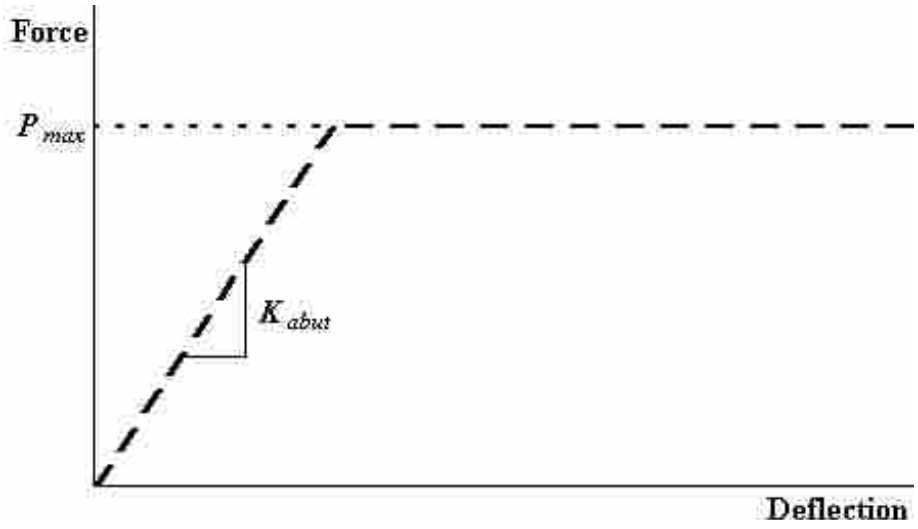

Figure 2.1: Passive Force-Deflection Model for Caltrans Seismic Design Method (Adapted from *Caltrans Seismic Design Criteria* Manual 2004)

PYCAP – Duncan and Mokwa

PYCAP is a simple Excel® spreadsheet based program created by Duncan and Mokwa (2001) that computes the passive resistance of a soil backfill with an accompanying failure surface. The ultimate passive force and failure surface are solved for iteratively using the log spiral theory corrected for three dimensional (3D) end effects by the Brinch Hansen correction factor until a minimum passive force value is found. The maximum possible value of the 3D correction factor in PYCAP is assumed to be limited to 2.0. A hyperbolic expression is then used in conjunction with the calculated ultimate passive force and an estimated soil stiffness value to predict the load-deflection relationship of an abutment. PYCAP is to be used in relatively simple situations where the ground is level, the walls are vertical, the surcharge is uniform, and the soil is homogeneous (Duncan and Mokwa 2001). Figure 2.2 shows the components of the log failure surface computed in PYCAP.

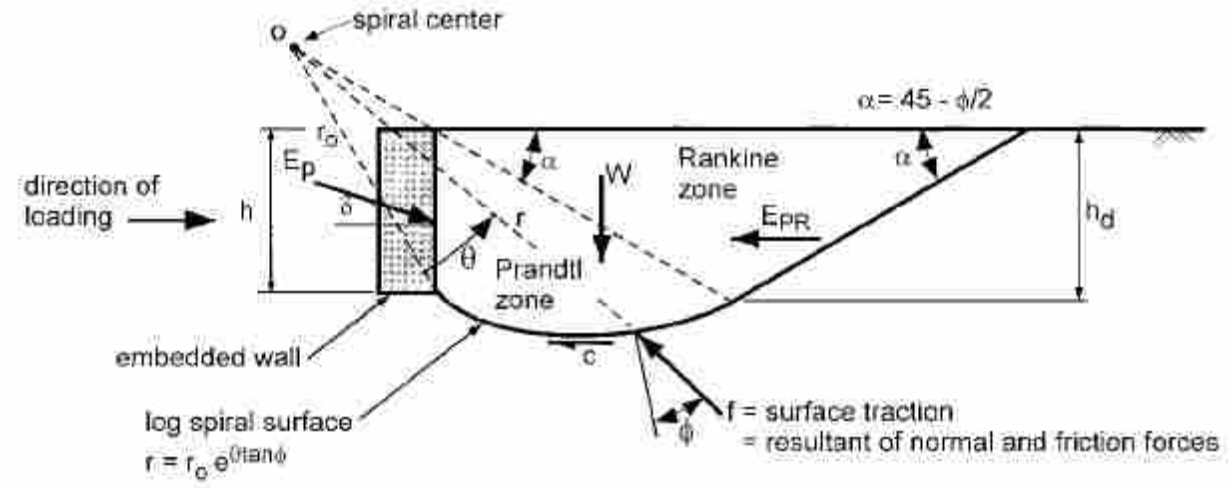

Figure 2.2: Log Spiral Failure Surface Features (Duncan and Mokwa 2001)

The passive load-deflection curve in PYCAP is calculated using a hyperbolic model. The equation representing this model is shown below as Equation 2.3:

$$P = \frac{y}{\left[\frac{1}{K_{max}} + R_f \frac{y}{P_{ult}}\right]} \quad \textbf{(2.3)}$$

where

P = passive resistance, kips

P_{ult} = ultimate passive resistance, kips

y = deflection of abutment, in.

K_{max} = initial stiffness, or the initial slope of the load-deflection curve, kip/in.

R_f = failure ratio, or P_{ult}/hyperbolic asymptote.

Figure 2.3 shows Equation 2.3 graphically plotted as force against deflection along with a representation of the location of K_{max}.

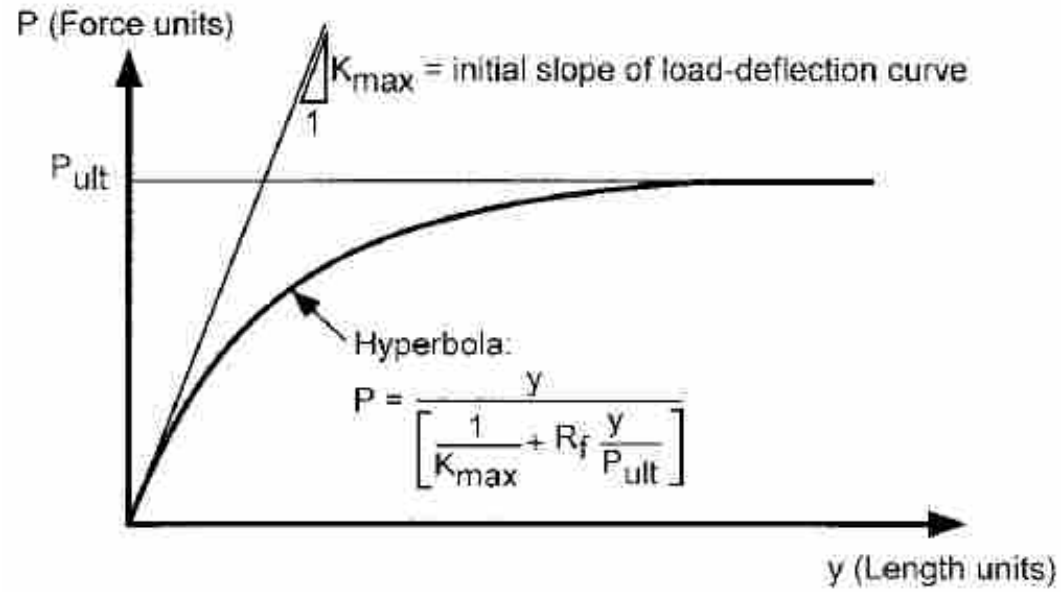

Figure 2.3: PYCAP Hyperbolic Load-Deflection Curve (Duncan and Mokwa 2001)

The K_{max} term is calculated using the elastic solution of a horizontal load on a rectangle as presented by Douglas and Davis (1964). In PYCAP, K_{max} is represented by two properties: initial Young's Modulus (E_i) and Poisson's ratio (ν). The following table, Table 2.1, was adapted from Duncan and Mokwa (2001) and shows typical values of E_i for shallow sands and gravels of different relative densities.

The R_f term is the ratio of the ultimate passive force and the hyperbolic asymptotic value of passive resistance. Duncan and Mokwa (2001) state that R_f can range from 0.75 to 0.95. A value of 0.85 was used in all of their computed solutions. R_f can also be eliminated from Equation 2.3 by solving the equation in terms of R_f when $P = P_{ult}$ and $y = y_{max}$ and substituting this result back into Equation 2.3 for R_f as suggested in Cole and Rollins (2006). The term y_{max} can then be approximated from the y_{max}/H (or Δ_{max}/H) ratio using suggested values presented in Cole and Rollins. H is the height of the abutment.

Table 2.1: Typical Initial Tangent Modulus (E_i) Values for Shallow Sands and Gravels (Adapted from Duncan and Mokwa 2001)

Density	Relative Density (D_r)	Normally Loaded	Preloaded or Compacted
Loose	40%	E_i = 200-400 ksf	E_i = 400-800 ksf
Medium	60%	E_i = 300-500 ksf	E_i = 500-1000 ksf
Dense	80%	E_i = 400-600 ksf	E_i = 600-1200 ksf

ABUTMENT – Shamsabadi

ABUTMENT is a computer program used to predict the passive force-deflection curve of a laterally loaded abutment developed by Shamsabadi et al. (2007). The program is based on the log spiral theory combined with a modified hyperbolic stress-strain relationship, also called the LSH relationship. The modified hyperbolic stress-strain relationship is a function of the strain properties, ε_{50} and R_f, of the backfill material. The ultimate passive force is calculated by dividing up the failure wedge into slices and applying force-based, limit-equilibrium equations to each slice as shown in Figure 2.4. The LSH model was compared to full scale abutment loading test results from Rollins and Cole (2006) and was found to produce results in good agreement with those reported by Rollins and Cole. The ABUTMENT results in comparison to the results from Rollins and Cole (2006) are shown in Figure 2.5.

AASHTO LRFD Approach

The American Association of State Highway and Transportation Officials (AASHTO) *Load and Resistance Factor Design (LRFD) Bridge Design Specifications*, 4th Edition (2007) suggests that the log spiral theory be utilized in calculating the ultimate passive resistance acting on an abutment. The manual specifies the use of log spiral charts developed by the U.S. Navy to simplify the process (U.S. Navy 1982). The manual also provides an estimate of how much abutment movement is necessary to develop the ultimate passive resistance in the backfill in

Table C3.11.1-1 (p. 3-68), also shown in Table 2.2 below (AASHTO 2007). The table states that the abutment movement required to develop the ultimate passive resistance is 4% of the wall height for loose sand, 2% for medium dense sand, and only 1% for dense sand. However, Section C3.11.5.4 (p. 3-74) explains that for loose sand, a displacement of 5% of the wall height may be needed to fully develop the passive resistance, and that a displacement of 5% of the wall height may be used as a conservative estimate for dense sand (AASHTO 2007). The *AASHTO Guide Specifications for LRFD Seismic Bridge Design* (2009) state that the wall friction angle used in the log spiral theory should be 2/3 of the soil friction angle as a conservative estimate for concrete-soil interfaces.

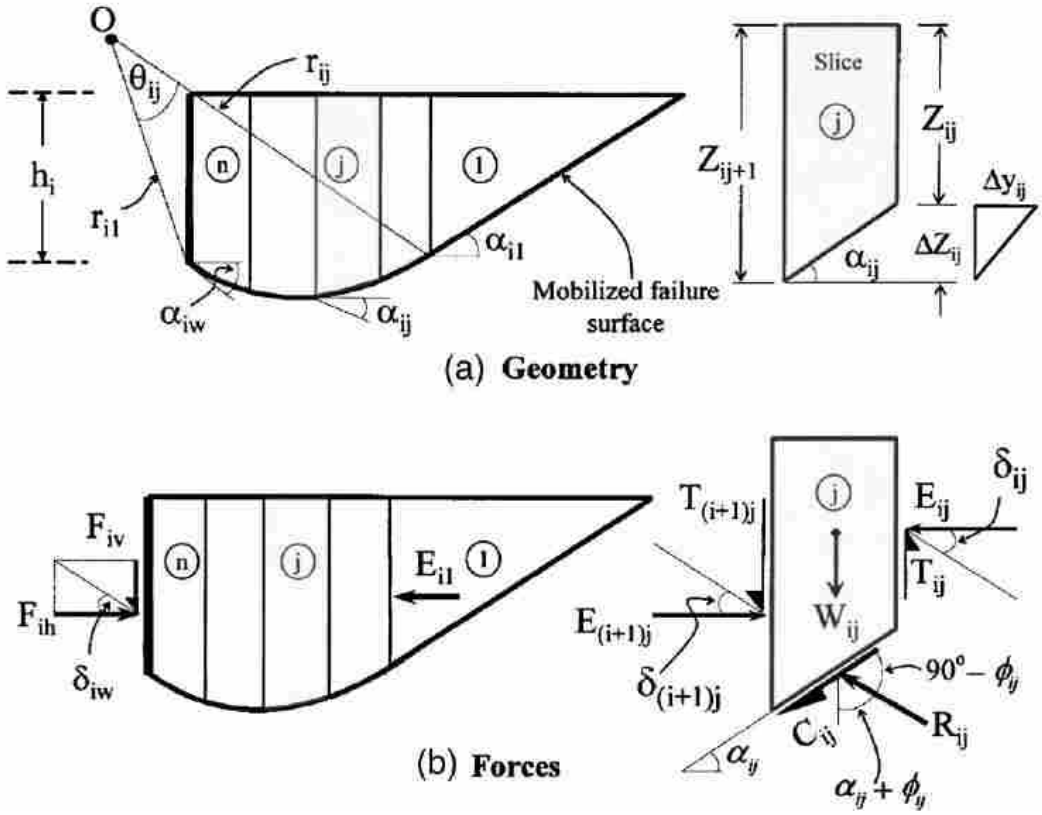

Figure 2.4: ABUTMENT Log Spiral Failure Surface Geometry and Forces (Shamsabadi et al. 2007)

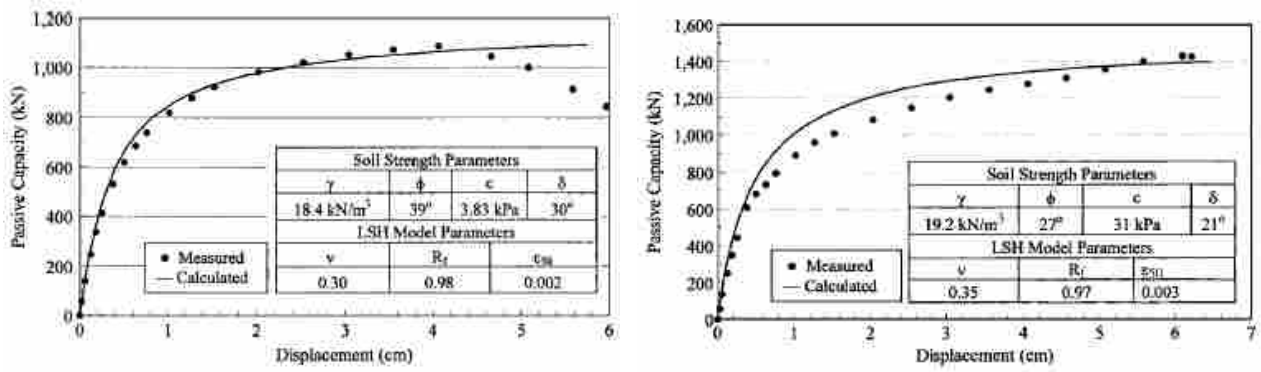

a) Clean Sand Results **b) Silty Sand Results**

Figure 2.5: Comparison of Field Test Measured and ABUTMENT Calculated Load-Displacement Results for a) Clean Sand and b) Silty Sand Backfill Types (Shamsabadi et al. 2007)

Table 2.2: Values of Wall Movement Required to Develop Active and Passive Earth Pressure Conditions (*AASHTO LRFD Bridge Design Specifications* 2007)

Type of Backfill	Values of Δ/H	
	Active	Passive
Dense sand	0.001	0.01
Medium dense sand	0.002	0.02
Loose sand	0.004	0.04
Compacted silt	0.002	0.02
Compacted lean clay	0.010	0.05
Compacted fat clay	0.010	0.05

2.2 Comparison of Triaxial and Plane Strain Soil Friction Angles

Shear Strength of Sands in Triaxial Compression, Plane Strain and Direct Shear (Rowe 1969)

To quantify the shear strength of different soils, an assortment of tests and variations of these tests exist, like the triaxial compression test and the direct shear test. A common variation of the triaxial shear test is plane strain loading conditions, where the confining stress are such

that $\sigma_1 > \sigma_2 > \sigma_3$ and $\varepsilon_2 = 0$. Rowe (1969) compared the relationship between these three shear tests for cohesionless soils. The results of his work showed that under plane strain loading conditions the strength parameter ϕ, or soil friction angle, was greater than that produced by the conventional triaxial compression test or the direct shear test. This suggests that the triaxial friction angle (ϕ_T) must be increased by some factor to be used under plane strain conditions.

Stress-Deformation and Strength Characteristics (Ladd et al. 1977)

Ladd et al. (1977) studied various factors influencing the behavior and strength characteristics of cohesionless soils with quantified results. One such factor addressed was the intermediate principal stress (σ'_2) and its influence on the soil friction angle. He concluded from the analysis of a number of cohesionless soil samples that as a sample is sheared under plane strain conditions, the peak friction angle increased above that measured during a conventional triaxial compression test. Figure 2.6 is a summary plot of the samples that were tested. It can be seen that as the parameter b increased from zero (triaxial compression conditions) to plane strain conditions ($b \approx 0.25$ to 0.4) the peak friction angle increased. The increase in the friction angle for plane strain conditions was approximately 4° to 9° for dense sands and 2° to 4° for loose sands.

Estimating Soil Properties for Foundation Design (Kulhawy and Mayne 1990)

Kulhawy and Mayne (1990) also provided a brief discussion on the increase of the soil friction angle when a sample is sheared under plane strain conditions as compared to triaxial compression. Based on a summary of test data available in the literature, Kulhawy and Mayne stated that the triaxial friction angle (ϕ_T) of a typical sand increased in the ranges of 7 to 17% with a mean of 11% for loose materials and 10 to 18% with a mean of 12% for dense materials when tested under plane strain conditions. Figure 2.7 shows the range of the ratio of a plane

strain soil friction angle to a triaxial compressive soil friction angle (ϕ_{PS}/ϕ_T) as a function of the intermediate principal stress (σ'_2) as given in the manual.

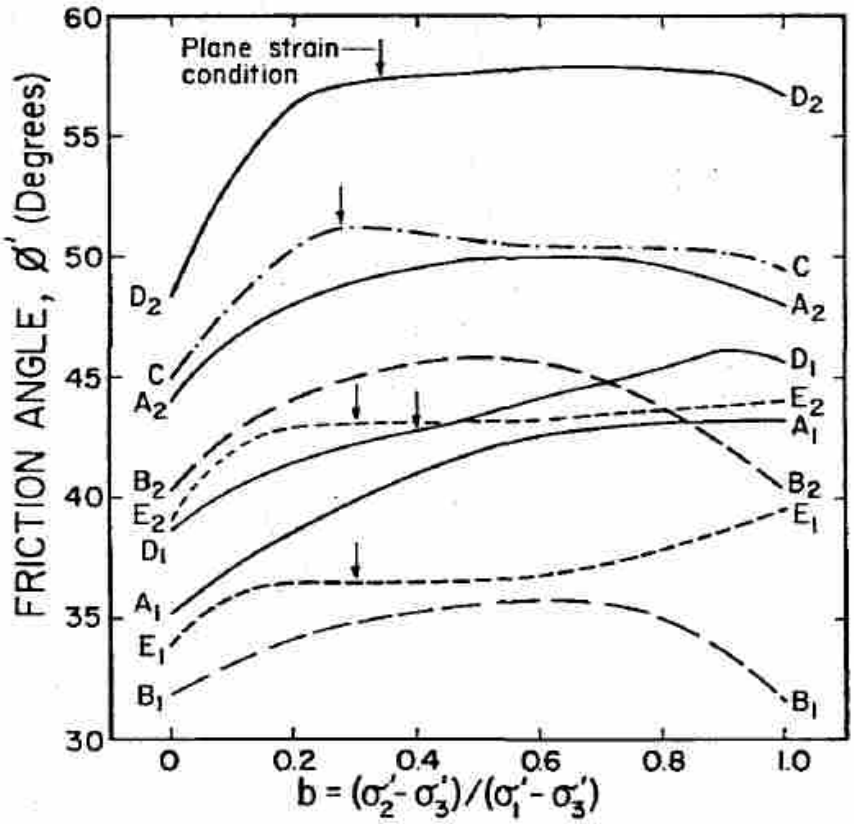

LINE	SAND	D_r (%)	REFERENCE
A_1	Ottawa	med. loose	Ko and Scott (1968)
A_2		med. dense	
B_1	Med Fine Loch Aline	30	Sutherland and Mesdary (1969)
B_2		80	
C	River Welland	dense	Proctor and Borden (1969)
D_1	Monterey No. 0	27	Lade and Duncan (1973)
D_2		98	
E_1	Ham River	loose	Reades and Green (1974)
E_2		dense	

Figure 2.6: Effects of the Intermediate Principal Stress (σ'_2) on the Friction Angle of Sands (Ladd et al. 1977)

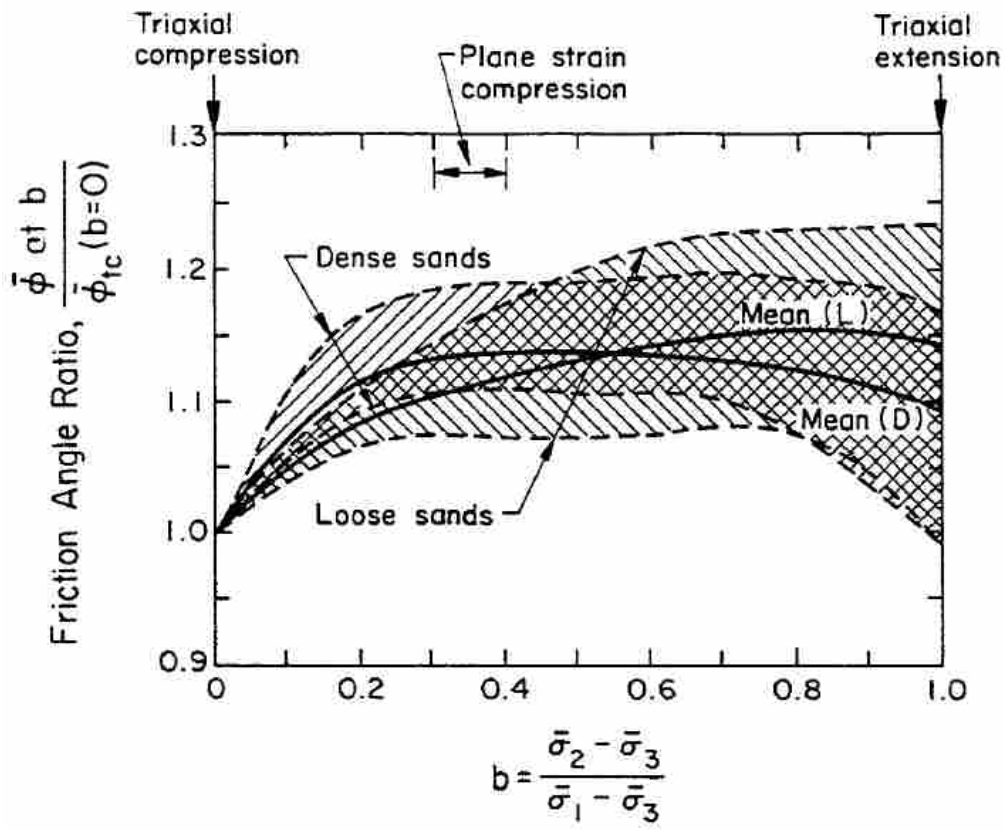

Figure 2.7: Influence of the Intermediate Principal Stress (σ'_2) on the Friction Angle of Sands (Kulhawy and Mayne 1990)

2.3 Design of MSE Walls with Reinforcement

MSE Walls and Reinforced Soil Slopes Design and Construction Guidelines (National Highway Institute 2001)

In March 2001, the National Highway Institute (NHI) in conjunction with the Federal Highway Administration (FHWA) published a report entitled *Mechanically Stabilized Earth Walls and Reinforced Soil Slopes Design and Construction Guidelines* to provide a basic design method for MSE walls and reinforced soil slopes. The design method presented in the report is based on Allowable Stress Design (ASD) procedures. This method was used to design the MSE wingwalls used during the testing described herein for internal stability. The AASHTO

simplified method was used to calculate the pullout resistance (P_r) of the reinforcing strips by the following equation, Equation 2.4:

$$P_r = F^* * \alpha * \sigma_v' * L_e * C \quad \textbf{(2.4)}$$

where

P_r = pullout resistance of the reinforcement per unit width of reinforcement, lb/ft

F^* = pullout resistance factor

α = scale effect correction factor to account for a non-linear stress reduction over the embedded length of highly extensible reinforcements (generally α = 1.0 for metallic reinforcement)

σ_v' = effective vertical stress at the soil-reinforcement interfaces, psf

L_e = embedment length in the resistive zone behind the failure surface, ft

C = reinforcement effective unit perimeter (typically C = 2 for strips, grids, and sheets).

(The author recognizes that the NHI has recently published a new version of the 2001 report in November 2009 which now implements LRFD procedures in MSE wall and reinforced soil slope design. At the time of the testing, program, and work presented in this thesis, the new manual had not yet been published.)

Predicted Loads in Steel Reinforced Soil Walls Using the AASHTO Simplified Method (Bathurst et al. 2009)

Bathurst et al. (2009) completed an in-depth statistical evaluation of a number of instrumented steel reinforced soil walls. The walls were reinforced with three different reinforcement types: bar mats, welded wire mesh, and steel strips. The data collected from each wall concerning the reinforcement load was compared to the calculated value from the AASHTO simplified method. As a result, the calculated value for the load carried by the reinforcement in

bar mat reinforced walls was found to be slightly conservative. This finding is consistent with the results of the field tests utilizing bar mat reinforcement which is presented subsequently in this thesis.

Passive Force-Deflection Curves for Abutments with MSE Confined Approach Fills (Heiner et al. 2008)

Prior to the testing reported herein, which was conducted in 2009, similar large scale field tests with and without MSE wingwalls were performed by Heiner et al. (2008). Heiner et al. not only conducted similar static tests, but mainly performed dynamic tests which included the use of an eccentric mass shaker. The group of field tests reported in this study was meant to expand upon the original tests completed by Heiner et al.

The results from Heiner et al. (2008) showed that the outward transverse displacement of the MSE wingwalls was approximately 40% of the longitudinal pile cap displacement with a maximum outward MSE wall displacement of 1.4 in. (35.6 mm). This large MSE wingwall deflection was thought to be a result of using the eccentric mass shaker. It was also found that, despite outward displacement of the MSE walls, the measured passive force per effective width of the pile cap was 28 kips/ft (409 kN/m) during the confined test, but only 25 kips/ft (365 kN/m) for the unconfined backfill.

3 TESTING METHODS

This section describes the site location, geotechnical conditions, and general testing setup and instrumentation of the large scale field tests conducted at the testing site.

3.1 Site Description

The test site is located at the Salt Lake City (SLC) International Airport approximately 1000 ft (300 m) north of the airport control tower. The land is currently unused by the airport and provides adequate conditions for testing because of its openness and flat topography. Because the location is unused, no utility lines run above ground or below ground to conflict with the completed large scale testing. The local water table was located at a depth of 5 to 5.5 ft (1.52 to 1.68 m) below the ground surface. An aerial photograph of the test area location in relation to the airport control tower is shown in Figure 3.1.

3.2 Geotechnical Site Characterization

A number of large scale lateral load tests of drilled shafts and driven pile groups have been conducted over the past 15 years at the airport location. During these previous tests much information regarding the subsurface site characteristics was collected through in-situ and laboratory testing. Figure 3.2 below shows the locations where in-situ tests were completed in relation to the location of existing drilled shafts and pile groups.

Figure 3.1: Aerial Photograph of Testing Site

From previous testing results, the upper 5 ft (1.5 m) of the soil profile consists of imported gravel fill. The underlying soils consist of alternating lean clay, sandy silt, and silty sand layers down to a depth of about 50 ft (15 m). The upper fill material around the drilled shafts and pile groups was eventually removed and replaced with clean sand for testing. An idealized soil profile created from the CPT test conducted near the 9-pile group location, along with other measured soil characteristics, is shown in Figure 3.3 and Figure 3.4. Additional subsurface soil information can be found in Christensen (2006), Snyder (2004), and Peterson (1996).

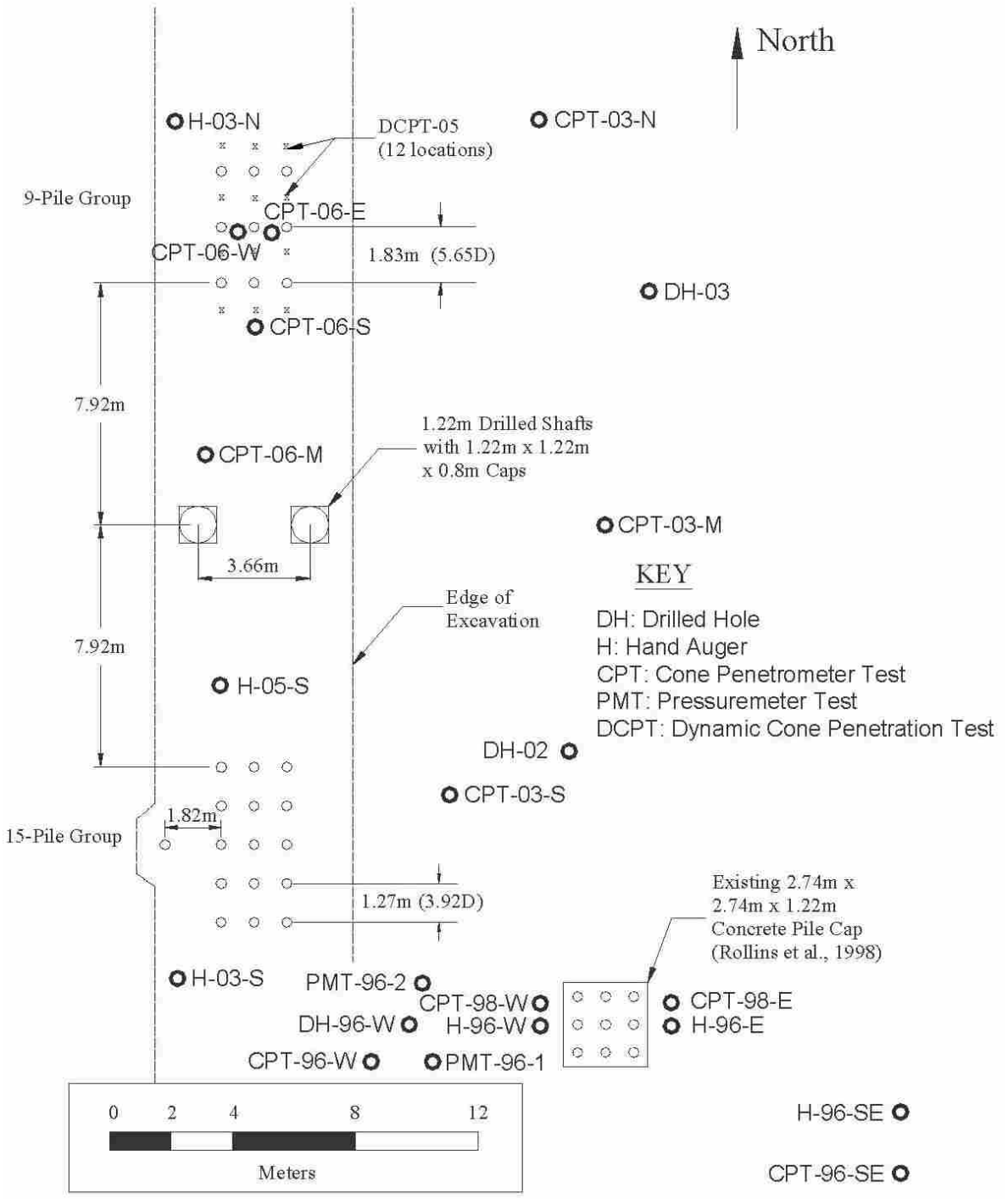

Figure 3.2: Locations of In-situ Tests at the Airport Testing Site (Christensen, 2006)

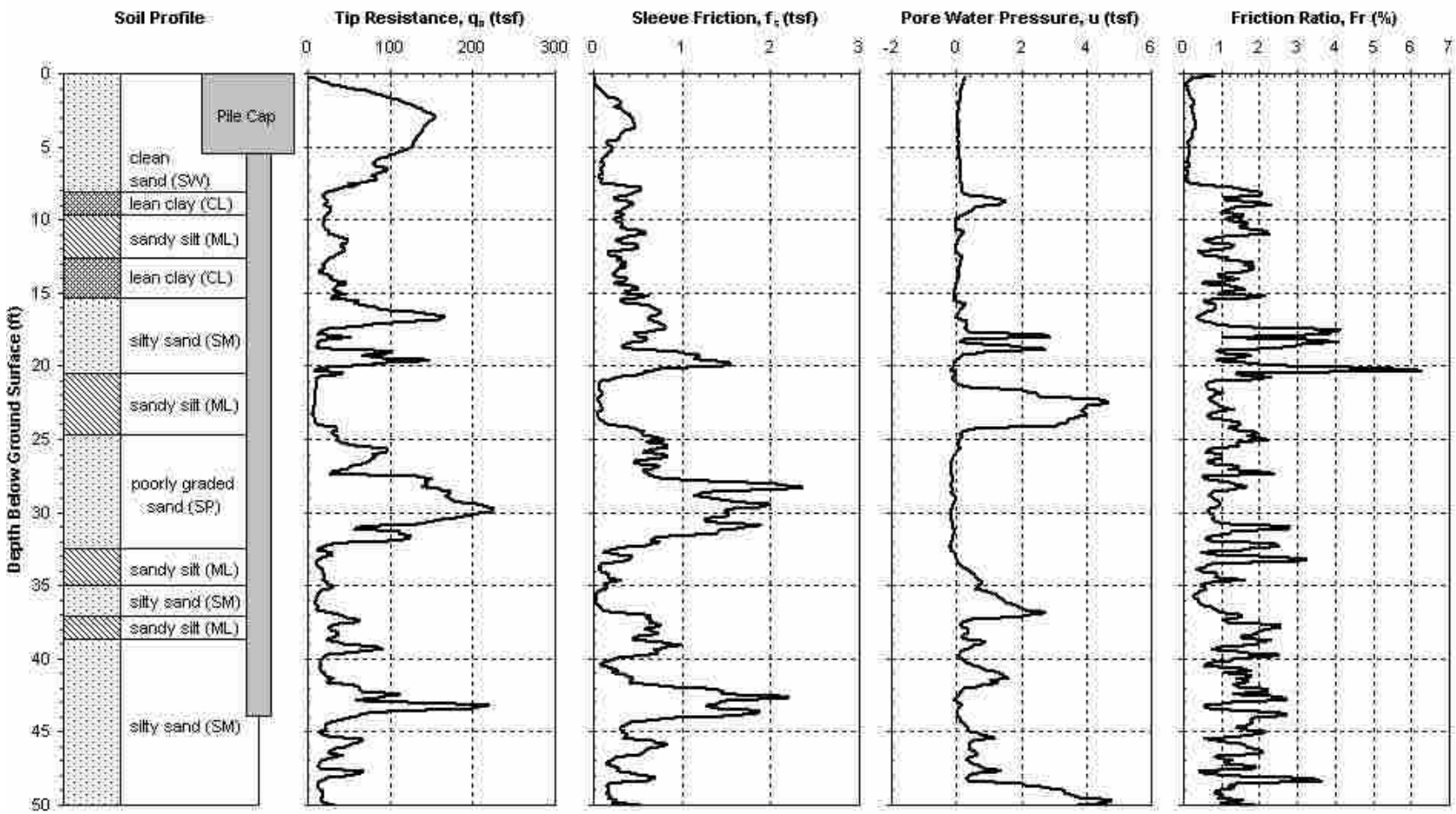

Figure 3.3: Idealized Soil Profile From CPT Test (Christensen, 2006)

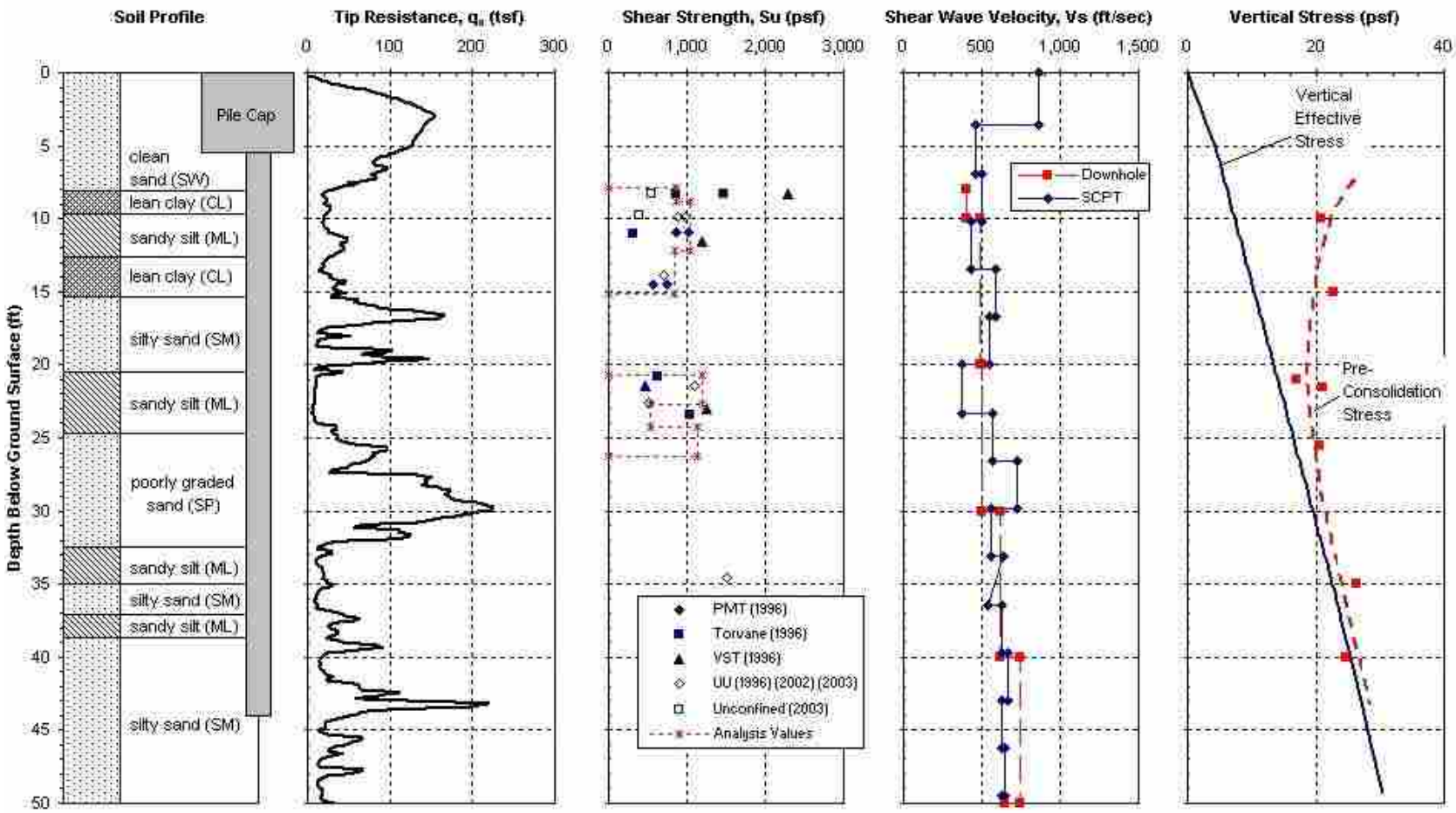

Figure 3.4: Idealized Soil Profile From CPT Data (Christensen, 2006)

3.3 Testing Setup

The testing setup consisted of four major components: a reaction foundation, a pile cap, a loading apparatus, and a backfill zone. Each of the components mentioned are explained in detail in the following sections. A drawing of the major components of the testing setup is shown in Figure 3.5.

3.3.1 Reaction Foundation

Two 4-ft (1.22-m) diameter drilled shafts was the centerpiece of the reaction foundation while a sheet pile wall, which spanned the north side of the shafts, and two large reinforced steel I-beams, lying horizontally on each side of the shafts, provided further lateral capacity to the foundation system. The shafts and sheet pile wall were installed during previous testing.

The center-to-center spacing of the shafts was 12 ft (3.66 m). The west and east shafts were drilled to depths of 55.2 ft (16.82 m) and 70.0 ft (21.35 m), respectively. A 4-ft square by 2-ft thick cap exists at the top of each shaft. The first 35 ft (10.67 m) of each shaft was reinforced with 18 #11 (#36) vertical bars. The spiral surrounding these bars was #5 (#16) bar with a pitch of 3 in. (75 mm) and a concrete cover of 4.75 in. (120 mm). From 35-55 ft (10.67-16.76 m) deep, only half of the previous 18 vertical bars were continued through the shafts and the spiral pitch changed to 12 in. (300 mm). The concrete has a compressive strength of 6000 psi (41 MPa).

The sheet piling placed on the north side of the drilled shafts was AZ-18 sheet piling constructed of ASTM A-572, Grade 50 steel. Sheet pile sections were placed using a vibratory hammer to depths ranging from 33.6 to 35.6 ft (10.24 to 10.85 m) below the excavated ground surface. During driving, the sheet piling was kept as near vertical and close to the drilled shafts as possible to provide support to the drilled shafts.

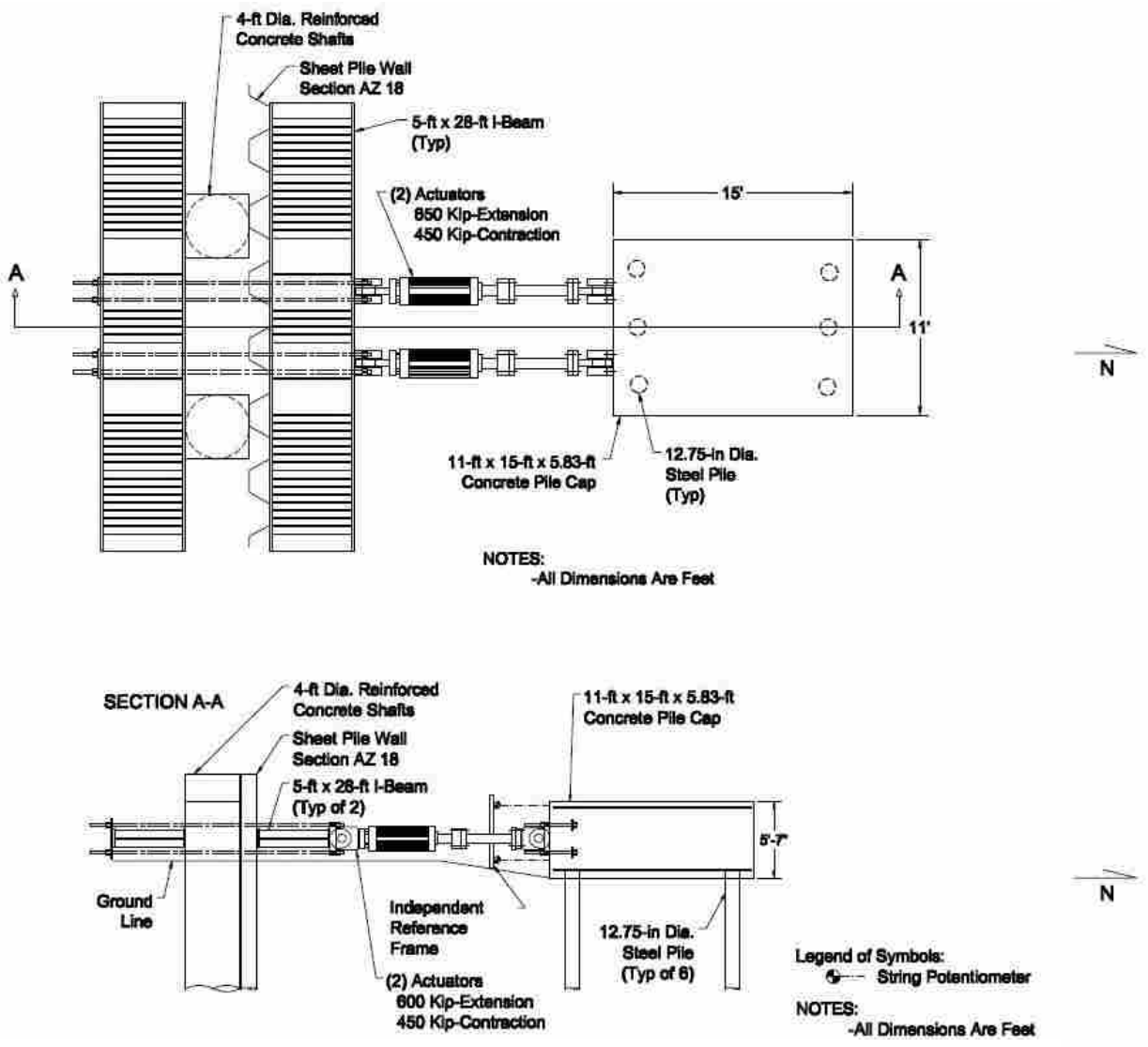

Figure 3.5: Aerial and Cross-section Views of the General Testing Layout

The two reinforced steel I-beams were 28-ft (8.53-m) long and 64-in. (1626-mm) high by 16-in. (406-mm) wide. Many stiffeners were inserted in the web of the beam to prevent the beams from buckling. The beams were placed on each side of the drilled shafts to help distribute loading evenly across the reaction foundation and to help the system react as a unit. The beams were tied to the sheet piling and drilled shafts using eight 2.5-in. (64-mm) high strength threaded bars post-tensioned to 100 kips (445 kN) each.

3.3.2 Pile Cap and Piles

During previous testing, a 9-pile group was installed a short distance to the north of the drilled shafts. These piles were ASTM A252 Grade 3 steel pipe and had an average yield strength of 57 ksi (393 MPa) with an outer diameter of 12.75 in. (324 mm) and a wall thickness of 0.375 in. (9.5 mm). The center-to-center spacing between rows of piles was 6 ft (1.83 m), with a center-to-center spacing between adjacent piles of 3.5 ft (1.07 m). All piles were driven closed-ended to a depth of about 43 ft (13.1 m) below the ground surface.

To create the pile cap on top of the 9-pile group, modifications were made to the pile group. First, the middle row of piles was removed to decrease the number of remaining piles to six. The removal of the middle piles increased the center-to-center spacing between the two remaining pile rows to 12 ft (3.66 m). Second, the piles were shorted to provide a minimum of 6 in. (150 mm) of embedment into the pile cap and filled with 6000-psi concrete. Rebar cages 18-ft (5.49 m) long were made of six #8 (#25) vertical bars and a #4 (#13) spiral at a pitch of 6 in. (152 mm) to connect the cap to the piles. The beginning 4.8 ft (1.47 m) of the 18-ft rebar cage was extended up into the pile cap to support the upper horizontal reinforcing mat in the cap while the remaining 13.2 ft (4 m) extended down into the pipe piles.

The pile cap was also cast using 6000-psi concrete with two horizontal reinforcing mats placed therein. The locations of the mats were the top and the bottom of the pile cap. The mats were made of #5 (#19) bars in both the transverse and longitudinal directions with a center-to-center spacing of 8 in. (203 mm) between bars. Resulting pile cap dimensions were 15-ft (4.57-m) long, 11-ft (3.35-m) wide, and 5.5-ft (1.68-m) tall with the top of the pile cap being approximately level with the backfill ground surface. Inclinometer tubes were cast in the center pile of both remaining rows of piles. Eight additional threaded 2.5-in diameter bars were also cast horizontally into the south end pile cap to provide a connection point between the pile cap and the loading apparatus.

3.3.3 Loading Apparatus

The loading apparatus consisted of two MTS hydraulic actuators shown in Figure 3.6. The actuators were seated horizontally between the reaction foundation and the pile cap. The post-tensioned threaded bars, mentioned previously, served as the connection between the reaction foundation and each actuator. The threaded bars embedded in the south end of the pile cap along with two 4-ft (1.22-m) long extensions provided the connection point from the actuators to the pile cap.

Each actuator was capable of applying 600 kips of horizontal force on the pile cap in compression, pushing the pile cap in the north direction, and 450 kips each in tension. The actuators had swivel-heads on each end, to eliminate the effect of moment on loading. The actuators were connected to the pile cap at a distance of 2.75 ft (0.84 m) above the base of the pile cap.

Figure 3.6: Photograph of MTS Hydraulic Actuators

3.3.4 Backfill Zone

The backfill zone was the area on the north side of the pile cap into which the pile cap was pushed. The area of the backfill zone was approximately 22-ft (6.7-m) wide and 24-ft (7.3-m) long for the unconfined (3D) tests with no walls, which considered probable 3D end effects as the pile cap displaced into the backfill. For those tests confined by the plywood side isolation panels or MSE wingwalls, the width of the backfill zone was limited to the width of the pile cap, or 11 ft. The first 8 ft (2.44 m) of the backfill extended to a depth of 7 ft (2.13 m) below the top of the pile cap for the unconfined test. After which, the depth of backfill decreased at a slope of approximately 3H:1V until the ground surface was reached. These backfill dimensions were chosen to minimize the amount of quality backfill needed for testing, but still be able to capture the predicted log-spiral failure surface. For the tests with wingwalls, the first 8 ft of the confined

backfill extended to a depth of 7 ft below the ground surface with the remaining 16 ft of backfill kept at a constant depth of about 5.5 ft (1.68 m) below the ground surface.

The backfill zone was filled in with material in lifts approximately 8 to 10 in. (203 to 254 mm) in height. The material was wetted as it was placed to aid in compaction. Jumping jack and vibratory drum compactors were used to compact each lift. Typically, three nuclear density tests were completed in random locations of each lift to help ensure proper density of the backfill and record soil unit weights and moisture contents.

3.3.5 General Instrumentation and Measurement

An independent reference frame was established between the reaction foundation and pile cap. This provided a fixed datum for measuring the pile cap displacement during loading. Six string potentiometers, also known as string pots, were mounted on the reference frame to measure the displacements. The string pots were Ametek model P-20 A units with a range of 20 inches, a tolerance of +/- 0.10%, and a linearity of 0.03% of full scale. Two of the string pots were connected to the north I-beam of the reaction foundation to measure displacements of the reaction frame towards the south. These two string pots were connected to the I-beam at a distance of about 8 ft (2.44 m) from the east and west ends at the same elevation as the connection point of the actuators to the pile cap. This also aligned the string pots with the approximate center of the drilled shafts. The remaining four string pots were attached at 3 and 51 in. (0.076 and 1.30 m) from the top of the pile cap on both the east and west edges of the south side of the pile cap. The displacements of the pile cap were captured by these four string pots and made it possible to detect any rotation that occurred during loading.

Seven other string pots were fixed to the top of the pile cap near the north face or backfilled side using a single angle iron. The angle iron was fixed at a distance of 10 in. (254

mm) from the pile cap face. The western most string pot was located at a distance of 46 in. (1.17 m) from the western edge of the pile cap. The remaining string pots were located at distances of 51.38, 56.50, 61.75, 72.63, 78.00, 83.25, and 88.50 in. (1.30, 1.44, 1.57, 1.84, 1.98, 2.11, and 2.25 m) also from the western edge of the pile cap. The string pots measured the surface displacement of the backfill zone. Steel stakes at locations in the backfill 2, 4, 6, 9, 12, 15, 18, and 24 ft (0.61, 1.22, 1.83, 2.74, 3.66, 4.57, 5.49, 7.32 m) away from the north face of the pile cap were the attaching points for the string pots. The string pots attached to stakes at the 2, 4, 6, 9, and 12 ft marks were Ametek Model P-20A units with a range of 20 in. (508 mm), a tolerance of +/- 0.10%, and a linearity of 0.03% of full scale. The string pots placed to measure the displacement at 15, 18, and 24 ft were UniMeasure Model P1010-5-S15 units with a range of 5 and 10 in. (127 and 254 mm), and a linearity of 0.18% of full scale.

As previously mentioned, inclinometer tubes were installed in the center pile of each pile row of the pile cap. The slotted tubes extended above the top of the pile cap about 1 ft (0.3 m) and to a depth of approximately 43 ft (13.1 m), or to the bottom of the piles. Each tube had an outer diameter of 2.75 in. (70 mm) and an inner diameter of 2.32 in. (60 mm). Inclinometer readings were taken at 2-ft (0.61-m) increments in both tubes before each test started and when the pile cap reached maximum displacement during each test. The inclinometer readings provided deflection versus depth profiles for the direction of loading.

Six pressure plates were installed prior to testing to measure the pressure of the backfill zone against the pile cap with depth. The plates were embedded into the pile cap allowing the face of the plates to be flush with the pile cap face as shown in Figure 3.7. Figure 3.8 shows the dimensioning of the pressure plates in relation to the pile cap. The pressure plates were nominal 9-in. diameter flat plates centered at depths of approximately 0.46, 1.38, 2.30, 3.22, 4.13, 5.05 ft

(5.5, 16.5, 27.5, 38.5, 49.5, and 60.5 in.; 0.14, 0.42, 0.70, 0.98, 1.26, and 1.54 m) below the ground surface after placement of the compacted fill. Reinforced backplates reduced point loading effects created by mounting the plates to a concrete or steel surface. The cells also contain a semi-conductor pressure transducer as opposed to a vibrating wire transducer to more accurately measure pressure changes during rapid loading. Steel channels were used to protect the pressure cell wiring from damage caused by the backfill material.

For each test, a 2 ft x 2 ft (0.61 m x 0.61 m) grid was painted on the surface of the backfill zone. Elevations were taken by a surveying level at each of the grid intersection points before each test started. After the pile cap reached maximum deflection, a second set of elevations was taken over the grid. The difference in elevations showed the vertical displacement of the backfill zone. Contour maps of the resulting vertical displacements of each test were then created.

Figure 3.7: Photograph of Pressure Plates Embedded in the Pile Cap

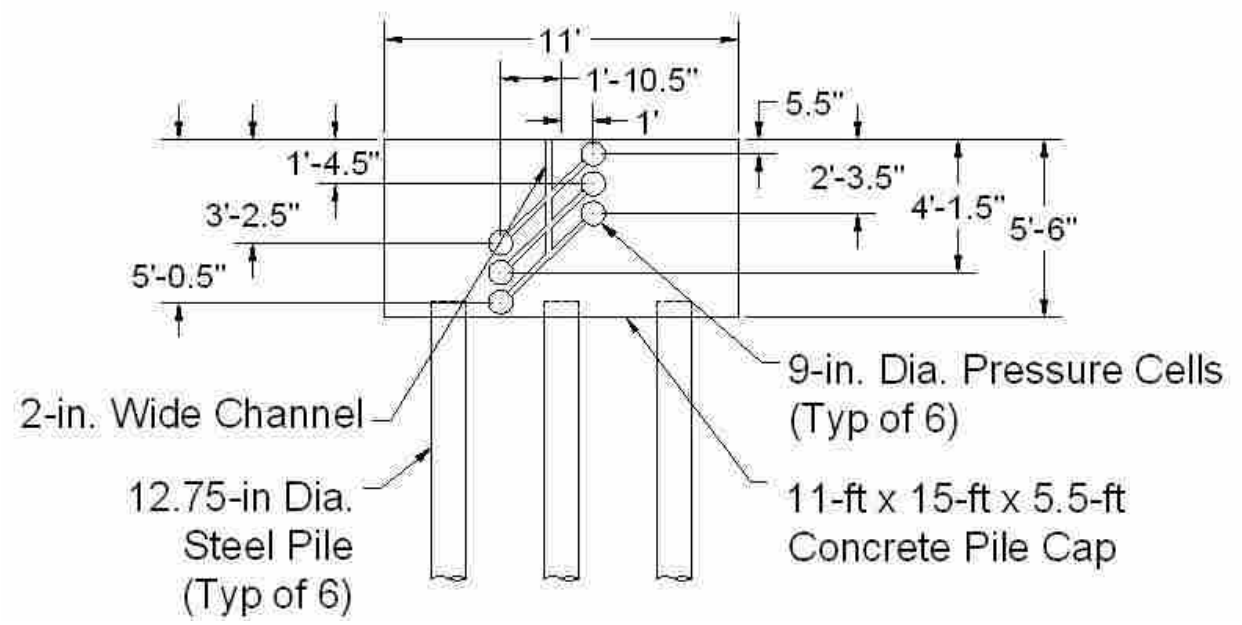

Figure 3.8: Drawing of the Imbedded Pressure Plates

During testing, surface cracking was also visually monitored. After each 0.25-in. (6.35-mm) displacement increment, the resulting cracks were marked with paint on the backfill and mapped on grid paper representing the backfill zone. Marking cracks on the backfill with paint allowed for new cracks to be distinguished more easily after subsequent displacement increments were completed. Each increment was mapped on the grid paper using a different color to highlight where new cracks had formed.

3.4 Backfill Soil Description

The backfill soil consisted of a well-graded sand (SW) according to the Unified Soil Classification System (USCS). An average particle size distribution curve is shown in Figure 3.9. Three sieve analyses were conducted throughout the testing period to produce the distribution. The resulting material was approximately 87% sand, 12% gravel, and 1% fines.

Table 3.1 gives a summary of other relevant soil characteristics determined from the particle size distribution curve.

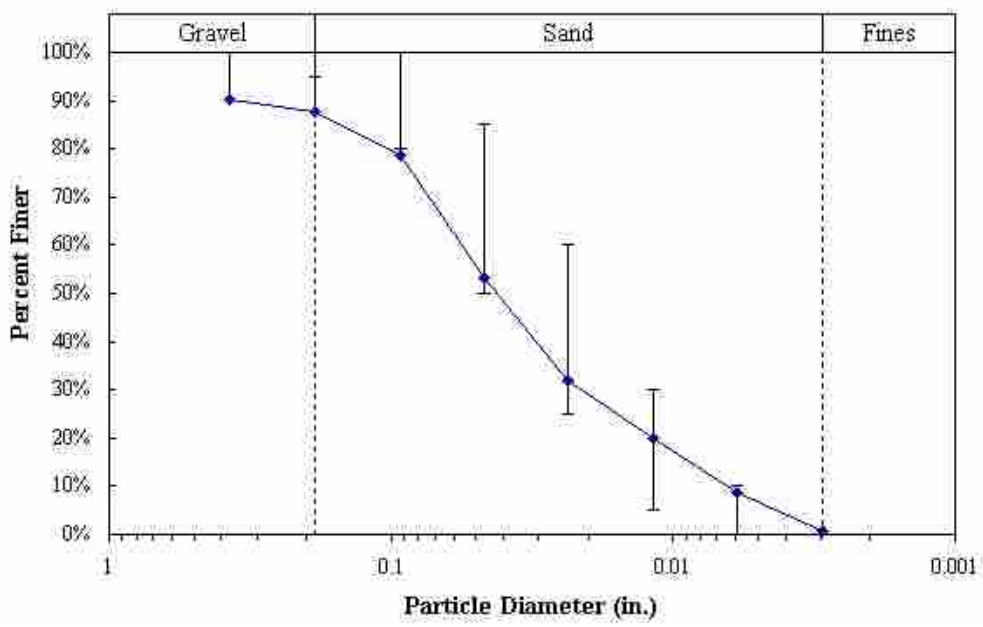

Figure 3.9: Particle Size Distribution Curve of the Backfill Soil

Table 3.1: Backfill Soil Grain Characteristics

Backfill Soil	Gravel %	Sand %	Fines %	D_{60} in.	D_{50} in.	D_{30} in.	D_{10} in.	C_u	C_c
Well-graded Sand	12	87	1	0.056	0.042	0.021	0.006	8.91	1.26

The modified Proctor maximum dry unit weight for the backfill sand was 124.2 pcf (19.51 kN/m^3) with an optimum moisture content (*w*) of 11.2%. The target on-site compaction level for the loose backfills was equal to 90% of the modified Proctor maximum dry unit weight, or 111.8 pcf (17.56 kN/m^3). The target on-site compaction level for the dense MSE backfill was equal to or greater than 96% of the modified Proctor maximum dry unit weight, or 119.23 pcf (18.73 kN/m^3). Figures 3.10, 3.11, 3.12, and 3.13 show the actual in-situ average dry unit

weights for the loose sand unconfined (3D), loose sand slip plane (2D), loose sand MSE, and dense sand MSE tests states of 107.0 pcf (16.80 kN/m^3), 109.5 pcf (17.20 kN/m^3), 109.1 pcf (17.14 kN/m^3), and 117.6 pcf (18.47 kN/m^3), respectively.

The backfill strength parameters of friction angle (ϕ) and cohesion (c) were found by conducting direct shear and triaxial shear tests in the BYU soils laboratory. Tests were performed by Joshua Pruett for the loose and dense sands. The results of all tests are shown in Tables 3.2 and 3.3. The ϕ and c values selected were from drained, partially saturated triaxial tests interpreted with no cohesion. The loose sand was found to have a friction angle of 36.0° with no cohesion. The dense sand was found to have a friction angle of 43.1° with no cohesion.

Using a correlation developed by Lee and Singh (1971) between relative density and relative compaction of granular soils, the relative density was computed for all four load tests. The correlation is shown below as Equation 3.1:

$$R = 80 + 0.2D_r \quad \textbf{(3.1)}$$

where

R = relative compaction, %

D_r = relative density, %.

Table 3.4 shows the actual relative compaction (R) achieved for each test using the densities provided in the previous section with the calculated relative densities (D_r). The difference between R for the loose tests is only 2 percentage points. However, a 2 percentage point difference in R produces a 10 percentage point difference in D_r and a 1.4 degree difference in friction angle (U.S. Navy 1982).

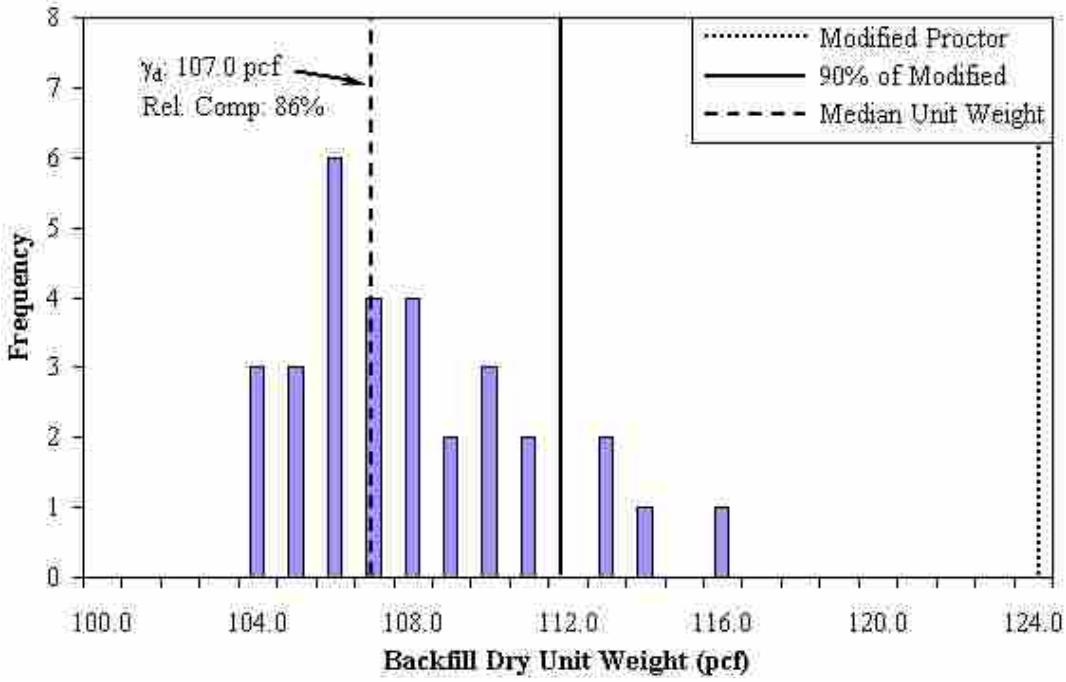

Figure 3.10: Backfill Dry Unit Weight Histogram for Loose Sand Unconfined (3D) Test

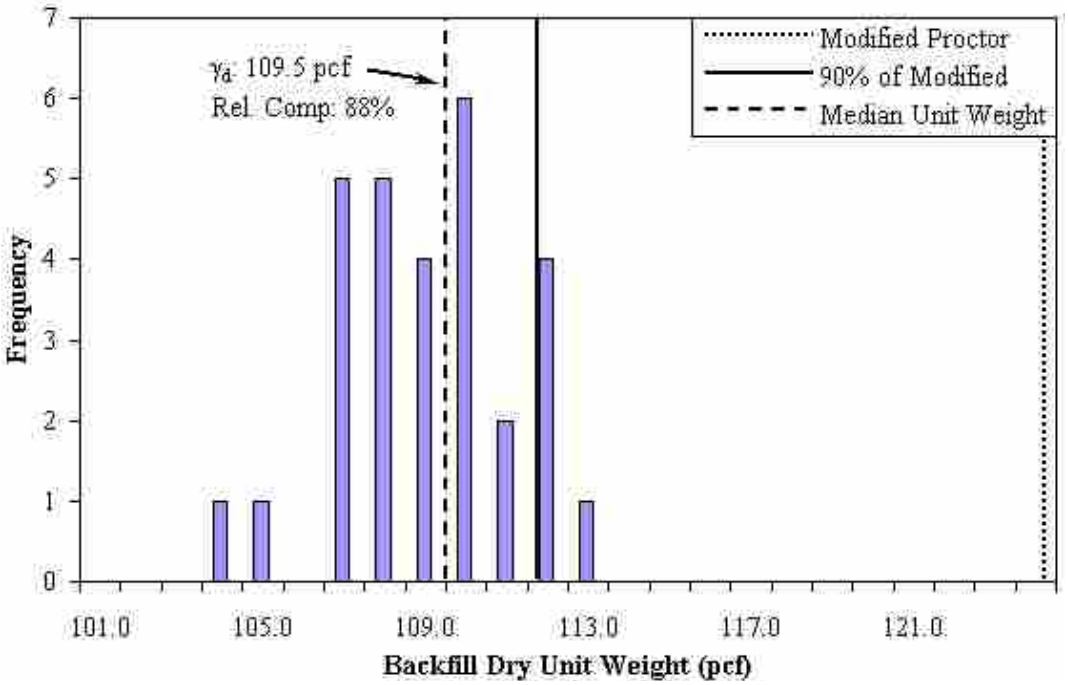

Figure 3.11: Backfill Dry Unit Weight Histogram for Loose Sand Slip Plane (2D) Test

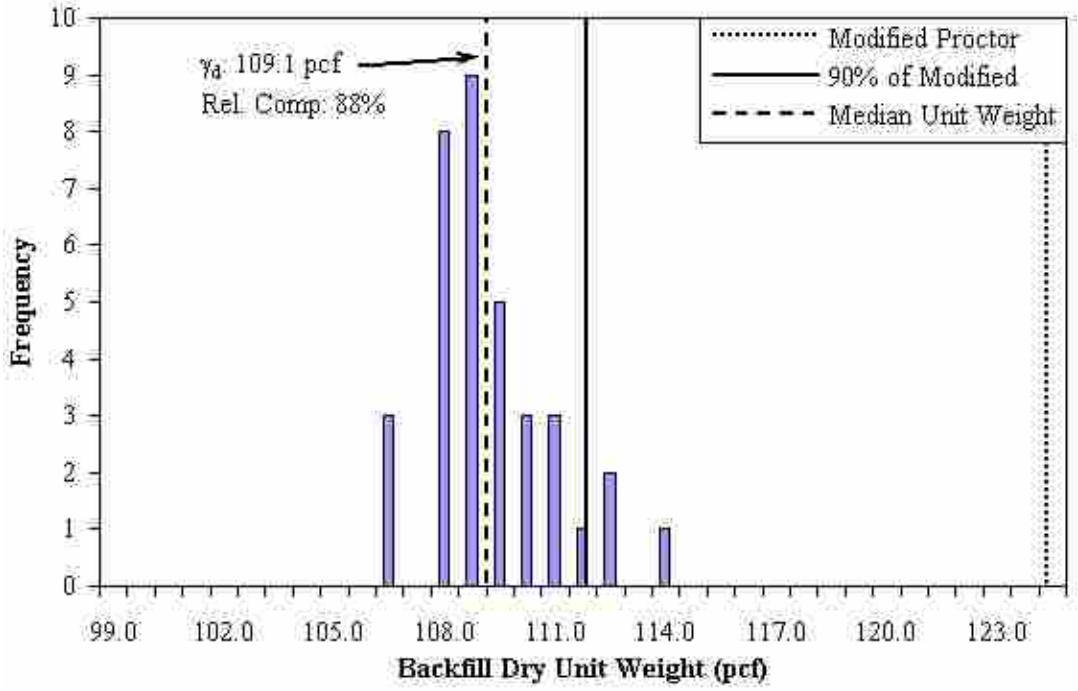

Figure 3.12: Backfill Dry Unit Weight Histogram for Loose Sand MSE Test

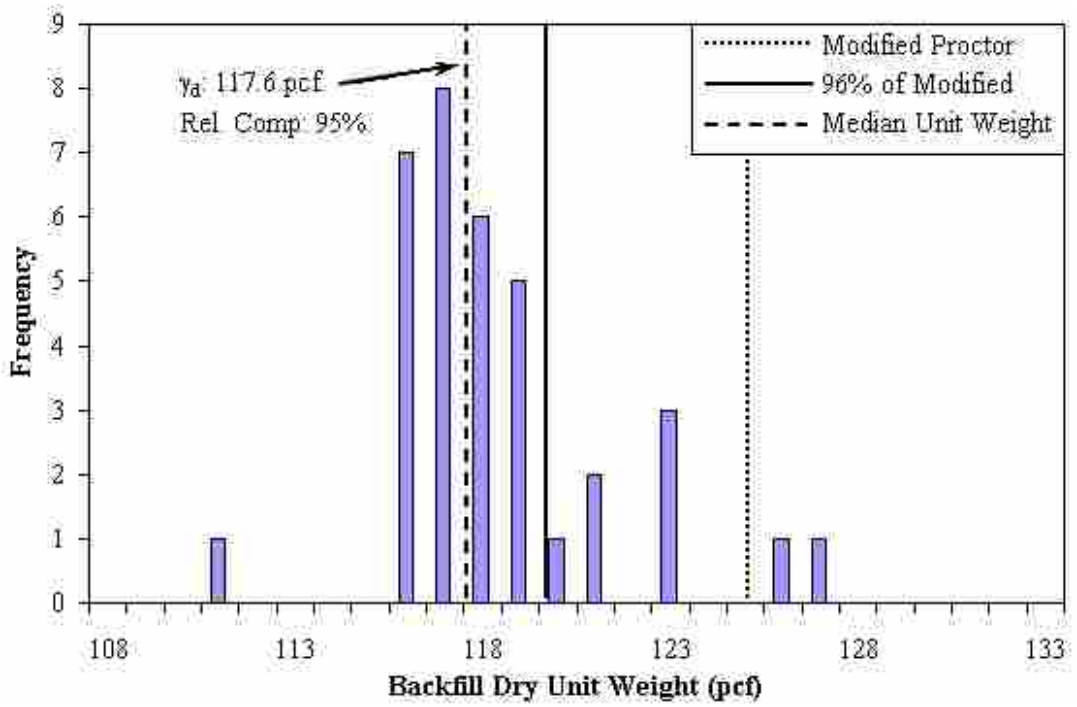

Figure 3.13: Backfill Dry Unit Weight Histogram for Dense Sand MSE Test

Table 3.2: Loose Sand Backfill Material Strength Parameters

Source of Test Result	Peak		Ultimate	
	φ (deg)	c (psf)	φ (deg)	c (psf)
Direct Shear (full range)	37.5	452	37.5	61.3
Direct Shear (full range, zero cohesion)	39.4	0.0	40.0	0.0
Direct Shear (250 psf to 3000 psf)	46.9	106	39.8	12.8
Direct Shear (250 psf to 3000 psf, zero cohesion)	48.3	0.0	37.7	0.0
Direct Shear (6000 psf to 12000 psf)	36.3	727	39.1	400
Direct Shear (6000 psf to 12000 psf, zero cohesion)	39.0	0.0	37.7	0.0
Triaxial	37.1	-137	34.6	-0.5
Triaxial (zero cohesion)	**36.0**	0.0	34.6	0.0

Table 3.3: Dense Sand Backfill Material Strength Parameters

Source of Test Result	Peak		Ultimate	
	φ (deg)	c (psf)	φ (deg)	c (psf)
Direct Shear (full range)	48	1020	37.3	15.9
Direct Shear (full range, zero cohesion)	50.9	0	37.4	0
Direct Shear (250 psf to 3000 psf)	52.2	751	36.2	47.4
Direct Shear (250 psf to 3000 psf, zero cohesion)	58.8	0	36.7	0
Direct Shear (6000 psf to 12000 psf)	44.3	2280	36.7	204
Direct Shear (6000 psf to 12000 psf, zero cohesion)	50.5	0	37.4	0
Triaxial	**43.1**	823	40.6	459
Triaxial (zero cohesion)	47.6	0	43.5	0

Table 3.4: Relative Compaction and Relative Density Values for All Tests

Backfill Property	Loose Sand Unconfined (3D)	Loose Sand Slip Plane (2D)	Loose Sand MSE	Dense Sand MSE
Median Dry Unit Weight (pcf)	107.0	109.5	109.1	117.6
Median Moisture Content (%)	5.6	7.9	9.5	9.4
Median Moist Unit Weight (pcf)	113.0	118.2	119.5	128.7
Relative Compaction (%)	86	88	88	95
Relative Density (%)	31	41	39	73

3.5 General Test Procedure

The general test procedure consisted of four basic steps: 1) wall placement, 2) backfilling, 3) displacement of the pile cap, and 4) data collection. A total of ten tests were conducted during the summer of 2009. Table 3.5 is a summary of all the tests with a short description of each. As mentioned previously, only detailed information regarding the second and third no backfill tests, loose sand unconfined (3D) test, loose sand slip plane (2D) test, and loose and first dense sand MSE tests is presented in this thesis.

Table 3.5: 2009 Testing Summary

Test Number	Test Date	Backfill Condition
1	3-Jun-09	No Backfill (Baseline)
2	4-Jun-09	No Backfill (Baseline)
3	8-Jun-09	Loosely Compacted Sand Unconfined (3D - No Walls)
4	12-Jun-09	Loosely Compacted Sand Slip Plane (2D - Plywood Walls with Plastic Sheeting)
5	18-Jun-09	Loosely Compacted Sand MSE Wingwall
6	22-Jun-09	Densely Compacted Sand MSE Wingwall 1
7	24-Jun-09	No Backfill (Baseline)
8	26-Jun-09	Densely Compacted Sand MSE Wingwall 2
9	2-Jul-09	Densely Compacted Sand Slip Plane (2D - Plywood Walls with Plastic Sheeting)
10	9-Jul-09	Densely Compacted Sand Unconfined (3D - No Walls)

The first step to complete each test was to place the walls which would be used for that test, if necessary. The baseline tests and the unconfined (3D) tests did not require walls. For the slip plane (2D) tests, 0.75-in. (19 mm) thick plywood panels covered with two layers of plastic sheeting acted as walls. These walls were designed to create 2D failure geometry with minimal friction on the sides of the sliding surface. This provided a setup most like plane strain loading conditions. The plywood panels were 4-ft (1.22-m) wide by 8-ft (2.44-m) long. Six panels

placed individually with the long dimension vertical were combined using 2 in. x 4 in. walers to make one wall 24-ft (7.32-m) long and 8-ft high.

The MSE tests used a total of four MSE panels for wingwalls. A MSE panel was approximately 12-ft (3.66-m) wide by 5-ft (1.52-m) tall. Each wingwall was then 24-ft (7.32-m) long. Figure 3.14 and Figure 3.15 show typical drawings of the MSE panels used during testing. The panels were placed on three standard 4 in. x 4 in. (102 mm x 102 mm) pieces of lumber inserted into the web of a steel I-beam to provide a stable and level base for the MSE wingwalls.

Once the walls were in place, backfilling was completed. The backfill was placed in 8 to 10 in. (200 to 254 mm) lifts. Each lift was compacted to the target unit weight. Material was placed both inside and outside of the plywood walls to prevent them from breaking. For the MSE tests, fill was only placed inside the wall panels, but the panels were braced to prevent them from displacing during construction. Reinforcing mats were also installed during the backfilling of the MSE wall tests. The mats were located at distances of 1.22 ft (0.37 m) and 3.72 ft (1.13 m) from the base of the panels.

Next, the tests were started with the pile cap deflecting into the backfill zone. The actuators were displaced in target intervals of 0.25 in. (6.35 mm) until the maximum passive force was developed or until the actuator load was close to the actuator capacity of 600 kips. After each 0.25-in. interval was reached, the actuators were held in place as the backfill zone surface was visually inspected for cracks. Each new crack was recorded on a grid. Typically, this process was repeated up to a maximum displacement of 3.25 in. (82.55 mm).

Grid elevations were taken at the beginning and end of each test to record the backfill zone overall vertical displacement. Inclinometer readings were also recorded at the beginning and end of each test to monitor the pile cap deflection with depth profiles.

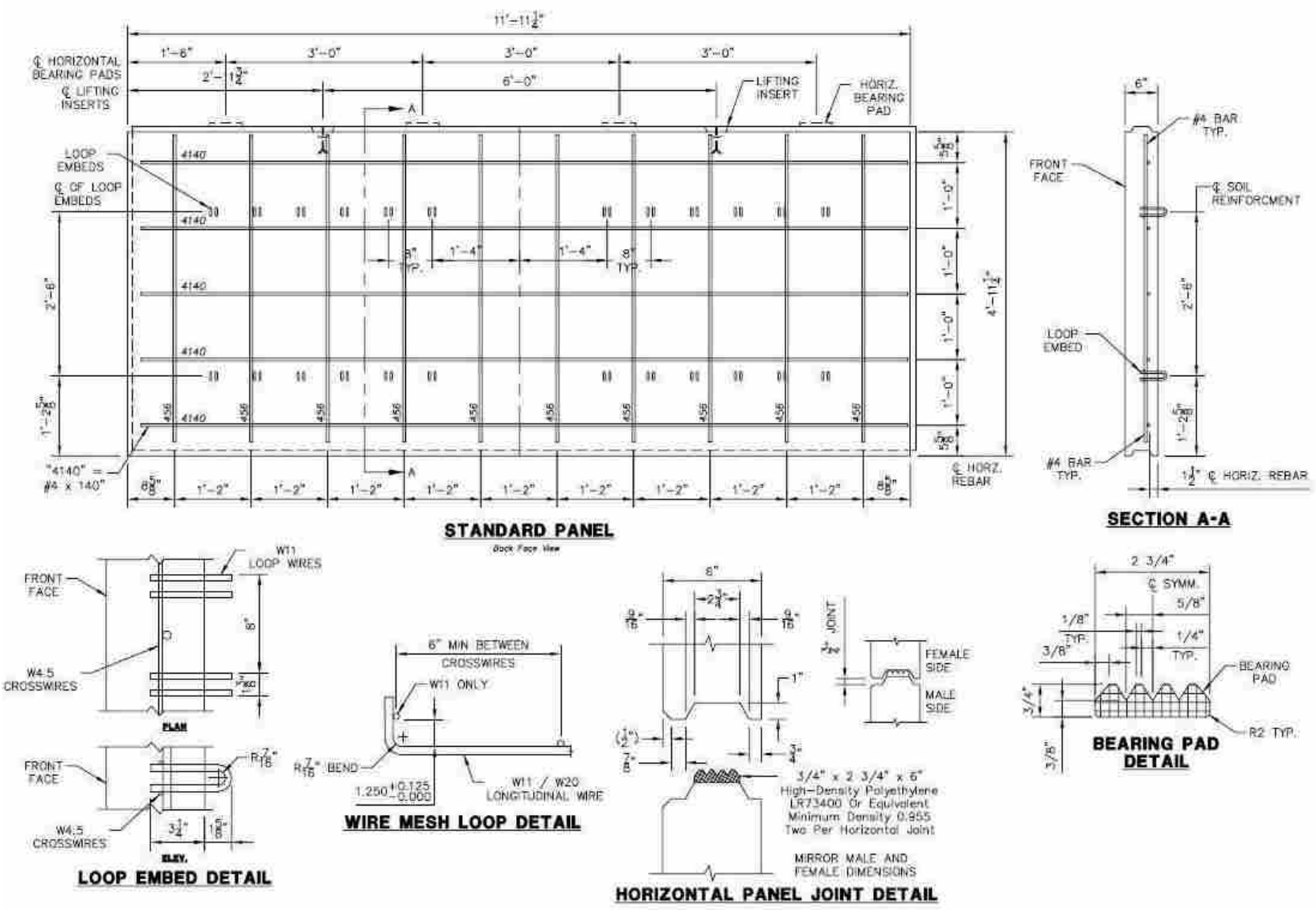

Figure 3.14: Standard MSE Panel Drawing (1)

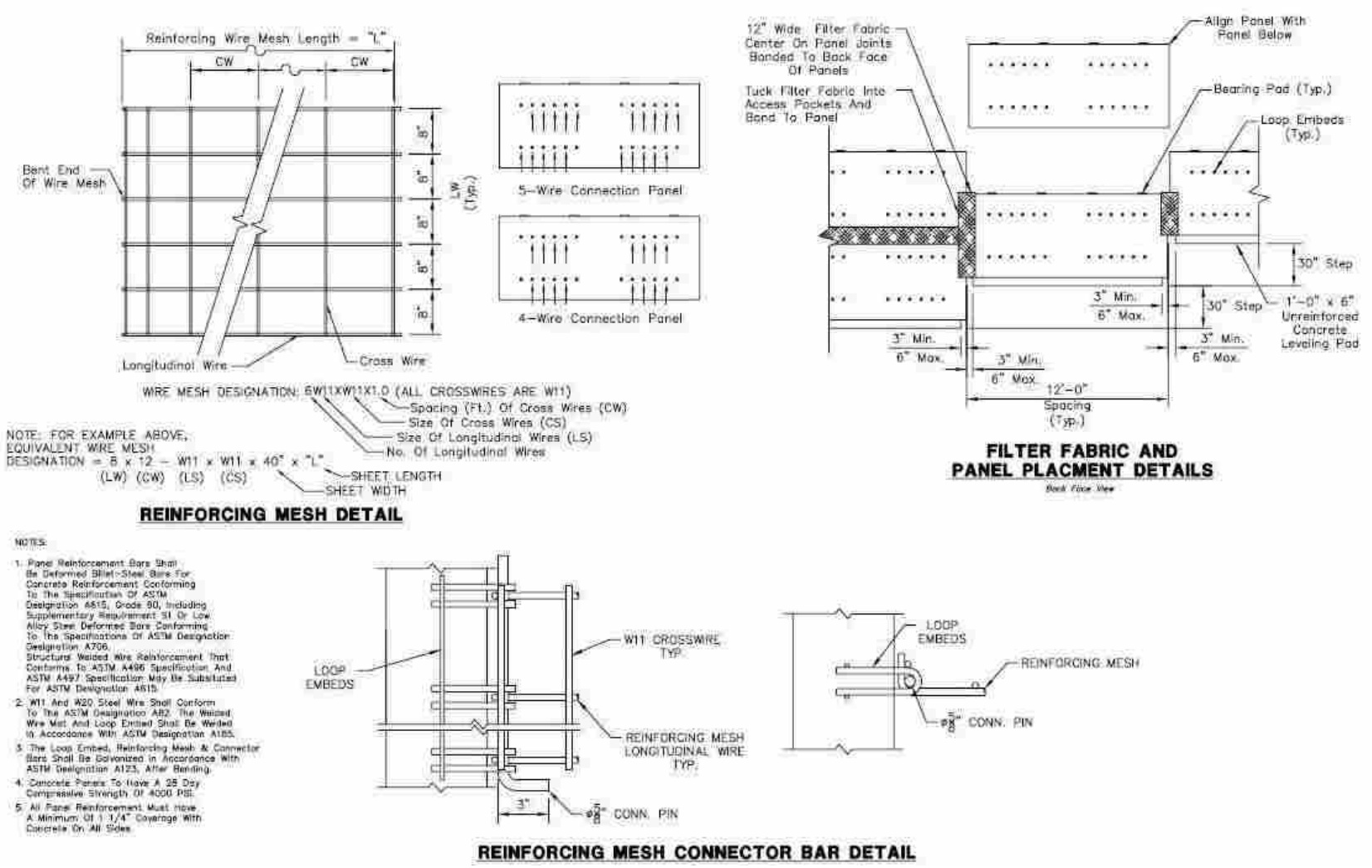

Figure 3.15: Standard MSE Panel Drawing (2)

4 ABUTMENT LOAD TESTING – LOOSE SAND UNCONFINED (3D) TEST

The loose sand unconfined (3D) test occurred on 8 June 2009. The test represented an abutment without a confined backfill, meaning no wingwalls were placed to truncate the backfill. The backfill in this case was considered loosely compacted because the median dry unit weight of the soil was approximately 86% of the modified Proctor. The purpose of this test was to capture the resulting log-spiral failure surface with the associated 3D geometry effects for comparison to the tests confined with walls. The test layout, instrumentation, procedure, and results are described in this chapter.

4.1 Test Layout, Instrumentation, and Procedure

The loose sand unconfined (3D) test did not require walls; therefore, the backfill zone was an area 22-ft wide by 24-ft long. The resulting effective pile cap width was 18 ft (5.49 m).The entire area was painted with the 2 ft x 2 ft grid to help assist in monitoring the movement of the backfill. No additional instrumentation was implemented during this test beyond that generally used for all tests. The general testing procedure also applied for this test. The pile cap was loaded in 0.25-in. displacement increments until a maximum cap deflection of 3.25 in. was reached. The backfill zone was visually inspected for cracks after each 0.25-in. increment. Figure 4.1 shows a photograph of the backfill zone setup for the test looking towards the backfill from the pile cap.

Figure 4.1: Photograph of the Loose Sand Unconfined (3D) Backfill Zone

4.2 Test Results

The following sections provide the results of the loose sand unconfined (3D) test. The results consist of passive force-displacement measured from the actuators, passive pressure versus depth curves, passive force-displacement measured from the pressure plates, inclinometer displacement versus depth curves, and backfill displacement data.

4.2.1 Load-Displacement Results – Actuators

Figure 4.2 plots the measured total peak actuator load versus pile cap displacement. The displacement values were calculated by taking the median displacement of the four string pots

attached to the pile cap at the end of each displacement increment. The maximum load recorded was 681 kips (3050 kN) at a displacement of 3.27 in. (83 mm).

The passive resistance of the backfill material was calculated from the total load-displacement curve and the baseline test results. The baseline response of the abutment was determined by conducting a lateral load test without backfill. Lateral pile resistance and base shear forces provided resistance to the pile cap movement during the baseline test and produced a baseline resistance of the pile cap system. The baseline resistance was then subtracted from the total actuator load to develop the passive resistance of the backfill. The total resistance, passive earth resistance, and baseline resistance are shown as a function of the pile cap displacement in Figure 4.2. The passive force-deflection curve shown does not have a distinct peak as would a dense material. The passive force gradually increased with displacement, consistent with a punching shear failure mechanism typical for loose materials.

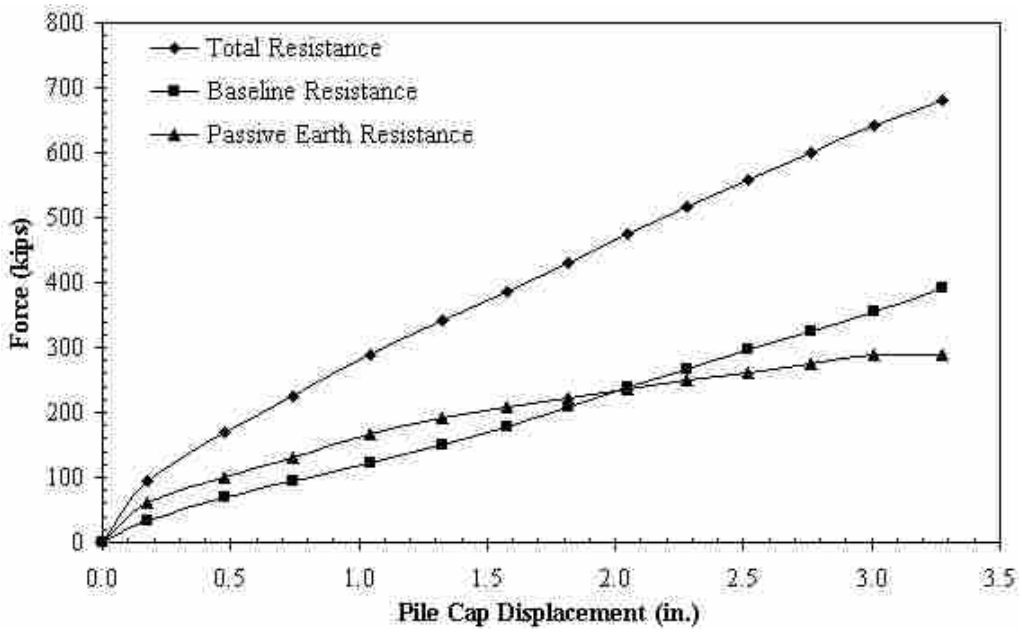

Figure 4.2: Force-Displacement Curves for the Loose Sand Unconfined (3D) Test

4.2.2 Load-Displacement Results – Pressure Cells

To help verify the load-displacement results from the actuators described in the previous section, measurements from the pressure cells embedded in the face of the pile cap were analyzed. During the test, pressure readings from the pressure cells were taken continuously. Figure 4.3 shows a plot of the backfill passive pressure as a function of the depth of the pile cap at the end of each displacement increment. The plot generally follows a trend of increasing pressure with increasing depth, but there are a few inconsistencies. For the upper three feet of the pile cap, the pressure did not change dramatically. As the depth increased greater than three feet, the pressure increased notably. Also, at a depth of 1.38 ft (0.42 m), the passive pressures recorded at this cell reached a peak value by the 1.33 in. (34 mm) increment and then proceeded to decrease significantly afterwards until the end of the test was reached.

To develop passive force-displacement curves from the passive pressure cell data, the readings were converted to force by multiplying the passive pressure by the tributary area of each pressure cell. The tributary area was computed as the vertical distance between the pressure cells, or approximately 11 in. (0.28 m), multiplied by the total width of the pile cap, or 11 ft (3.35 m). This calculation assumed a uniform pressure across the width of the pile cap. Figure 4.4 shows a plot of the pressure cell passive force versus the pile cap displacement compared to the backfill passive resistance calculated from the actuators.

Typically, the pressure cell passive force-displacement curves were lower than the actuator passive force-displacement curves by approximately 30 to 40%. This discrepancy can likely be attributed to assuming a uniform pressure across the width of the pile cap. Soil-structure analyses frequently show increased stress concentrations near the edges of a concrete mat or pile cap. Because the pressure cells were located near the center of the pile cap, an

increased pressure near the edges of the pile cap was not captured and an underestimation of the actual pressure across each horizontal segment of the pile cap occurred. The "pressure cells with multiplier" curve, in Figure 4.4, accounts for this concern by showing what the passive force-displacement curve appears like when multiplied by a factor of 1.67. This curve is slightly above the measured passive earth resistance curve calculated from the actuators, but maintains the same general shape. The maximum passive forces of both the "passive earth resistance" and the "pressure cells with multiplier" curves are nearly identical.

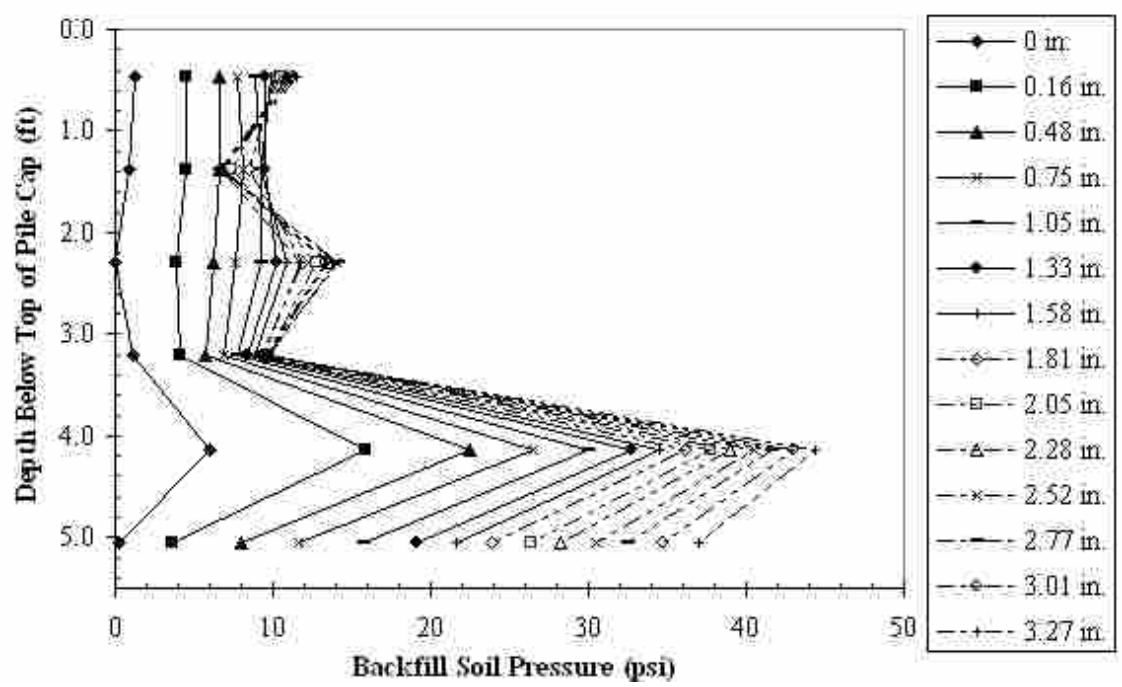

Figure 4.3: Backfill Passive Pressure Versus Depth at Each Displacement Increment for the Loose Sand Unconfined (3D) Test

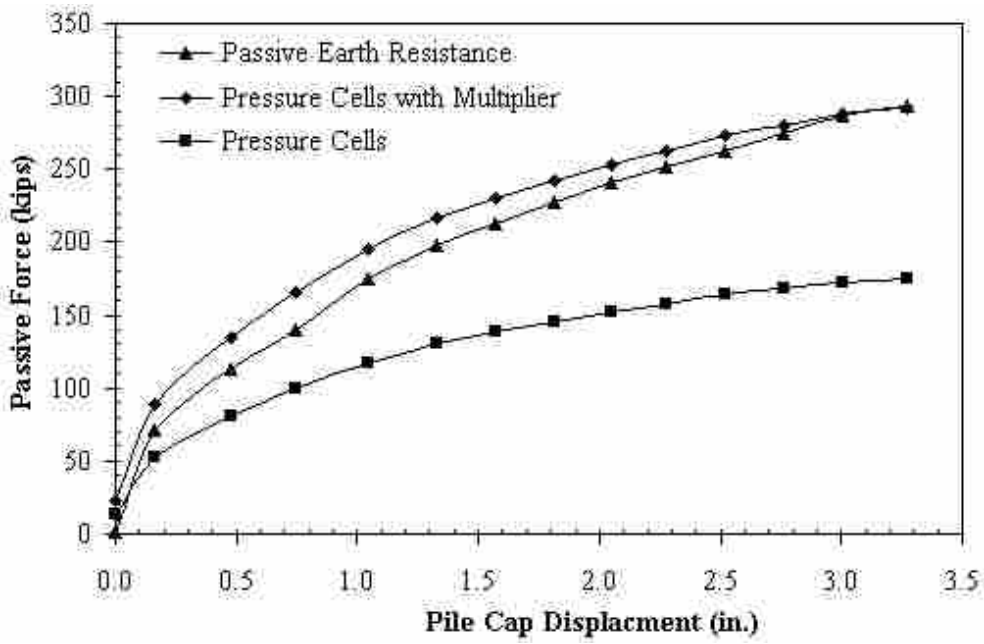

Figure 4.4: Pressure Cell Passive Force Resistance Compared to the Measured Passive Earth Resistance for the Loose Sand Unconfined (3D) Test

4.2.3 Inclinometer Data

Before and after each test was conducted, inclinometer readings were taken in both the north and south inclinometer tubes embedded in the pile cap. The readings measured the pile cap and pile deflection over the depth of the piles parallel to the direction of loading. Figure 4.5 shows the north and south deflection results when the pile cap reached maximum deflection during the loose sand unconfined (3D) test. The curves shown were generated by subtracting the initial readings at the start of the test from the final readings at the end of the test. Positive deflection values correlate with the northerly direction of loading. A depth of zero corresponds to the top of the pile cap. The zero displacement of the piles occurred at a depth of approximately 20 ft (6.10 m), which depth is about 19 pile diameters. The maximum displacement values recorded by the four string pots attached to the pile cap were also plotted.

The string pot values confirm the inclinometer results. From the inclinometer plot, it can be seen that the pile cap experienced very little rotation during loading, typical of a fixed head boundary condition.

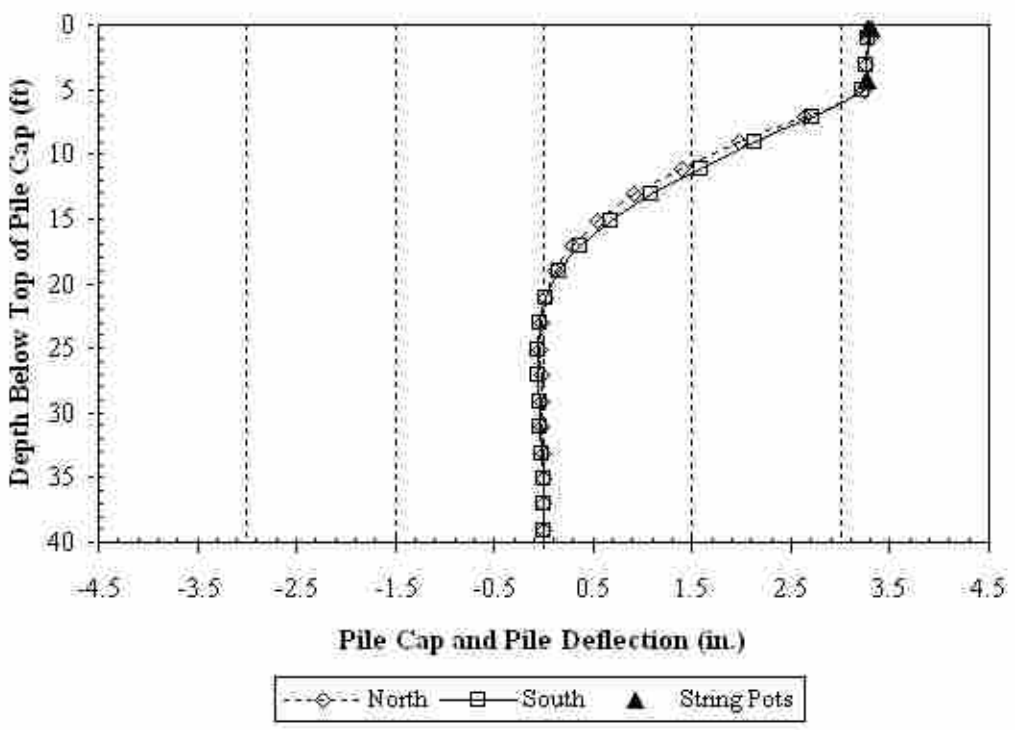

Figure 4.5: Inclinometer Readings of the Loose Sand Unconfined (3D) Test

4.2.4 Backfill Displacement Data

During testing, the backfill displacement was monitored with string pots located in the configuration described previously in Section 3.3.5. Figure 4.6 shows the absolute displacement of the backfill plotted against the distance from the pile cap recorded from these string pots. To simplify the plot, backfill displacements from selected pile cap displacements increments are shown. The results of the loose unconfined test show that more backfill displacement occurred close to the pile cap while at distances greater than about 10 ft (3.05 m), the material was less

affected by the cap movement and little displacement occurred. The minimum horizontal displacement recorded at a distance of 24 ft (7.32 m) from the pile cap face was approximately 0.17 in. (4.3 mm). This observation can be understood by recognizing that loose sands tend to exhibit a local shear failure as compared to a general shear failure condition typical of dense sands. General shear failure would lead to movement throughout the failure zone while local shear failure would primarily lead to movement close to the pile cap.

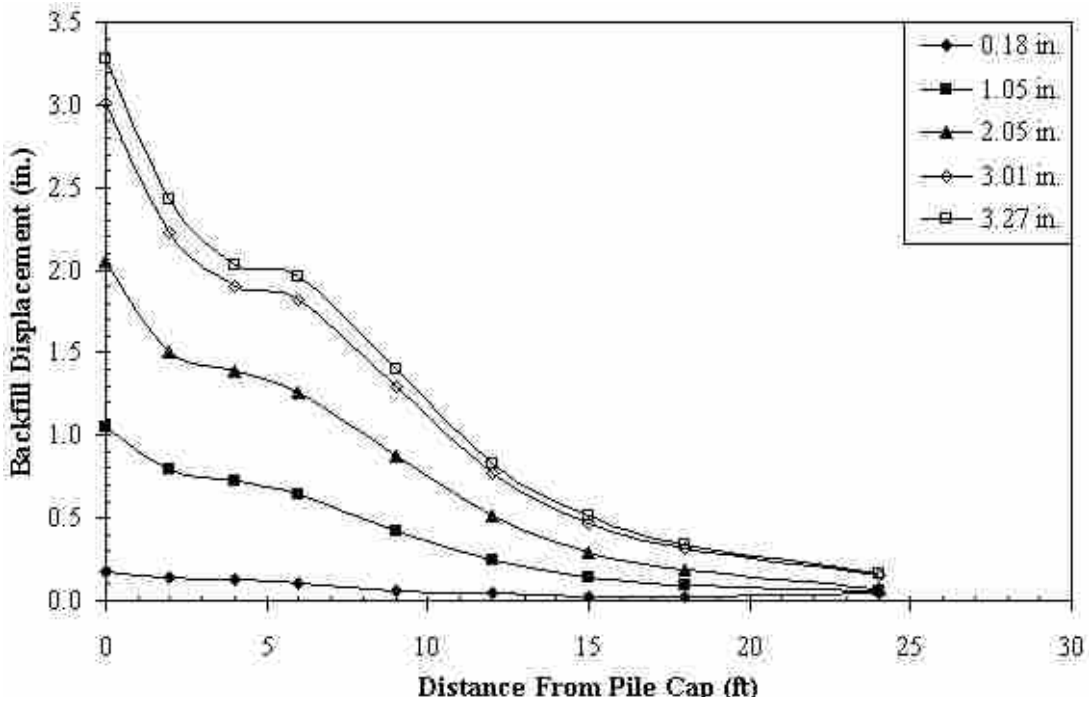

Figure 4.6: Absolute Backfill Displacement Versus Distance from the Pile Cap for the Loose Sand Unconfined (3D) Test

From the displacement data in Figure 4.6, the compressive strain (in./in.) was calculated for each distance between string pot stakes (i.e., 0-2 ft, 2-4 ft, 4-6 ft, 6-9 ft, etc.) with the following equation, Equation 4.1:

$$\varepsilon = \Delta L / L \quad \textbf{(4.1)}$$

where

ε = compressive strain

ΔL = change in string pot length per displacement interval, in.

L = north-south distance between adjacent stakes, in.

Figure 4.7 shows the compressive strain calculation results for selected displacement intervals. Not all intervals are shown to simplify the plot. The overall trend can still be seen with the intervals plotted. The highest compressive strain rates occur in the first two feet of backfill. The strain rates are approximately equal in the 6 to 12 ft (1.83 to 3.66 m) interval. However, the compressive strain levels decrease as the distance from the pile cap increases beyond 12 ft.

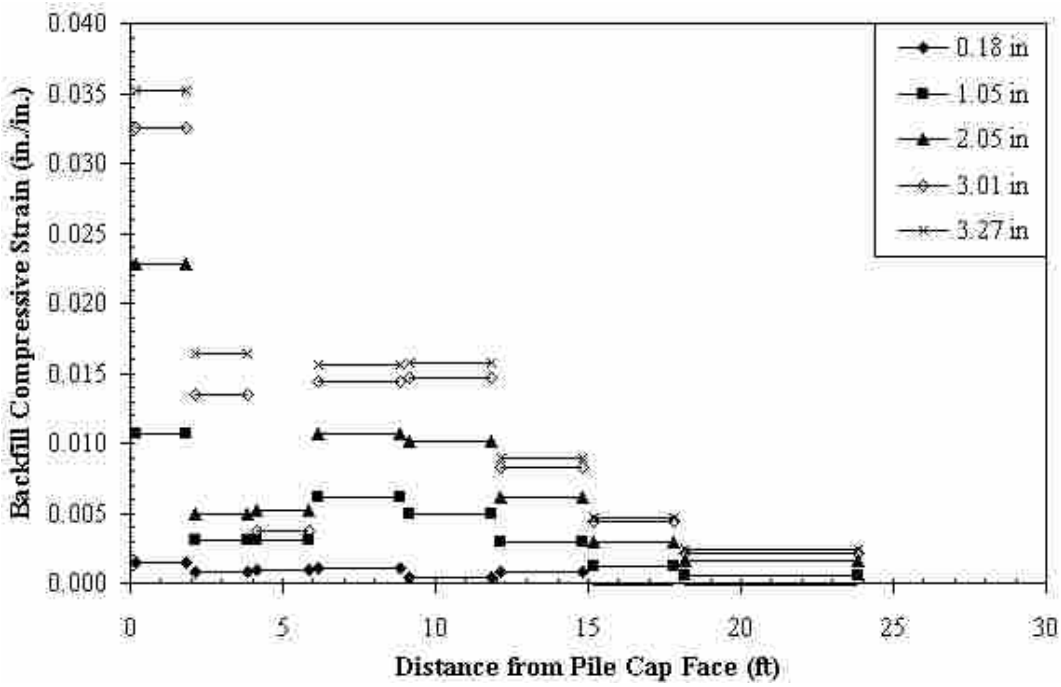

Figure 4.7: Backfill Compressive Strain for the Loose Sand Unconfined (3D) Test

The vertical displacement of the backfill was also determined for the test. To determine vertical displacement, the elevation of the backfill grid was recorded before and after the test. The difference between the elevations showed how much the backfill displaced from the loading of the pile cap. Figure 4.8 shows a contouring of the backfill zone for the loose sand unconfined (3D) test measured in inches. Positive values reflect heave, or upward movement, of the backfill while negative values indicate settlement of the material. The contours appear generally in a circular pattern in front of the pile cap face. This circular pattern is representative of the 3D end shearing effects of the pile cap. The maximum vertical displacement occurred was approximately 2.0 in. (51 mm) at a distance of 4 ft (1.22 m) from the pile cap. Along the 12-ft and 18-ft gridlines, three instances of settlement occurred where the backfill settled approximately 0.25 in. (6.35 mm). Practically no heave occurred after the 22-ft gridline. It was also interesting to note the region 18 ft (5.50 m) from the cap face where there was an increase in vertical displacement up to approximately 1.25 in. (32 mm). This increase may be an indication of the log-spiral failure surface exit location in the material.

Figure 4.9 shows the crack pattern that developed in the backfill during testing. The backfill was visually inspected for cracks after each displacement increment. The most significant cracking during testing occurred approximately 2 ft to 4 ft (0.61 m to 1.22 m) from the pile cap face around the pile cap corners. The corner cracking provides support to believe that end effects from pile caps do produce a 3D log-spiral failure surface that is wider that the pile cap or abutment. The shear zones extent 4 to 5 ft (1.22 to 1.52 m) beyond the edge of the pile cap to create an effective pile cap width of approximately 18 ft (5.49 m). No visual cracking appeared beyond the 16-ft grid line. The cracks tend to follow a similar pattern as the heave contours shown in Figure 4.8.

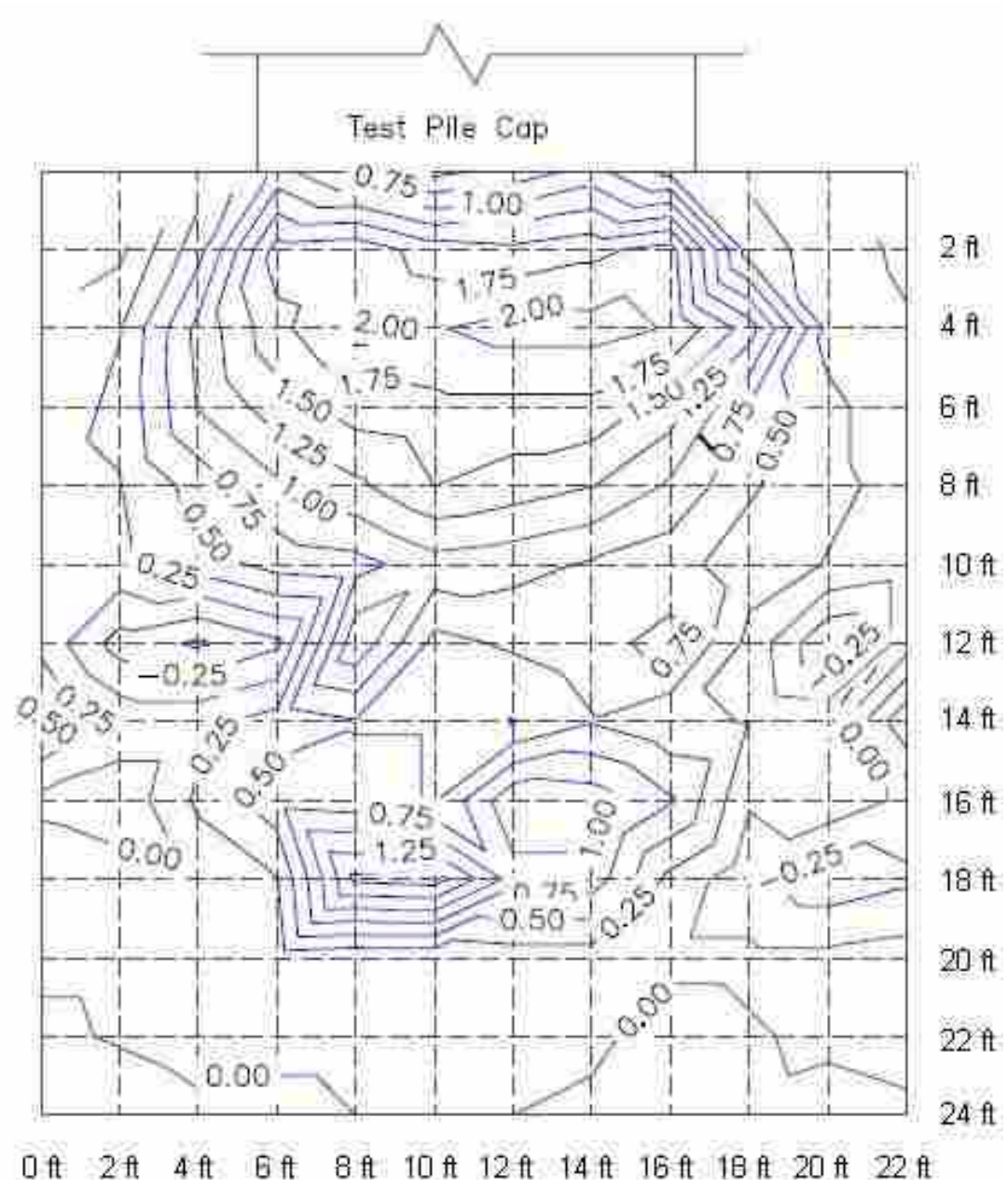

Figure 4.8: Backfill Vertical Displacement Contour of the Loose Sand Unconfined (3D) Test

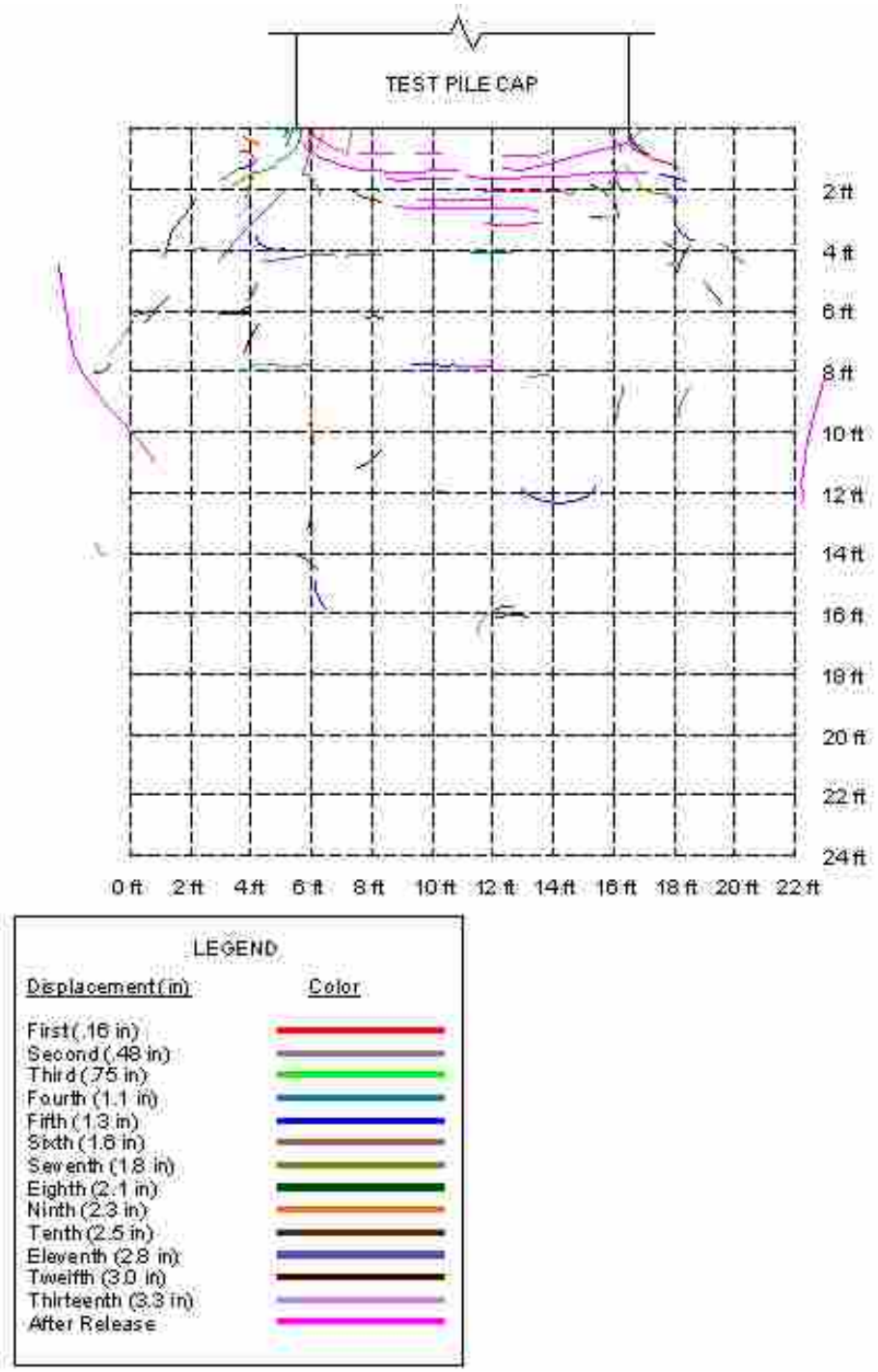

Figure 4.9: Observed Backfill Cracking During the Loose Sand Unconfined (3D) Test

5 ABUTMENT LOAD TESTING – LOOSE SAND SLIP PLANE (2D) TEST

The loose sand slip plane (2D) test occurred on 12 June 2009. The test represented an abutment with a confined backfill, where walls were placed to truncate the backfill to the width of the pile cap. In this test, the backfill was considered loosely compacted because the median dry unit weight of the soil was approximately 88% of the modified Proctor. The purpose of this test was to remove the 3D end effects experienced during the unconfined (3D) test by producing a 2D situation most like plane strain conditions and capture the resulting log-spiral failure surface. The test layout, instrumentation, procedure, and results are described in this chapter.

5.1 Test Layout

Plan and profile views of the loose sand slip plane (2D) test layout are shown in Figure 5.1. The plywood panels utilized were 4-ft (1.22-m) wide, 8-ft (2.44-m) tall, and 0.625-in. (16-mm) thick. Six panels were placed on each side of the pile cap to create two 24-ft (7.32-m) long wingwalls. The panels were connected together using standard 2 in. x 4 in. pieces of lumber to prevent any separation between panels. Two layers of plastic sheeting (Visqueen) lined the inside of the plywood walls. The purpose of using the plastic sheeting was to provide a low-friction surface between the walls and the backfill material, thus creating 2D failure geometry. Backfill material was placed and compacted on both sides of the walls to prevent the walls from flexing excessively by balancing the normal stress placed on the walls.

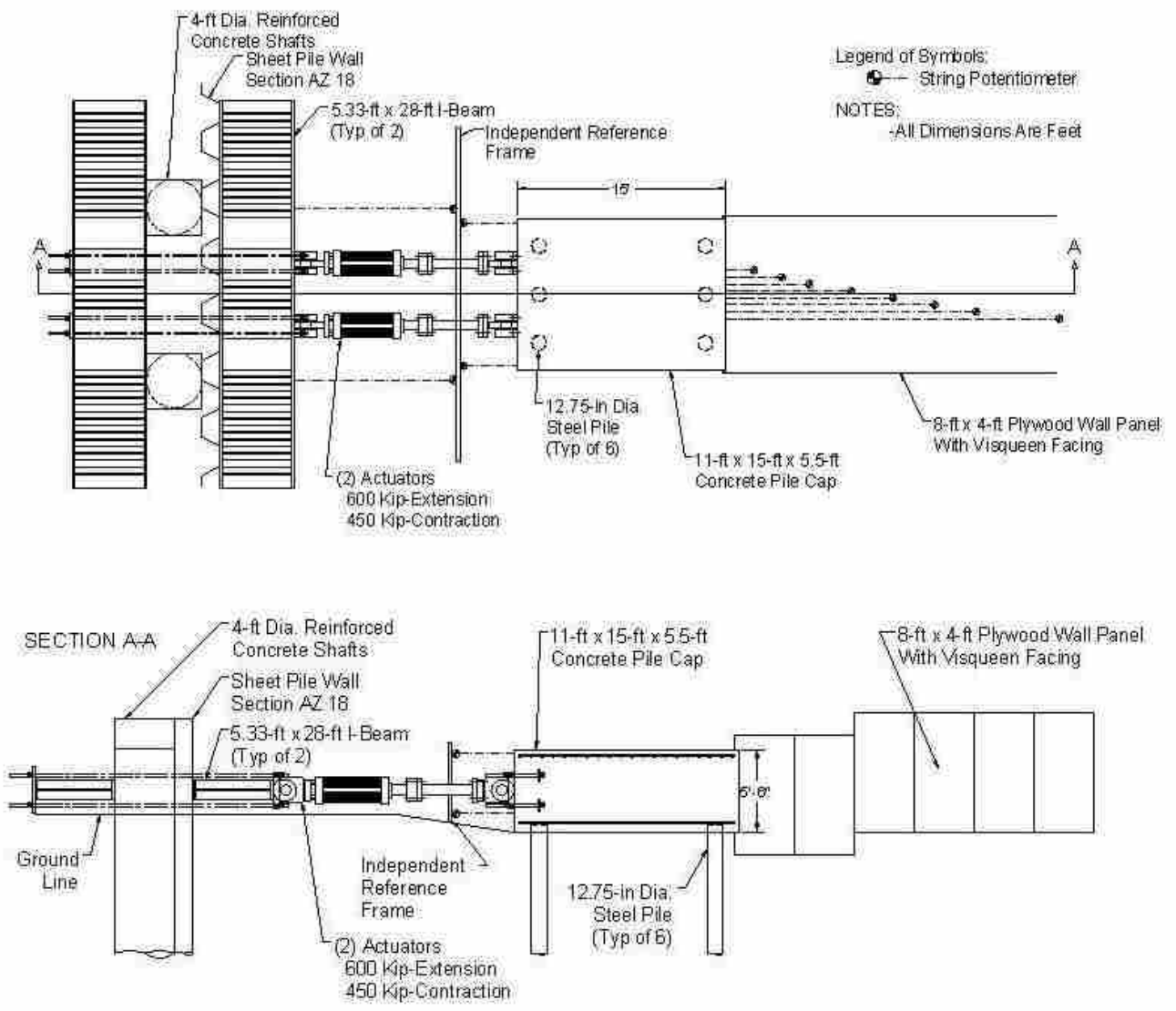

Figure 5.1: Layout of Loose Sand Slip Plane (2D) Test

5.2 Test Instrumentation and Equipment

In addition to the general instrumentation previously described in Section 3.3.5, string pots were attached to the west plywood wall just above the ground surface. A total of three string pots were attached along the first 12 ft (3.66 m) of the west wall, located at distances of approximately 2, 6, and 12 ft (0.61, 1.83, and 3.66 m) from the pile cap face. The string pots used were UniMeasure Model P1010-5-S15, with a range of 5 and 10 in., and a linearity of 0.18% of full scale. The ends of the string pots were connected to steel stakes placed beyond the backfilled area for the test to avoid any movement of the stake. The string pots monitored the outward movement of the walls during testing. Figure 5.2 shows the placement of the string pots along the wall.

Figure 5.2: Location of String Pots During Loose Sand Slip Plane (2D) Test

5.3 Test Procedures

The testing procedure followed for the loose sand slip plane (2D) test was exactly as stated previously in Section 3.5. The pile cap was loaded incrementally by the hydraulic actuators to a maximum pile cap deflection of 3.25 in. Each displacement increment increased the pile cap deflection by a target value of 0.25 in. After the maximum deflection was reached and necessary data collected, the actuators were used to pull the pile cap back into its initial unloaded condition.

5.4 Test Results

The following sections provide the results of the loose sand slip plane (2D) test. The results consist of passive force-displacement measured from the actuators, passive pressure versus depth curves, passive force-displacement measured from the pressure plates, inclinometer displacement versus depth curves, and backfill displacement data.

5.4.1 Load-Displacement Results – Actuators

Figure 5.3 plots the measured total peak actuator load versus pile cap displacement as the "total resistance." The displacement values were calculated by taking the median displacement of the four string pots attached to the pile cap at the end of each displacement increment. The maximum load recorded was 719 kips (3197 kN) at a displacement of 3.24 in. (82 mm).

The contribution of the backfill passive resistance to the total resistance was also calculated from the force-displacement data. As previously stated, the baseline resistance was subtracted from the total measured actuator load to develop the passive resistance provided by the backfill only. The baseline resistance used in the calculation for this test was that which was

also used for the unconfined (3D) test and from the baseline test conducted on 4 June 2009. Figure 5.3 plots of the backfill passive resistance and baseline resistance with the total resistance. The passive force did not exhibit a distinct peak, but continued to gradually increase with displacement throughout the test.

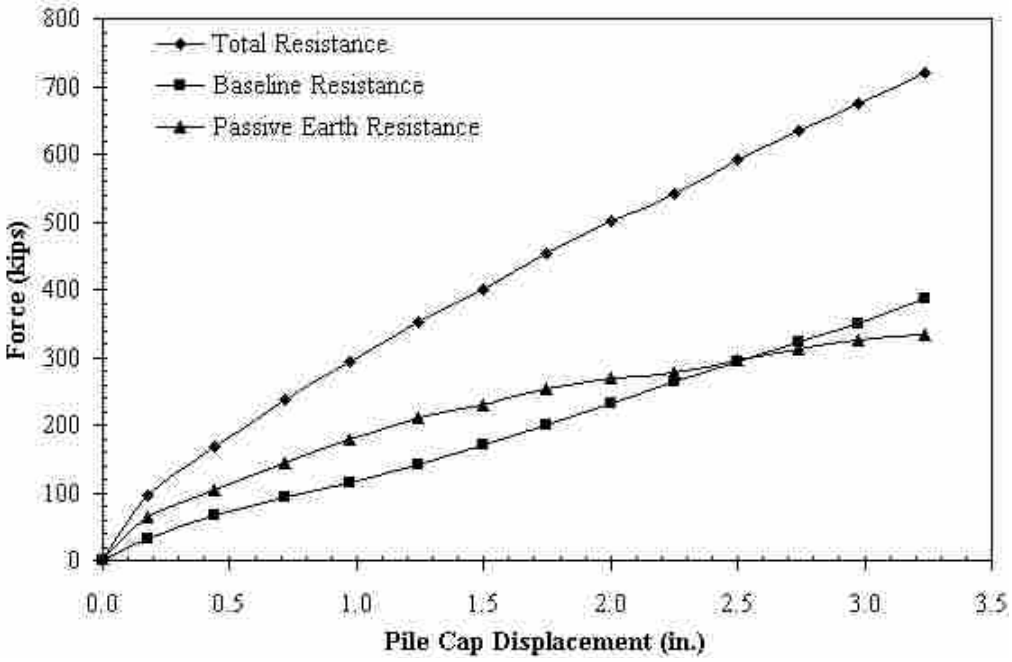

Figure 5.3: Load-Displacement Comparison For Loose Sand Slip Plane (2D) Test

5.4.2 Load-Displacement Results – Pressure Cells

To help verify the load-displacement results from the actuators described in the previous section, measurements from the pressure cells embedded in the north face of the pile cap were analyzed. During the test, pressure readings from the cells were taken continuously. Figure 5.4 shows a plot of the backfill passive pressure as a function of the depth of the pile cap at each displacement increment. The plot generally follows a trend of increasing pressure with increasing depth, but there are a few inconsistencies. For the upper three feet of the pile cap, the

pressure did not change dramatically. As the depth increased greater than three feet, the pressure increased notably. Also, at a depth of 5.05 ft (1.54 m), in Figure 5.4, the pressures recorded at this cell reached a peak value by the 1.50 in. (38 mm) increment and then proceeded to decrease until the end of the test was reached.

As explained in Section 4.2.2, the passive pressure was converted to force by multiplying the pressures by the tributary area of each pressure cell. Figure 5.5 shows a plot of the passive force from the pressure cells versus the pile cap displacement compared to the backfill passive resistance calculated from the actuators. Typically, the pressure cell passive force-displacement curves were lower than the measured passive force-displacement curves by approximately 30 to 40% due to the assumption of uniform pressure acting across the width of the pile cap. The "pressure cells with multiplier" curve, in Figure 5.5, accounts for this concern by showing what the pressure cell passive force-displacement curve looks like when multiplied by a factor of 1.33. This multiplier was lower than for the other tests. The "pressure cells with multiplier" curve is slightly above the measured passive earth resistance curve, but maintains the same general shape.

5.4.3 Inclinometer Data

Before and after each test was conducted, inclinometer readings were taken in both the north and south inclinometer tubes embedded in the pile cap. The readings measured the pile cap and pile deflection over the depth of the piles parallel to the direction of loading. Figure 5.6 shows the north and south deflection results when the pile cap reached maximum deflection during the loose slip plane (2D) test. Positive deflection values correlate with the northerly direction of loading. The zero displacement of the piles occurred at a depth of approximately 20 ft (6.10 m), which depth is about 19 pile diameters. The maximum displacement values recorded by the four string pots attached to the pile cap were also plotted. The string pot values confirm

the inclinometer results. From the inclinometer plot, it can also be seen that the pile cap experienced very little rotation during loading, typical of a fixed head boundary condition.

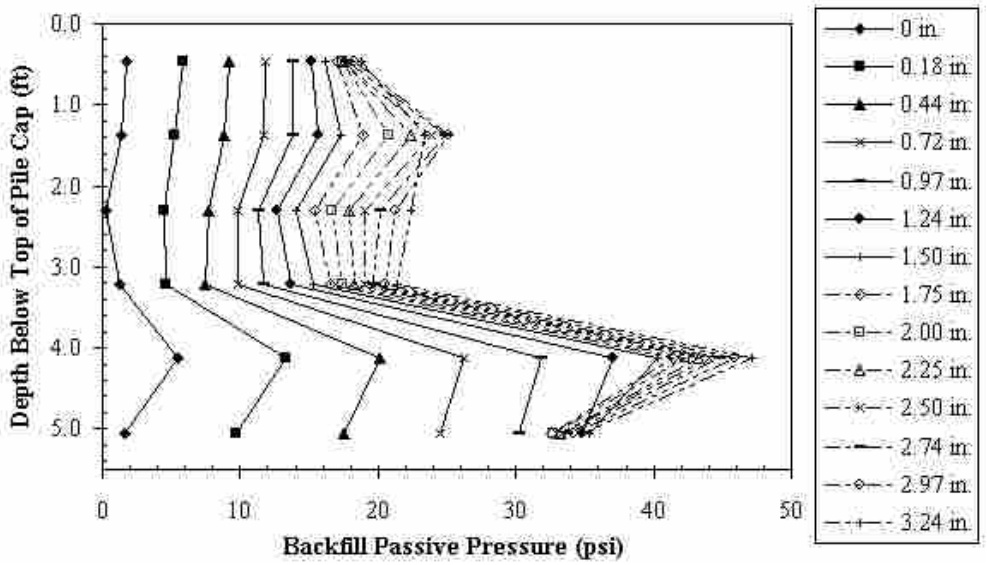

Figure 5.4: Backfill Passive Pressure Versus Depth at Each Displacement Increment for the Loose Sand Slip Plane (2D) Test

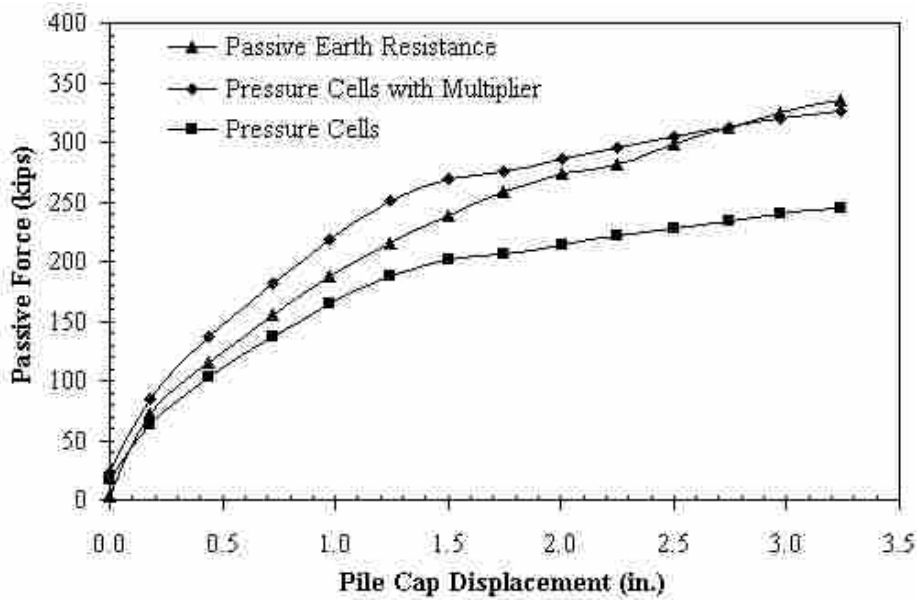

Figure 5.5: Pressure Cell Passive Resistance Compared to the Measured Passive Earth Resistance of the Loose Sand Slip Plane (2D) Test

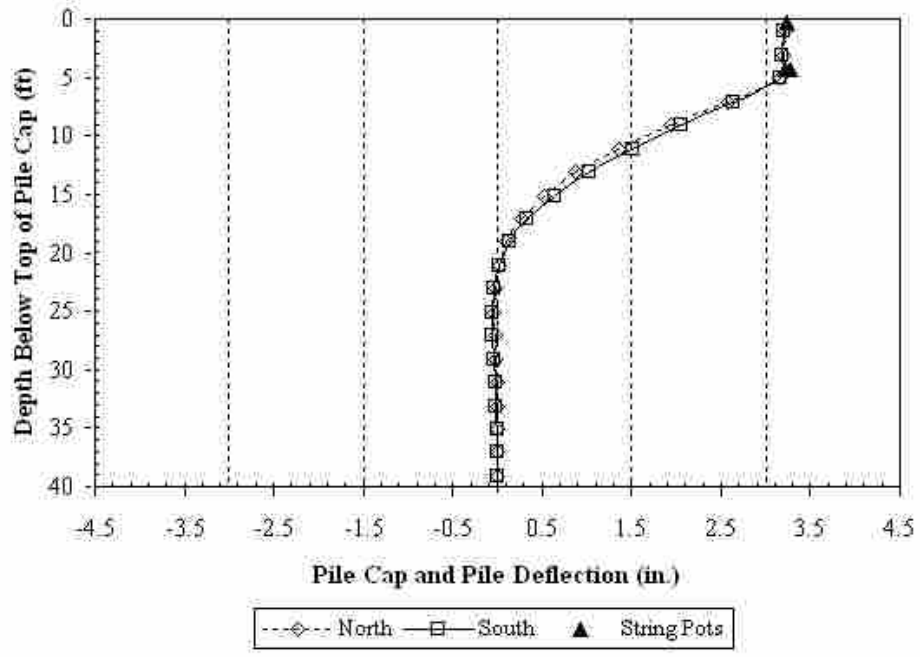

Figure 5.6: Inclinometer Readings of the Loose Sand Slip Plane (2D) Test

5.4.4 Backfill Displacement Data

During testing, the backfill displacement was monitored with string pots located in the configuration described in Section 3.3.5. Figure 5.7 shows the absolute displacement of the backfill plotted against the distance from the pile cap recorded from these string pots. To simplify the plot, backfill displacements from selected pile cap displacements increments are shown. The results of the loose slip plane test were similar to the previous loose test and show that more backfill displacement occurred close to the pile cap while at distances greater than about 10 ft (3.05 m), the material was less affected by the cap movement and little displacement occurred. The minimum horizontal displacement recorded at a distance of 24 ft (7.32 m) from the pile cap face was approximately 0.28 in. (7.1 mm). These observations can be understood by recognizing that loose sands tend to exhibit a local shear failure as compared to a general shear failure condition typical of dense sands. General shear failure would lead to movement

throughout the failure zone while local shear failure would primarily lead to movement close to the pile cap.

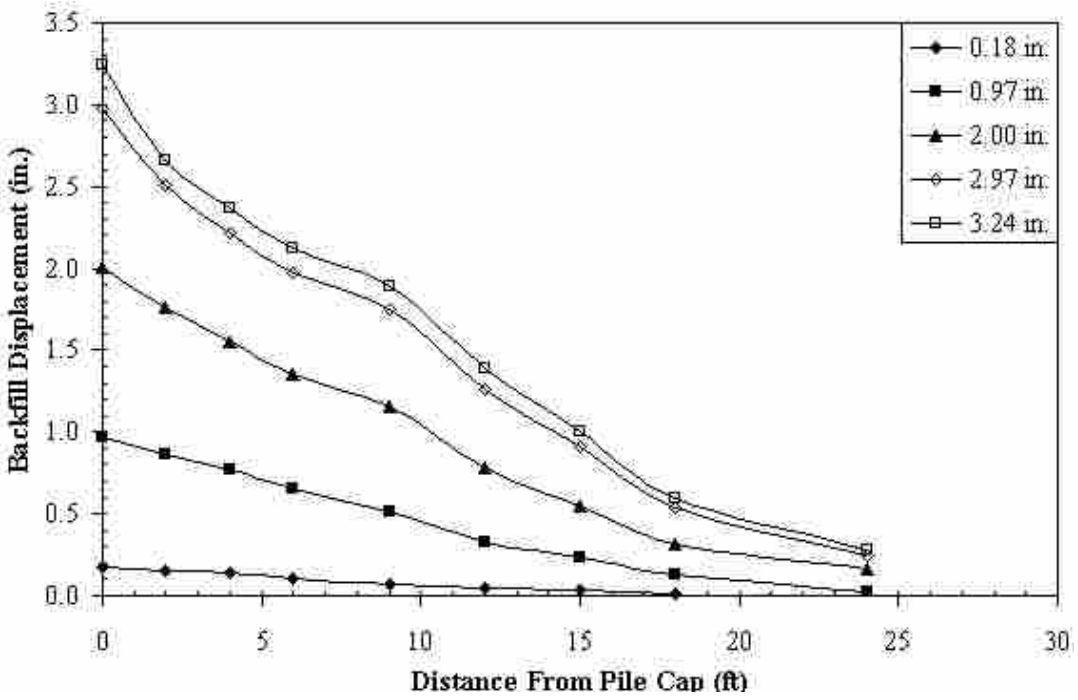

Figure 5.7: Absolute Backfill Displacement Versus Distance from the Pile Cap for the Loose Sand Slip Plane (2D) Test

From the displacement data in Figure 5.7, the longitudinal compressive strain (in./in.) was calculated for each distance between string pot stakes (i.e., 0-2 ft, 2-4 ft, 4-6 ft, 6-9 ft, etc.) with Equation 4.1, shown previously. Figure 5.8 shows the compressive strain calculation results for selected displacement intervals. Not all intervals are shown to simplify the plot. The overall trend can still be seen with the intervals plotted. The highest compressive strain rates of approximately 0.024 occur in the first two feet of backfill. The strain rates in the 9 to 18 ft (2.74 to 5.49 m) interval are similar. As the distance from the pile cap face increased, the compressive strain levels decreased.

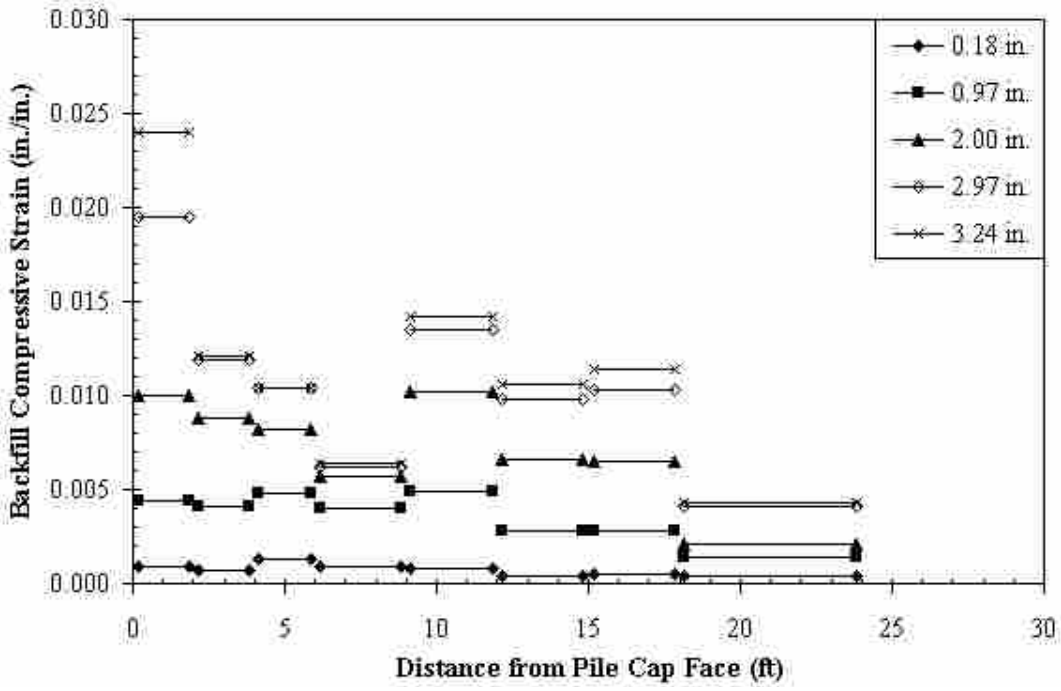

Figure 5.8: Backfill Compressive Strain for the Loose Sand Slip Plane (2D) Test

The vertical displacement of the backfill was also determined for the test. To determine vertical displacement, the elevation of the backfill grid was recorded before and after the test. The difference between the elevations showed how much the backfill displaced from the loading of the pile cap. Figure 5.9 shows a contouring of the backfill zone for the loose sand slip plane (2D) test. The maximum vertical displacement was approximately 1.75 in. (51 mm) and occurred in two locations: 4 ft (1.22 m) and 6 ft (1.83 m) from the pile cap face.

Figure 5.10 shows the crack pattern that developed in the backfill during testing. The backfill was visually inspected for cracks after each displacement increment. The most significant cracking occurred approximately 2 ft (0.61 m) from the pile cap face in between the panels after the release of the actuators. Only a small amount of cracking appeared in the first 4 ft of the backfill during loading. No cracking occurred beyond the 18-ft (5.49-m) grid line. Two

longitudinal cracks developed about 2 ft back from each wall face. This may be the boundary between the active and passive zones behind the slip plane walls.

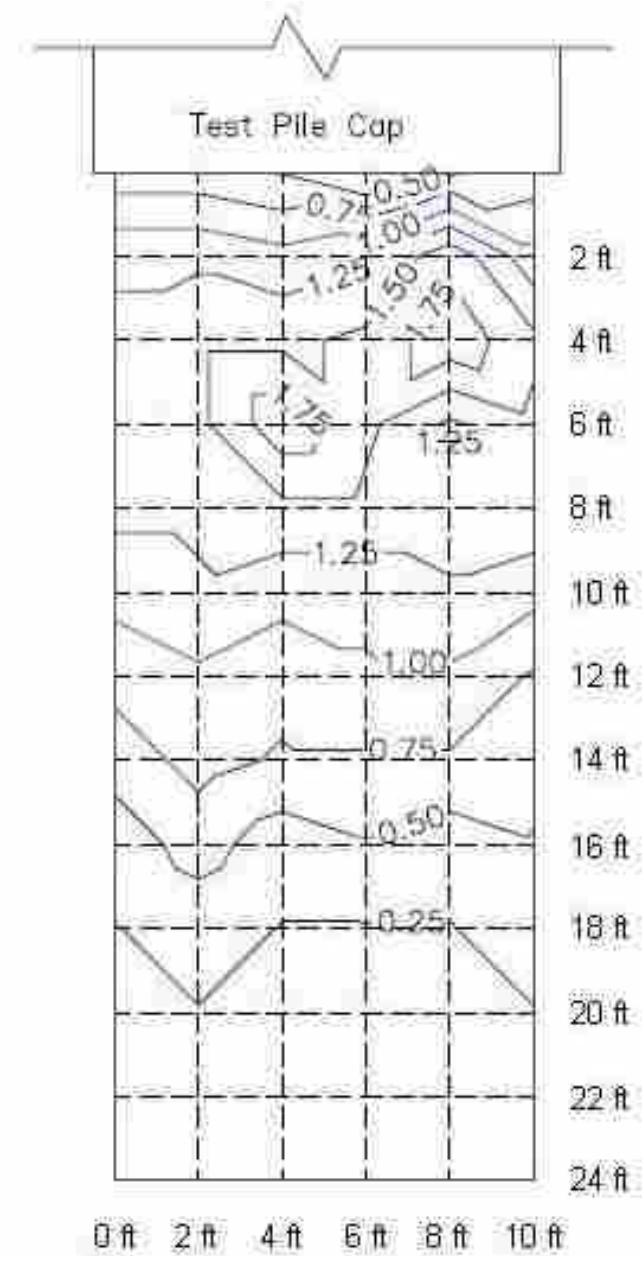

Figure 5.9: Backfill Vertical Displacement Contour of the Loose Sand Slip Plane (2D) Test

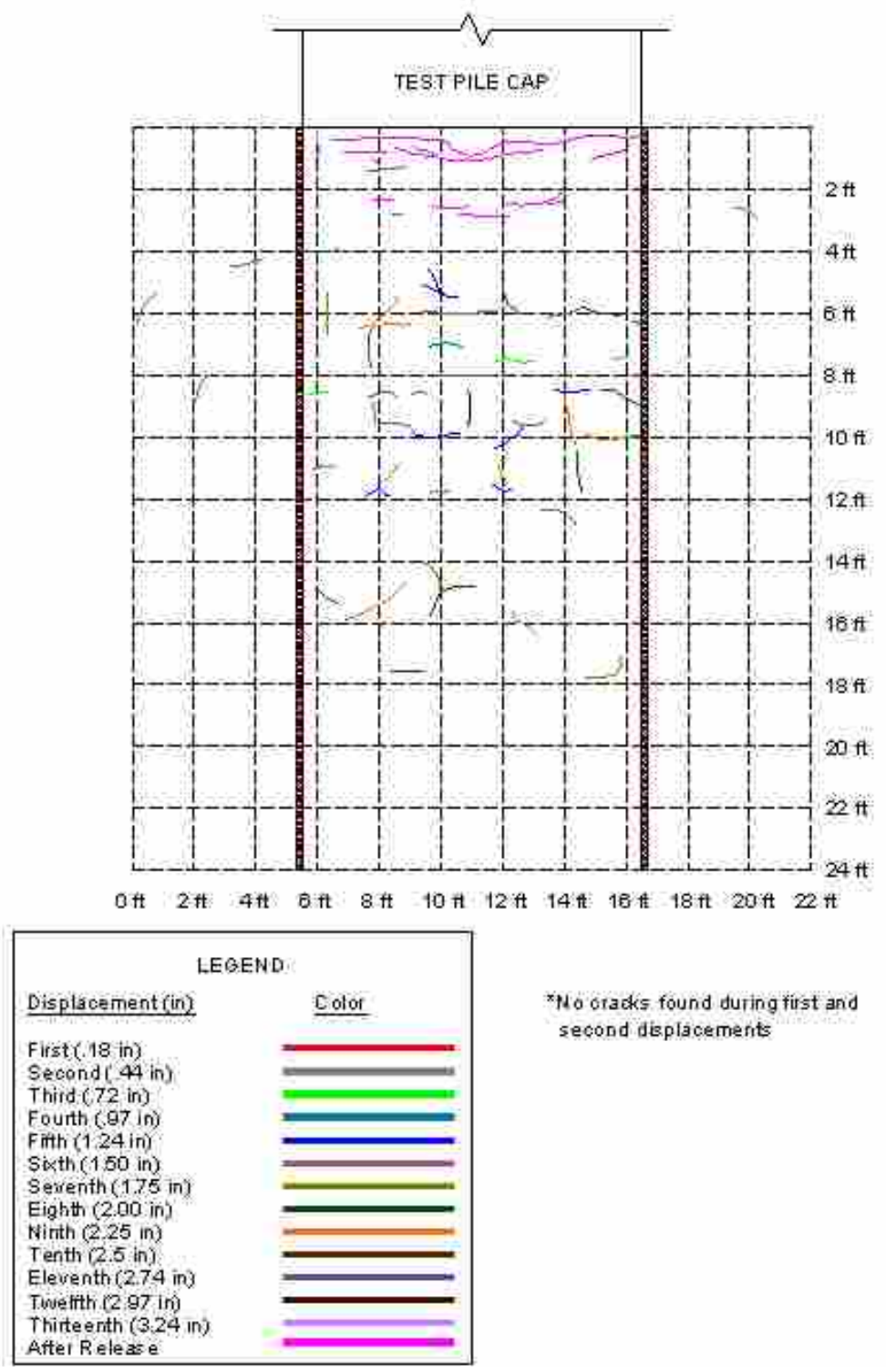

Figure 5.10: Observed Backfill Cracking During the Loose Sand Slip Plane (2D) Test

5.4.5 Transverse Wall Displacement Results

To measure the transverse deflection of the wall panels during loading of the pile cap and backfill, three string pots were attached to the outside of the west wall at locations of 2, 6, and 12 ft (0.61, 1.83, and 3.66 m) from the face of the pile cap. The string pots were located approximately 1 to 2 in. (25 to 51 mm) above the backfill surface (see Figure 5.2). Figure 5.11 shows the deflection of the wall during loading at several pile cap displacement increments. The plot viewpoint places the viewer looking west at the west wall with the pile cap on the left. The wall deflections are shown for every 0.5-in. increment, starting at the first increment until the last. The most deflection occurred at the string pot located approximately 6 ft from the pile cap face with a maximum displacement of approximately 0.16 in. (4 mm) during the final pile cap displacement increment. The wall displacements are small in relation to the scale of the test and the longitudinal backfill displacement, which allows this test to be considered similar to plane strain loading conditions. The increased lateral displacements at 6 ft appear to correlate with the longitudinal cracks which occurred at a similar distance from the pile cap face.

Figure 5.12 shows the passive force plotted against the panel displacement for each of the three string pots attached to the wall. As would be expected, the string pot the furthest from the pile cap face (12 ft) deflected the least with the increase in load. It also appears that the majority of the deflection occurred during the 0 to 275 kip (0 to 1220 kN) range. After this point, the slope of the passive force-displacement curves increased.

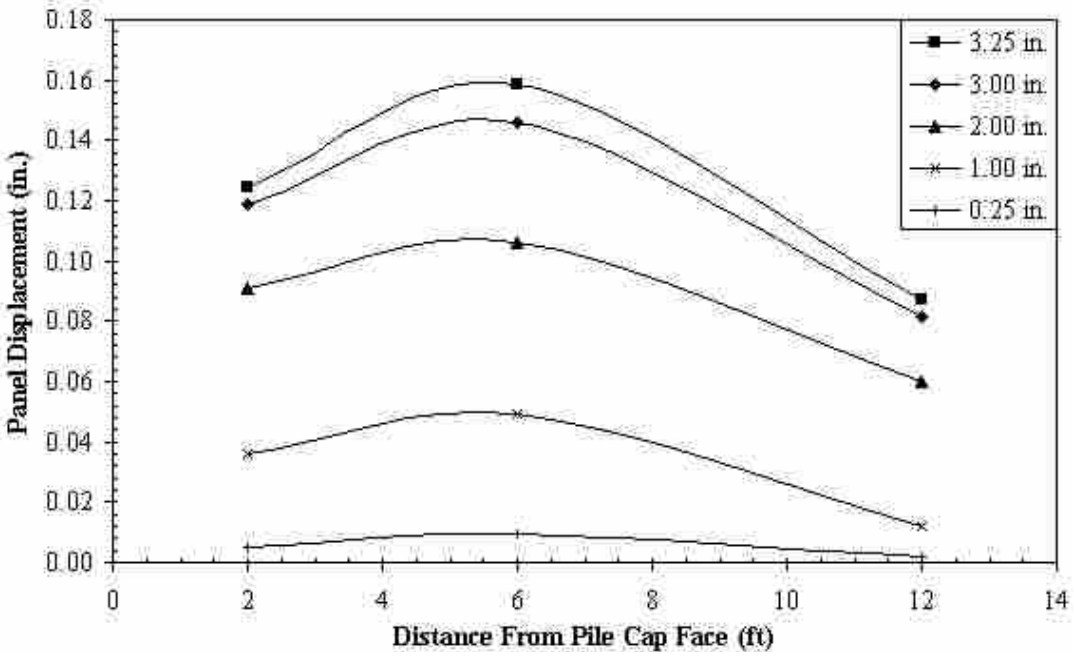

Figure 5.11: Slip Plane (2D) Panel Displacement Plot at Select Pile Cap Displacement Increments

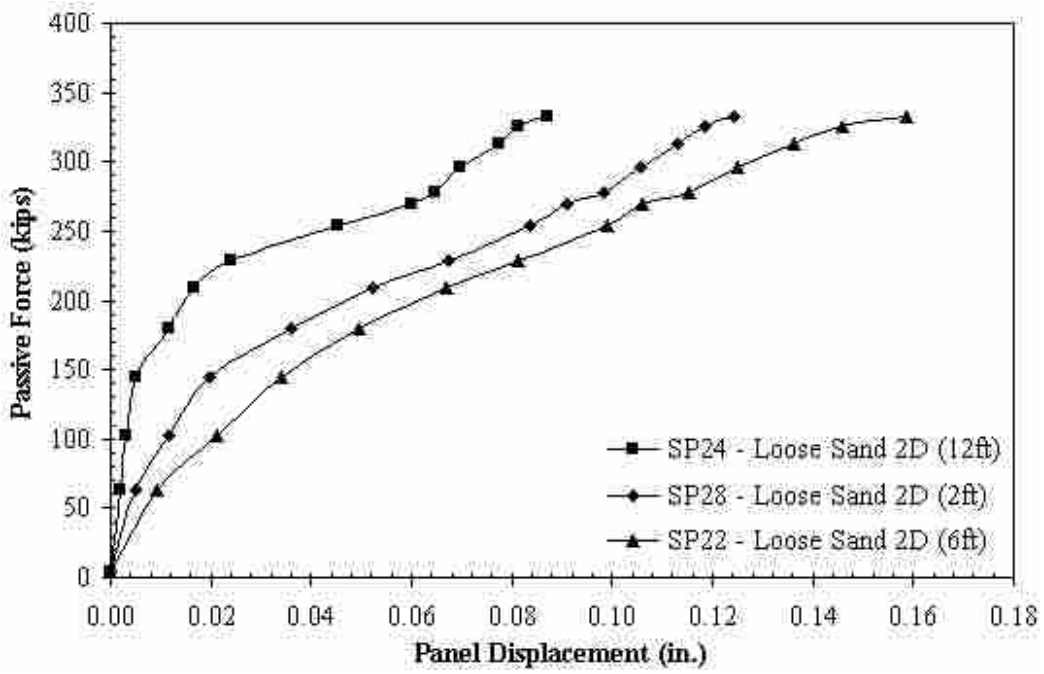

Figure 5.12: Passive Force-Panel Displacement Plot for Loose Sand Slip Plane (2D) Test

6 ABUTMENT LOAD TESTING – LOOSE SAND WITH MSE WINGWALLS

The first load test which utilized the MSE panels was conducted on 18 June 2009. This test was originally designed with an average static factor of safety against pullout of the reinforcing mats of at least 1.65. The backfill in this case was considered loosely compacted because the median dry unit weight of the soil was approximately 88% of the modified Proctor. The test layout, instrumentation, procedure, and results are described in this chapter.

6.1 Test Layout

Plan and profile views of the loose sand MSE test layout are shown in Figure 6.1. The MSE panels utilized were 12-ft (3.66-m) wide, 5-ft (1.52-m) tall, and 0.5-ft (0.152-m) thick. Two panels were placed on each side of the pile cap to create two 24-ft (7.32-m) long wingwalls. The panels were placed on three standard 4 in. x 4 in. (102 mm x 102 mm) pieces of lumber inserted into the web of a steel I-beam to provide a stable and level base for the walls. Extensions were added to the top of the MSE panels to increase the panel height to be approximately level with the top of the pile cap for a total panel height of about 5.5 ft (1.68 m). The extensions consisted of 8-ft (2.44-m) long 2 in. x 8 in. (51 mm x 203 mm) pieces of lumber.

Each MSE panel was reinforced into the backfill by four steel reinforcing mats. The two lower mats were connected to the panel at 1.22 ft (0.37 m) from the base of the panel. The two upper mats connected to the panel at a distance of 3.72 ft (1.13 m) from the base of the panel and

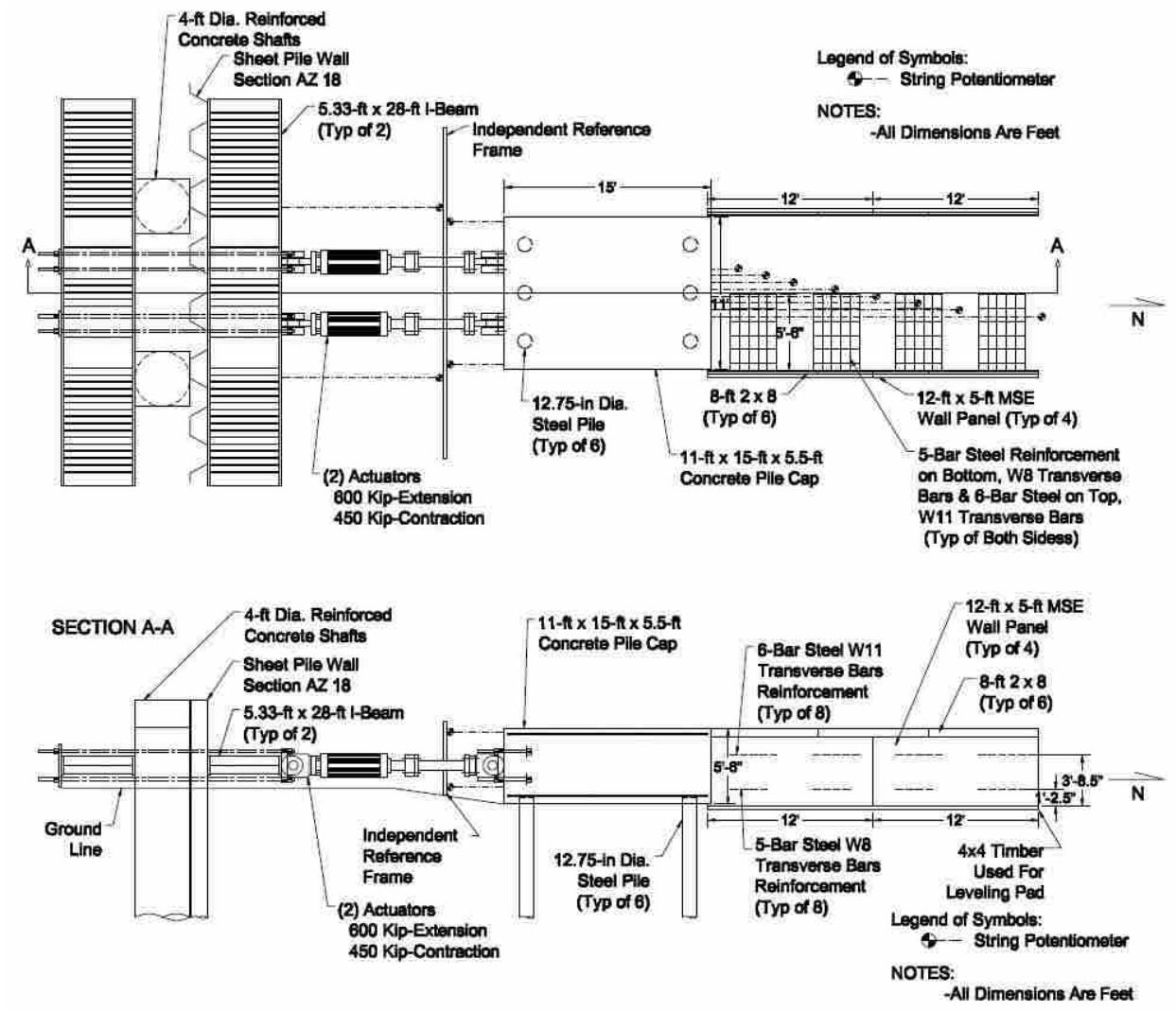

Figure 6.1: Plan and Profile Views of the Layout of Loose Sand MSE Test

2.5 ft (0.76 m) above the location of the lower mats. All eight of the lower mats were composed of five W11 longitudinal bars and W8 cross bars spaced 1 ft (0.305 m) on center. The upper mats consisted of six W20 longitudinal bars with W11 cross bars also spaced 1 ft (0.305 m) on center. The longitudinal bar spacing and total length of all the mats was 0.67 ft (0.203 m) on center and 5.5 ft (1.68 m), respectively. Figure 6.2 is a schematic of the upper and lower mats.

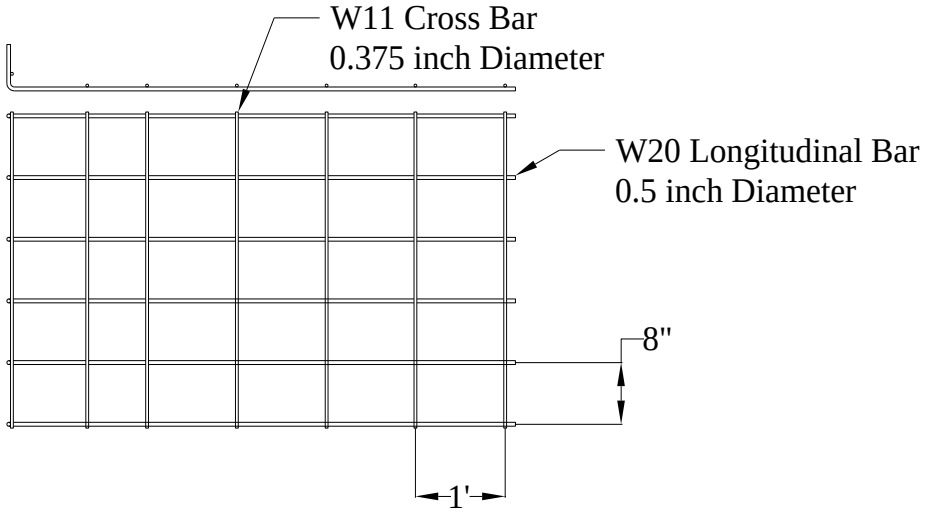

a) Upper Reinforcing Mat

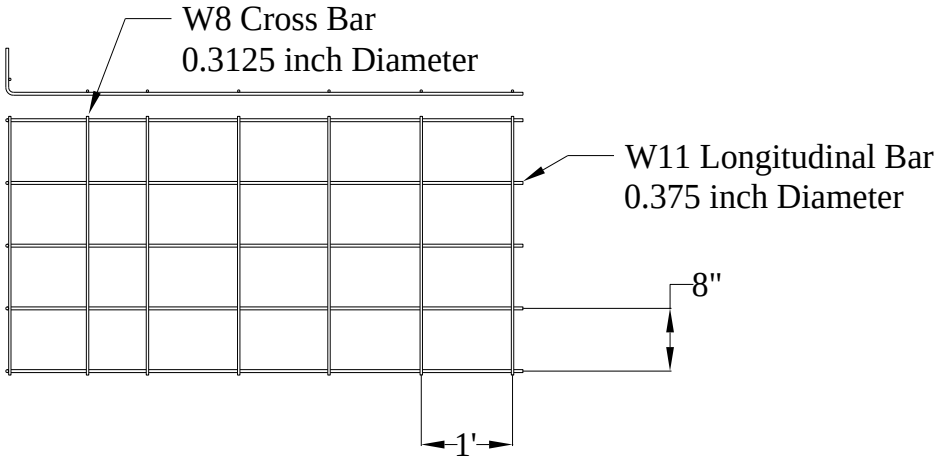

b) Lower Reinforcing Mat

Figure 6.2: Schematic of a) Upper and b) Lower Bar Mats

6.2 Test Instrumentation and Equipment

In addition to the backfill and pile cap string pots, four string pots were attached to the southeast MSE panel as shown in Figure 6.3. The string pots were UniMeasure Model P1010-5-S15 units with a range of 5 and 10 in. (127 and 254 mm) and a linearity of 0.18% of full scale. The ends of the string pots were attached to T-posts placed in the excavation and reinforced against movement with cables. Two of the string pots were located at a distance of 44 in. (1.12 m) above the bottom of the panel, approximately level with the upper bar mats. The other two string pots were located at a distance of 14 in. (0.36 m) above the bottom of the panel, approximately level with the lower bar mats. The four string pots measured MSE wall displacement and rotation throughout the test at distances of 21 in. (0.53 m) and 103 in. (2.62 m) from the pile cap face to where the center of the mats was located.

Figure 6.3: String Pot Configuration on MSE Panel for Loose Sand MSE Test

To monitor the development of load in the reinforcing mats during the test, the four bar mats connected to the southeast MSE panel were instrumented with FLA-2-11 strain gauges. The tolerance of the gauges was +/-0.85 μm/m/°C, with a gauge factor of 2.11+/-1.0%, and a coefficient of 11.8x10^-6/°C. For the bottom two mats, the strain gauges were placed on the center longitudinal bar. The top two mats had six longitudinal bars and the gauges were placed on the northern-most longitudinal bar of the two center bars. A total of sixteen gauges were affixed to each mat, located at distances of 2, 5, 9, 19.5, 28, 37, 47, and 56 in. (51, 127, 229, 495, 711, 940, 1194, and 1422 mm) from the panel face. Two gauges were placed at each location, one on the top and bottom of the bar, to reduce effects from bending.

To adhere the strain gauges to the steel bar, the following procedure was used. First, the steel bar was sanded with successively finer grit sand paper at the specified gauge locations until the protective zinc coating was removed and the surface was smoothed. Next, acetone was used to clean the bar of dust or other debris. Scotch tape was then placed next to the gauge location to prevent the exposed wires of the stain gauges from touching the steel surface once the gauges were attached. The gauges were glued to the sanded areas. After the glue had set, a non-conductive epoxy was placed on the gauges and their surrounding area to keep them in place and protect the gauges from being damaged. Lastly, the bars to which the gauges were affixed, gauges, and gauge wires were wrapped with electrical tape to keep out moisture and provide an added layer of protection to the setup.

6.3 Testing Procedure

The testing procedure followed for the loose sand MSE test was exactly as stated in Section 3.5. The pile cap was loaded incrementally by the hydraulic actuators to a maximum

pile cap deflection of about 3.25 in. Each displacement increment increased the pile cap deflection by a target value of 0.25 in. After the maximum deflection was reached and necessary data collected, the actuators were used to pull the pile cap back to its initial unloaded condition.

6.4 Test Results

The following sections provide the results of the loose sand MSE test. The results consist of passive force-displacement measured from the actuators, passive pressure versus depth curves, passive force-displacement measured from the pressure plates, inclinometer displacement versus depth curves, and backfill displacement data.

6.4.1 Load-Displacement Results – Actuators

Figure 6.4 plots the measured total peak actuator load versus pile cap displacement as the "total resistance." The displacement values were calculated by taking the median displacement of the four string pots attached to the pile cap at the end of each displacement increment. The maximum load recorded was 708 kips (3151 kN) at a displacement of 3.16 in. (80 mm).

The contribution of the backfill passive resistance to the total resistance was calculated from the load-displacement data collected. As previously stated, the baseline resistance was subtracted from the total measured actuator load to develop the passive resistance provided by the backfill only. Figure 6.4 plots of the backfill passive resistance and baseline resistance in comparison with the total resistance. As seen in previous tests, the passive force did not exhibit a distinct peak, but continued to gradually increase with displacement throughout the test.

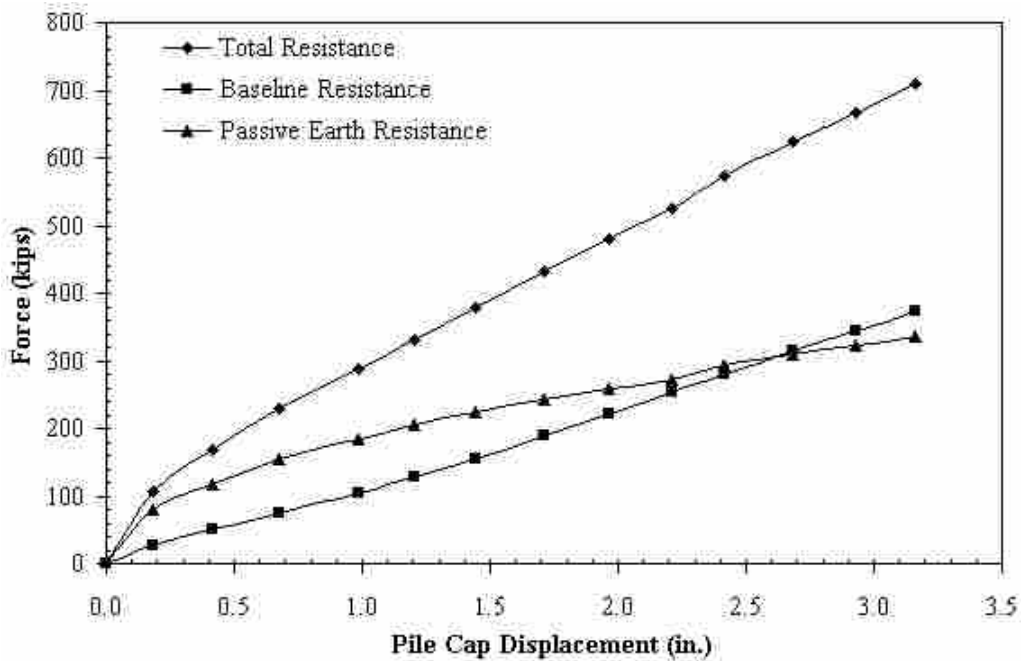

Figure 6.4: Force-Displacement Comparison For Loose Sand MSE Test

6.4.2 Load-Displacement Results – Pressure Cells

To help verify the load-displacement results from the actuators described in the previous section, measurements from the pressure cells embedded in the north face of the pile cap were analyzed. During the test, pressure readings from the cells were taken continuously. Figure 6.5 shows a plot of the backfill passive pressure as a function of the depth of the pile cap at each displacement increment. The plot generally follows a trend of increasing pressure with increasing depth, but there are a few inconsistencies. Notable increases and decreases in pressure occurred across the full range of depth. Also, at a depth of 1.38 ft (0.42 m), in Figure 6.5, the pressures recorded at this cell reached a peak value by the 1.44 in. (37 mm) increment and then proceeded to decrease until the end of the test was reached.

As explained in Section 4.2.2, the passive pressure readings were converted to force by multiplying the pressures by the tributary area of each pressure cell. Figure 6.6 shows a plot of

the pressure cell passive force versus the pile cap displacement compared to the backfill passive resistance calculated from the actuators. Typically, the pressure cell passive force-displacement curves were lower than the actuator load-displacement curves by approximately 30 to 40% due to the assumption of uniform pressure acting across the width of the pile cap. The "pressure cells with multiplier" curve, in Figure 6.6, accounts for this concern by showing what the load-displacement curve looks like when multiplied by a factor of 1.67. The "pressure cells with multiplier" curve shows an increased initial stiffness during the first portion of the curve. However, the maximum measured passive force measured from the actuators is approximately 50 kips (226 kN) greater than the maximum pressure cell passive force.

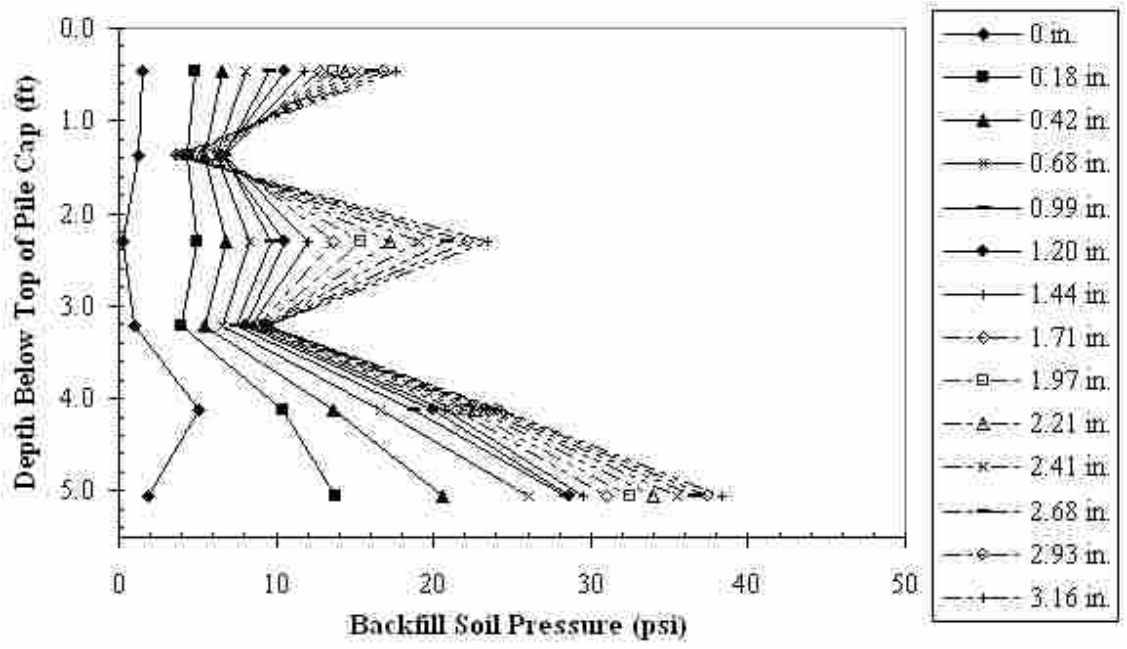

Figure 6.5: Backfill Passive Pressure Versus Depth at Each Displacement Increment for the Loose Sand MSE Test

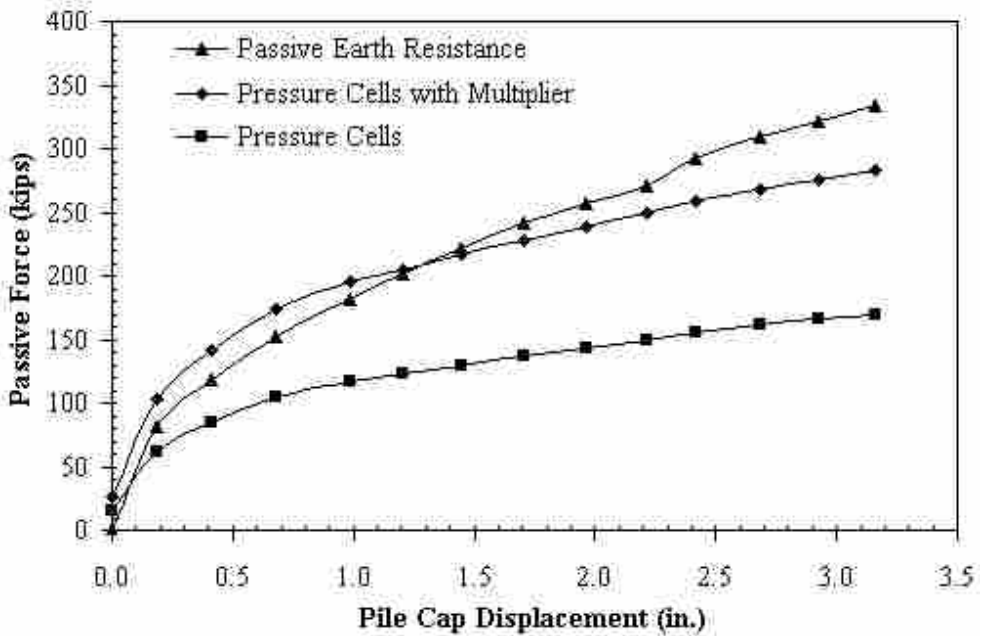

Figure 6.6: Pressure Cell Passive Resistance Compared to the Measured Passive Earth Resistance of the Loose Sand MSE Test

6.4.3 Inclinometer Data Results

Before and after each test was conducted, inclinometer readings were taken in both the north and south inclinometer tubes embedded in the pile cap. The readings measured the pile cap and pile deflection over the depth of the piles parallel to the direction of loading. Figure 6.7 shows the north and south deflection results when the pile cap reached maximum deflection during the loose sand MSE test. Positive deflection values correlate with the northerly direction of loading. The zero displacement of the piles occurred at a depth of approximately 20 ft (6.10 m), which depth is about 19 pile diameters. The maximum displacement values recorded by the four string pots attached to the pile cap are also plotted. The string pot values confirm the inclinometer results. From the inclinometer plot, it can also be seen that the pile cap experienced very little rotation during loading, typical of a fixed head boundary condition.

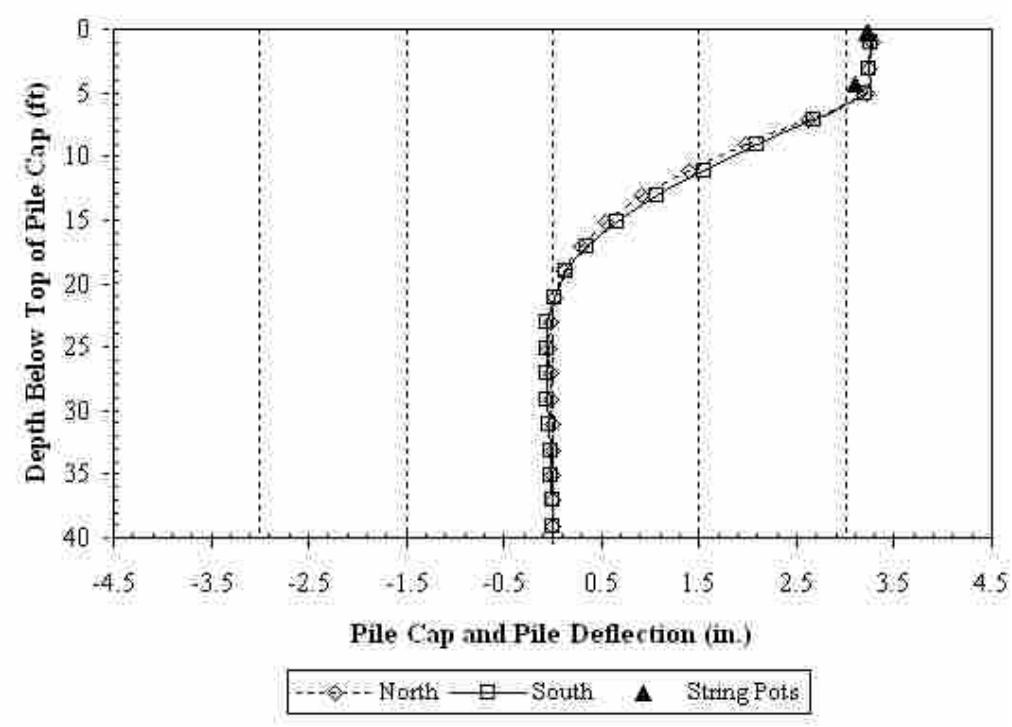

Figure 6.7: Inclinometer Readings of the Loose Sand MSE Test

6.4.4 Backfill Displacement Results

During testing, the backfill displacement was monitored with string pots located in the configuration described previously in Section 3.3.5. Figure 6.8 shows the absolute displacement of the backfill plotted against the distance from the pile cap recorded from these string pots. To simplify the plot, backfill displacements from selected pile cap displacements increments are shown. The results of the loose MSE test were similar to the two previous loose tests and show that more backfill displacement occurred close to the pile cap while at distances greater than about 10 ft (3.05 m), the material was less affected by the cap movement and little displacement occurred. The minimum horizontal displacement recorded at a distance of 24 ft (7.32 m) from the pile cap face was approximately 0.28 in. (7.1 mm). These observations can be understood by recognizing that loose sands tend to exhibit a local shear failure as compared to a general shear

failure condition typical of dense sands. General shear failure would lead to movement throughout the failure zone while local shear failure would primarily lead to movement close to the pile cap.

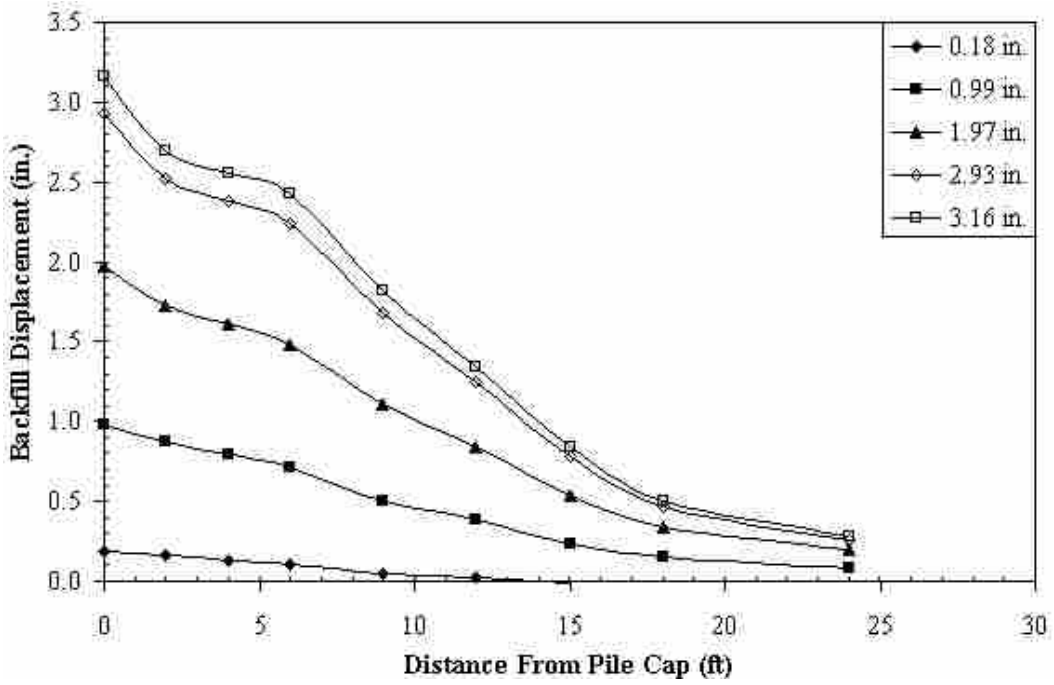

Figure 6.8: Absolute Backfill Displacement Versus Distance from the Pile Cap for the Loose Sand MSE Test

From the displacement data in Figure 6.8, the longitudinal compressive strain (in./in.) was calculated for each distance between string pot stakes (i.e., 0-2 ft, 2-4 ft, 4-6 ft, 6-9 ft, etc.) with Equation 4.1, shown previously. Figure 6.9 shows the compressive strain calculation results for selected displacement intervals. Not all intervals are shown to simplify the plot. The overall trend can still be seen with the intervals plotted. The highest compressive strain rates occur in the first two feet of backfill. The strain rates in the 2 to 6 ft (0.61 to 1.83 m) range are similar. As the distance from the pile cap face increases, the compressive strain levels decrease.

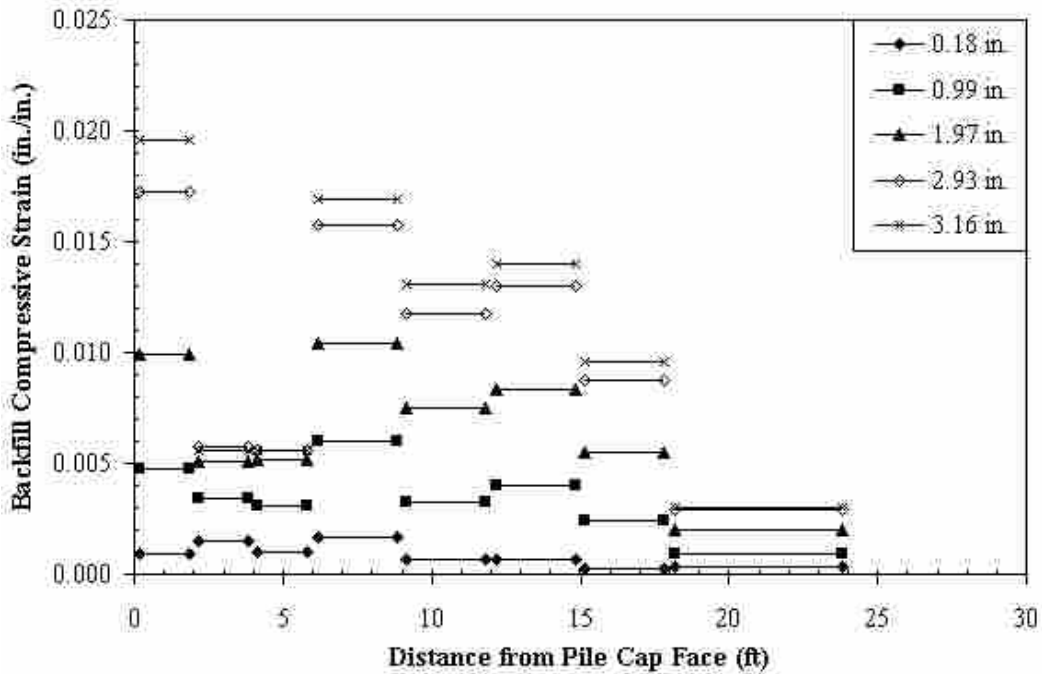

Figure 6.9: Backfill Compressive Strain for the Loose Sand MSE Test

The vertical displacement of the backfill was also determined for the test. To determine vertical displacement, the elevation of the backfill grid was recorded before and after the test. The difference between the elevations showed how much the backfill displaced from the loading of the pile cap. Figure 6.10 shows a contouring of the backfill zone for the loose sand MSE test. The maximum vertical displacement was approximately 1.0 in. (25.4 mm) occurring along the MSE walls between 2 to 6 ft (0.61 to 1.83 m) from the pile cap face. Minute amounts of heave were seen beyond the 16-ft grid line.

Figure 6.11 shows the crack pattern that developed in the backfill during testing. The backfill was visually inspected for cracks after each displacement increment. The most significant cracking occurred approximately 2 ft (0.61 m) from the pile cap face in between the panels after the actuators were released. Only a small amount of cracking appeared in the first 4 ft (1.22 m) of the backfill during loading. The majority of cracking during loading occurred

approximately 4 to 8 ft (1.22 to 2.44 m) from the pile cap face. No cracking occurred beyond the 16-ft grid line.

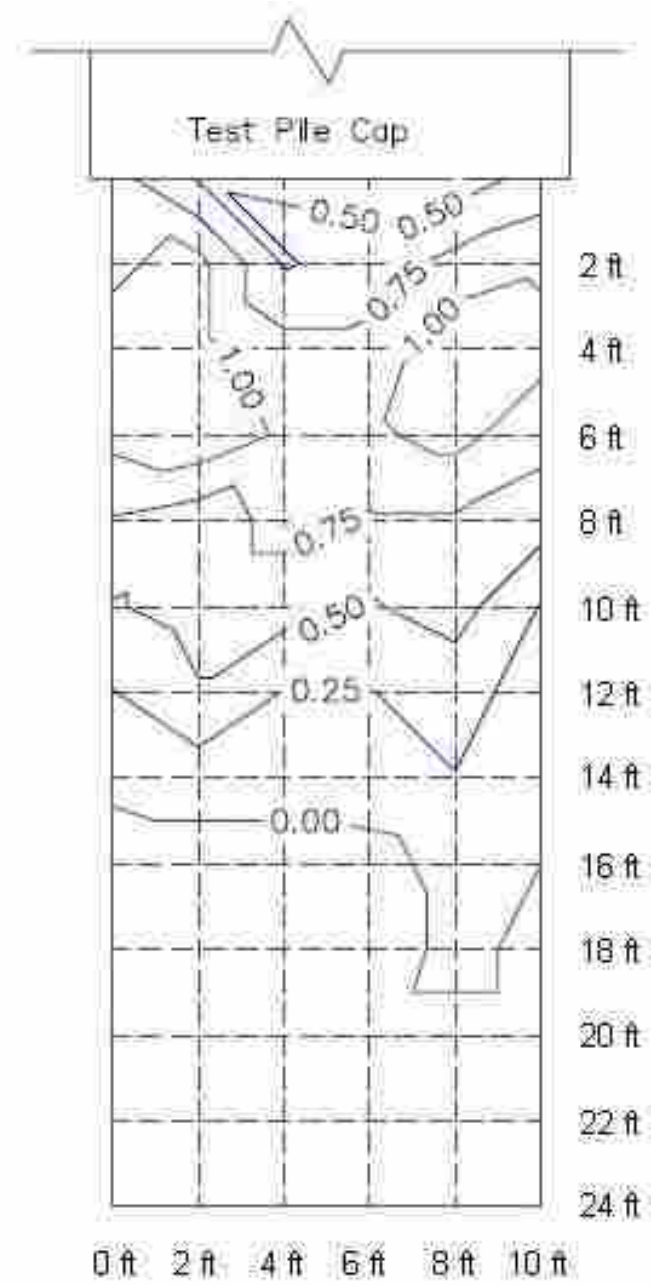

Figure 6.10: Backfill Vertical Displacement Contour of the Loose Sand MSE Test

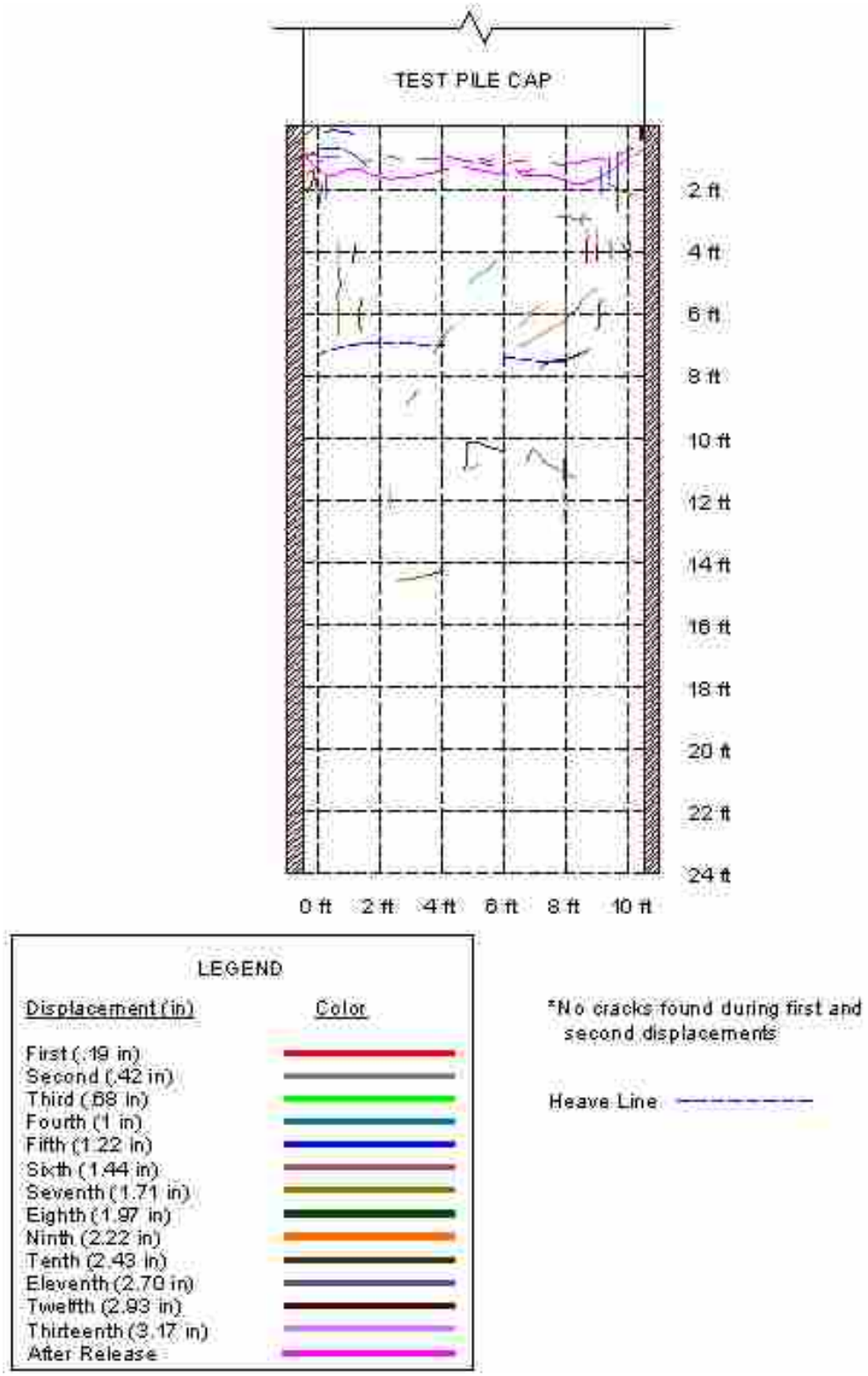

Figure 6.11: Observed Backfill Cracking During the Loose Sand MSE Test

6.4.5 Transverse Wingwall Displacement Results

As mentioned in Section 6.2, to monitor the MSE wingwall movement during the tests, four string pots were attached to the southeast MSE panel. Figure 6.12 a) and b) are plots of the transverse MSE wingwall movement recorded during testing from both sets of string pots located 21 in., or 1.75 ft (0.53 m), and 103 in., or 8.58 ft (2.62 m), from the pile cap face. The data were extrapolated linearly to show the total movement of the wingwall from top to bottom. The markers on each line represent the location of the string pots. Each line shows the movement of the wingwall for each 0.25-in. displacement increment. As seen from the plots, the panels appear to have rotated during the test. Some rotation was expected because the shallow upper bar mats carried less load than the deep lower bar mats. Since the lower mats were placed deeper in the backfill, a greater soil weight was transferred to the mats preventing the wingwall from rotating as depth increased.

In Figure 6.12 a), the values of the string pot located at a depth of 52 in. were modified due to some irregularities in the string pot measurements. After the 1-in. displacement increment, the string pot measurement values increased dramatically until the 3-in. increment was reach. At this point the measurement decreased to a value which followed the original trend produced by the string pot. Therefore, the displacement measurements from the 1.25-in. to the 2.75-in. increments were interpolated based on the displacement trend from the previous and subsequent displacement increments. Figure 6.12 a) reflects the interpolated values for the string pot at a depth of 52 in. The other string pot located at the same distance from the pile cap face experienced no issues during the test.

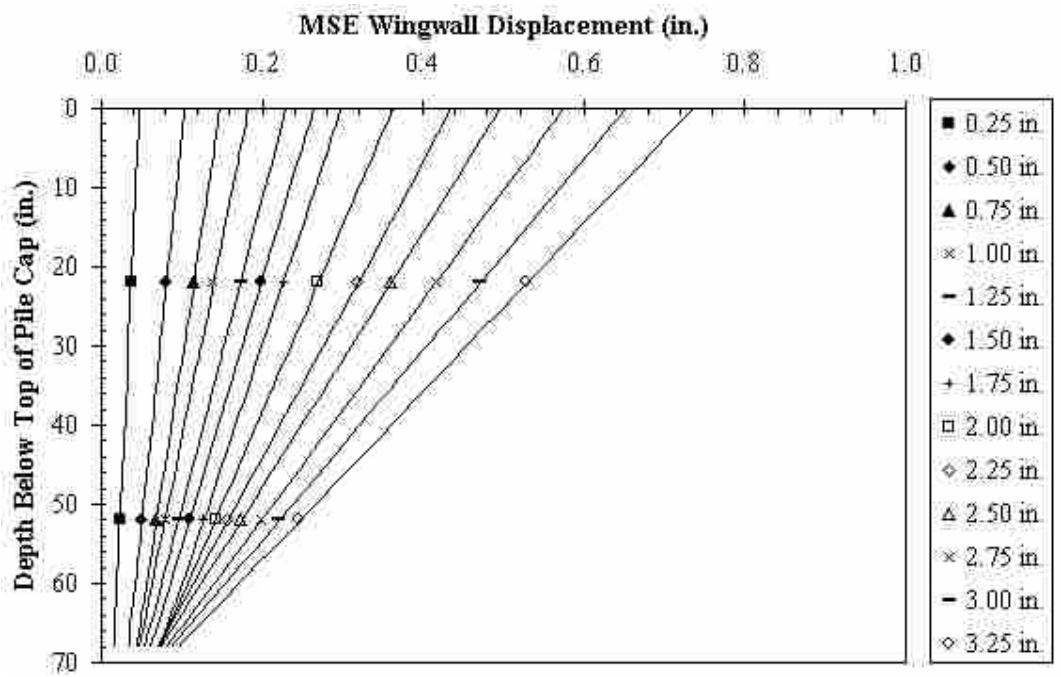

a) Distance of 21 in. From the Pile Cap Face (Modified)

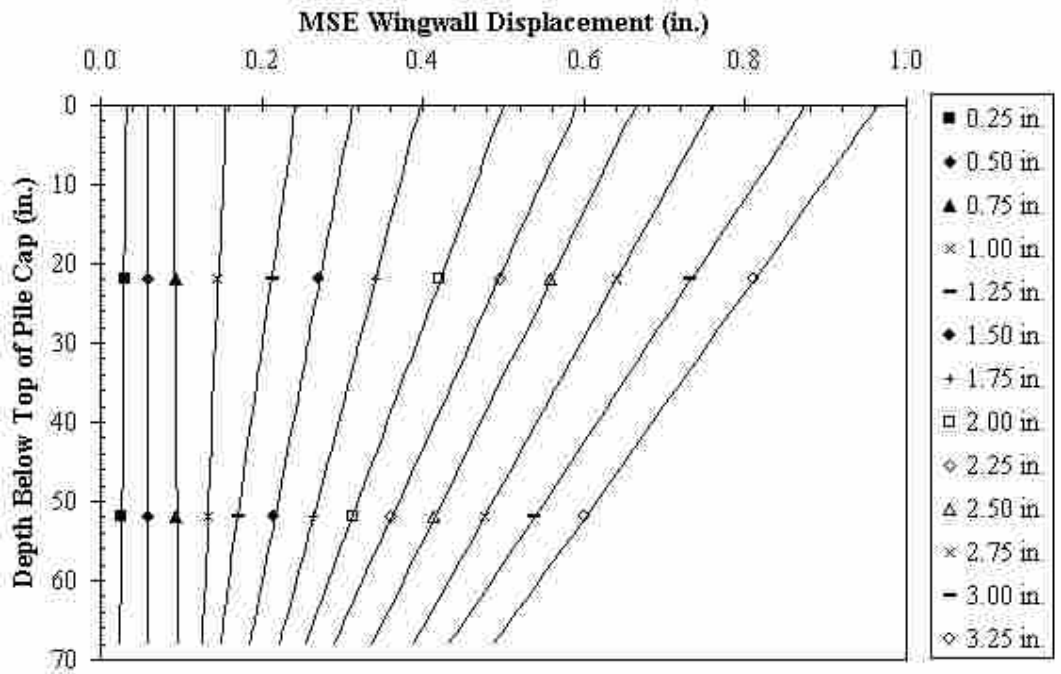

b) Distance of 103 in. From the Pile Cap Face

Figure 6.12: Outward MSE Wingwall Displacement per Pile Cap Displacement Increment for Loose Sand MSE Test

The graph in Figure 6.13 shows the MSE wingwall rotation plotted against the passive force at the location of both sets of string pots. The overall trend shows that as the passive force increased, the rotation of the wingwall also increased. For the data representing the string pots located 103 in. from the pile cap face, there appeared to be some small initial movement of the wingwalls after the first displacement increment. This may be an initial deformation response of the MSE panels.

Figure 6.14 presents the transverse movement of the MSE wingwalls from an aerial prospective. Data were collected at each 0.25-in. displacement increment. However, to simplify the plot, data are only shown for every 0.50 in. of pile cap displacement. The markers in the plot represent the location of the top string pots. From the plot, it can be seen that as the distance from the pile cap face increased, the amount of outward movement increased.

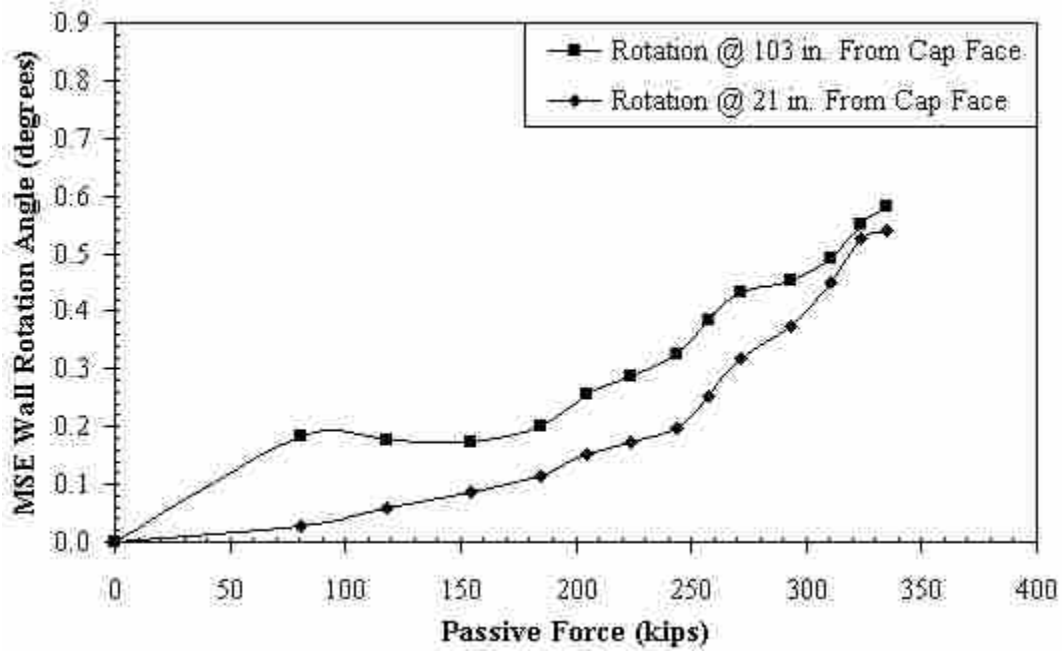

Figure 6.13: MSE Wingwall Rotation-Passive Force Plot for Loose Sand MSE Test

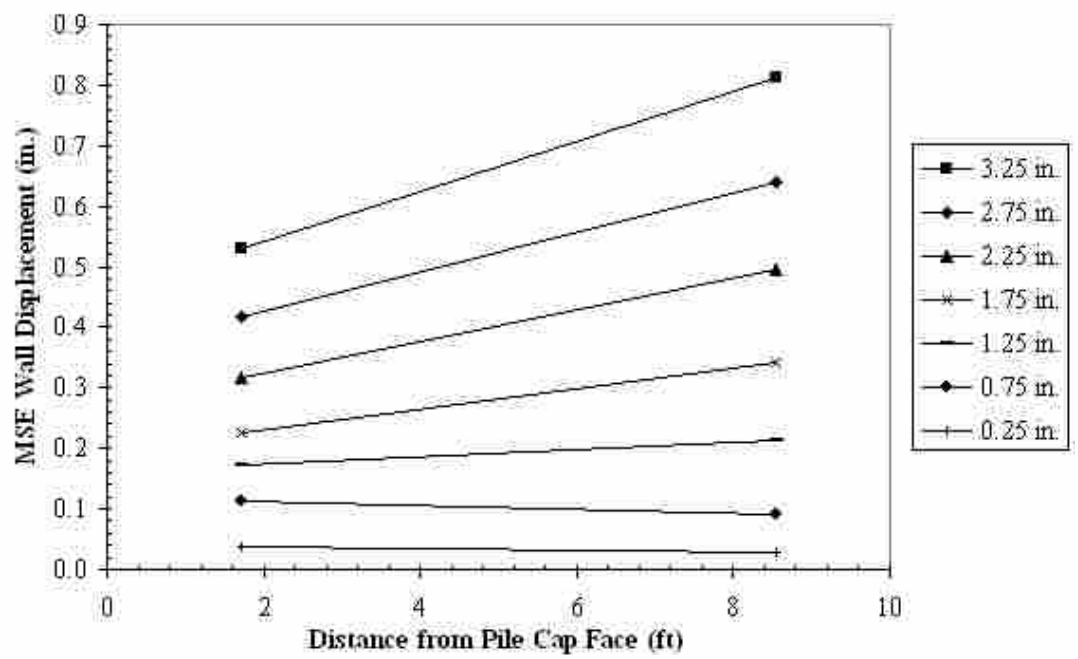

Figure 6.14: Transverse MSE Wingwall Displacement of the Top String Pots for Loose Sand MSE Test

Figure 6.15 and Figure 6.16 also provide a look at how the wingwalls displaced in regards to passive force and the pile cap displacement. The graphs show the wingwall response at both the 21 in. and 103 in. distances from the pile cap face. The displacements plotted represent the movement of the very top of the MSE wingwalls, which was extrapolated from the string pot measurements. The trends show from the concave shapes of the plots that as the passive force increased, the wingwall displacement increased. If this trend continued, eventually a peak passive force would be reached and "failure," or severe displacements of the wingwalls, would occur. For MSE wingwalls, failure occurs when the reinforcing mats start pulling out of the backfill at large displacement levels per displacement increment.

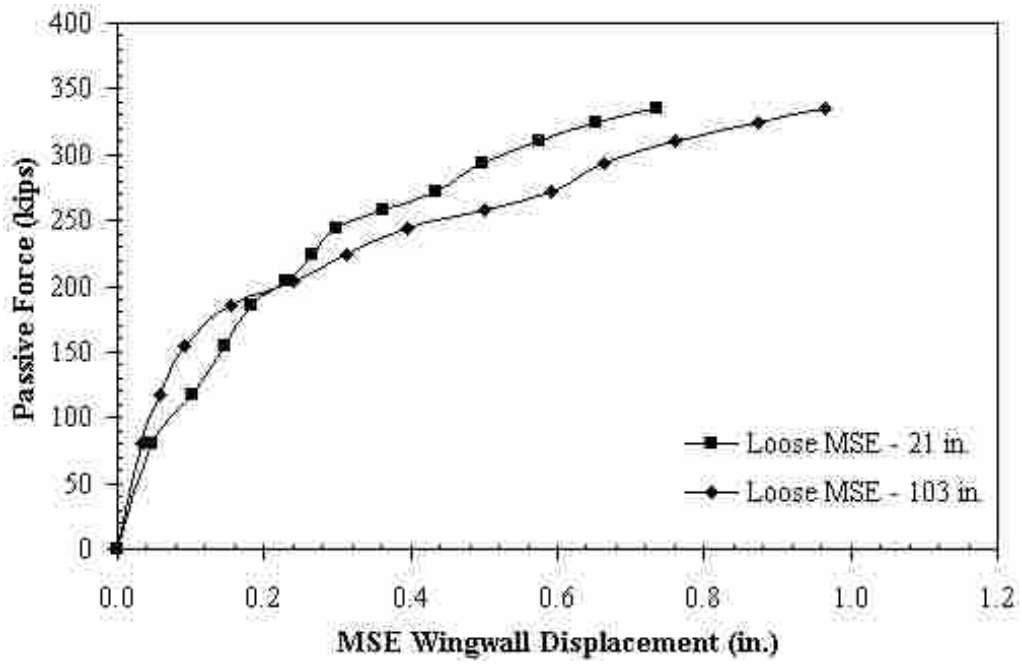

Figure 6.15: Outward MSE Wingwall Displacement-Passive Force Plot for Loose Sand MSE Test

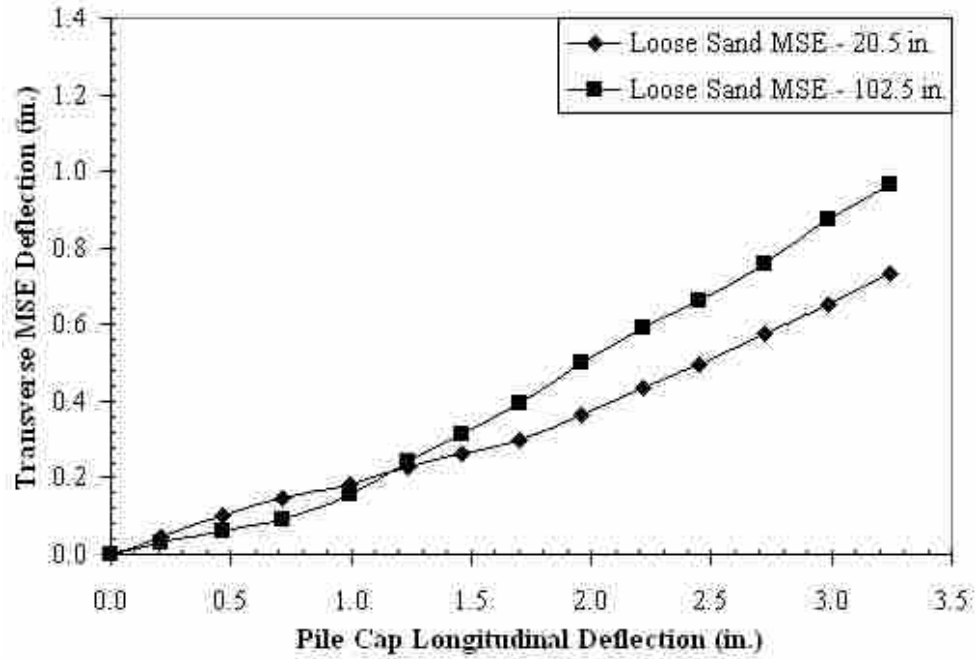

Figure 6.16: MSE Wingwall Displacement-Pile Cap Displacement Plot for Loose Sand MSE Test

6.4.6 Reinforcing Mat Load Results

As stated in Section 6.2, strain gauges were attached to the reinforcing mats used in conjunction with the MSE panels to monitor the development of load in the mats. The mat loads calculated were then compared to the displacement of the MSE wingwalls to develop load-deflection curves for the bar mats. These load-deflection curves provided a reasonable means of detecting the capacity of the walls before failure occurred.

To calculate the force in a reinforcing mat, the strain data collected from each set of strain gauges (meaning, the top and bottom strain gauges at a given distance from the MSE panel face) was used in the following equation, Equation 6.1:

$$F = \bar{\varepsilon} * E * A * B \qquad \textbf{(6.1)}$$

where

F = total force in the reinforcing mat, kips

$\bar{\varepsilon}$ = average strain of a set of strain gauges, in./in.

E = modulus of elasticity of steel, 29000 ksi

A = cross-sectional area of one longitudinal bar, in.^{2}

B = n – 1

n = number of longitudinal bars of a mat.

The outermost longitudinal bars of a mat only provided half of the tributary area that an inner bar provided, thus B in the equation above subtracts one from the total number of longitudinal bars of a mat. The average strain, $\bar{\varepsilon}$, in the above equation, considered the strain recorded during construction of the backfill and during the load test. As the test setup was completed, an initial

strain was placed on the mats from the backfill material. This was accounted for when computing the total load, *F*, in each reinforcing mat by including the measured initial strain with that measured during the load test.

Figure 6.17 and Figure 6.18 are plots of the total force calculated in the bar mats along the entire length of each mat compared to the ultimate pullout forces calculated at specific displacement increments. Each marker in the plots represents the location of a set of strain gauges. Due to the sensitivity and reliability of the strain gauges, not all data collected from the strain gauges were useful. If data from a specific set of gauges were deemed inaccurate, the marker representing that set was removed from the plot and the curve was continued between the accepted values. The graphs which plot data from the upper reinforcing mats placed at a depth of 1.83 ft (0.56 m) below the top of the pile cap are referred to as "top." Graphs which plot data from the lower reinforcing mats placed at a depth of 4.33 ft (1.32 m) below the top of the pile cap are referred to as "bottom." The center longitudinal bar of the mats described as "near cap" were located at a distance of approximately 3 ft (0.91 m) from the pile cap face while the center longitudinal bar of the mats described as "away from cap" were located at a distance of approximately 9 ft (2.74 m) from the pile cap face.

The strain gauges located in the 2 to 9 in. (51 to 229 mm) range were the most inconsistent in providing reasonable measurements. Because these gauges were located at a short distance from the MSE panel face, bending effects (evident in the rotation of the wall panels) or damage during construction may have affected the accuracy of the gauges. The gauges located at 2 in. (51 mm) from the panel face were especially susceptible to construction damage from the pins used to secure the reinforcing mats to the MSE panels.

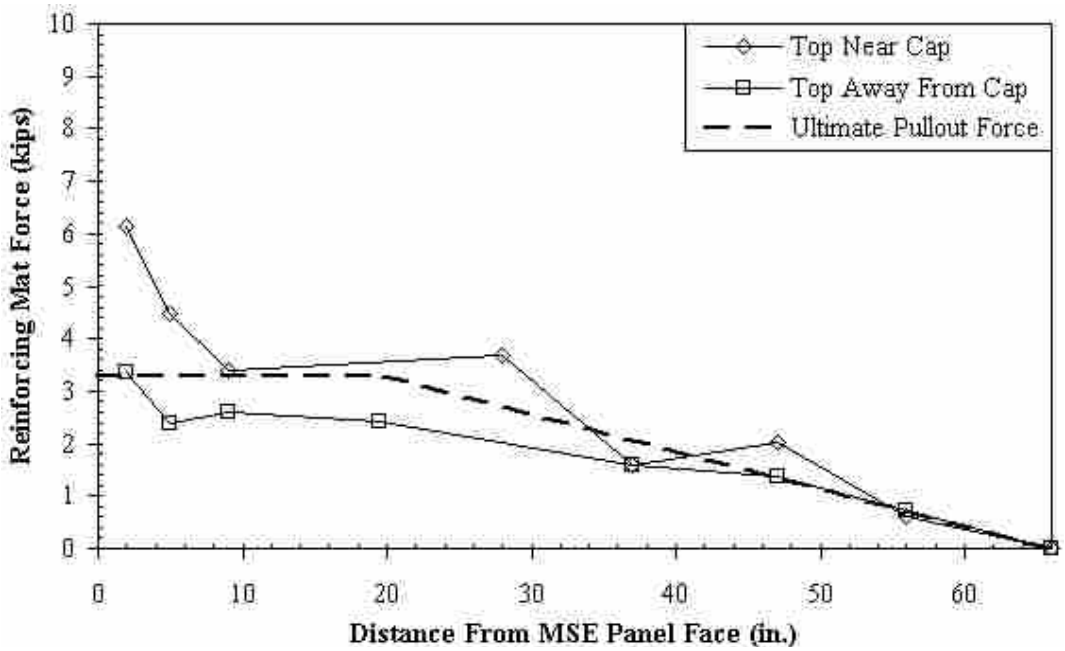

a) 0.5-in. Pile Cap Displacement Increment

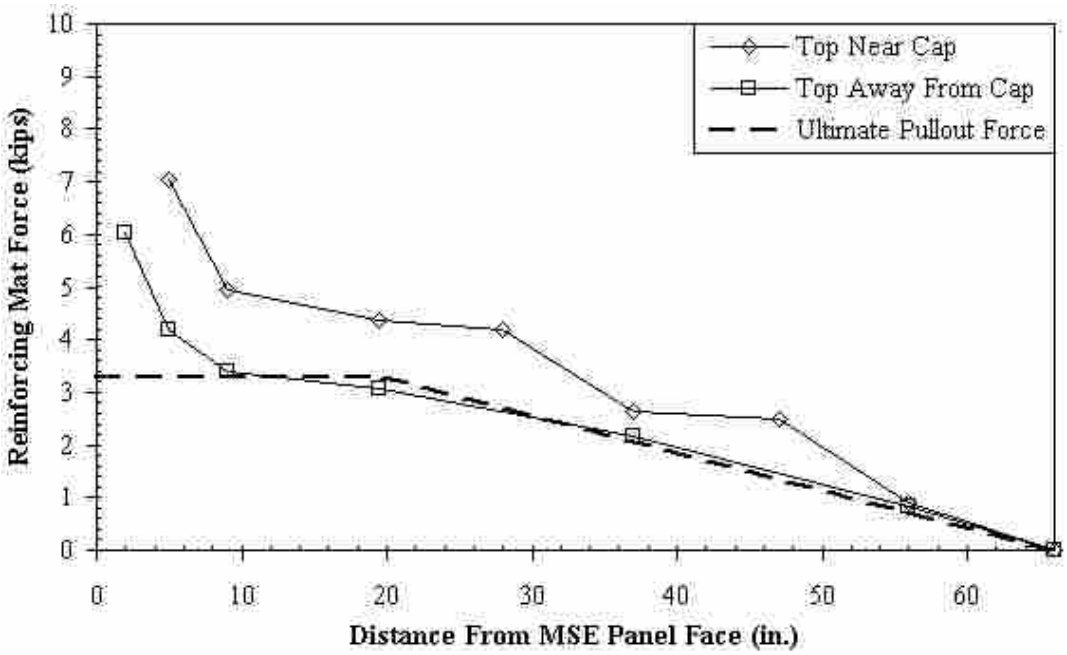

b) 1.0-in. Pile Cap Displacement Increment

Figure 6.17: Calculated Total Force in Top Reinforcing Mats for Loose Sand MSE Test at Selected Pile Cap Displacement Increments

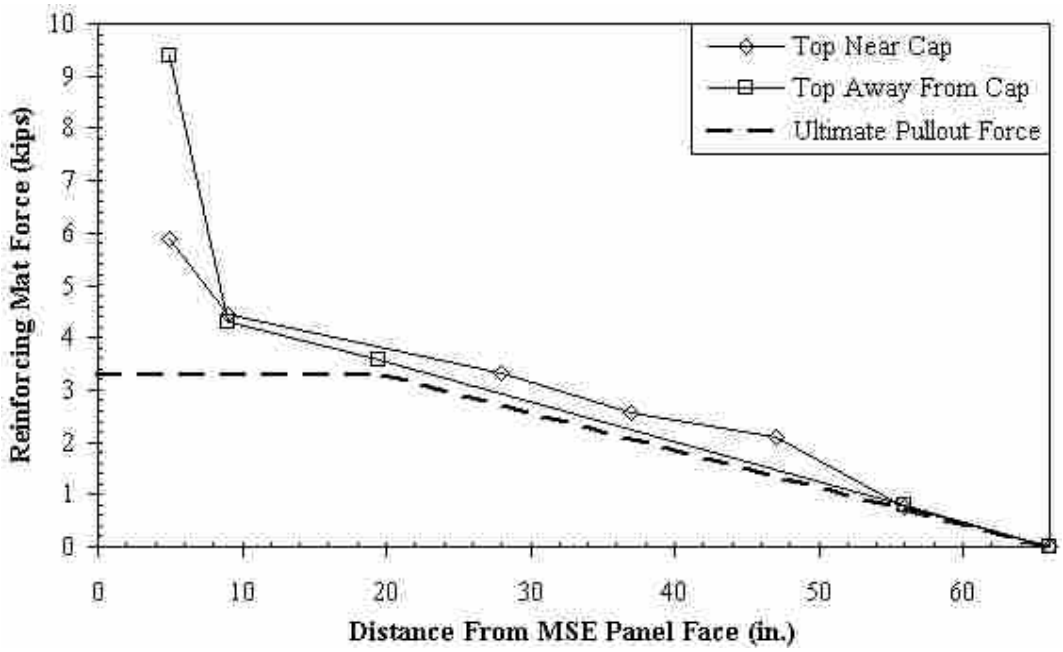

c) 2.0-in. Pile Cap Displacement Increment

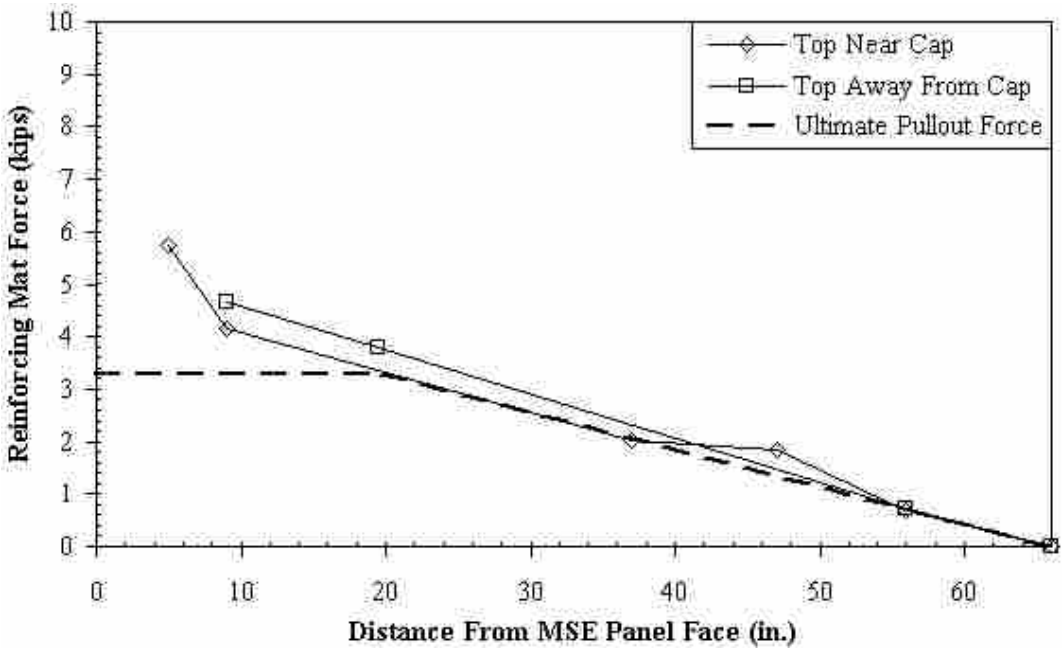

d) 3.0-in. Pile Cap Displacement Increment

Figure 6.17 (continued): Calculated Total Force in Top Reinforcing Mats for Loose Sand MSE Test at Selected Pile Cap Displacement Increments

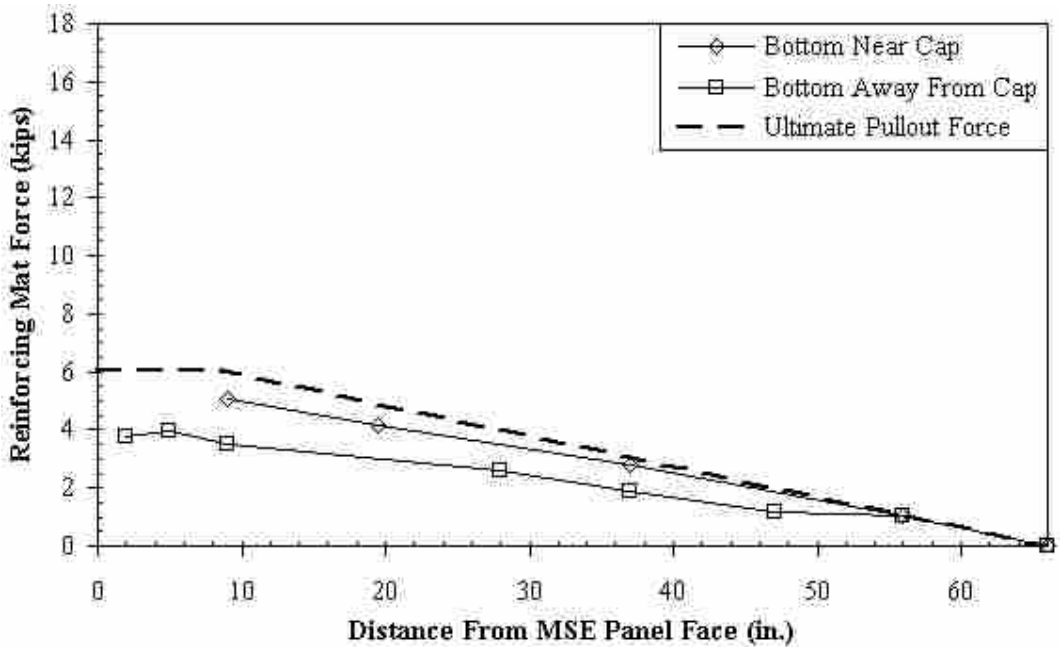

a) 0.5-in. Pile Cap Displacement Increment

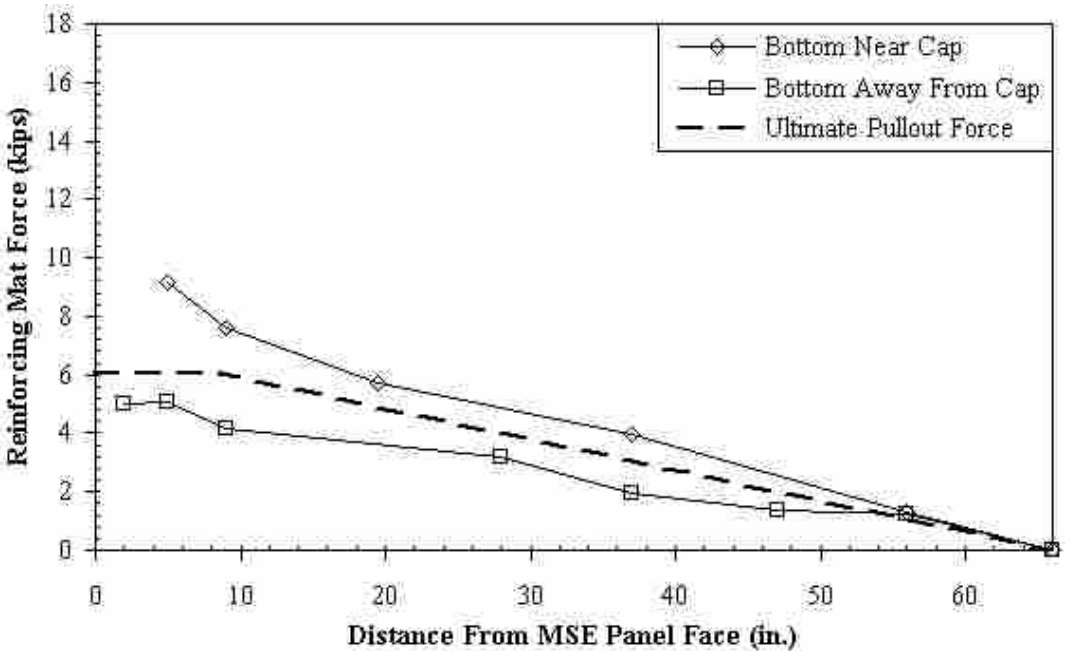

b) 1.0-in. Pile Cap Displacement Increment

Figure 6.18: Calculated Total Force in Bottom Reinforcing Mats for Loose Sand MSE Test at Selected Pile Cap Displacement Increments

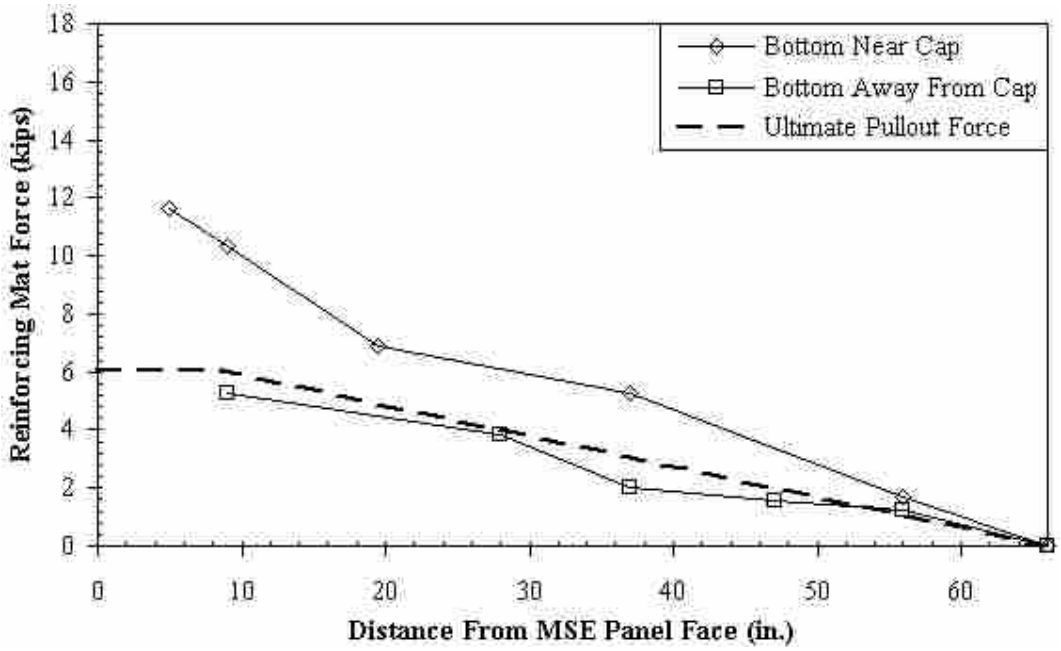

c) 2.0 in. Pile Cap Displacement

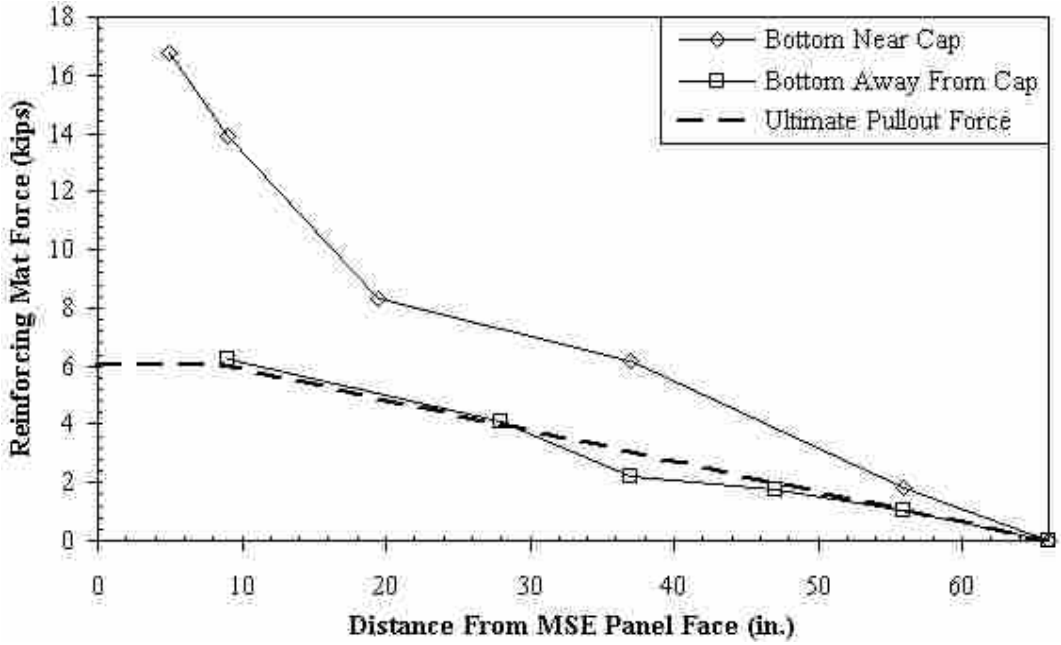

d) 3.0 in. Pile Cap Displacement

Figure 6.18 (continued): Calculated Total Force in Bottom Reinforcing Mats for Loose Sand MSE Test at Selected Pile Cap Displacement Increments

The dashed line in the plots above represents the ultimate pullout force of the mat. The line was calculated according to NHI guidelines. The flat portion of the line is equal to the ultimate force of the mat and extends to a distance of 0.3H above the mid-height of the wall. Below mid-height, the distance is interpolated between zero and at the base of the wall and 0.3H at the mid-height of the wall. The force value then tapered to zero until the total length of the reinforcing mat was reached.

The graphs show that the total calculated bar mat forces follow the trend established by the ultimate pullout force line. The force in each mat tapered toward zero at the end of the mat and generated the greatest force close to the MSE panel. It can also be seen that the development of force in the mats is also likely a function of how close the mat is to the source of load, the pile cap. In most of the plots, the "near cap" mats recorded greater values of force than the "away from cap" mats. The bottom, or deeper, mats also consistently recorded a greater force than the upper mats. Although the force in the upper bar mats was very close to the expected force, the force in one of the bottom bar mats was greater than the expected force. This is likely a result of the conservative nature of the ultimate pullout force equation.

Figure 6.19 shows the reinforcing mat forces plotted against the transverse MSE wingwall displacements for the "bottom" and "top" mats. The ultimate pullout force is plotted for comparison. The plot of the top reinforcing mats reveals that the peak force in the mats was 1 to 2 kips (4.45 to 8.90 kN) greater than the ultimate value. The lower bar mat plot shows that the mat forces increased to about the same level as the ultimate force for the reinforcing mat further away from the cap face and were much greater than the ultimate force in the bottom mat near the cap. This difference is thought to be, in part, the result of inaccurate MSE wall deflection measurements taken at this location as expressed previously in Section 6.4.5.

Typically, the maximum force in the reinforcing mats is developed with a small wall displacement of 0.2 to 0.3 in. (5 to 8 mm).

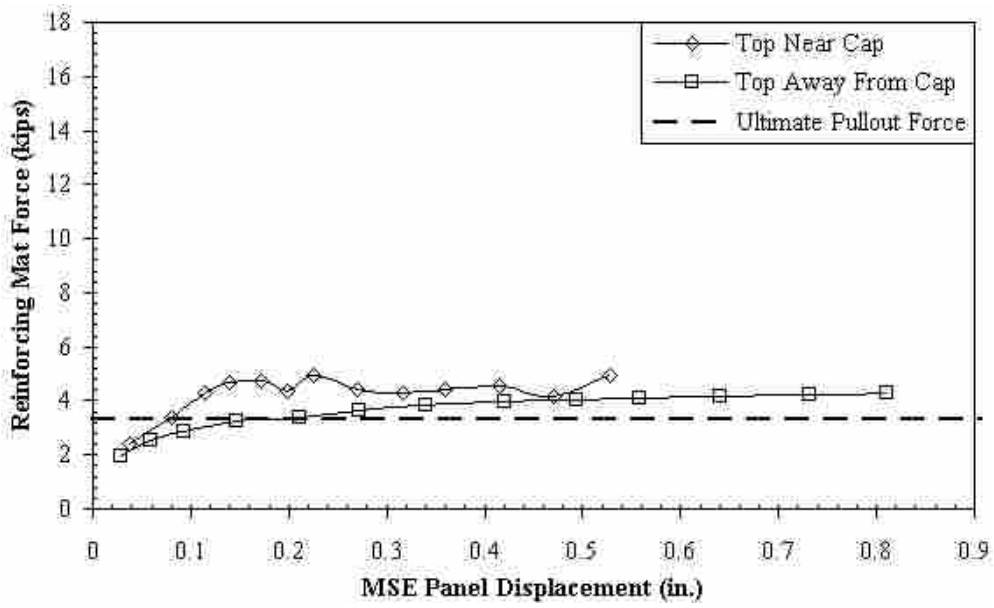

a) Top Reinforcing Mats

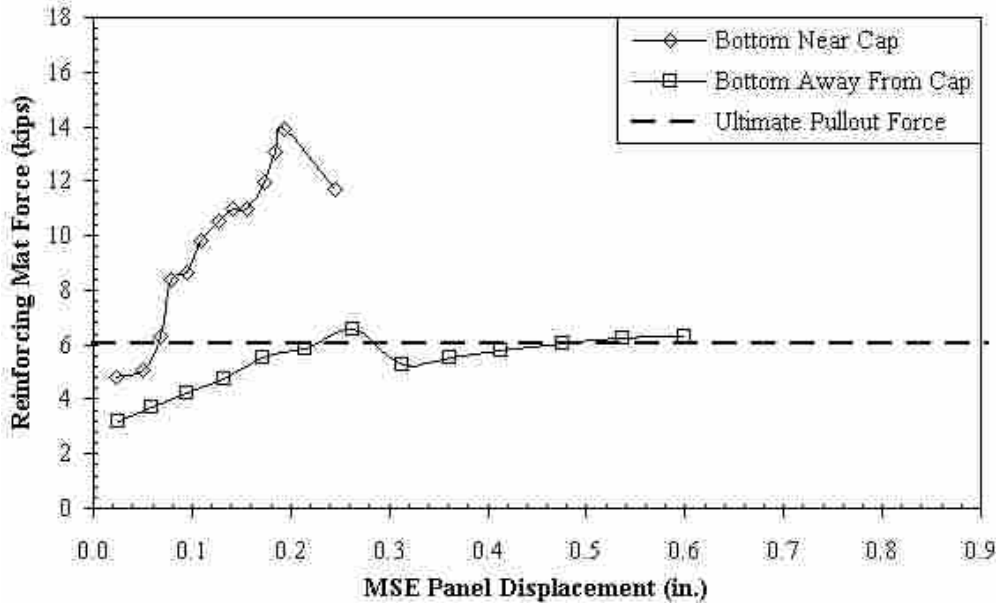

b) Bottom Reinforcing Mats

Figure 6.19: Calculated Bar Mat Force-MSE Panel Displacement Plot for Loose Sand MSE Test

Figure 6.20 shows a plot of the ratio of the pressure on the MSE wingwalls to the pressure on the pile cap face as a function of the distance of the strain gauges on each reinforcing mat from the pile cap face. The pressure on the MSE panels was calculated as the load measured in a reinforcing mat divided by the tributary area of the MSE panel of that mat. The load in the bar mat does not include the forces generated from the load test setup before testing started. The pressure on the face of the pile cap was determined by first, assuming the passive pressure distribution was in a triangular shape, meaning that the pressure was zero at the top of the pile cap and increased linearly to the bottom of the pile cap. Next, the resultant passive earth force was assumed to act at a height of one-third of the pile cap height measured from the bottom of the pile cap, thus allowing the maximum pressure at the base of the pile cap to be calculated. Last, the pressures on the pile cap at the same depths of the reinforcing mats were linearly interpolated from the maximum pressure. The MSE wall pressure was divided by the pile cap pressure at each pile cap displacement increment. The median values of all the displacement increments for each bar mat were plotted against the distance of the strain gauges on each bar mat from the pile cap face, and a linear trendline was fitted to the data points.

The maximum pressure ratio value calculated was approximately 0.09 for the loose sand MSE test with a minimum value of zero suggested by the trendline at a distance of approximately 192 in., or 16 ft (4.88 m), from the pile cap face. This distance correlates with a zero heave measurement on the backfill contour map shown previously in Figure 6.10, suggesting that no pressure may be present on the MSE walls at this distance. The statistical R^2 value, or the coefficient of determination, for the trendline was approximately 0.433, which shows some amount of correlation in the pressure ratio-distance from the pile cap relationship.

Figure 6.21 is similar to Figure 6.20, except the pressure data were reduced to remove any opportunity for pullout of the bar mats to affect the pressure ratio relationship. This was accomplished by determining at which lateral wall displacement the mats appear to begin pulling out by plotting the total MSE wall force against the average lateral wall displacement as shown in Figure 6.22. From the plot, a value of 0.2 in. (5 mm) was selected to represent the maximum amount of allowable lateral wall displacement. Only the pile cap displacement increments up to the wall displacement value of 0.2 in. were then used to find the median wall pressure. This reduced the deviation between the pressure ratios and improved the correlation in the pressure ratio-distance relationship for the loose sand MSE test. The subsequent maximum pressure ratio was approximately 0.115 while a zero pressure ratio was located at a distance of about 170 in., or 14.17 ft (4.32 m). This distance correlates with a 0 to 0.25 in. heave measurement on the backfill contour map shown previously in Figure 6.10. The R^2 value increased to 0.780.

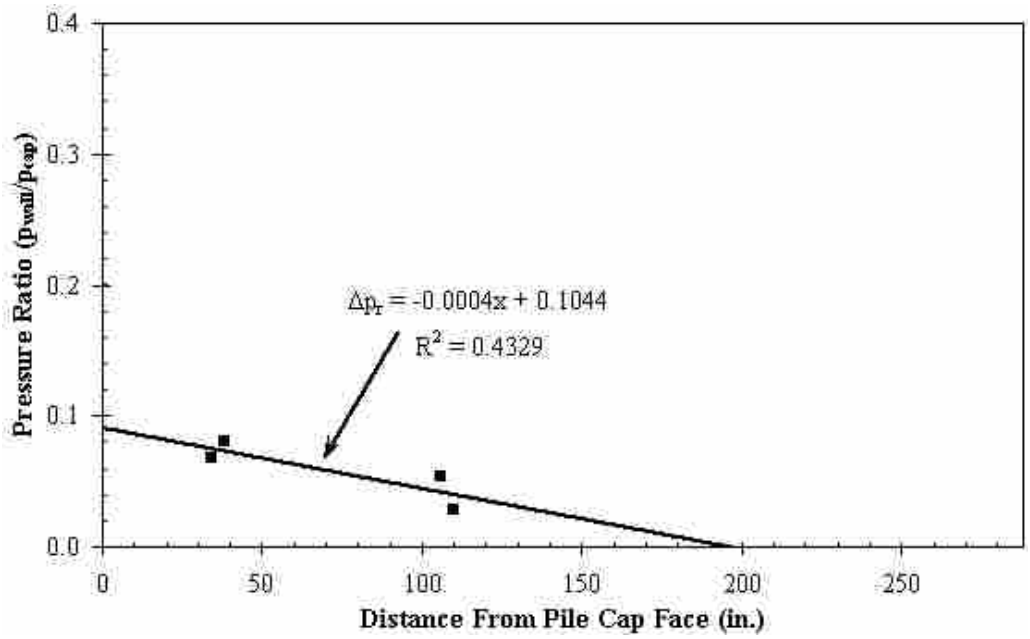

Figure 6.20: Pressure Ratio-Distance Relationship for Loose Sand MSE Test

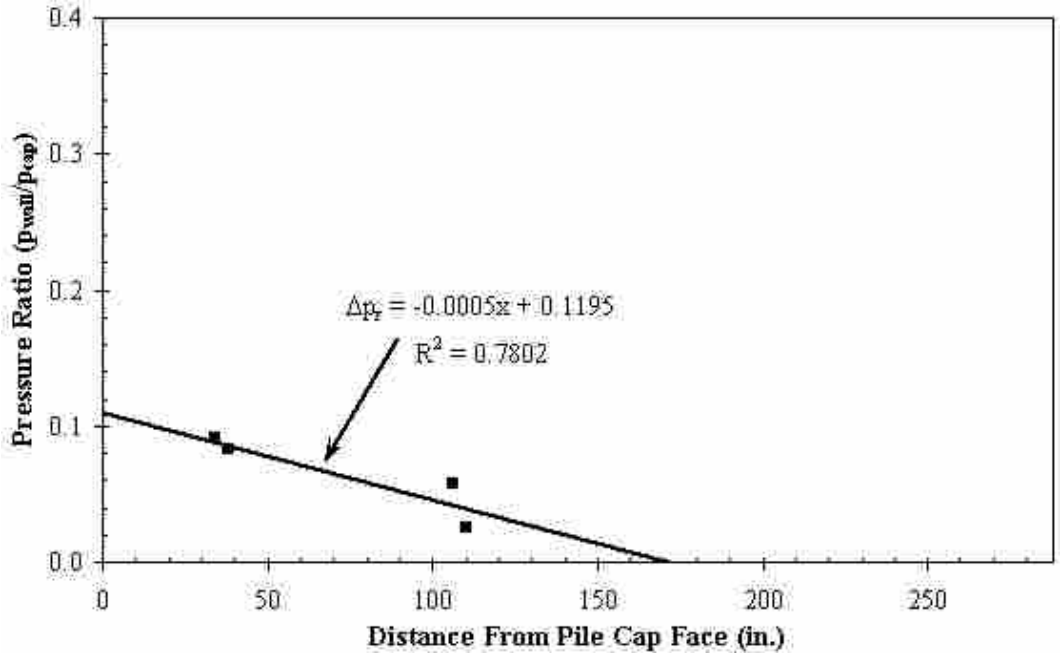

Figure 6.21: Reduced Pressure Ratio-Distance Relationship for Loose Sand MSE Test

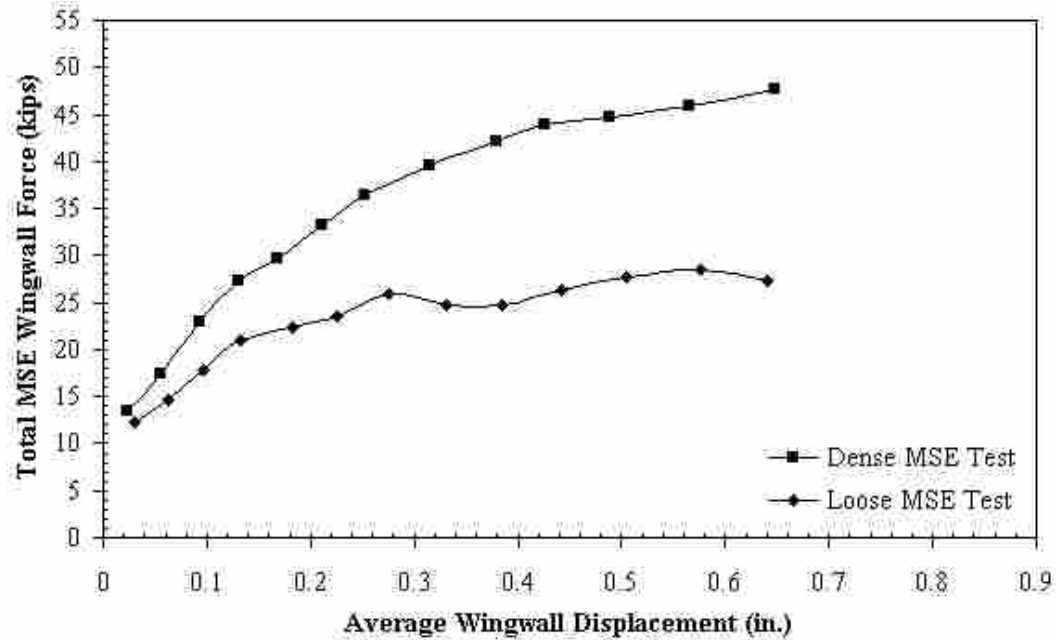

Figure 6.22: Total MSE Wingwall Force-Average MSE Wingwall Displacement Plot for the Loose and Dense MSE Tests

7 ABUTMENT LOAD TESTING – DENSE SAND WITH MSE WINGWALLS

The second load test which utilized the MSE panels was conducted on 22 June 2009. This test was originally designed with an average static factor of safety against pullout of the reinforcing mats of at least1.65. The backfill in this case was considered densely compacted because the median dry unit weight of the soil was approximately 95% of the modified Proctor. The test layout, instrumentation, procedure, and results are described in this chapter.

7.1 Test Layout

The test layout for the dense sand MSE test was identical to that described previously for the loose sand MSE test. The significant difference between the two tests was the compaction level of the backfill. The same MSE panels were utilized again. Also, the reinforcing mat layout was identical with the slightly larger mats occupying the upper mat location and the smaller mats occupying the lower mat location of the panels. Figure 6.1 and Figure 6.2, shown previously, represent the layout of the dense sand MSE test.

7.2 Test Instrumentation and Equipment

The additional instrumentation used during this test was in the same configuration as used during the loose sand MSE test. The string pots attached to the southeast MSE panel were utilized and were placed at the same locations. The reinforcing mats placed in the backfill were

also instrumented with strain gauges in an identical manner as described previously in Section 6.2. Figure 7.1 shows a photograph of the dense sand test layout before testing started.

Figure 7.1: Backfill String Pot Layout During Dense Sand MSE Test

7.3 Testing Procedure

The testing procedure followed for the dense sand MSE test was identical to that described previously in Section 3.5. The pile cap was loaded incrementally by the hydraulic

actuators to a maximum pile cap deflection of 3.25 in. (83 mm). Each displacement increment increased the pile cap deflection by a target value of 0.25 in. (6.35 mm). After the maximum deflection was reached and necessary data collected, the actuators were used to pull the pile cap back to its initial unloaded condition.

7.4 Test Results

The following sections provide the results of the dense sand MSE test. The results consist of passive force-displacement measured from the actuators, passive pressure versus depth curves, passive force-displacement measured from the pressure plates, inclinometer displacement versus depth curves, and backfill displacement data.

7.4.1 Load-Displacement Results – Actuators

Figure 7.2 plots the measured total peak actuator load versus pile cap displacement as the "total resistance." The displacement values were calculated by taking the median displacement of the four string pots attached to the pile cap at the end of each displacement increment. The maximum load recorded was 959 kips (4266 kN) at a displacement of 3.17 in. (80 mm).

The contribution of the backfill passive resistance to the total resistance was calculated from the load-displacement data collected. As previously stated, the baseline resistance was subtracted from the total measured actuator load to develop the passive resistance provided by the backfill only. Figure 7.2 plots of the backfill passive resistance and baseline resistance in comparison with the total resistance. As seen in previous tests, the passive force did not exhibit a distinct peak, but continued to gradually increase with displacement throughout the test.

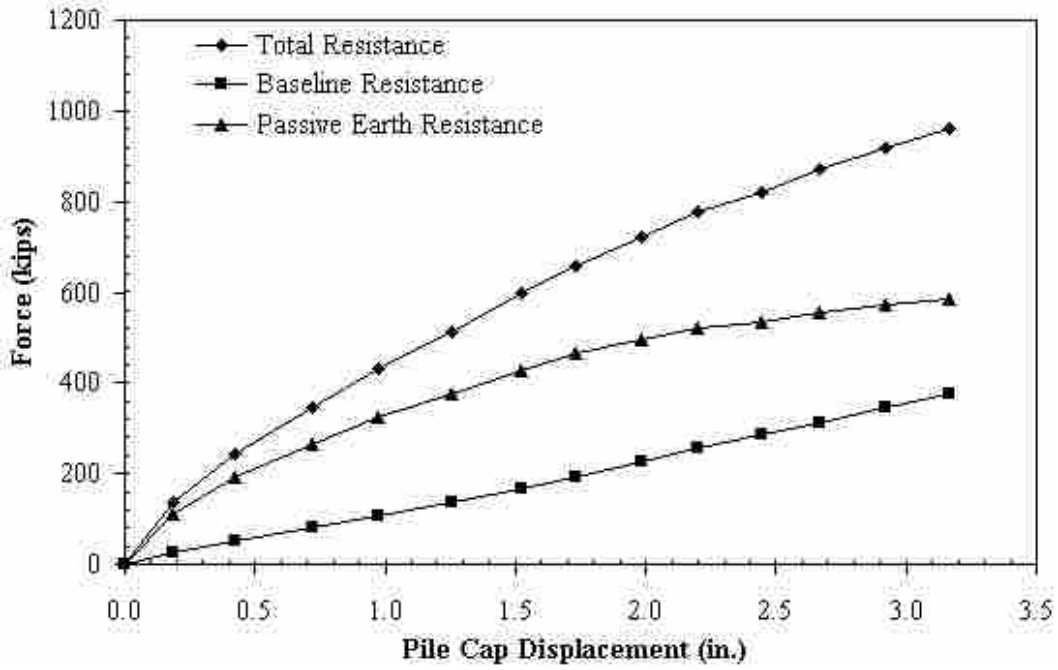

Figure 7.2: Force-Displacement Comparison For Dense Sand MSE Test

7.4.2 Load-Displacement Results – Pressure Cells

To help verify the load-displacement results from the actuators described in the previous section, measurements from the pressure cells embedded in the north face of the pile cap were analyzed. During the test, pressure readings from the cells were taken continuously. Figure 7.3 shows a plot of the backfill passive pressure as a function of the depth of the pile cap at each displacement increment. The plot generally follows a trend of increasing pressure with increasing depth, but there are a few inconsistencies. Notable increases and decreases in pressure occurred across the full range of depth. Also, at depths of 1.38 ft (0.42 m) and 4.13 ft (1.26 m), in Figure 7.3, the pressures recorded at these cells reached a peak value by the 1.52 in. (39 mm) and 2.44 in. (62 mm) increments, respectively, and then proceeded to decrease until the load test was completed.

As explained in Section 4.2.2, the passive pressure readings were converted to force by multiplying the pressures by the tributary area of each pressure cell. Figure 7.3 shows a plot of the pressure cell passive force versus the pile cap displacement compared to the backfill passive resistance calculated from the actuators. Typically, the pressure cell passive force-displacement curves were lower than the actuator passive force-displacement curves by approximately 30 to 40% due to the assumption of uniform pressure acting across the width of the pile cap. The "pressure cells with multiplier" curve, in Figure 7.4, accounts for this concern by showing what the load-displacement curve looks like when multiplied by a factor of 1.33. The "pressure cells with multiplier" curve is slightly above the measured passive earth resistance curve, but maintains the same general shape. The maximum passive force of the "pressure cells with multiplier" curve is less than the same value for the measured maximum passive force.

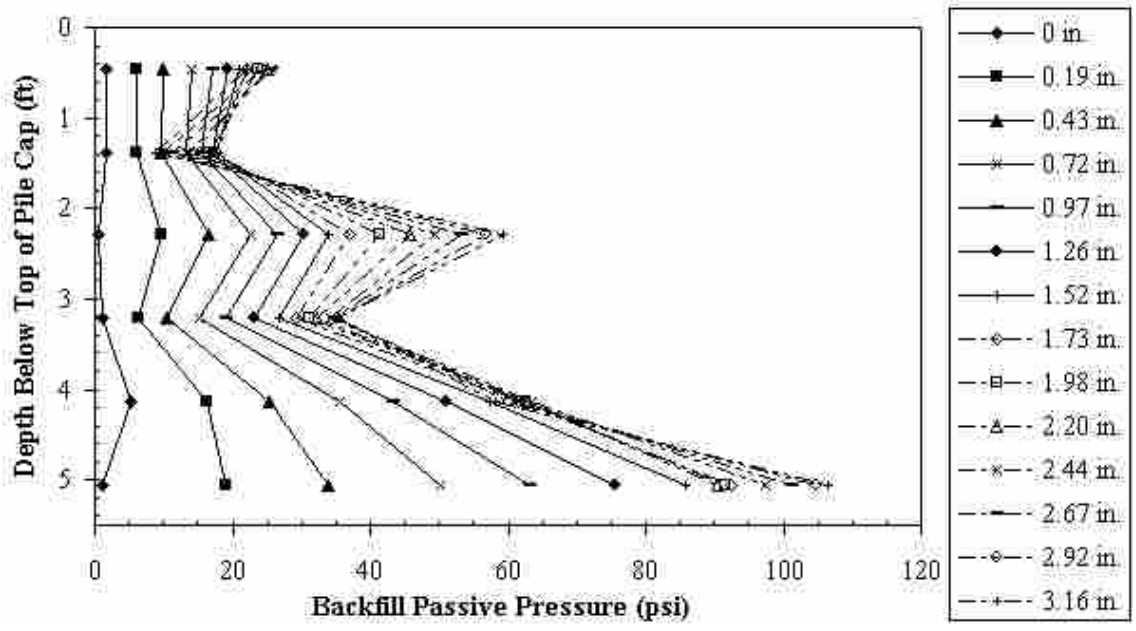

Figure 7.3: Backfill Passive Pressure-Depth Plot at Each Displacement Increment for the Dense Sand MSE Test

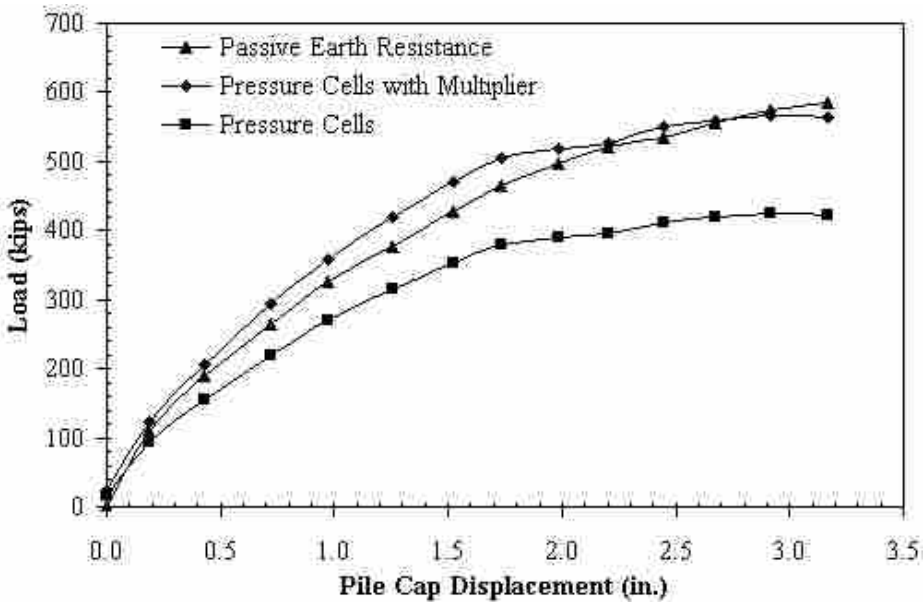

Figure 7.4: Pressure Cell Passive Force Resistance Compared to the Measured Passive Earth Resistance of the Dense Sand MSE Test

7.4.3 Inclinometer Data Results

Before and after each test was conducted, inclinometer readings were taken in both the north and south inclinometer tubes embedded in the pile cap. The readings measured the pile cap and pile deflection over the depth of the piles parallel to the direction of loading. Figure 7.5 shows the north and south deflection results when the pile cap reached maximum deflection during the dense sand MSE test. Positive deflection values correlate with the northerly direction of loading. The zero displacement of the piles occurred at a depth of approximately 20 ft (6.10 m), which depth is about 19 pile diameters. The maximum displacement values recorded by the four string pots attached to the pile cap are also plotted. The string pot values confirm the inclinometer results. From the inclinometer plot, it can also be seen that the pile cap experienced very little rotation during loading, typical of a fixed head boundary condition.

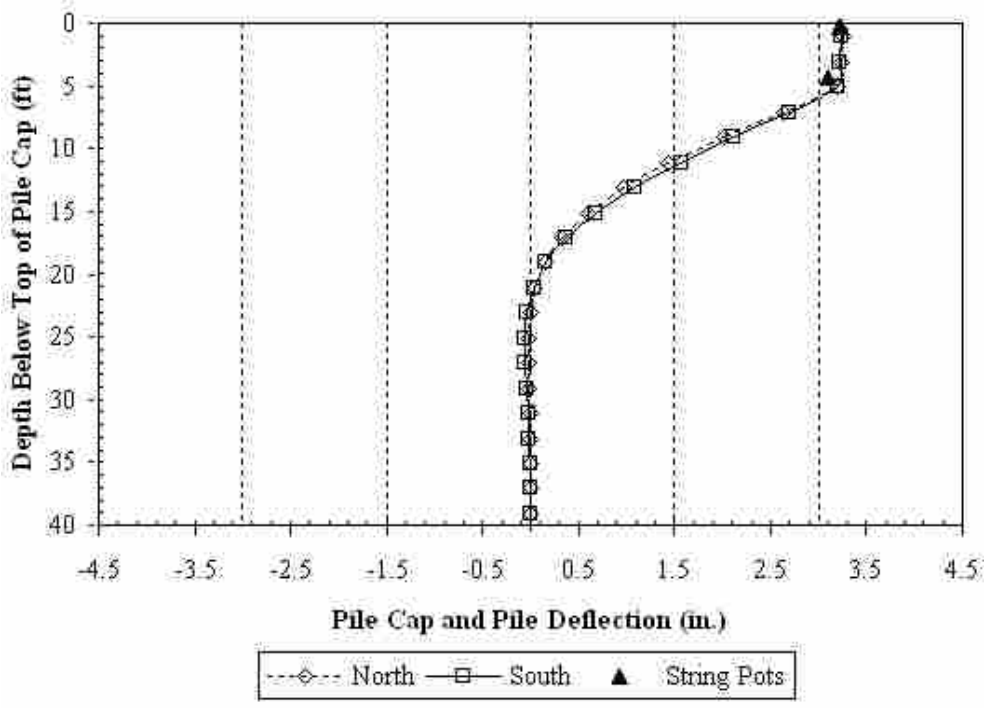

Figure 7.5: Inclinometer Displacement Readings of the Dense Sand MSE Test

7.4.4 Backfill Displacement Results

During testing, the backfill displacement was monitored with string pots located in the configuration described in Section 3.3.5. Figure 7.6 shows the absolute displacement of the backfill plotted against the distance from the pile cap recorded from these string pots. To simplify the plot, backfill displacements from selected pile cap displacements increments are shown. The results of the dense MSE test were different from the three previous loose tests and show that a steady and consistent decrease in displacement level occurred throughout the load test. The minimum horizontal displacement recorded at a distance of 24 ft (7.32 m) from the pile cap face was approximately 0.78 in. (19.8 mm), which was 0.5 in. (12.7 mm) more than the minimum value of any of the loose tests. These observations can be understood by recognizing that dense sands tend to exhibit a general shear failure as compared to a local shear failure

condition typical of loose sands. General shear failure would lead to movement throughout the failure zone while local shear failure would primarily lead to movement close to the pile cap.

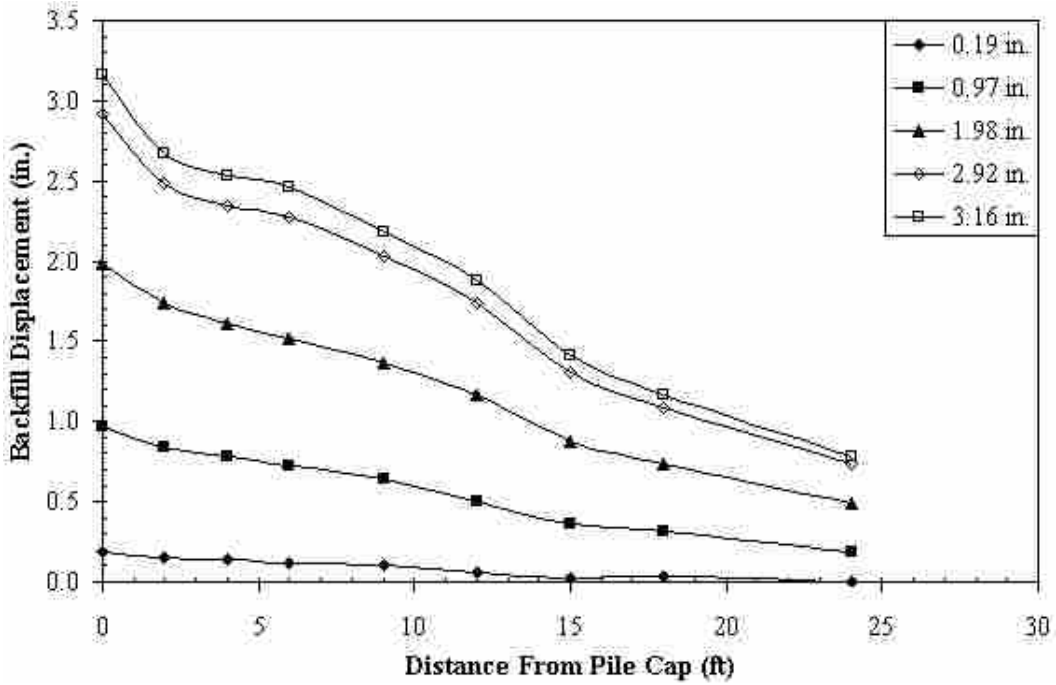

Figure 7.6: Absolute Backfill Displacement Versus Distance from the Pile Cap for the Dense Sand MSE Test

From the displacement data above, the compressive strain (in./in.) was calculated for each distance between string pot stakes (i.e., 0-2 ft, 2-4 ft, 4-6 ft, 6-9 ft, etc.) with Equation 4.1. Figure 7.7 shows the compressive strain calculation results for selected displacement intervals. While not all intervals are shown, the overall trend can still be seen with the intervals plotted. The highest compressive strain rates occur in the first two feet of backfill. Generally, as the distance from the pile cap face increased, the compressive strain levels decreased. During the dense sand MSE test, the strain rate decreased dramatically after the first 2 ft (0.61 m), increased in the 12 to 15 ft (3.66 to 4.57 m) range, and then decreased again after that.

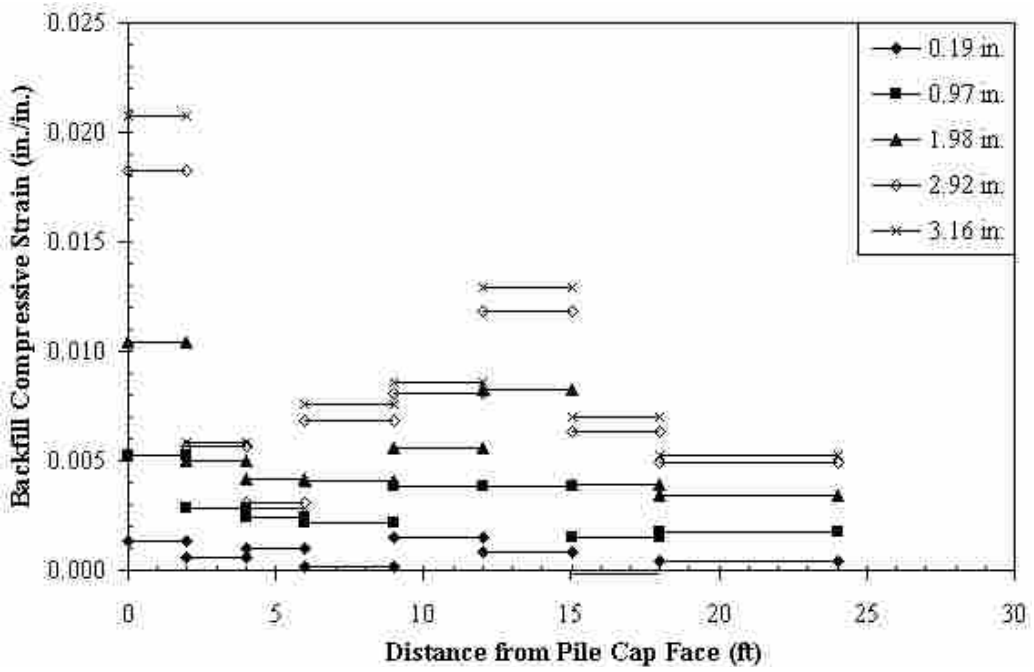

Figure 7.7: Backfill Compressive Strain for the Dense Sand MSE Test

The vertical displacement of the backfill was also determined for the test. To determine vertical displacement, the elevation of the backfill grid was surveyed before and after the test. The difference between the elevations showed how much the backfill displaced from the loading of the pile cap. Figure 7.8 shows a contouring of the backfill zone for the dense sand MSE test. The maximum vertical displacement was approximately 1.75 in. (44.5 mm) occurring along the 6-ft grid line with at least 0.5 in. (12.7 mm) of heave also occurred along much of the 24-ft grid line.

Figure 7.9 shows the crack pattern that developed in the backfill during testing. The backfill was visually inspected for cracks after each displacement increment. The most significant cracking occurred perpendicular to the pile cap face coinciding with the ends of the reinforcing mats around the 4 and 6 ft north-south gridlines. This cracking appeared as two parallel trend lines extending from 4 ft (1.22 m) to nearly 20 ft (6.10 m) from the pile cap face at

distances of 1 ft (0.30 m) from either side of the backfill centerline. No significant cracking occurred beyond the 20 ft (5.49 m) gridline. It is interesting to note that because the backfill was more densely compacted during this test, more cracking was visible than during the loose sand MSE test.

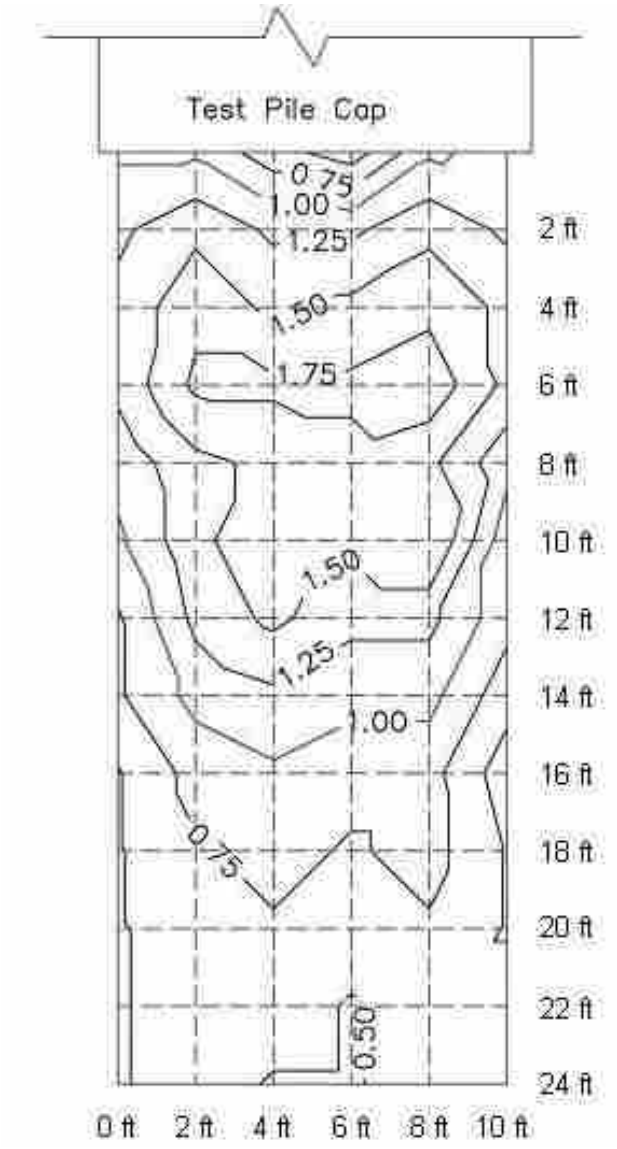

Figure 7.8: Backfill Vertical Displacement Contour of the Dense Sand MSE Test

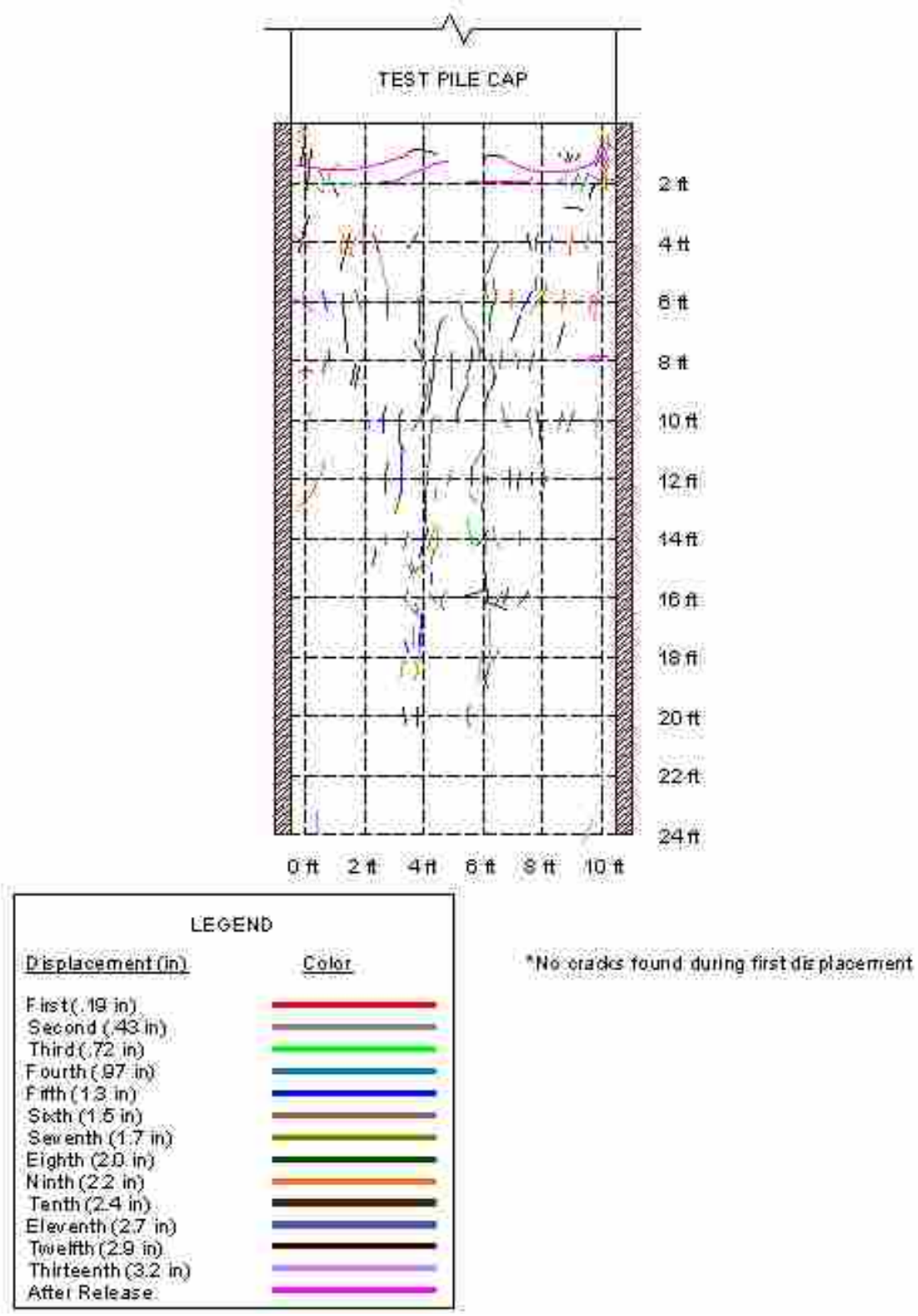

Figure 7.9: Observed Backfill Cracking During the Dense Sand MSE Test

7.4.5 Transverse Wingwall Displacement Results

As mentioned in Section 6.2, to monitor the MSE wingwall movement during the tests, four string pots were attached to the southeast MSE panel. Figure 7.10 is a plot of the transverse MSE wingwall movement recorded during testing from the pair of string pots located 103 in., or 8.58 ft (2.62 m), from the pile cap face. The data from the pair of string pots located 21 in., or 1.75 ft (0.53 m) from the pile cap face are not shown because one of the string pots was erratic during testing. The data in the graph were extrapolated linearly to show the total movement of the wall from top to bottom. The markers on each line represent the location of the string pots. Each line shows the movement of the wall for each 0.25-in. displacement increment. As seen from the plot, the panels appear to have rotated during the test. The rotation was expected because the shallow upper bar mats carried less load than the deep lower bar mats. Since the lower mats were placed deeper in the backfill, a greater soil weight was transferred to the mats preventing the wall from rotating as depth increased.

Figure 7.11 shows the MSE wingwall rotation plotted against the passive force at the 103 in. location of string pots. Very little rotation occurred during the first three displacement increments, but the overall trend of the plot shows that as the load increased, the rotation of the wall also increased. A maximum rotation of approximately 0.27 degrees was measured.

Figure 7.12 presents the transverse movement of the MSE wingwalls from an aerial prospective. Data were collected at each 0.25-in. displacement increment. However, to simplify the plot, data are only shown for every 0.50 in. of pile cap displacement. The markers in the graph represent the location of the string pots. From the plot, it can be seen that as the distance from the pile cap face increased, the amount of outward movement increased.

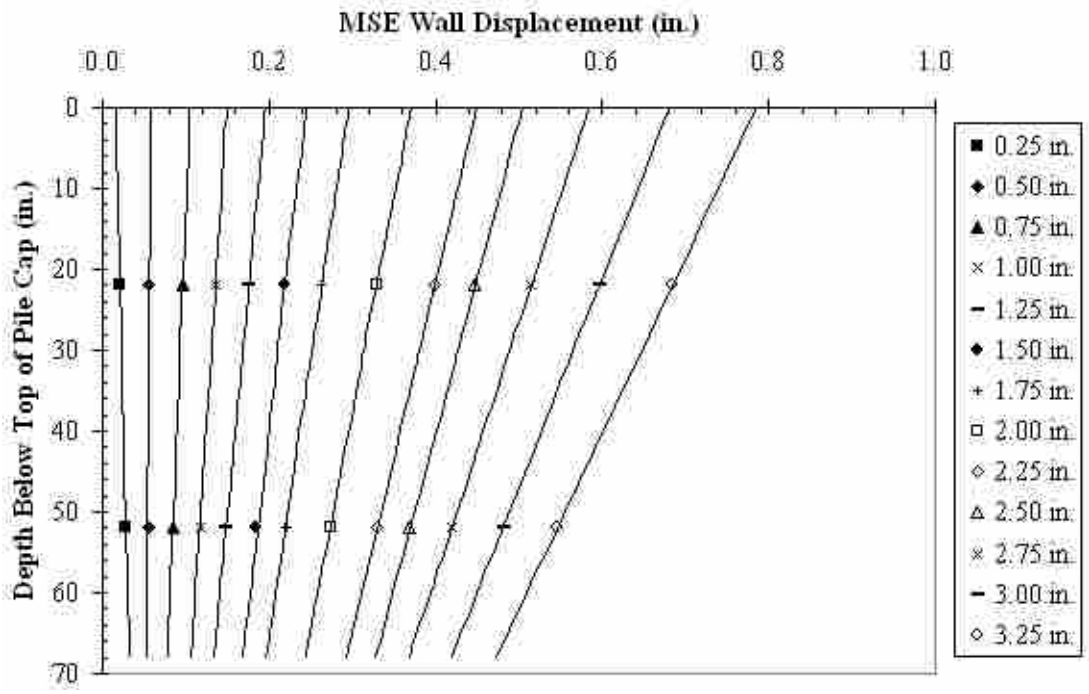

Figure 7.10: MSE Wingwall Displacement at 103 in. From the Pile Cap for Dense Sand MSE Test

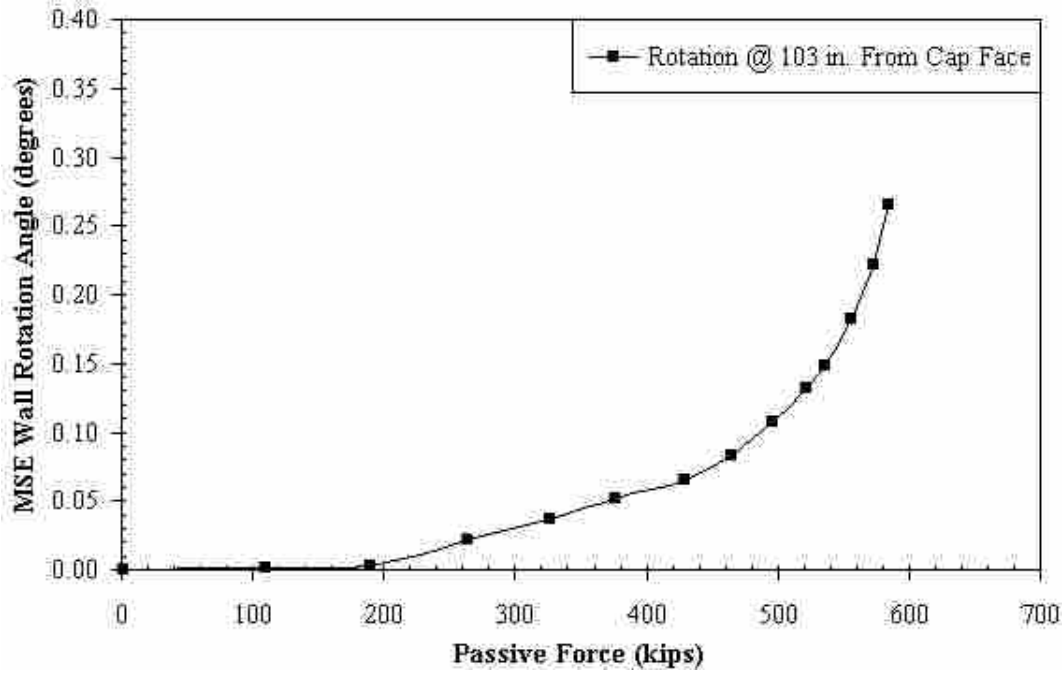

Figure 7.11: MSE Wingwall Rotation-Measured Passive Force Plot for Dense Sand MSE Test

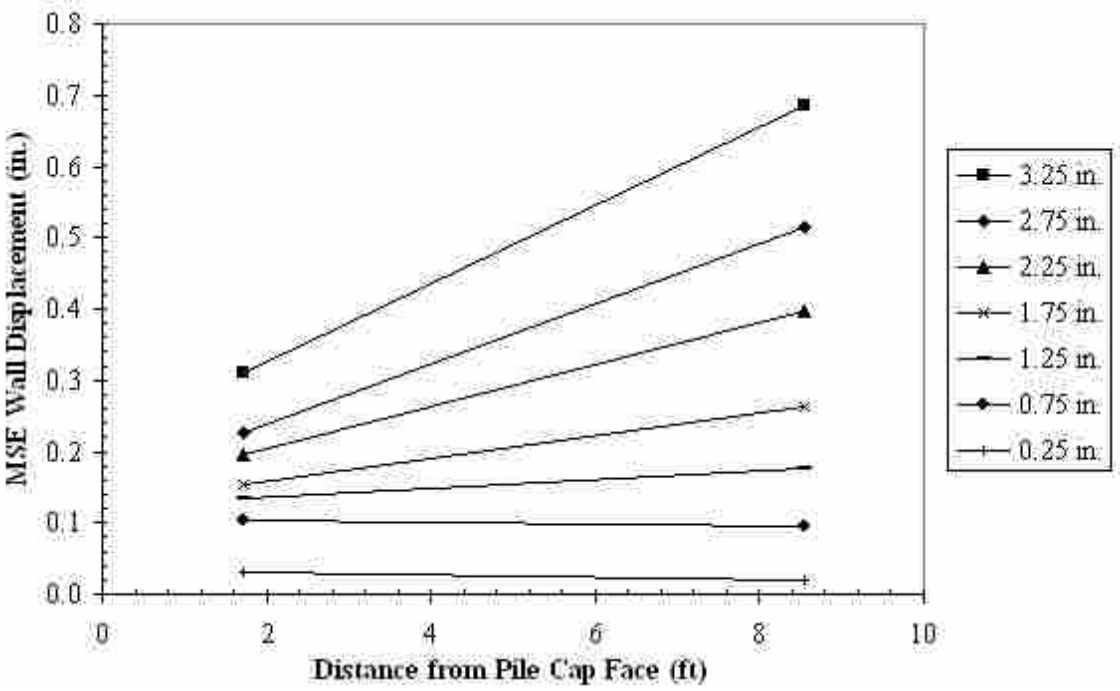

Figure 7.12: Transverse MSE Wingwall Displacement for Dense Sand MSE Test

Figure 7.13 and Figure 7.14 also provide a look at how the wingwalls displaced in regards to passive force and the pile cap displacement. The plots show the wingwall response at the 103 in. string pot location. The displacements plotted represent the movement of the very top of the MSE wingwalls, which was extrapolated from the string pot measurements. The trends show from the concave shapes of the plots that as the passive force increased, the wingwall displacement increased. If this trend continued, eventually a peak load would be reached and "failure," or severe displacements of the wingwalls, would occur. For MSE wingwalls, failure occurs when the reinforcing mats start pulling out of the backfill at large displacement levels per displacement increment.

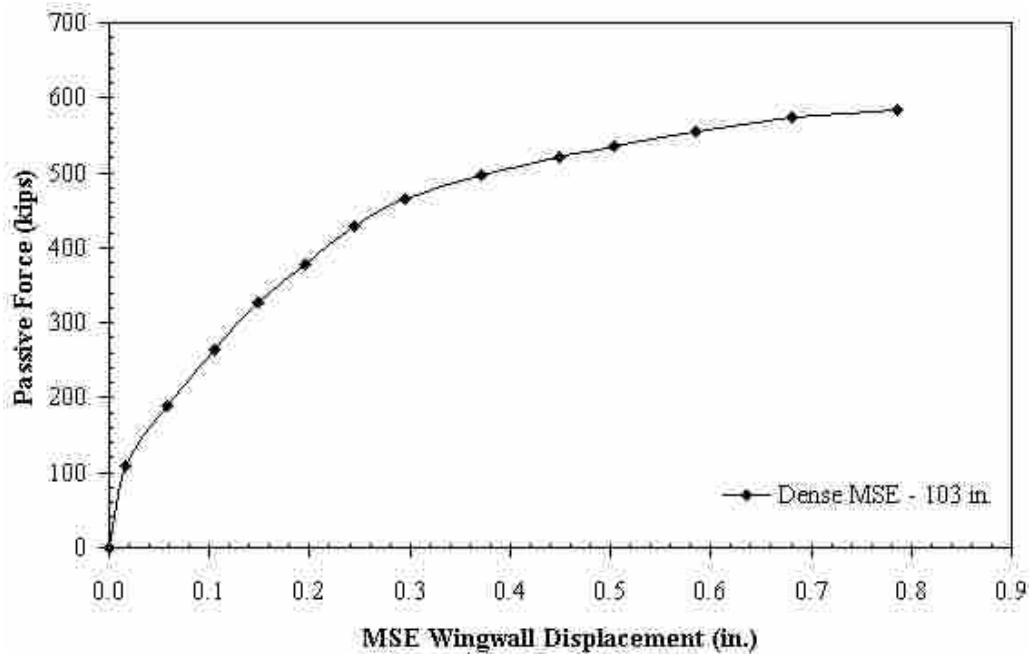

Figure 7.13: Outward MSE Wingwall Displacement-Measured Passive Force Plot for Dense Sand MSE Test

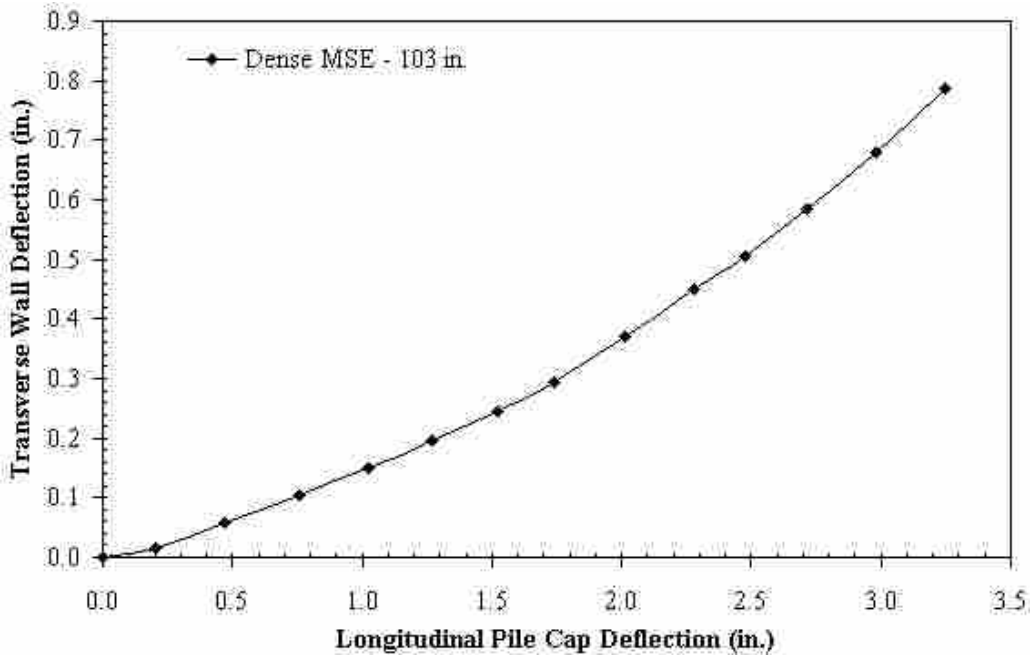

Figure 7.14: MSE Wingwall Displacement-Pile Cap Displacement Plot for Dense Sand MSE Test

7.4.6 Reinforcing Mats Load Results

As stated in Section 7.2, strain gauges were implemented on the reinforcing mats used in conjunction with the MSE wingwalls to monitor the development of load in the mats. The mat loads calculated were then compared to the displacement of the MSE wingwalls to develop load-deflection curves for the bar mats. These load-deflection curves provided a reasonable means of detecting the capacity of the walls before failure occurred.

To calculate the force in a reinforcing mat, the strain data collected from each set of strain gauges was used in Equation 6.1. The average strain, $\bar{\varepsilon}$, in the equation considered the strain recorded during construction of the test and during the test. As the test setup was completed, an initial strain was placed on the mats from the backfill material. This was accounted for when computing the total load, *F*, in each reinforcing mat by including the measured initial strain with that measured during the load test.

Figure 7.15 and Figure 7.16 are plots of the total force calculated in the bar mats compared to the ultimate pullout forces calculated at specific displacement increments. Each marker in the plots represents the location of a set of strain gauges. Due to the sensitivity and reliability of the strain gauges, not all data collected from the strain gauges were useful. If data from a specific set of gauges were deemed inaccurate, the point representing that set was removed from the plot and the curve was continued between the existing points. The graphs plotting data from the upper reinforcing mats placed at a depth of 1.83 ft (0.56 m) below the top of the pile cap are referred to as "top." Graphs which plot data from the lower reinforcing mats placed at a depth of 4.33 ft (1.32 m) below the top of the pile cap are referred to as "bottom." The center of the mats described as "near cap" and "away from cap" were located at distances of 3 ft (0.91 m) and 9 ft (2.74 m) from the pile cap face, respectively.

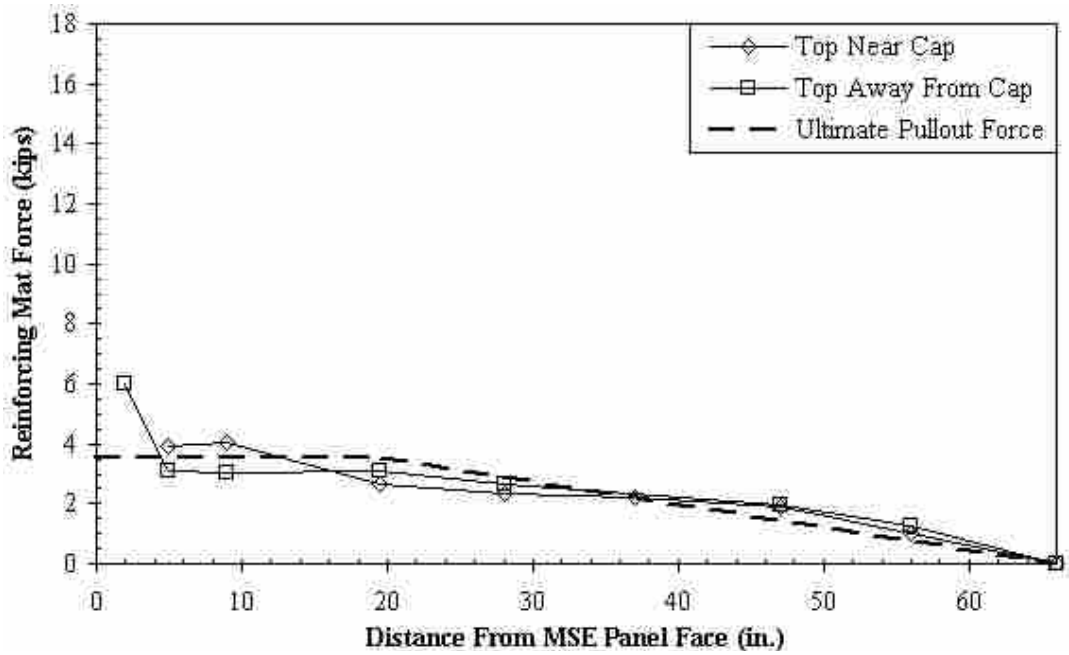

a) 0.5-in. Pile Cap Displacement Increment

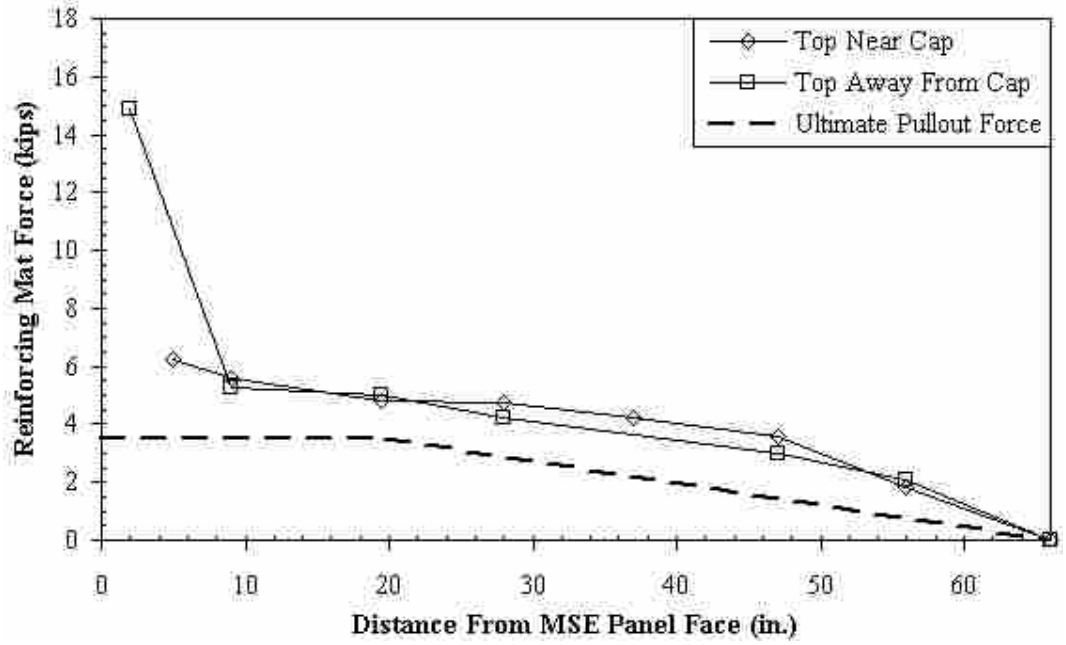

b) 1.0-in. Pile Cap Displacement Increment

Figure 7.15: Calculated Total Force in Top Reinforcing Mats for Dense Sand MSE Test at Selected Pile Cap Displacement Increments

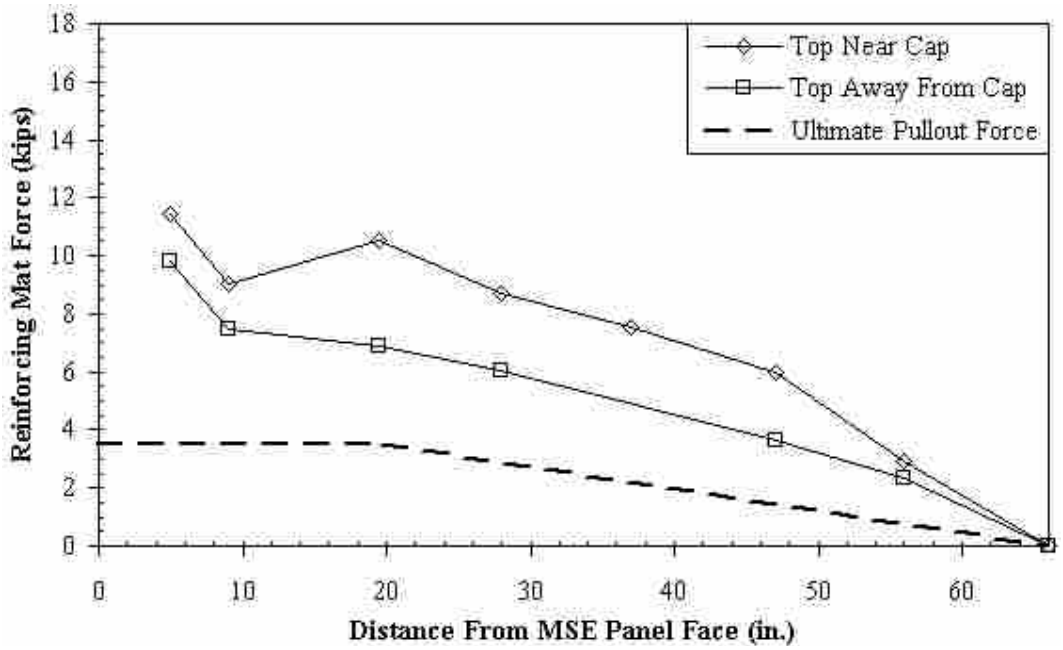

c) 2.0-in. Pile Cap Displacement Increment

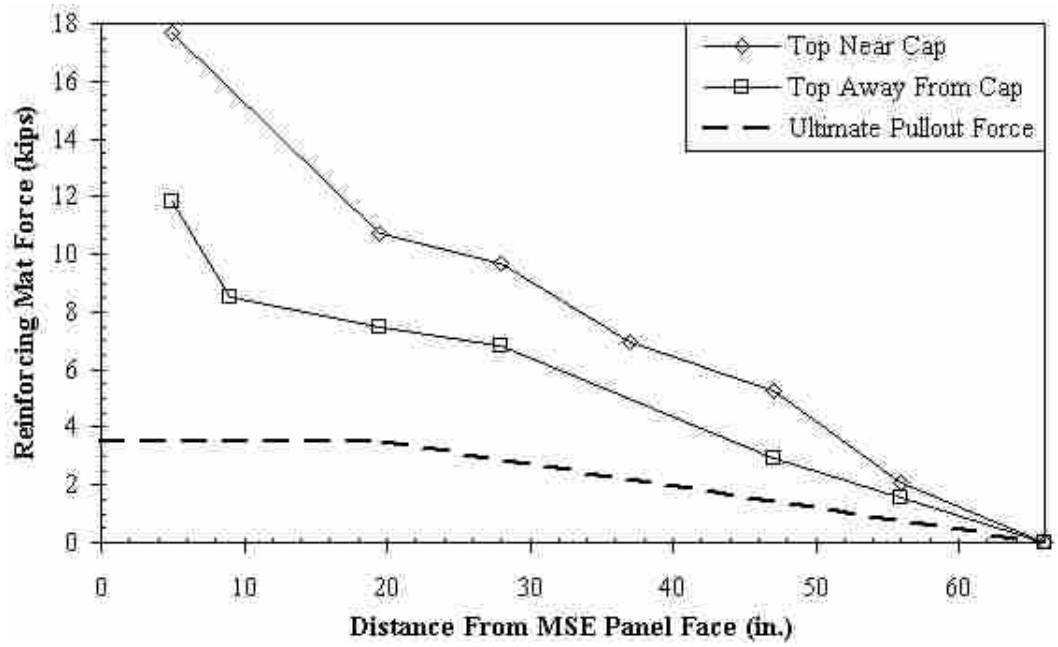

d) 3.0-in. Pile Cap Displacement Increment

Figure 7.15 (continued): Calculated Total Force in Top Reinforcing Mats for Dense Sand MSE Test at Selected Pile Cap Displacement Increments

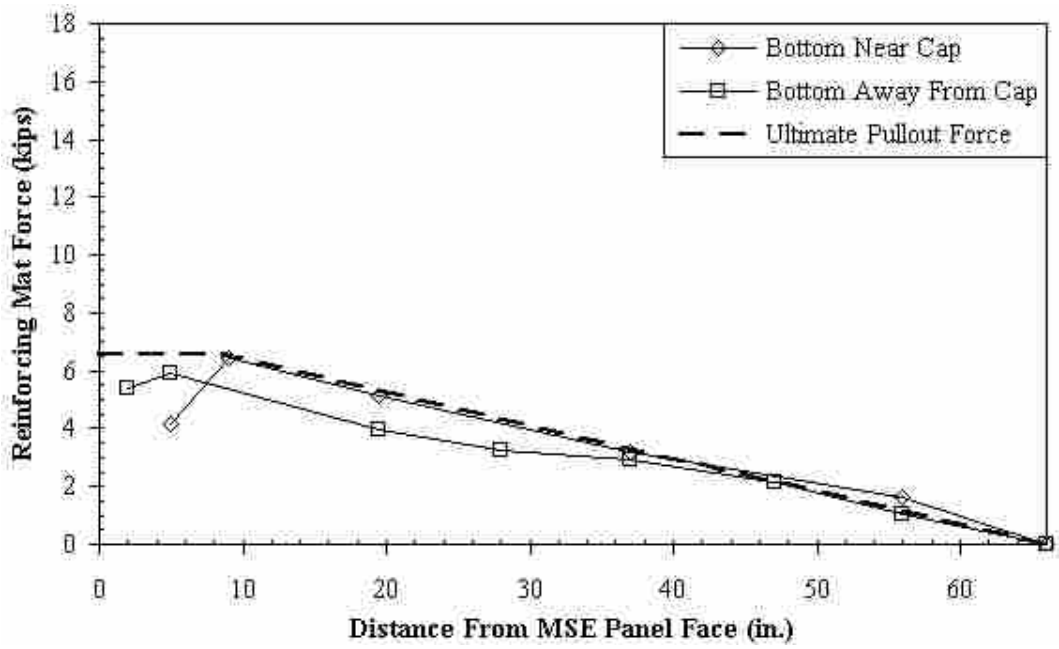

a) 0.5-in. Pile Cap Displacement Increment

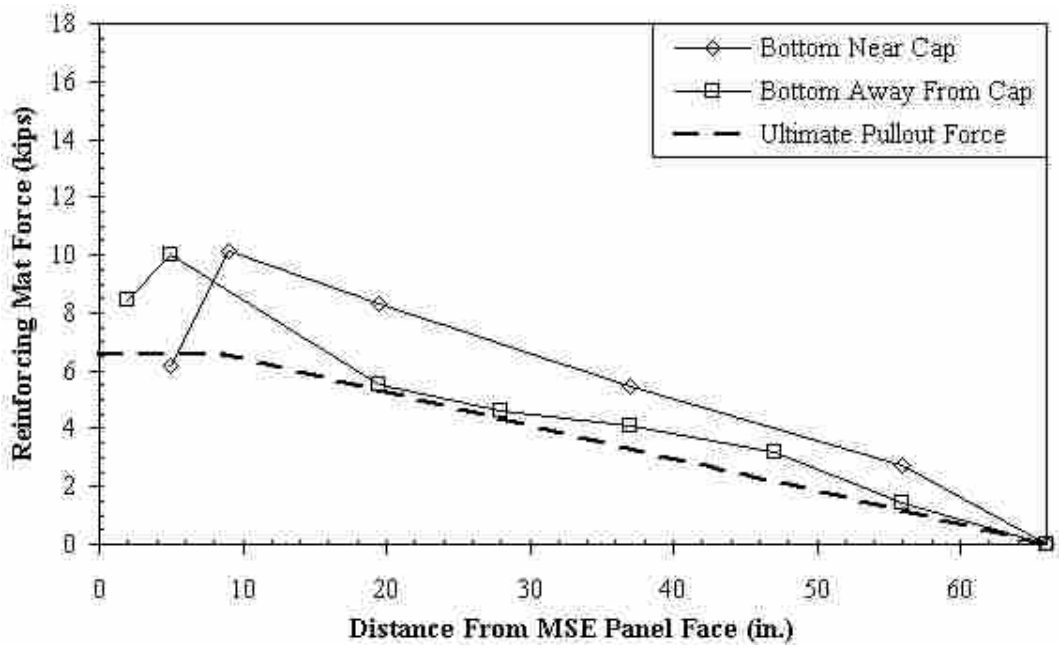

b) 1.0-in. Pile Cap Displacement Increment

Figure 7.16: Calculated Total Force in Bottom Reinforcing Mats for Dense Sand MSE Test at Selected Pile Cap Displacement Increments

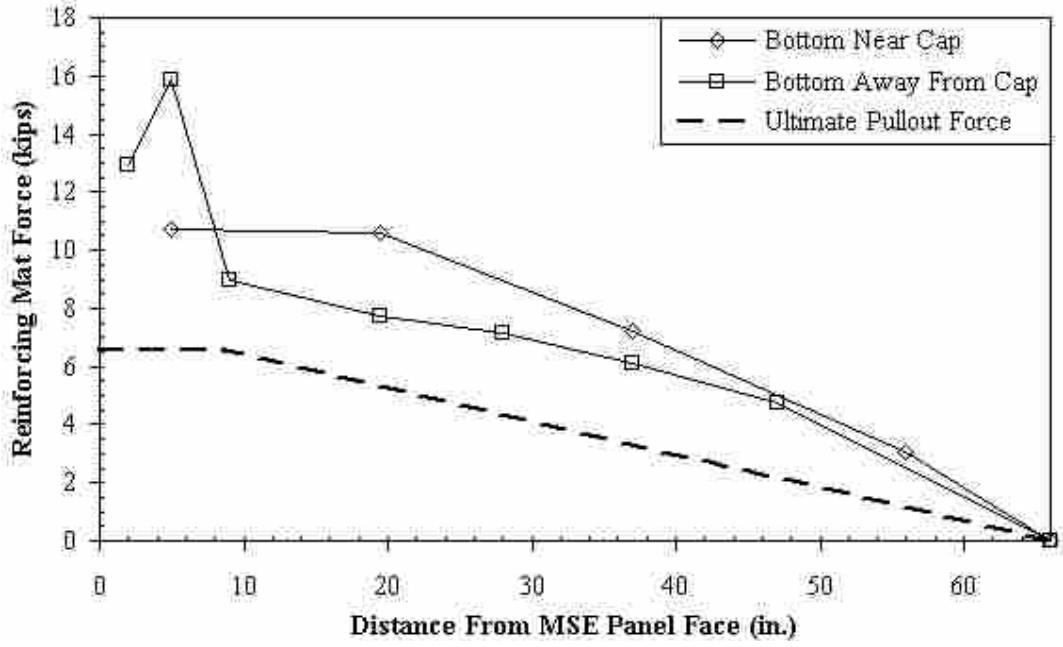

c) 2.0 in. Pile Cap Displacement

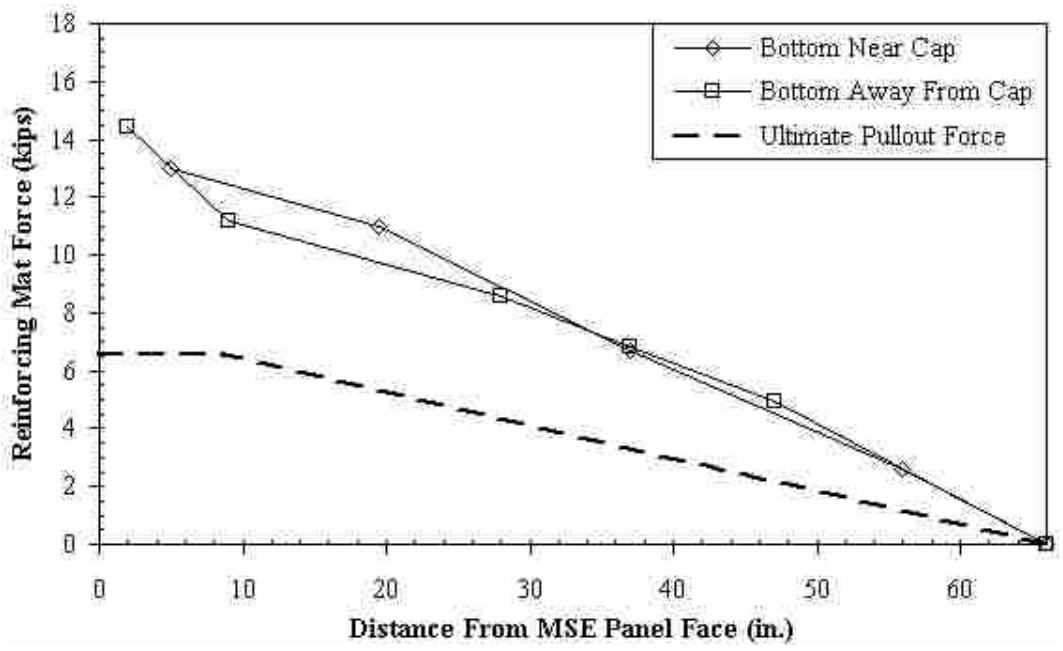

d) 3.0 in. Pile Cap Displacement

Figure 7.16 (continued): Calculated Total Force in Bottom Reinforcing Mats for Dense Sand MSE Test at Selected Pile Cap Displacement Increments

The strain gauges located in the 2 to 9 in. (51 to 229 mm) range were the most inconsistent in providing reasonable measurements. Because these gauges were located at a short distance from the MSE panel face, bending effects or damage during construction may have affected the accuracy of the gauges. The gauges located at 2 in. (51 mm) from the panel face were especially susceptible to construction damage from the pins used to secure the reinforcing mats to the MSE panels.

The dashed line in the plots represents the ultimate pullout force of the mats. The line was calculated according to NHI guidelines. The flat portion of the line is equal to the ultimate pullout force of the mat and extends to a distance of 0.3H above the mid-height of the wall. Below the mid-height, the distance is interpolated between zero at the base of the wall and 0.3H at the mid-height of the wall. The force value was then tapered to zero until the total length of the reinforcing mat was reached.

The plots show that the calculated bar mat forces follow the trend established by the ultimate pullout force line. The force in each mat tapered toward zero at the end of the mat and generated the greatest forces closer to the MSE panel. The forces calculated increased with each successive pile cap displacement increment. It can also be seen that the development of force in the mats is also likely a function of how close the mat is to the source of load. In most of the graphs, the mats that were considered “near cap” recorded greater values of force than those mats considered “away from cap.” The bottom, or deeper, mats also consistently recorded the greater amounts of force than the upper reinforcing mats. Shown in most of the graphs, the amount of force in the mat was greater than the design pullout force. This is most likely a result of the conservative nature of the ultimate pullout force equations. At approximately the 1.0-in. pile cap

increment was where the mat force typically began to exceed the ultimate pullout force in both the top and bottom mats.

Figure 7.17 shows the reinforcing bar mat forces plotted against the transverse MSE wall displacements for the "top" and "bottom" mats. The ultimate pullout forces are also plotted for comparison. The plots reveal that the mat forces increased to levels significantly greater than the ultimate pullout forces. Eventually, the load values began to peak after a wall displacement of 0.4 in. (10.2 mm) for the "away from cap" mats and 0.14 in. (3.56 mm) for the "near cap" mats. The only exception to this finding is the bottom mat near the pile cap face plotted in Figure 7.17 b). The MSE wall displacements measured at this location were inaccurate as concerns over the string pot placed there were expressed earlier in Section 7.4.5. Typically, the maximum force in the mats is developed with a relatively small wall displacement of 0.2 to 0.3 in. (5 to 8 mm).

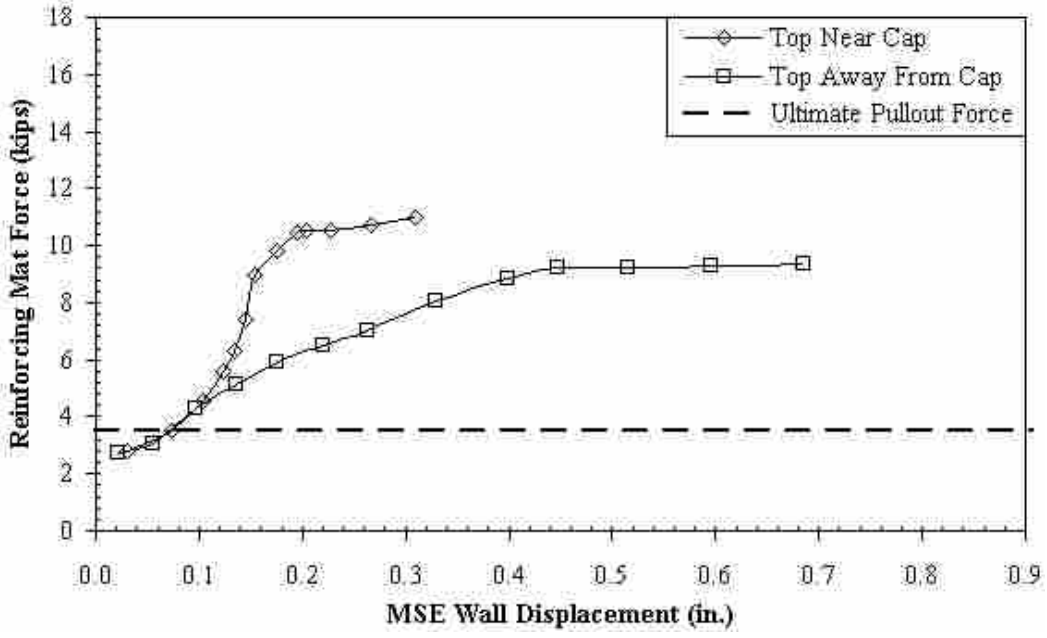

a) Top Reinforcing Mats

Figure 7.17: Reinforcing Mat Force-MSE Panel Displacement Plot for Dense Sand MSE Test

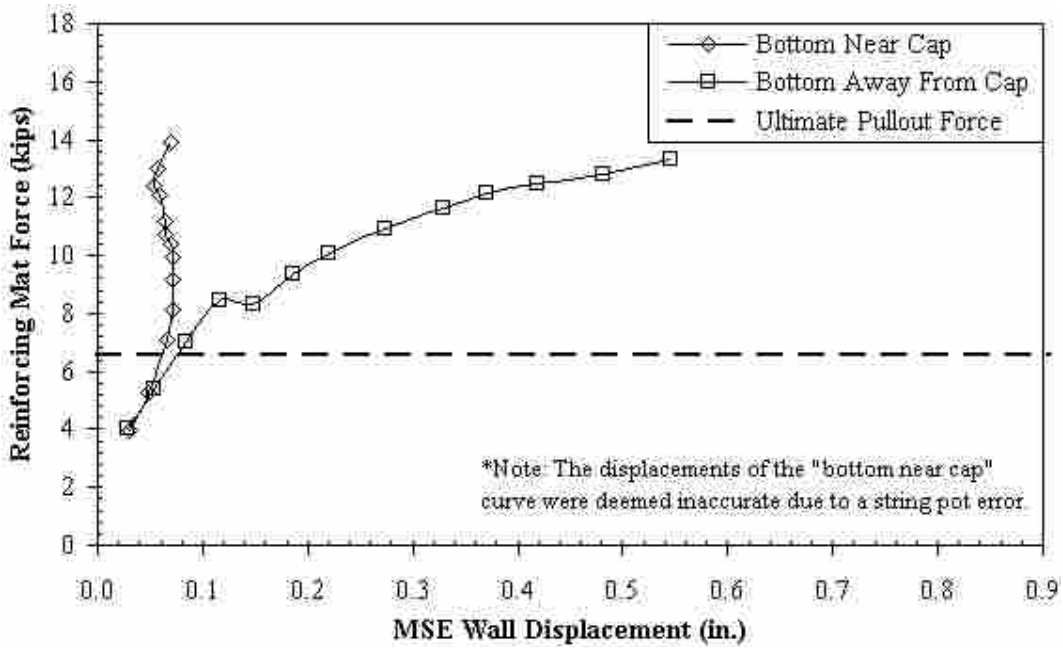

b) Bottom Reinforcing Mats

Figure 7.17 (continued): Reinforcing Mat Force-MSE Panel Displacement Plot for Dense Sand MSE Test

Figure 7.18 shows a plot of the ratio of the pressure on the MSE wingwalls to the pressure on the pile cap face as a function of the distance of the strain gauges on each reinforcing mat from the pile cap face. The pressure on the MSE panels was calculated as the load measured in a reinforcing mat divided by the associated tributary area of the MSE panel of that mat. The load in the bar mat does not include the forces generated from the load test setup before testing started. The pressure on the face of the pile cap was determined by first, assuming the pressure distribution was in a triangular shape, meaning that the pressure was zero at the top of the pile cap and increased linearly to the bottom of the pile cap. Next, the resultant passive earth force was assumed to act at a height of one-third of the pile cap height measured from the bottom of the pile cap, thus allowing the maximum pressure at the base of the pile cap to be calculated. Last, the pressures on the pile cap at the same depths of the reinforcing mats were linearly

interpolated from the maximum cap pressure. The MSE wingwall pressure was divided by the pile cap pressure at each pile cap displacement increment. The median values of all the displacement increments for each reinforcing mat were plotted against the distance of the strain gauges on each reinforcing mat from the pile cap face, and a linear trendline was fitted to the data points.

The maximum pressure ratio value calculated was approximately 0.08 for the dense sand MSE test. A zero pressure ratio is not reached with the trendline for the dense MSE test. This suggests that some pressure acts along the entire length of the wall. The statistical R^2 value for the trendline was approximately 0.175, which shows a small amount of correlation in the pressure ratio-distance from the pile cap relationship.

Figure 7.19 is similar to Figure 7.18, except the pressure data were reduced to remove any opportunity for pullout of the reinforcing mats to affect the pressure ratio relationship. This was accomplished by determining at which lateral wall displacement the mats appear to begin pulling out by plotting the total MSE wall force against the average lateral wall displacement as shown in Figure 6.22. From the plot, a value of 0.2 in. was selected to represent the maximum amount of allowable lateral wall displacement. All of the pile cap displacement increments up to the wall displacement value of 0.2 in. were then used to find the median wall pressure. This reduced the deviation between the pressure ratios and improved the correlation in the relationship between the pressure ratio and distance from the pile cap for the dense sand MSE test. An improved R^2 value of 0.260 was generated. The subsequent maximum pressure ratio was approximately 0.06 with a minimum of about 0.03.

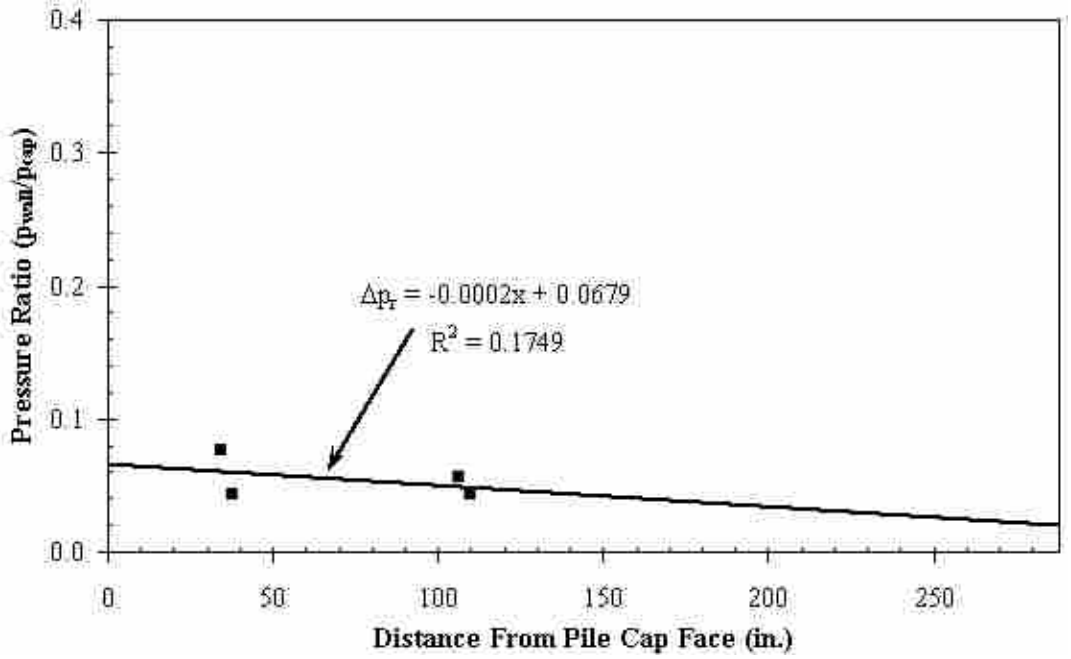

Figure 7.18: Pressure Ratio-Distance Relationship for Dense Sand MSE Test

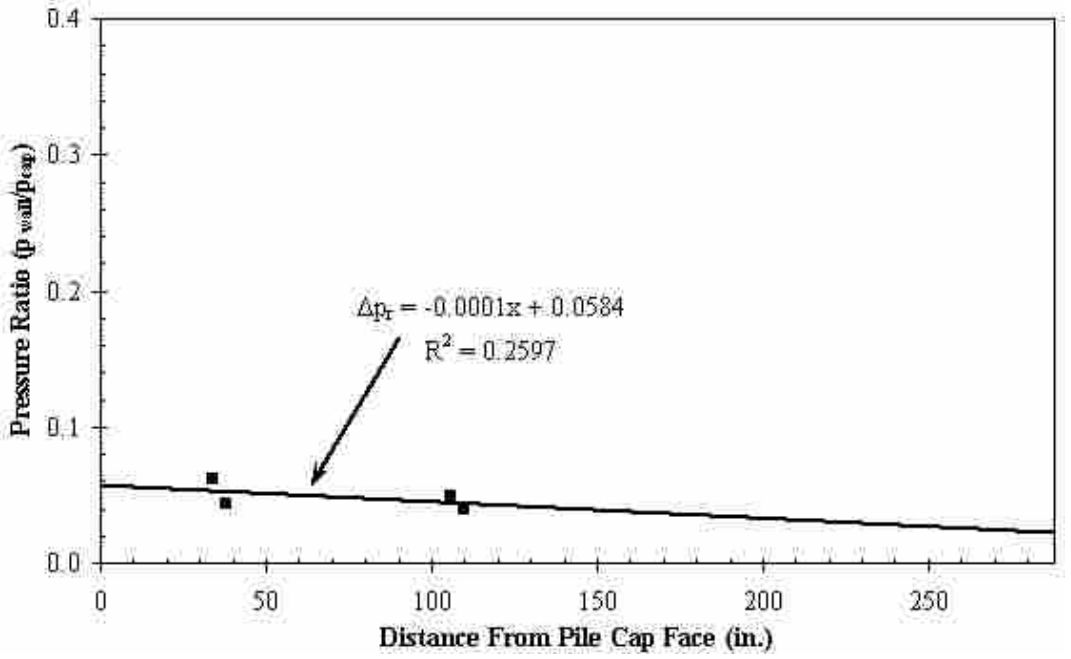

Figure 7.19: Reduced Pressure Ratio-Distance Relationship for Dense Sand MSE Test

8 COMPARISON OF TEST RESULTS

After the completion of field testing, the data collected from all tests were compared and contrasted in several areas, namely: passive force-displacement measured from the actuators, backfill displacement, transverse wingwall displacement, and reinforcing mat forces. This chapter is a summary of that comparison for the following tests: loose sand unconfined (3D), loose sand slip plane (2D), loose sand MSE, dense sand MSE, dense sand unconfined (3D), and dense sand slip plane (2D). As stated previously in Section 1.3, the dense sand unconfined and dense sand slip plane test data were not detailed in this thesis as the two tests were more specifically presented in Bingham (2010). The comparison of the data was focused on the differences between tests with loose and dense backfills.

8.1 Load-Displacement Comparison – Actuators

The passive force-displacement curves for the six tests mentioned in the chapter introduction are plotted in Figure 8.1. The three dense tests show maximum passive force values all greater than 585 kips (2602 kN) with the unconfined (3D) test recording the greatest peak passive force value of approximately 780 kips (3470 kN). The three loose tests are all within a range for the maximum passive force of approximately 290 to 335 kips (1290 to 1490 kN) with the unconfined test providing the lowest maximum passive force.

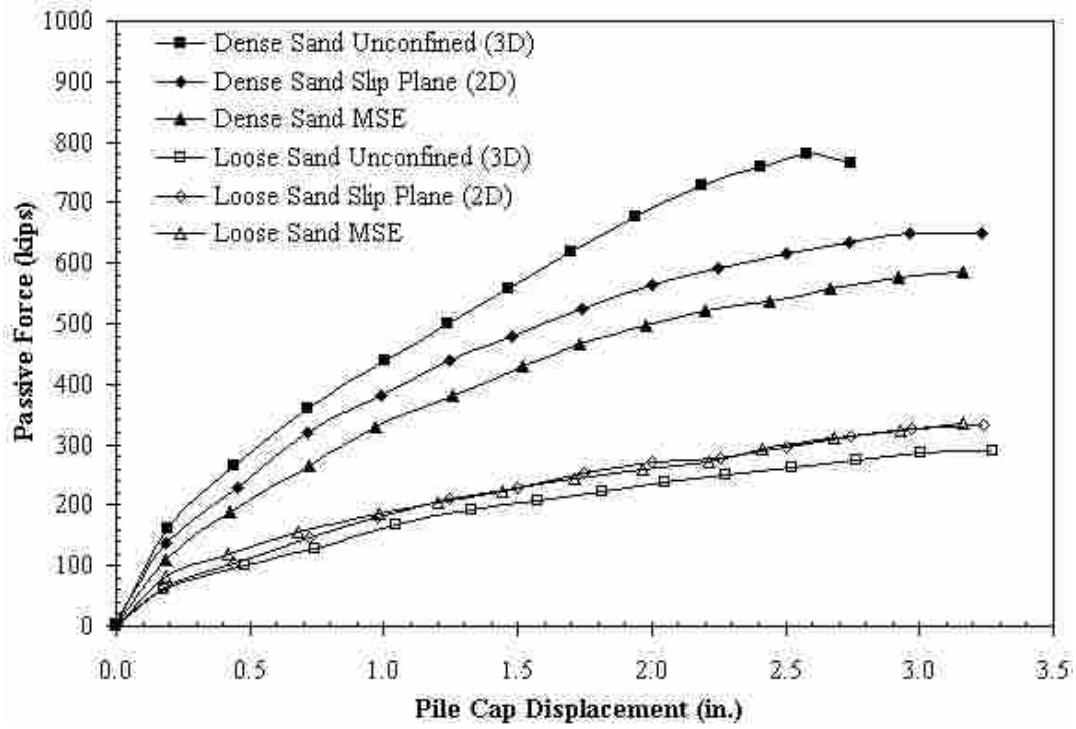

Figure 8.1: Comparison of Passive Force-Displacement Curves for all Loose and Dense Tests

For the unconfined tests, no wingwalls were used to limit the 3D end effects from the pile cap, thus increasing the effective width of the pile cap to approximately 18 ft (5.49 m) for the loose test and 22 ft (6.71 m) for the dense test. The increased effective width influenced the increase in the peak passive force for the dense unconfined test, but for the loose unconfined test, no increase in the peak force was noticeable. The peak passive force of the loose unconfined test was the lowest of the three loose tests. This suggests that the 3D end effects from the pile cap play a larger role in developing the maximum passive force with denser soils than with looser soils. In dense sands, a general shear failure would be expected whereas local shear failure would be expected in loose sands. Therefore, greater benefits in lateral resistance resulting from 3D end effects would be expected from general shear failure in dense sands than local shear failure in loose sands.

From Figure 8.1, it can also be seen that the slip plane (2D) and MSE tests for both loose and dense backfills produced similar force-displacement curves. The loose slip plane and MSE tests recorded a peak passive force value within three kips (13 kN) of each other. The maximum passive force developed during the dense MSE test was about 90% of the maximum passive force developed during the dense slip plane test. This helped to validate the use of the plane strain friction angle for predicting the passive force-deflection curves of all of the slip plane and MSE tests.

Table 8.1 shows a comparison between the passive forces per effective pile cap width for all six tests. To compute the passive force per effective width, the maximum passive force recorded from each passive force-displacement curve was divided by its effective pile cap width. The effective pile cap width was found by multiplying the Brinch Hansen 3D correction factor by the actual pile cap width of 11 ft (3.35 m). Only for the two unconfined tests was the effective pile cap width larger than the actual pile cap width.

The largest passive force per effective width value of 59.1 kip/ft (863 kN/m) developed during the dense sand slip plane test. A slightly lower value was found for the dense sand MSE test. The loose and dense unconfined tests recorded the lowest values. With a wider effective width, the passive resistance generated by the backfill was spread out over a larger width, thus lowering the passive force per effective width value. The greater passive force per width values for the slip plane and MSE cases, relative to the unconfined cases, points out the increased passive resistance provided by the plane strain-like failure geometry. Although the soil is essentially the same in both cases, the plane strain-like failure geometry leads to greater resistance per width. It is also important to note that the passive force per effective width values for the loose tests were lower than the dense tests by approximately 40 to 50%.

Table 8.1: Comparison of Passive Force per Effective Width of Pile Cap

Test	Effective Pile Cap Width (ft)	Max. Passive Force (kips)	Max. Passive Force/ Effective Width (kip/ft)	Δ_{max}/H
Dense Unconfined (3D)	22	781	35.5	0.042
Dense Slip Plane (2D)	11	650	59.1	0.049
Dense MSE	11	586	53.2	0.048*
Loose Unconfined (3D)	18	289	16.1	0.050*
Loose Slip Plane (2D)	11	332	30.2	0.049*
Loose MSE	11	335	30.5	0.048*

* There is a small increasing slope in passive force-deflection curve at max. displacement

Table 8.1 also shows the ratio between the maximum pile cap deflection and the pile cap height (Δ_{max}/H) for each test. The Δ_{max}/H values for all of the tests are in the 0.04 to 0.05 range. These results follow the high end of the range suggested by AASHTO guidelines stated previously in Section 2.1, however, there was a small upward slope on some of the passive force-displacement curves at the peak displacement reached during the tests.

8.2 Backfill Displacement

The comparison graphs shown in Figure 8.2 plot the absolute longitudinal displacement of the backfill during testing. To simplify the plots, backfill displacements from selected pile cap displacements increments are shown. The results of the loose tests show, in relation to the dense tests, that more backfill displacement occurred close to the pile cap while at distances greater than about 10 ft (3.05 m), the material was less affected by the cap movement and little displacement occurred. The dense material showed a steady and consistent decrease in displacement level throughout the load tests. These observations can be understood by recognizing that loose sands tend to exhibit a local shear failure while dense sands develop a general shear failure condition. General shear failure would lead to movement throughout the failure zone while local shear failure would primarily lead to movement close to the pile cap.

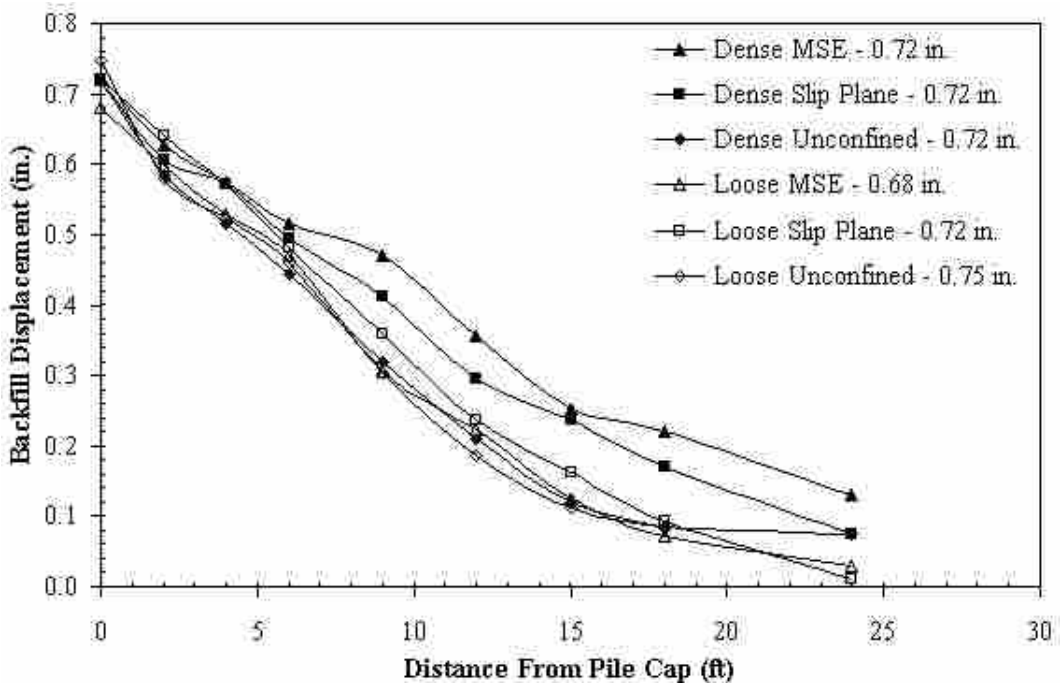

a) 0.75-in Pile Cap Displacement Increment

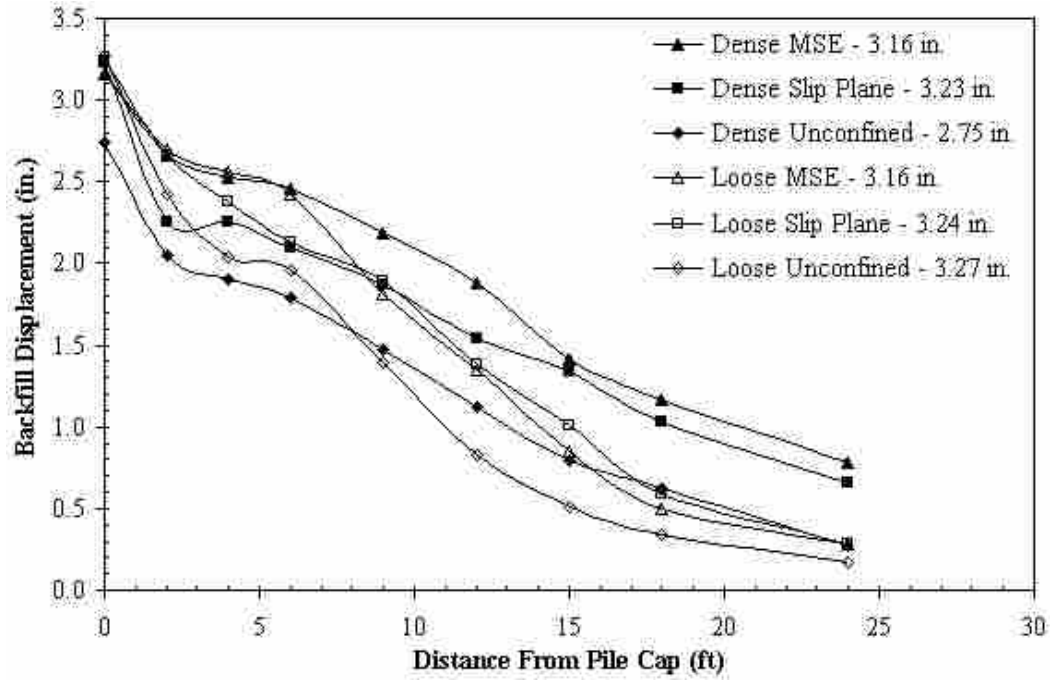

b) Last Pile Cap Displacement Increment

Figure 8.2: Absolute Backfill Displacement Versus Distance from the Pile Cap for Six Field Tests at Two Selected Displacement Increments

The compressive strain rates within the backfill were also calculated and plotted for each field tests based on data from Figure 8.2. The comparison graphs in Figure 8.3, below, show a plot of the backfill strain at the 0.75-in. and last displacement increments of the pile cap. The strain is shown as a function of distance from the pile cap. Each of the plots show an overall trend of having a high strain rate across the first 2 ft (0.61 m) of backfill, followed by a considerable decreased in the 2 to 6 ft (0.61 to 1.83 m) range. An increase again occurred typically after 6 ft (1.83 m) from the pile cap face, which then tended to decrease until the final stake is reached at a distance of 24 ft (7.32 m) from the pile cap. The overall trend also shows that the loose tests experience more strain as compared to the dense tests in the 2 ft to 12 ft range. This suggests that the loose material was generally compressing in this range while the dense sand was compressing less and translating more as would be expected for a general shear failure.

To monitor the vertical backfill displacement, the elevation of the backfill was surveyed before and after each test was completed. Elevations were taken on the grid which was painted on the backfill. The graphs in Figure 8.4 show the change in elevation measured in inches for each test in a side-by-side comparison. Positive contour values show upward movement.

In Figure 8.4 a) and b), the loose and dense unconfined (3D) tests, heave was seen to occur out 11 ft (3.35 m) from the center of the pile cap in both west and east directions in circular patterns. The largest heave measurements occurred approximately 4 ft (1.22 m) from the pile cap face during the loose test and 8 ft (2.44 m) from the pile cap face during the dense test. The dense test produced increased heave values overall in comparison with the loose test and an increased maximum heave value of approximately 2.50 in. (64 mm). The maximum heave value recorded from the loose test was approximately 2.0 in. (51 mm).

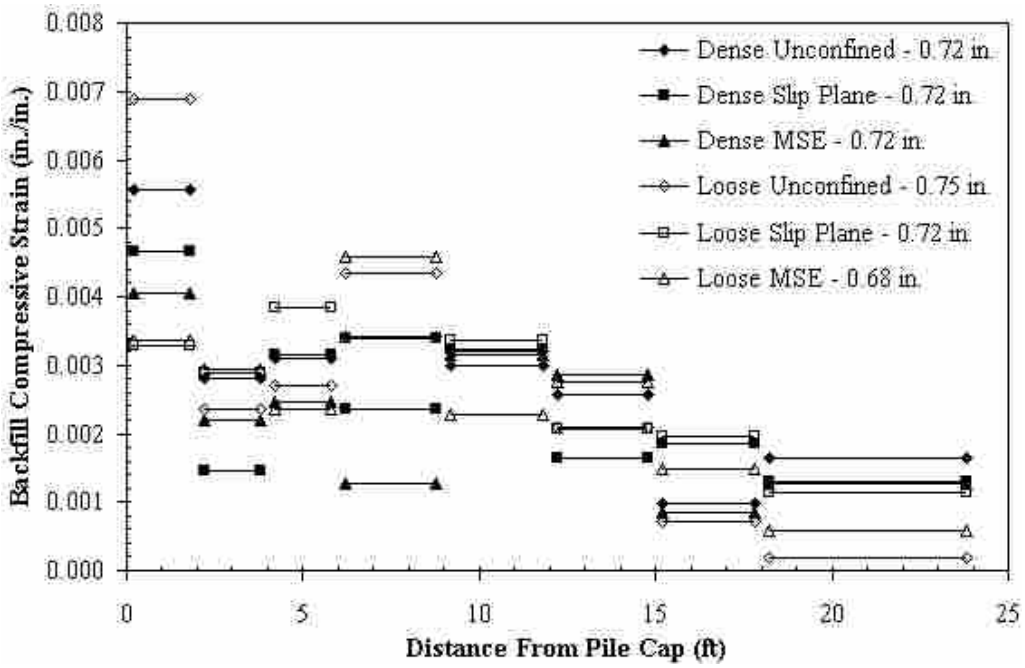

a) 0.75-in. Pile Cap Displacement Increment

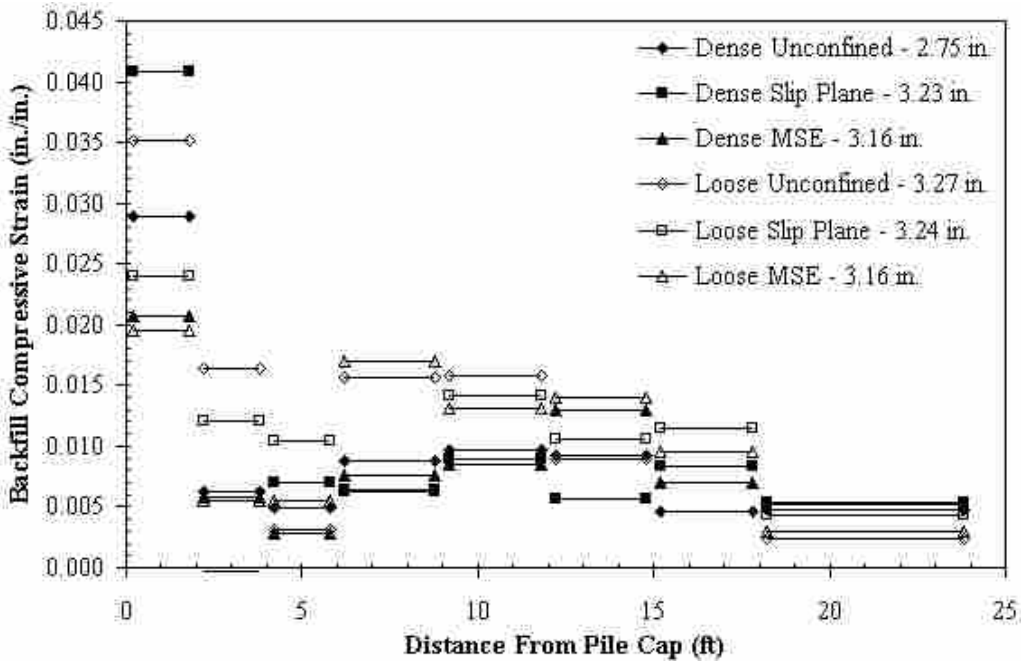

b) Last Pile Cap Displacement Increment

Figure 8.3: Comparison of Backfill Compressive Strain Versus Distance from the Pile Cap for Six Field Tests

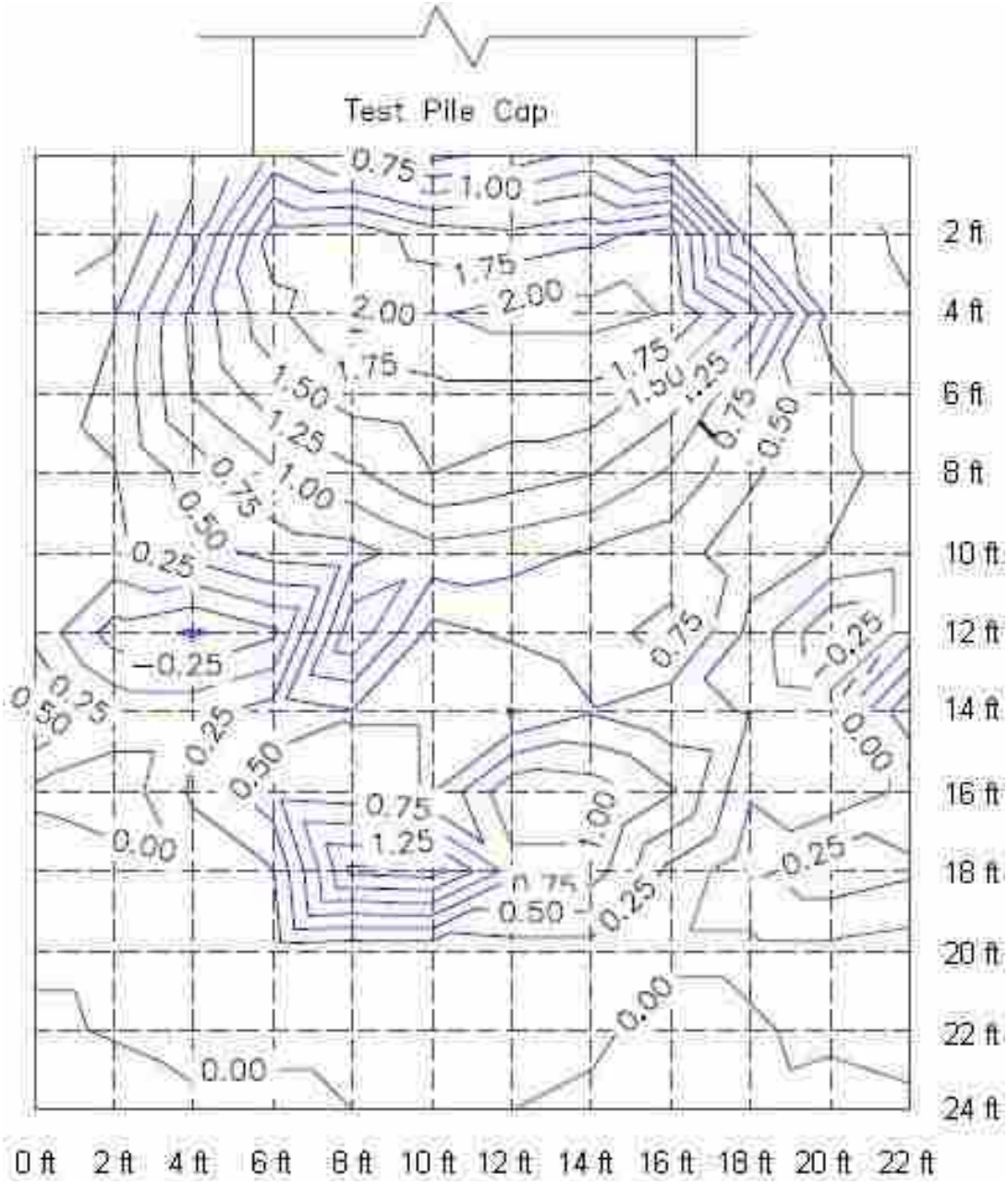

a) Loose Sand Unconfined (3D)

Figure 8.4: Backfill Elevation Change Maps for Six Field Tests

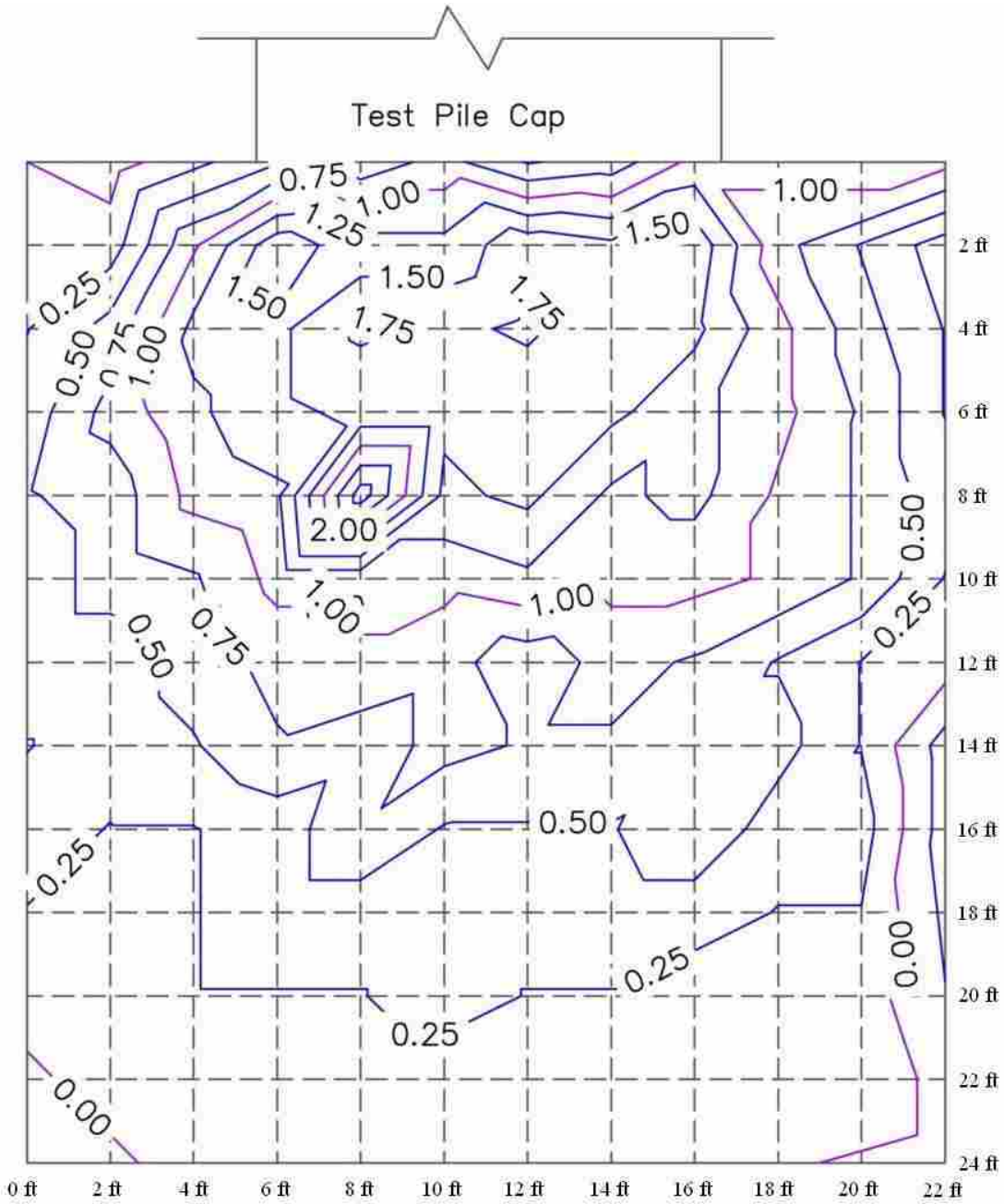

b) Dense Sand Unconfined (3D)

Figure 8.4 (continued): Backfill Elevation Change Maps for Six Field Tests

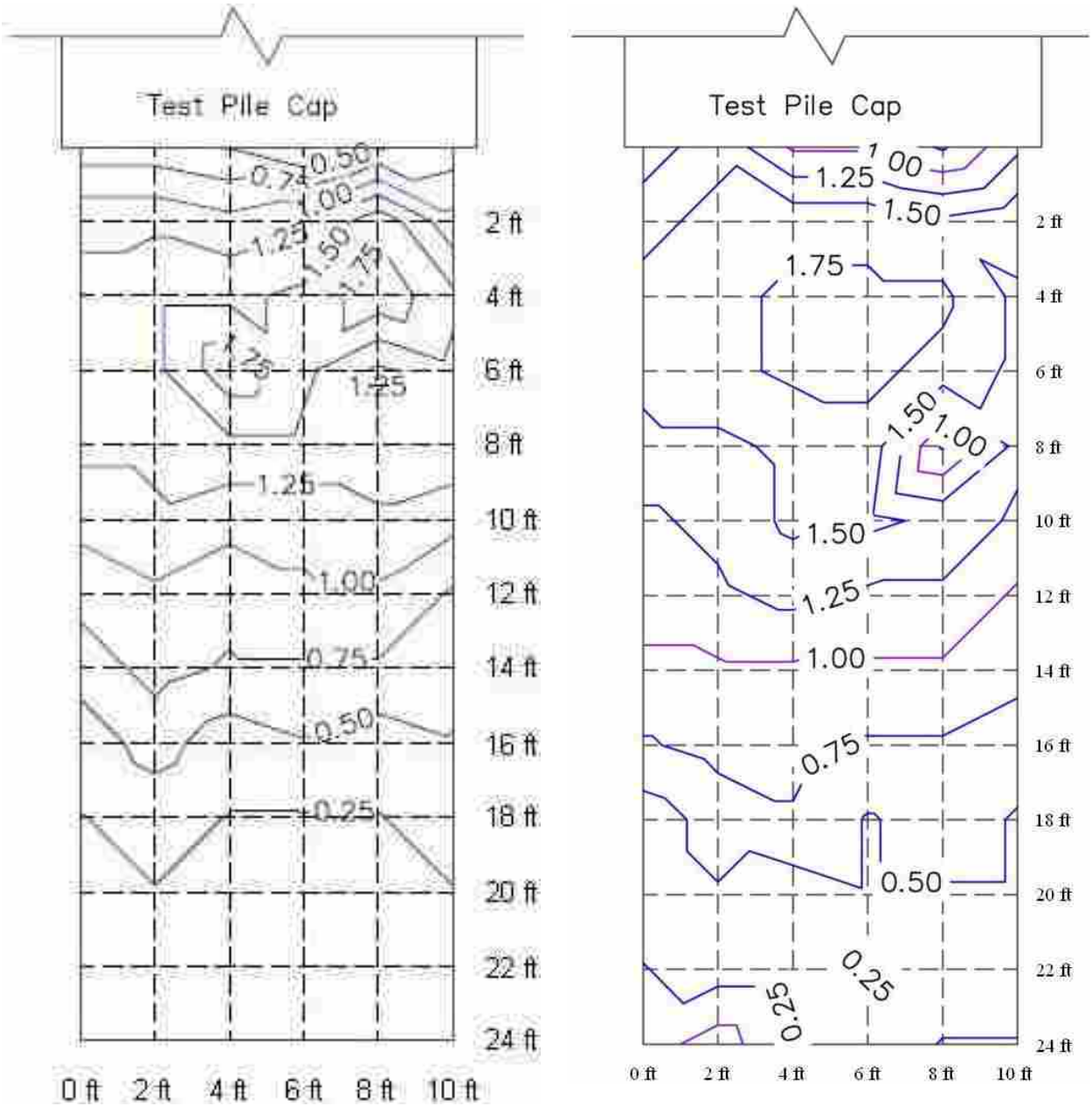

c) Loose Sand Slip Plane (2D) **d) Dense Sand Slip Plane (2D)**

Figure 8.4 (continued): Backfill Elevation Change Maps for Six Field Tests

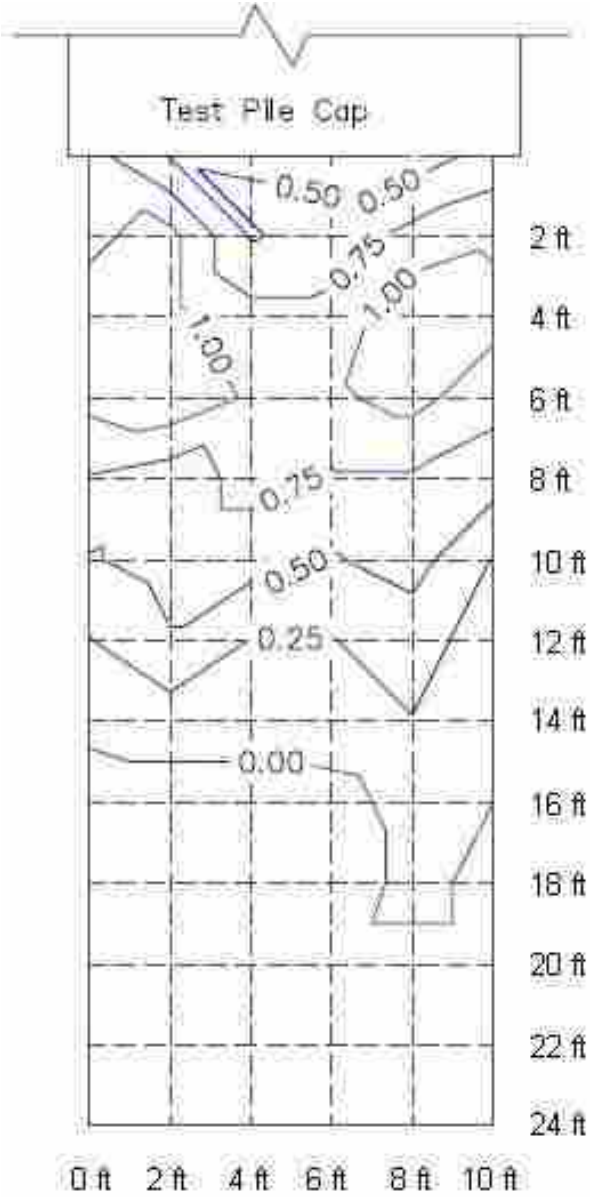

e) Loose Sand MSE

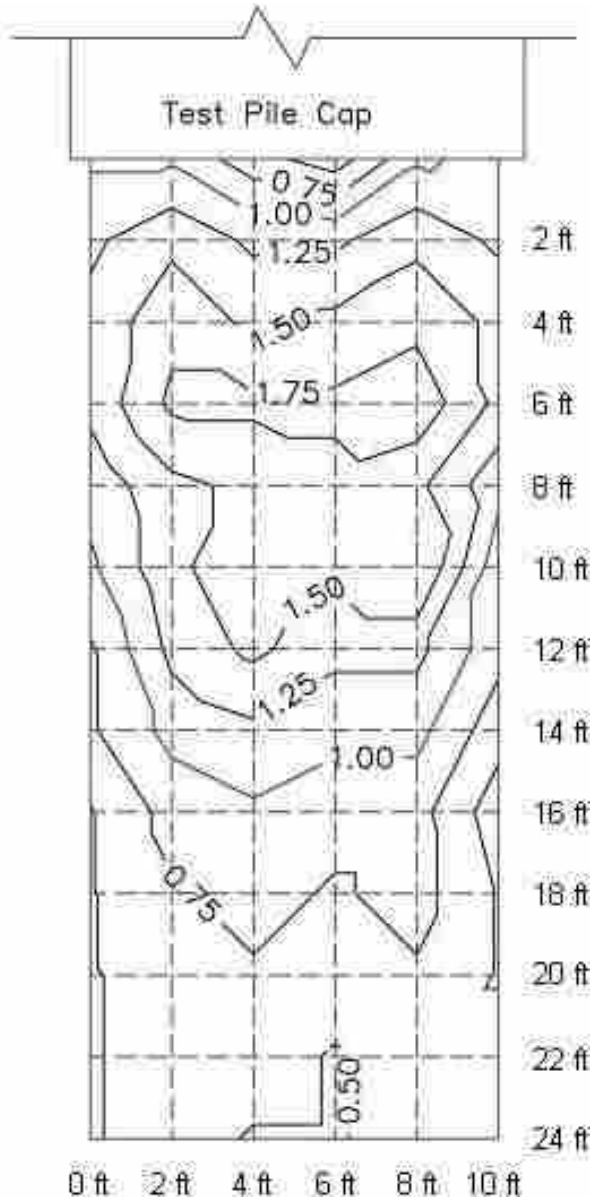

f) Dense Sand MSE

Figure 8.4 (continued): Backfill Elevation Change Maps for Six Field Tests

The heave contouring for the loose and dense slip plane (2D) tests was very similar. Again, the overall pattern of the contouring was a semi-circular shape truncated by the side isolation panels. A maximum value of heave measured 1.75 in. (44 mm) during both slip plane tests at about the same location of 4 to 6 ft (1.22 to 1.83 m) from the pile cap face.

When comparing the heave contours of the loose and dense MSE tests in Figure 8.4 e) and f), one will notice the same semi-circular pattern to the contouring as mentioned for the slip plane tests. The difference in the maximum heave values between the loose and dense MSE tests was also noticeable during the MSE tests like the unconfined tests. The loose MSE test showed a maximum heave value of approximately 1.0 in. (25.4 mm) while the dense MSE test showed a maximum heave value of approximately 1.75 in. (44 mm). The zone of heaving for the dense MSE test also extended to a greater distance in comparison with the loose MSE test. The zero heave contour developed at distance of about 15 ft (4.57 m) from the pile cap face during the loose MSE test while the same contour is not visible in the gridded backfill zone for the dense MSE test.

Visual inspections of the backfill surface during each test were completed to record the cracking history of the backfill after each displacement increment. The plots below in Figure 8.5 show a side-by-side comparison of the cracking history for each test. The cracking pattern of the unconfined tests showed strong evidence of the 3D edge effects of the pile cap with limited cracking occurring in the middle of the backfill. The cracks extend to a greater width for the dense test than for the loose test. The slip plane tests produced cracking patterns that were mostly longitudinal in direction concentrated in between the side isolation panels most likely resulting from the plane strain-like backfill conditions provided by the side panels. Cracking was relatively minimal in both cases when compared to the unconfined tests.

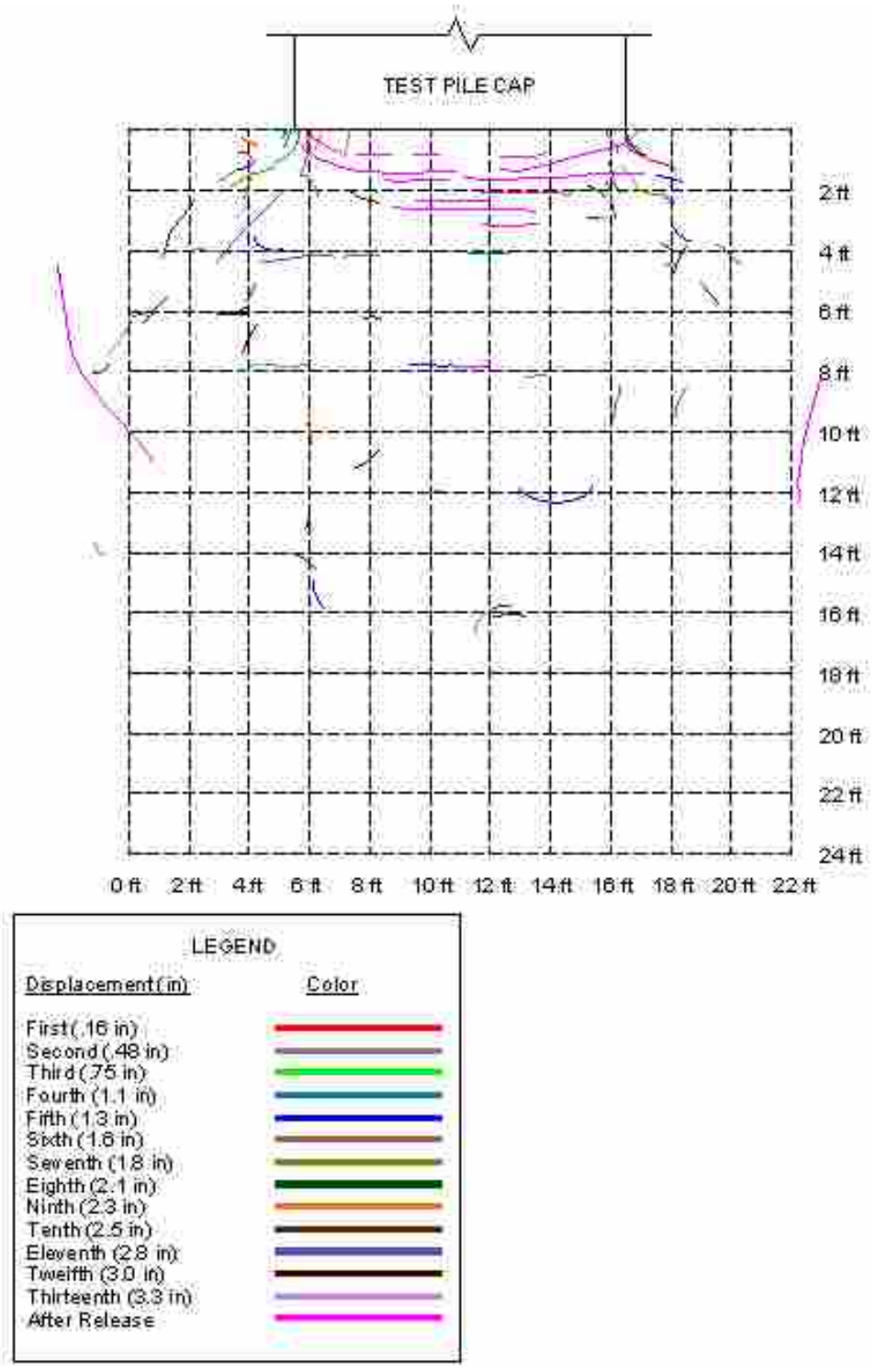

a) Loose Sand Unconfined (3D)

Figure 8.5: Comparison of Observed Backfill Cracking During Six Field Tests

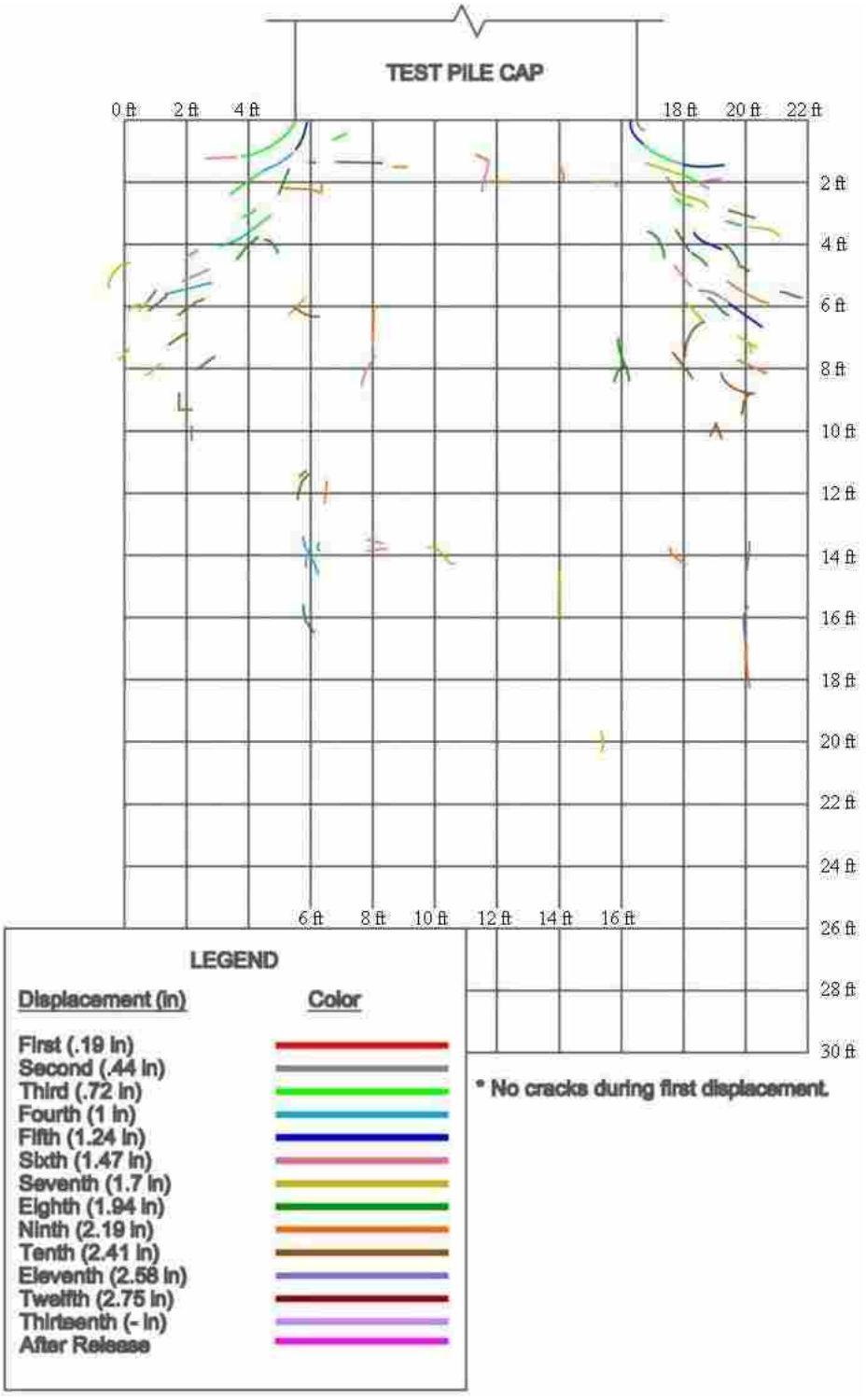

b) Dense Sand Unconfined (3D)

Figure 8.5 (continued): Comparison of Observed Backfill Cracking During Six Field Tests

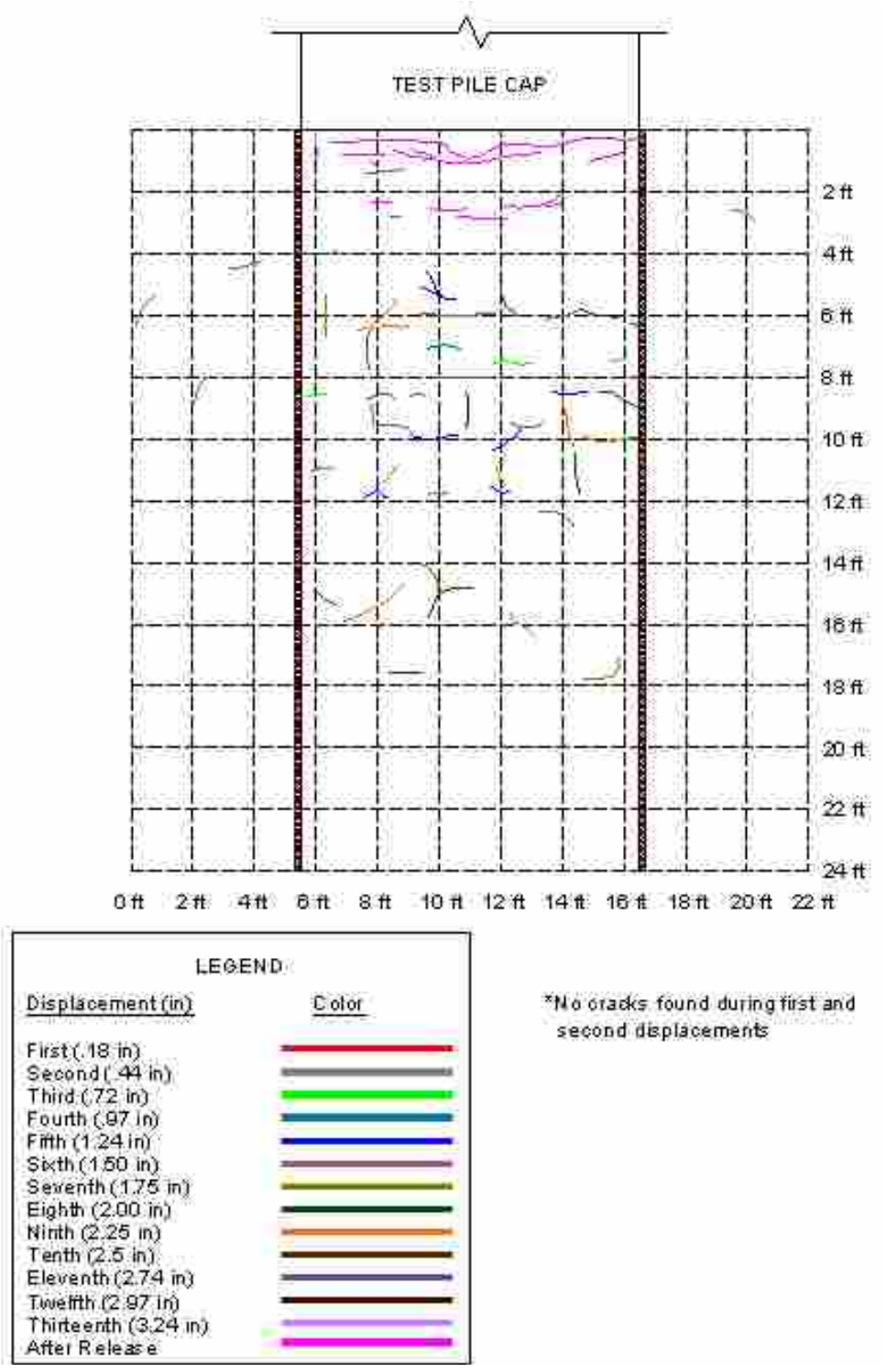

c) Loose Sand Slip Plane (2D)

Figure 8.5 (continued): Comparison of Observed Backfill Cracking During Six Field Tests

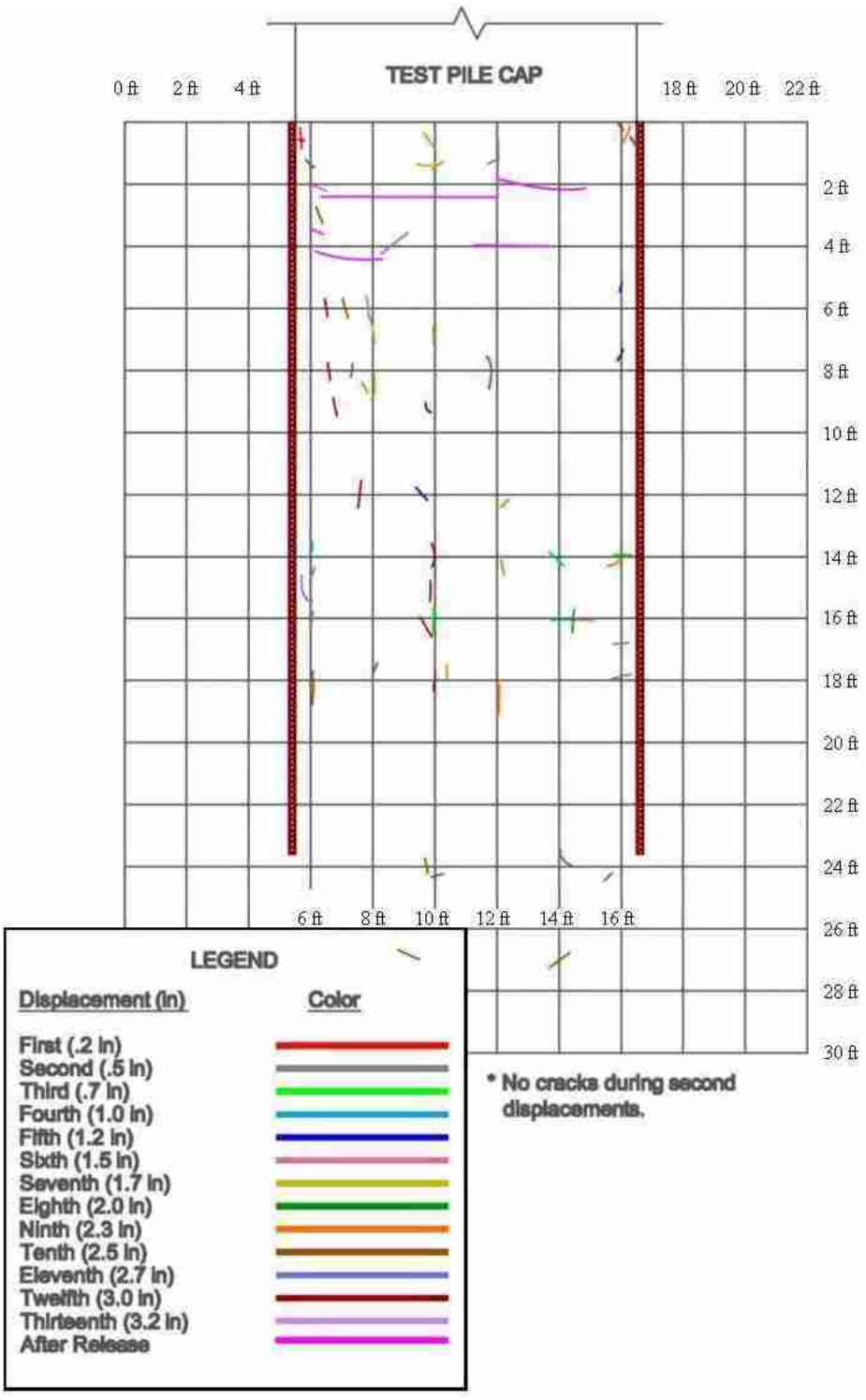

d) Dense Sand Slip Plane (2D)

Figure 8.5 (continued): Comparison of Observed Backfill Cracking During Six Field Tests

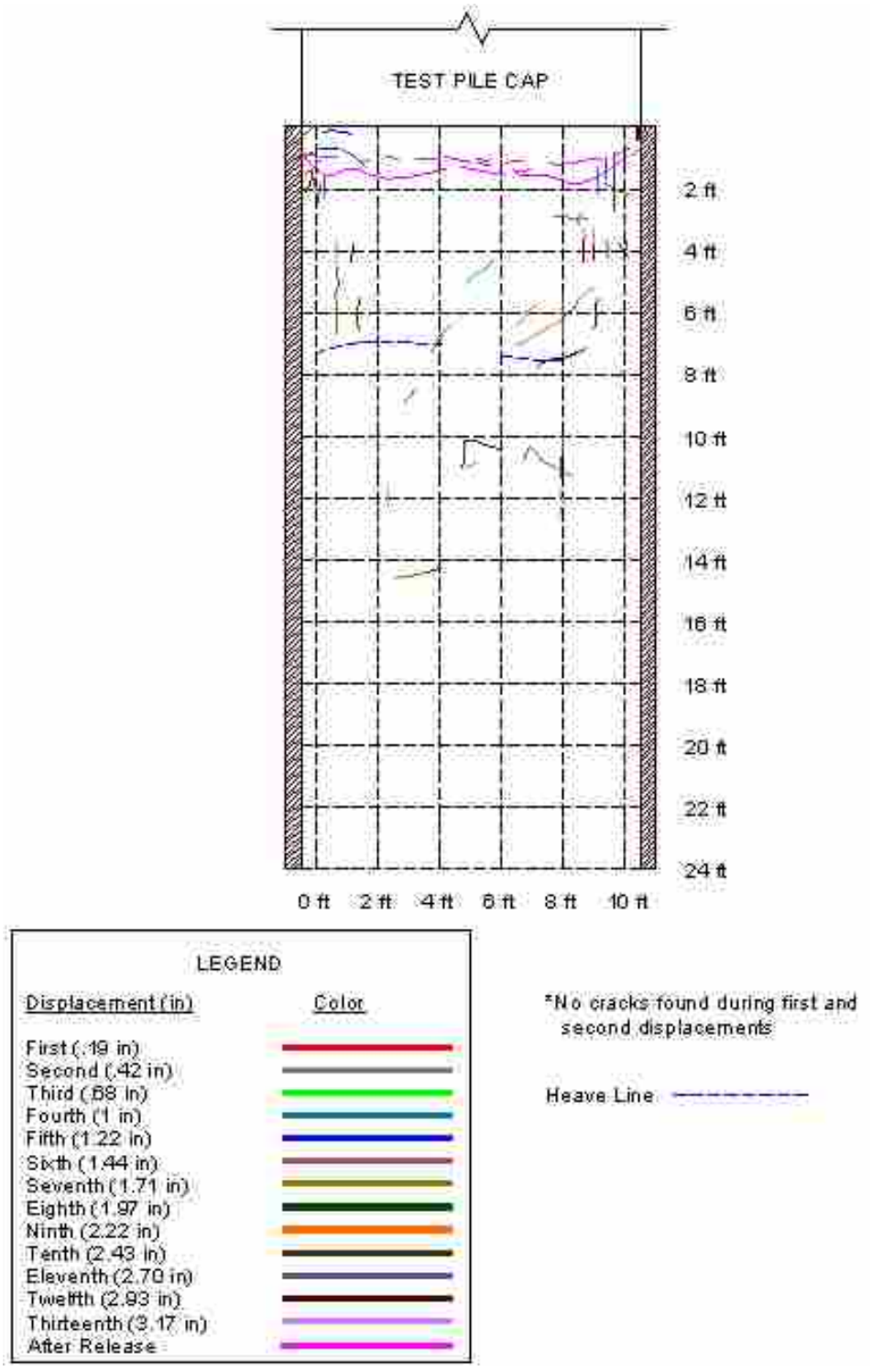

e) Loose Sand MSE

Figure 8.5 (continued): Comparison of Observed Backfill Cracking During Six Field Tests

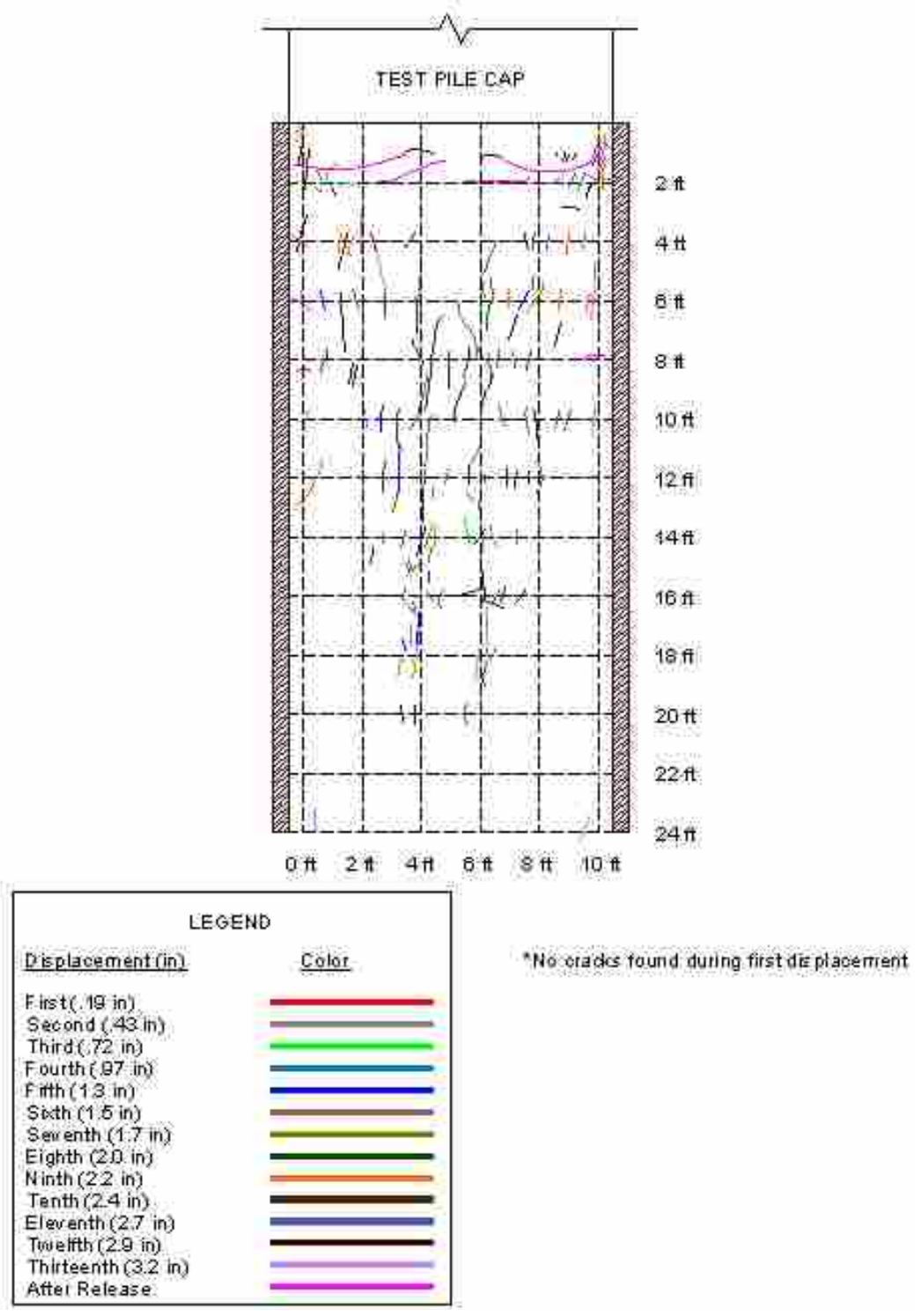

f) Dense Sand MSE

Figure 8.5 (continued): Comparison of Observed Backfill Cracking During Six Field Tests

The cracking patterns produced during the MSE tests also show a majority of the cracks developing the in longitudinal direction, parallel to the wingwalls. The dense MSE test showed an increased number of cracks relative to the loose test. The majority of the cracks ran perpendicular to the end of the reinforcing mats. The increased backfill density along with the pullout effects of the reinforcing mats placed in the backfill were the cause of the increased crack density near the center of the backfill grid for the dense MSE test.

8.3 Transverse Wingwall Displacement

A comparison of the various wingwall displacement results for the two slip plane (2D) tests and the two MSE tests are shown below. The panels used in the loose slip plane test were instrumented with three string pots on the outside of the panels located just above the backfill surface at distances of 2, 6, and 12 ft (0.61, 1.83, 3.66 m) from the pile cap face. The panels used in the dense slip plane test were instrumented with four string pots on the outside of the panels located at distances of 2, 6, 12, and 18 ft (0.61, 1.83, 3.66, and 5.50 m) from the pile cap face. The MSE walls, for both the loose and dense cases, were instrumented with four string pots located approximately over the center of the four reinforcing mats connected to the wall.

Figure 8.6 shows the outward movement of the plywood panels recorded at each string pot as a function of distance from the pile cap for both slip plane tests. The plots are in plan view with the pile cap on the left being loaded to the right. The maximum wall displacement of the loose test was approximately 0.16 in. (4 mm) at a distance of 6 ft (1.83 m) from the pile cap face. The maximum wall displacement of the dense test was approximately 0.22 in. (5.6 mm) at the same distance from the pile cap face despite recording a greater maximum passive load of

650 kips (2891 kN) during the dense test relative to a maximum passive load of 332 kips (1477 kN) during the loose test.

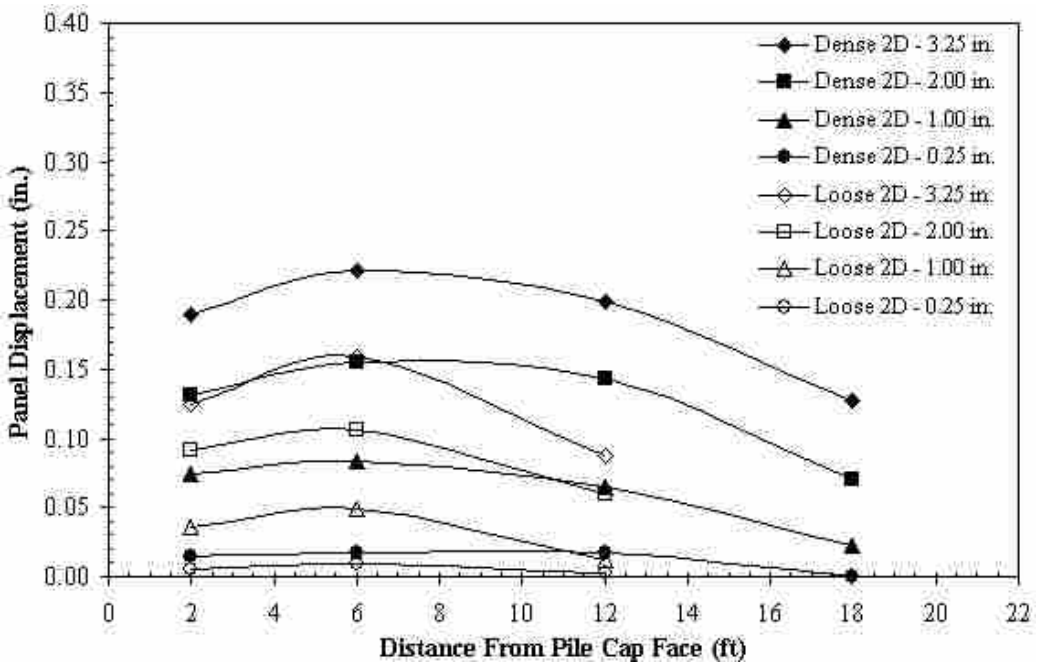

Figure 8.6: Comparison of Loose Slip Plane (2D) and Dense Slip Plane (2D) Outward Panel Displacement Plotted Against Distance From the Pile Cap Face

Figure 8.7 shows the passive force as a function of the outward panel displacement recorded by each string pot for the loose and dense plane strain tests. The plot clearly demonstrates that the plywood panels experienced less deflection as the distance from the pile cap increased. The three string pots located at distances of 2, 6, and 12 ft during the dense slip plane test all exhibit similar non-linear, or hyperbolic, shaped passive load-displacement curves, while the string pot located at 18 ft exhibits a much more dramatic non-linear shaped curve with much less displacement. The plot also shows that more deflection will occur as more force is placed on the pile cap. This reflects the effect the increase in backfill unit weight had on the load and displacement levels that are shown when comparing the dense to loose tests.

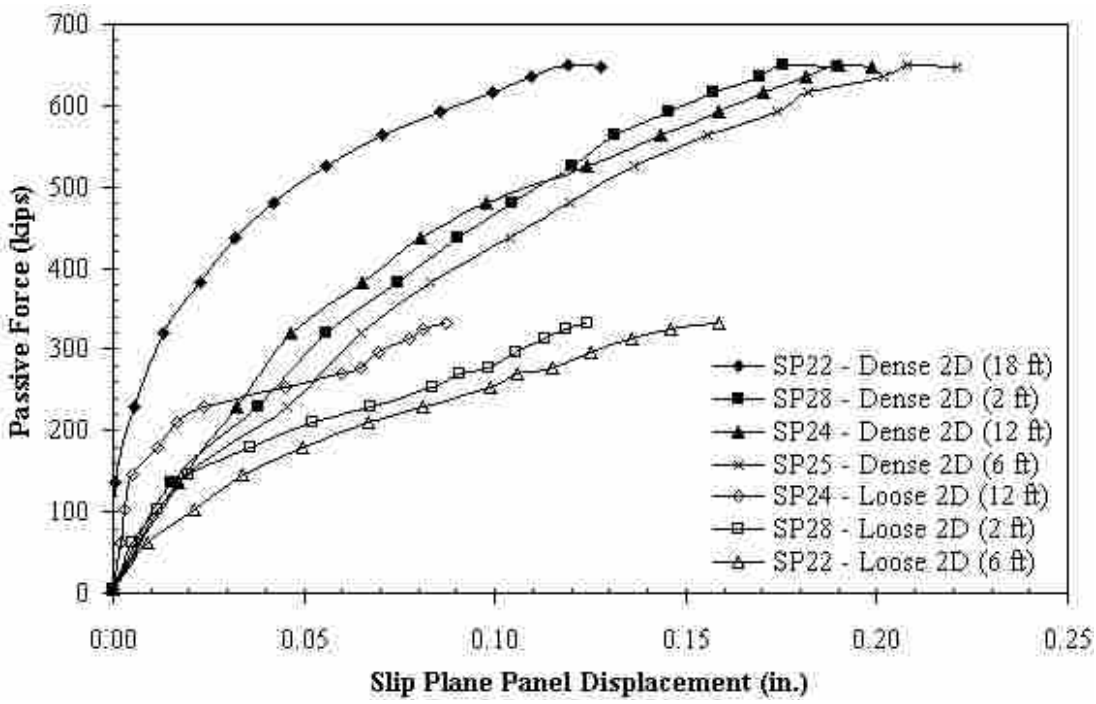

Figure 8.7: Comparison of Loose and Dense Slip Plane (2D) Passive Force Plotted Against Individual String Pot Displacements

Figure 8.8 shows the outward displacement of the loose and dense MSE tests as a function of backfill depth for each displacement increment. The plots appear as if looking at a cross-sectional view of the backfill and walls. Two plots are shown for the loose MSE test representing two pairs of string pots at 21 and 103 in. (0.53 and 2.62 m) from the pile cap face. Only one plot is shown for the dense MSE test for the string pot pair at 103 in. from the pile cap face. One of the string pots from the other pair did not record properly during the entire dense MSE test; therefore, no plot is shown for the pair at 21 in. from the pile cap face. A depth of zero inches represents the backfill surface. A depth of 68 in. (1.73 m) represents the bottom of the MSE walls.

The string pot located at 22 in. (0.56 m) below the ground surface in Figure 8.8 a) recorded a maximum displacement of 0.53 in. (13.5 mm). The string pot located at the same

location during the dense MSE test recorded a maximum displacement of 0.31 in. (7.9 mm). (A plot of this string pot is not shown because the string pot below did not work properly during the dense MSE test.) The MSE wingwalls during the loose test displaced more than the wingwalls did during the dense test. This observation is confirmed by comparing Figure 8.8 b) and c), which represent the MSE wingwall displacement as recorded by the pair of string pots located at a distance of 103 in. from the pile cap face. The maximum displacements of the loose MSE test at 22 in. and 52 in. (1.32 m) below the ground surface are 0.81 in. and 0.60 in. (20.6 mm and 15.2 mm), respectively. The maximum displacements of the dense MSE test at 22 in. and 52 in. below the ground surface are 0.68 in. and 0.55 in. (17.3 and 14.0 mm, respectively. The denser backfill provided more resistance to pullout, thus reducing the MSE wingwall displacement.

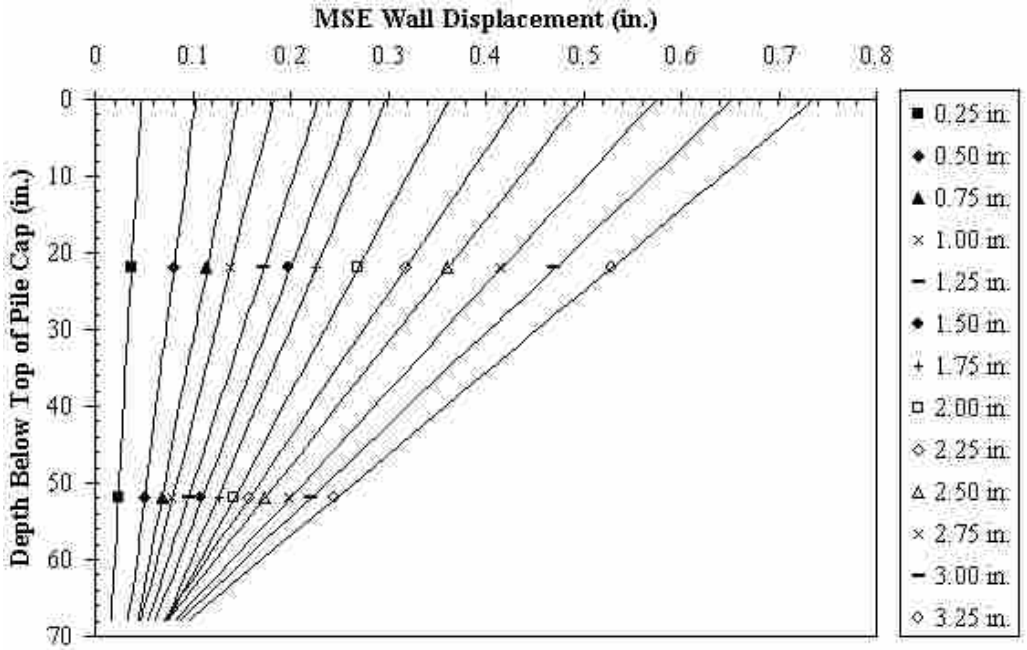

a) Loose MSE Test at 21 in. From Pile Cap Face

Figure 8.8: Comparison of Loose and Dense MSE Test Outward MSE Wall Displacement Plotted Against Depth Below the Top of the Pile Cap

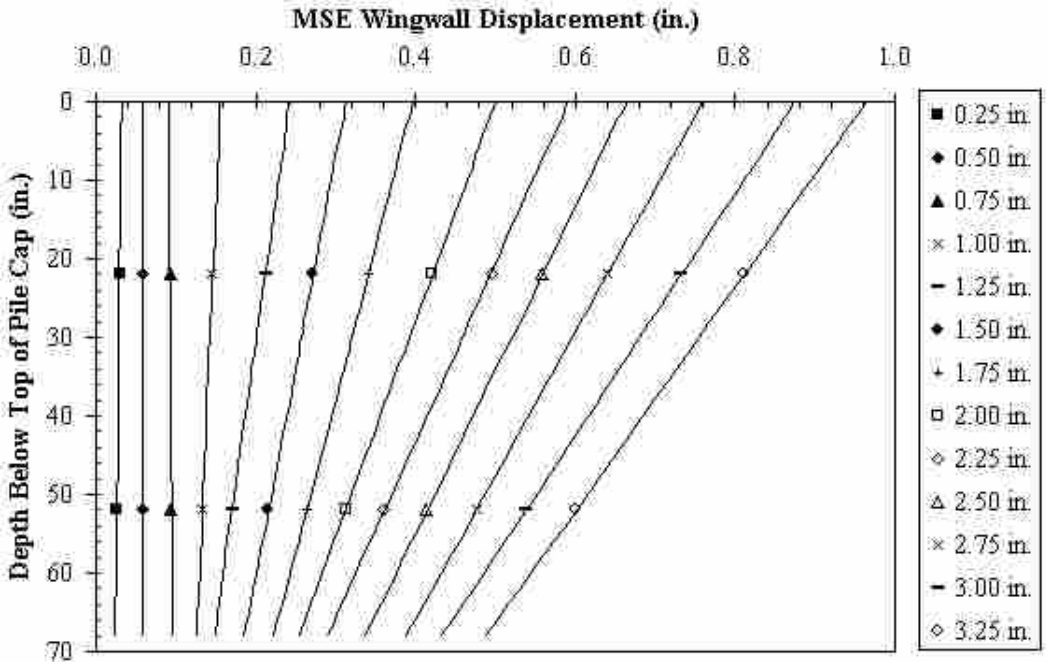

b) Loose MSE Test at 103 in. From Pile Cap Face

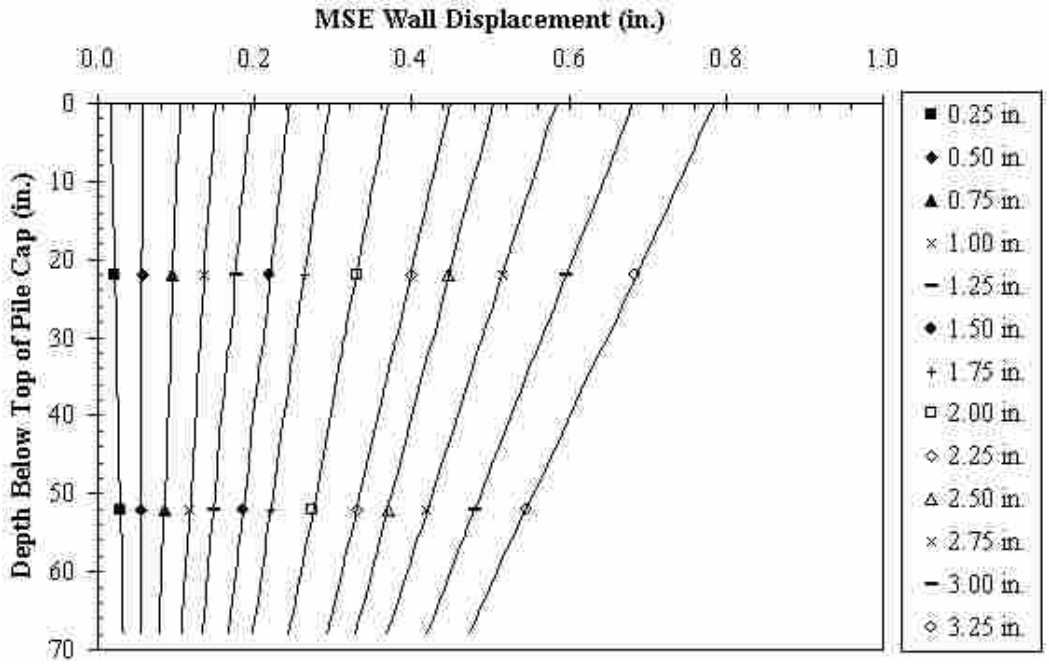

c) Dense MSE Test at 103 in. From Pile Cap Face

Figure 8.8 (continued): Comparison of Loose and Dense MSE Test Outward MSE Wall Displacement Plotted Against Depth Below the Top of the Pile Cap

In addition to the displacement information provided in Figure 8.8, Figure 8.9 is a comparison of the rotation angle of the MSE wingwalls during testing for both the loose and dense MSE tests. The plot supports the observation above in that the MSE walls displaced and rotated less during the dense test than during the loose test. The maximum rotation angle for the loose MSE test was approximately 0.6 degrees. The maximum rotation angle for the dense MSE test was approximately half of the angle for the loose test at 0.3 degrees. The more rotation and displacement observed from the MSE walls, the greater the possibility that pullout or failure might occur. The denser backfill material was a means for increased capacity from the MSE reinforcement.

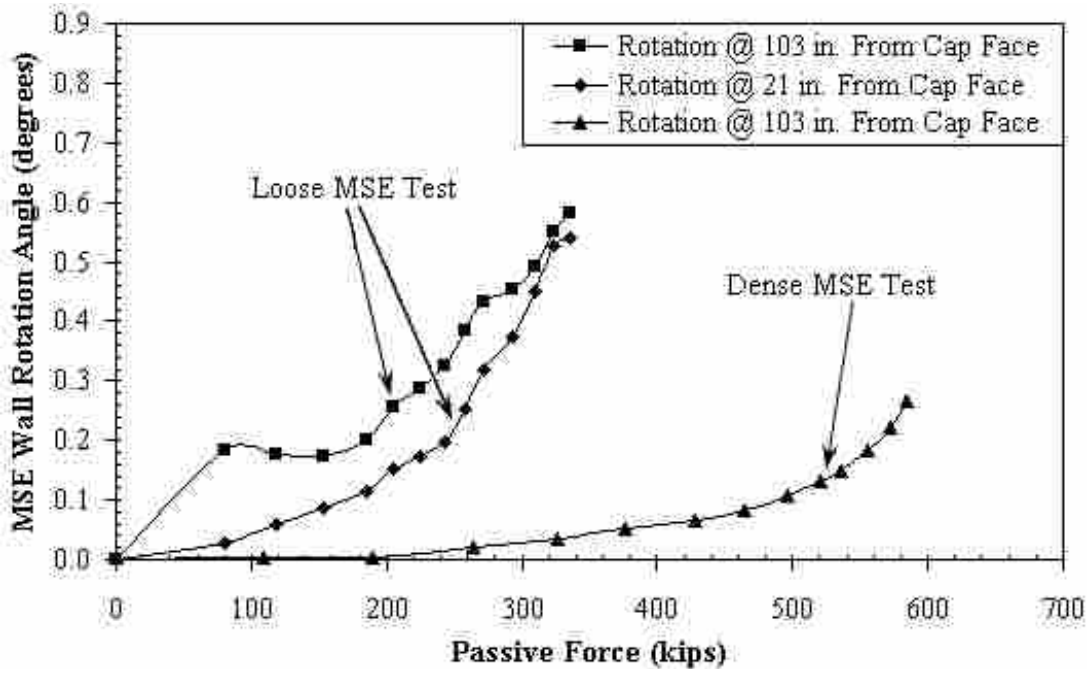

Figure 8.9: Comparison of MSE Wingwall Rotation Angle for Loose and Dense MSE Tests Plotted Against Passive Force

Figure 8.10 provides a view of the transverse wingwall displacement for the two slip plane and two MSE tests plotted as a function of the longitudinal pile cap displacement. The

transverse wall displacements shown were taken at locations along the MSE wingwalls and plywood panels that were level with the ground surface. For the slip plane cases, the wall containing the dense backfill deflected somewhat more than the wall containing the loose backfill. However, considering that the load applied by the actuator was about twice as large for the pile cap with dense backfill as for that with loose backfill, the dense wall is still considerably stiffer. In addition, it can be seen that the dense MSE wingwalls deflected less per pile cap displacement increment than did the loose MSE wingwalls. The MSE wingwalls deflected more than the slip plane walls indicating that the bar mat reinforcements did not provide the same confinement as having soil on the outside of the wall.

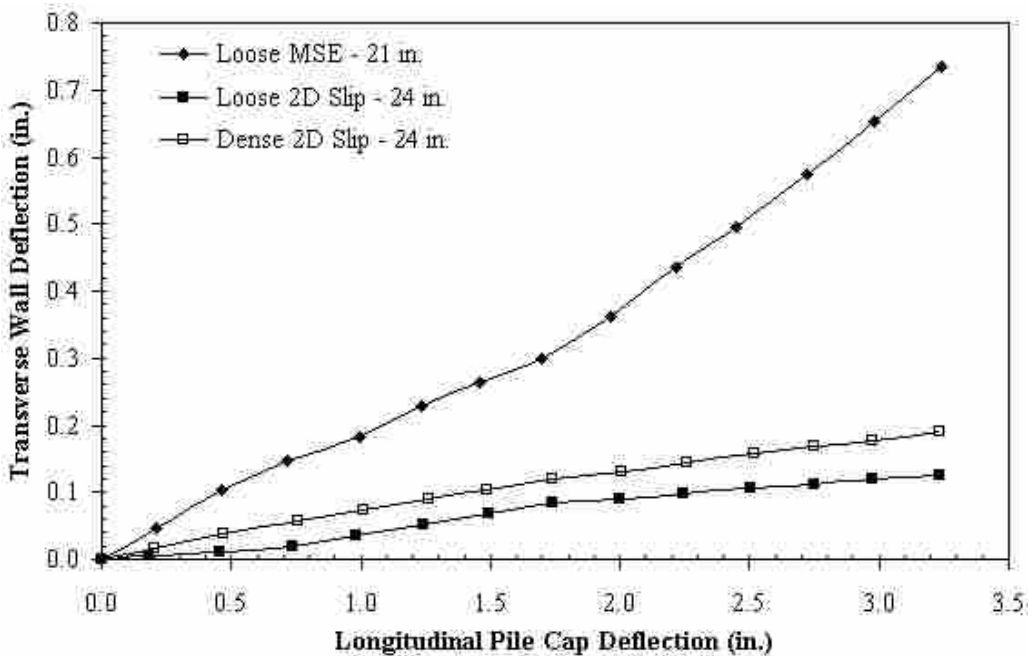

a) Transverse Wall Displacement at 21 in. and 24 in. From the Pile Cap Face

Figure 8.10: Comparison of the Transverse Wall Displacement as a Function of Longitudinal Cap Displacement at Two Distances From the Pile Cap Face

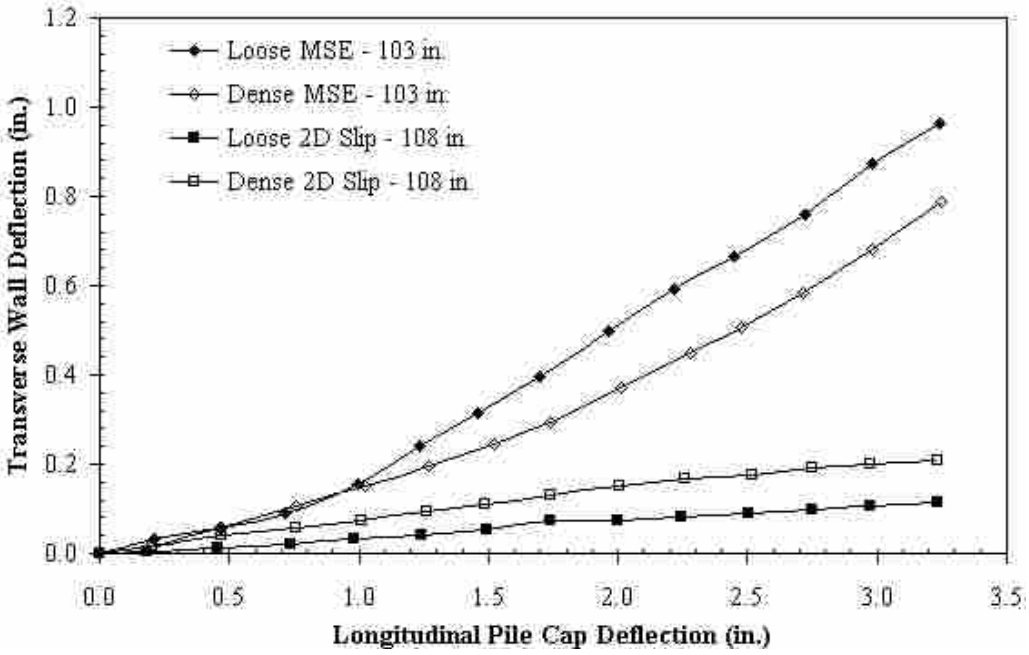

b) Transverse Wall Displacement at 103 in. and 108 in. From the Pile Cap Face

Figure 8.10 (continued): Comparison of the Transverse Wall Displacement as a Function of Longitudinal Cap Displacement at Two Distances From the Pile Cap Face

8.4 Reinforcing Mat Force Results

The reinforcing mats used during the loose and dense MSE tests were instrumented with strain gauges to record the strain from which the forces placed on the mats while the pile cap was laterally loaded were calculated. This section compares the total load computed for the reinforcing mats, including the construction loads, and the ratio of the lateral pressure placed on the MSE wingwalls to the lateral pressure placed on the pile cap of the two MSE tests conducted. Earlier discussions of the strain results and how the force in the mats was calculated for the MSE tests can be found in Sections 6.4.6 and 7.4.6.

Figure 8.11 and Figure 8.12 are plots of the force calculated on the top reinforcing mats compared to the ultimate pullout forces at the 0.5-in. and 3.0-in. displacement increments for the

loose and dense MSE test. Figure 8.13 and Figure 8.14 are plots of the force calculated on the bottom reinforcing mats compared to the ultimate pullout forces at the 0.5-in. and 3.0-in. displacement increments for the loose and dense MSE test. Each marker in the plots represents the location of a set of strain gauges. The graphs which plot data from the upper bar mats placed at a depth of 1.83 ft (0.56 m) below the top of the pile cap are referred to as "top." Graphs which plot data from the lower bar mats placed at a depth of 4.33 ft (1.32 m) below the top of the pile cap are referred to as "bottom." The center of the mats described as "near cap" were located at a distance of 3 ft (0.91 m) from the pile cap face while the center of the mats described as "away from cap" were located at a distance of 9 ft (2.74 m) from the pile cap face. The scale of each set of graphs was kept consistent for easy comparison.

The dashed line in the plots represents the ultimate pullout force of the mat. The line was calculated according to NHI guidelines with the appropriate backfill parameters for both tests. The force value was greatest at the beginning of the mats and then tapered to zero until the total length of the bar mat was reached. The ultimate pullout force of the top mats for the loose and dense cases was 3.28 kips and 3.54 kips (14.6 and 15.7 kN), respectively, with an average factor of safety (FS) of 1.38. The ultimate pullout force of the bottom mats for the loose and dense cases was 6.07 kips and 6.55 kips (27.0 and 29.1 kN), respectively, with an average FS of 1.90.

The graphs show that the calculated force in the mats increased above the ultimate pullout force as the displacement increment increased from 0.5 in. to 3.0 in., except in the top mats of the loose MSE test. The increase in force appears to approximately double the ultimate pullout force for the dense tests. This shows that NHI guidelines may be conservative in computing the force in bar mats for dense sands, especially at large displacement increments.

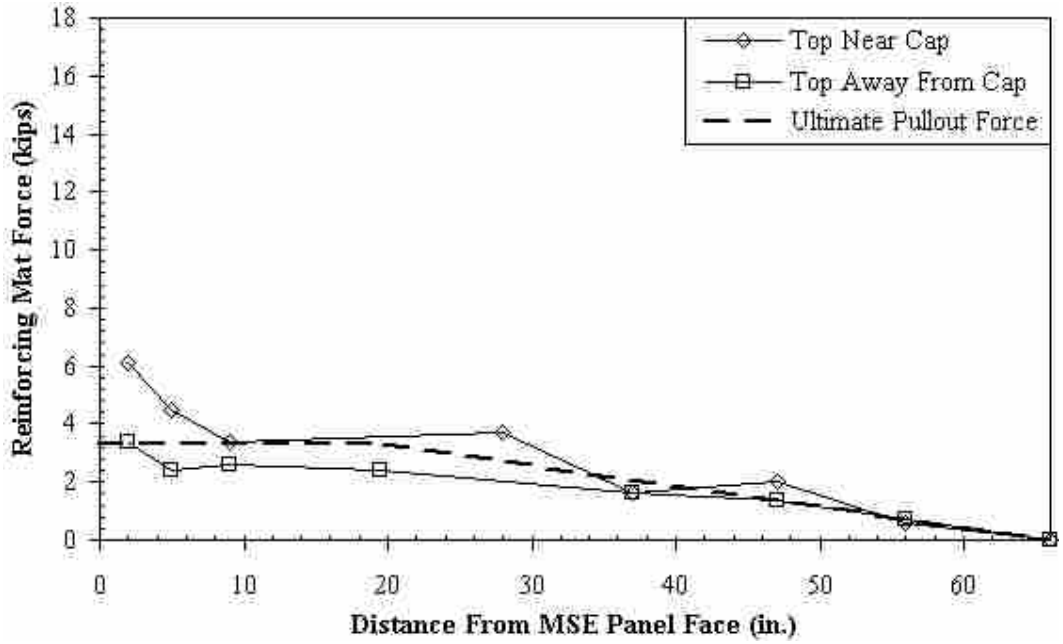

a) Loose MSE Test 0.5-in. Pile Cap Displacement Increment

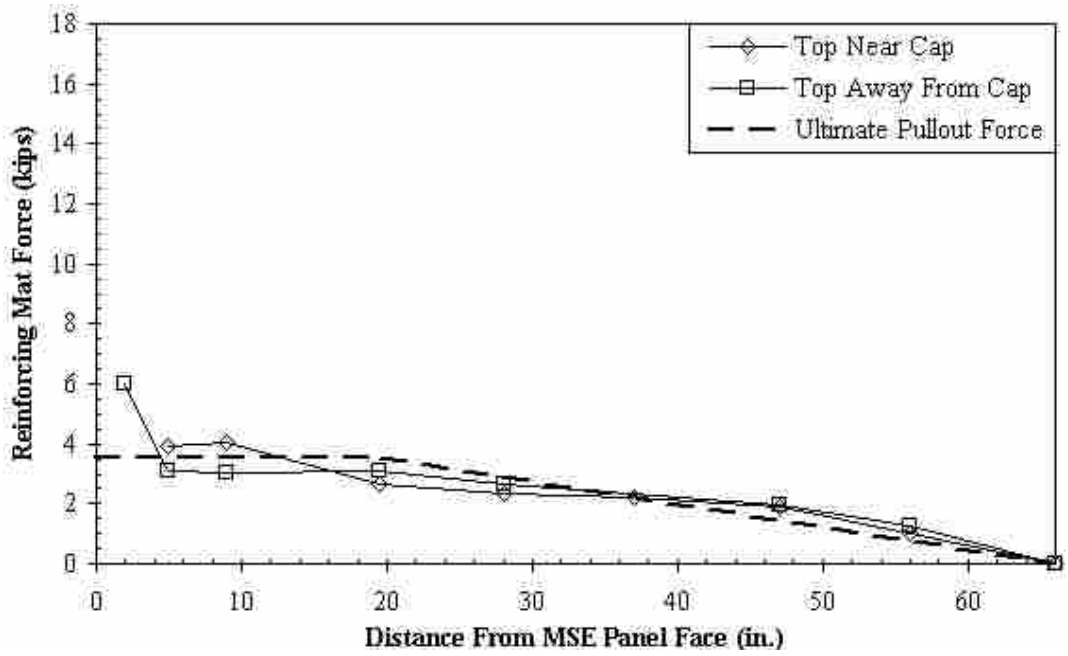

b) Dense MSE Test 0.5-in. Pile Cap Displacement Increment

Figure 8.11: Comparison of the Calculated Force in the Top Reinforcing Mats During the 0.5-in. Displacement Increment for the Loose and Dense Sand MSE Test

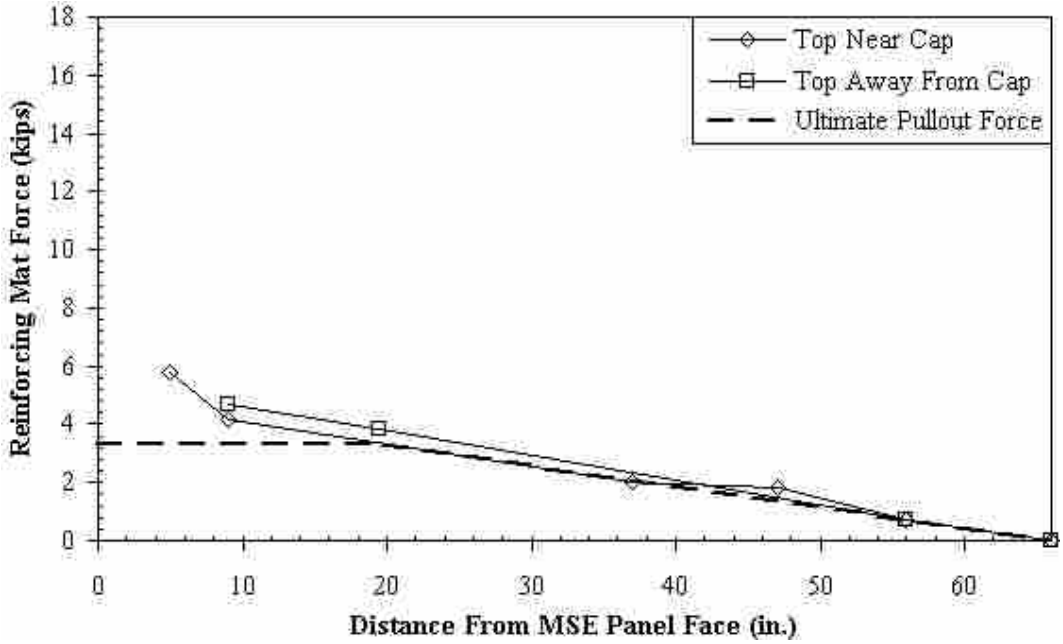

a) Loose MSE Test 3.0-in. Pile Cap Displacement Increment

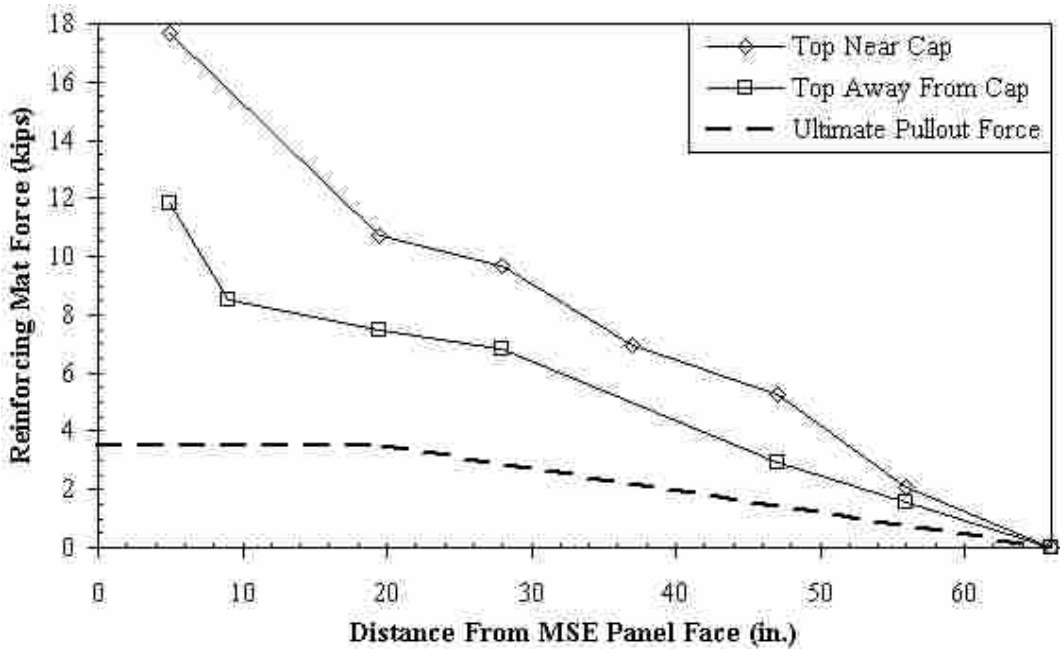

b) Dense MSE Test 3.0-in. Pile Cap Displacement Increment

Figure 8.12: Comparison of the Calculated Force in the Top Reinforcing Mats During the 3.0-in. Displacement Increment for the Loose and Dense Sand MSE Test

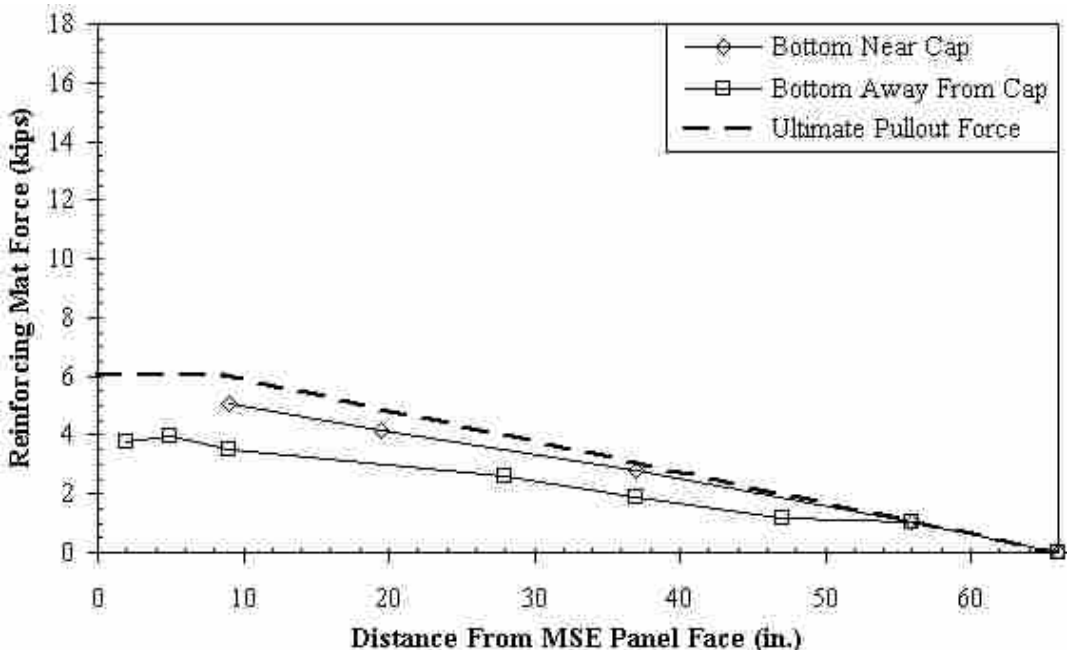

a) Loose MSE Test 0.5-in. Pile Cap Displacement Increment

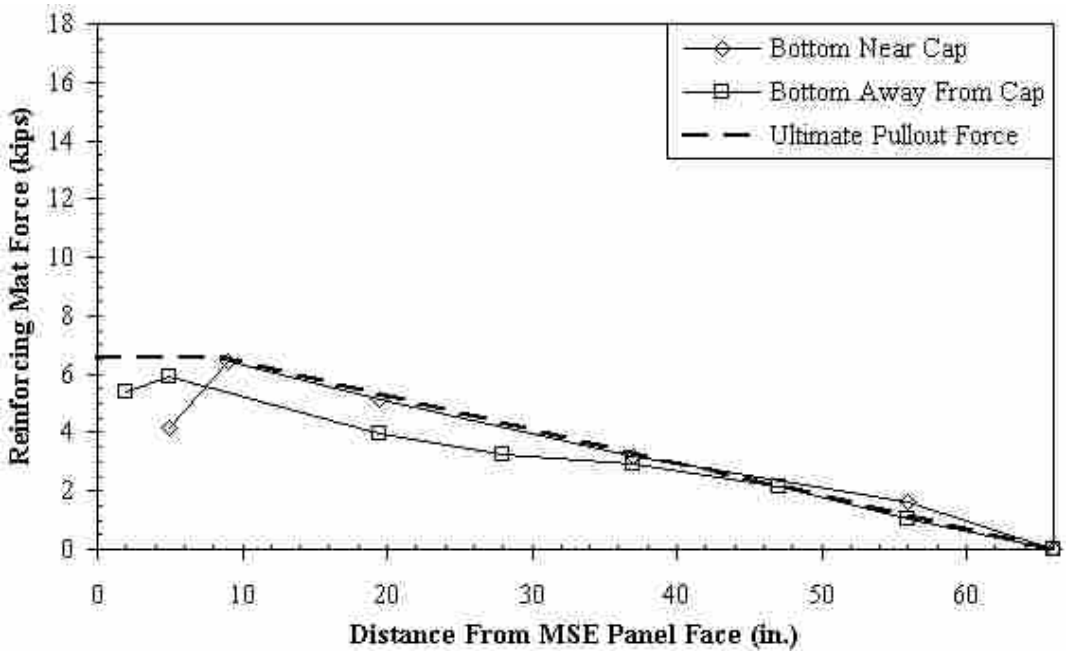

b) Dense MSE Test 0.5-in. Pile Cap Displacement Increment

Figure 8.13: Comparison of the Calculated Force in the Bottom Reinforcing Mats During the0.5-in. Displacement Increment for the Loose and Dense Sand MSE Test

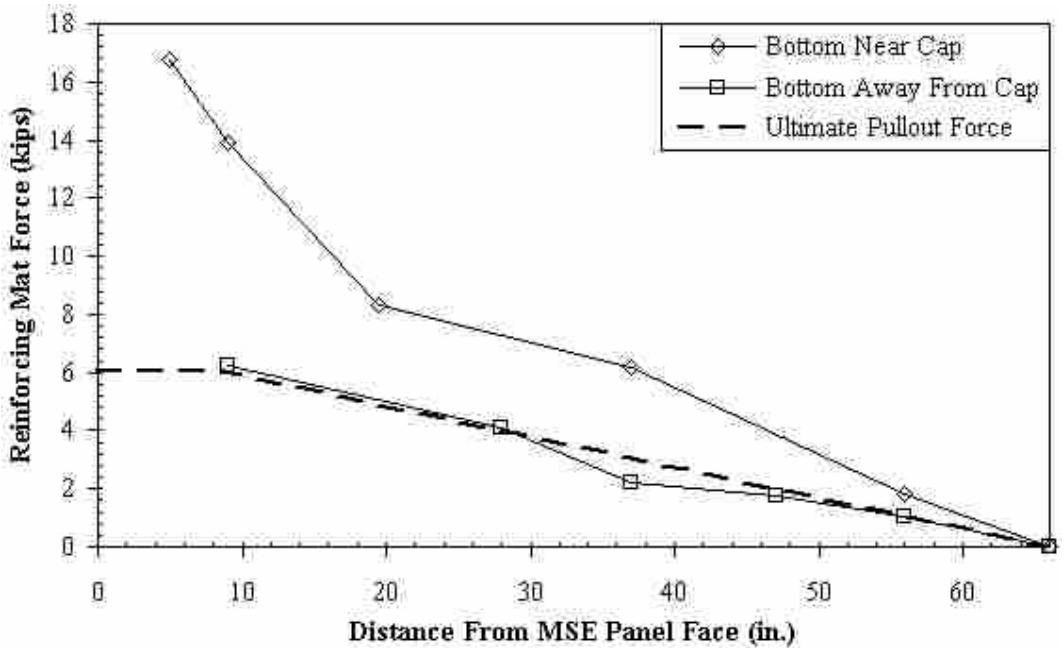

a) Loose MSE Test 3.0-in. Pile Cap Displacement Increment

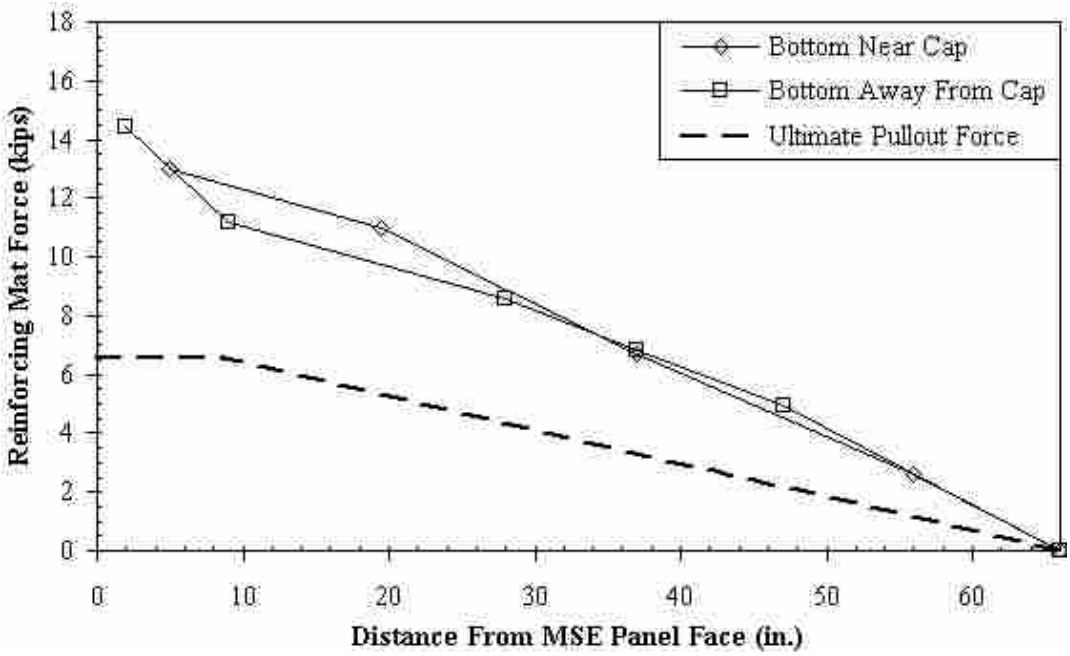

b) Dense MSE Test 3.0-in. Pile Cap Displacement Increment

Figure 8.14: Comparison of Calculated Force in the Bottom Reinforcing Mats During the 3.0-in. Displacement Increment for the Loose and Dense Sand MSE Test

The total MSE wall force calculated from the bar mat forces was also plotted as a function of the MSE wall displacement in Figure 8.15 and Figure 8.16. These graphs compare the force generated by the top and bottom bar mats for both the loose and dense tests. The ultimate pullout force is also plotted for comparison.

Generally, the trends in the bar mat force show that force in the mats of the dense MSE test was about double the amount of force in the loose MSE test. The force in the mats of the dense test was also greater than the computed pullout force while the force in the mats of the loose test compared relatively well to the ultimate pullout force.

As explained previously in Sections 6.4.6 and 7.4.6, the ratio between the additional pressure exerted on the MSE wingwalls during testing and the pressure exerted on the pile cap was computed and plotted against the distance from the pile cap face to the locations of the strain gauges on the mats. The plots of the reduced pressure ratio against distance from the pile cap are shown in Figure 8.17 with a linear trendline. These plots reduce the pressure data to a maximum average MSE wall displacement of 0.2 in. to remove any effect of pullout of the bar mats from influencing the pressure ratio.

A comparison of the plots for the loose and dense cases indicates that the loose sand has higher pressure ratios than the dense sand and that the ratios decrease more rapidly with distance from the cap. The induced pressure ratio ranged from 0.03 to 0.09 for the loose MSE test data points and 0.04 to 0.06 for the dense MSE test. The loose case plot shows a stronger coefficient of determination (R^2), or correlation, between the pressure ratio and distance away from the pile cap of 0.780 as opposed to 0.260 for the dense plot. For the loose test, a zero pressure ratio can be determined from the trendline at a distance of 170 in., or 14.17 ft (4.32 m). This location is between the 0 to 0.25 in. heave lines of the backfill elevation contour map shown in Figure 6.10.

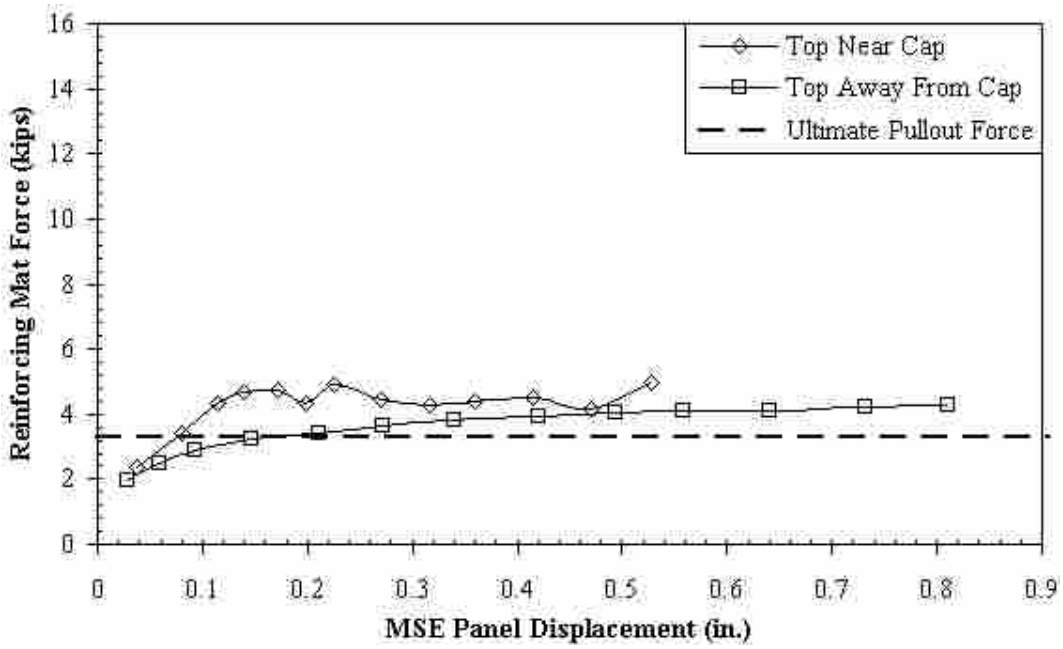

a) Loose MSE Test Top Reinforcing Mats

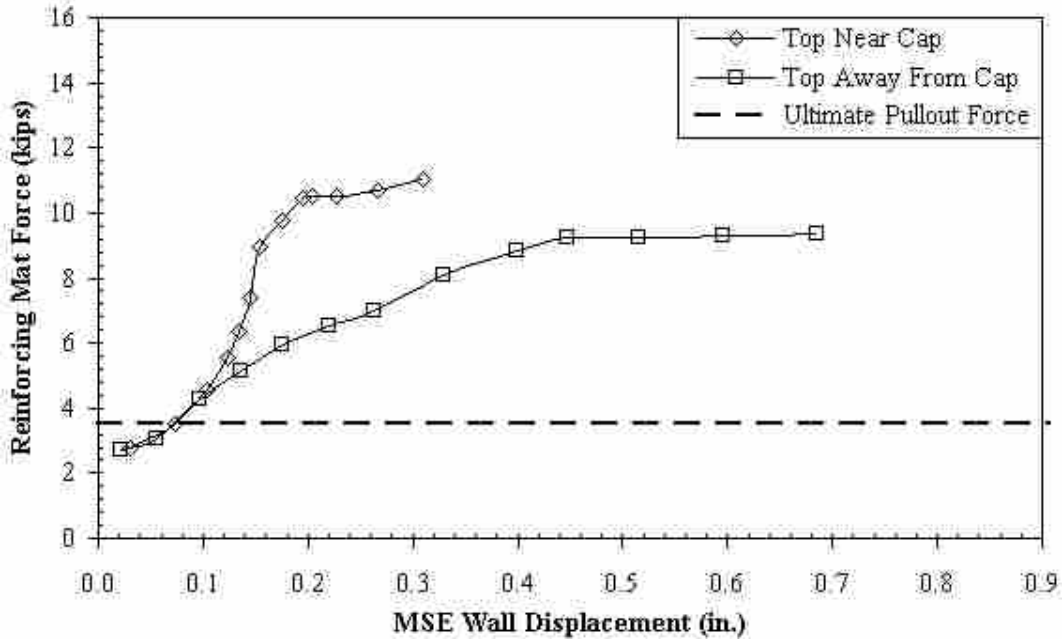

b) Dense MSE Test Top Reinforcing Mats

Figure 8.15: Comparison of the Top Bar Mar Force Plotted Against MSE Wall Displacement for the Loose and Dense MSE Tests

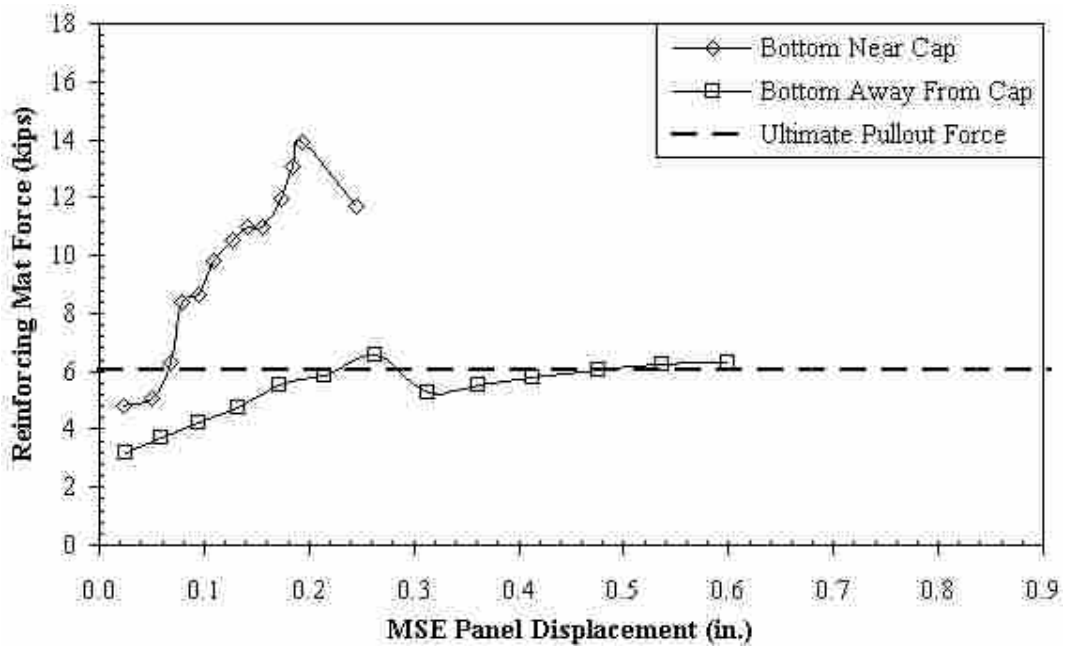

a) Loose MSE Test Bottom Reinforcing Mats

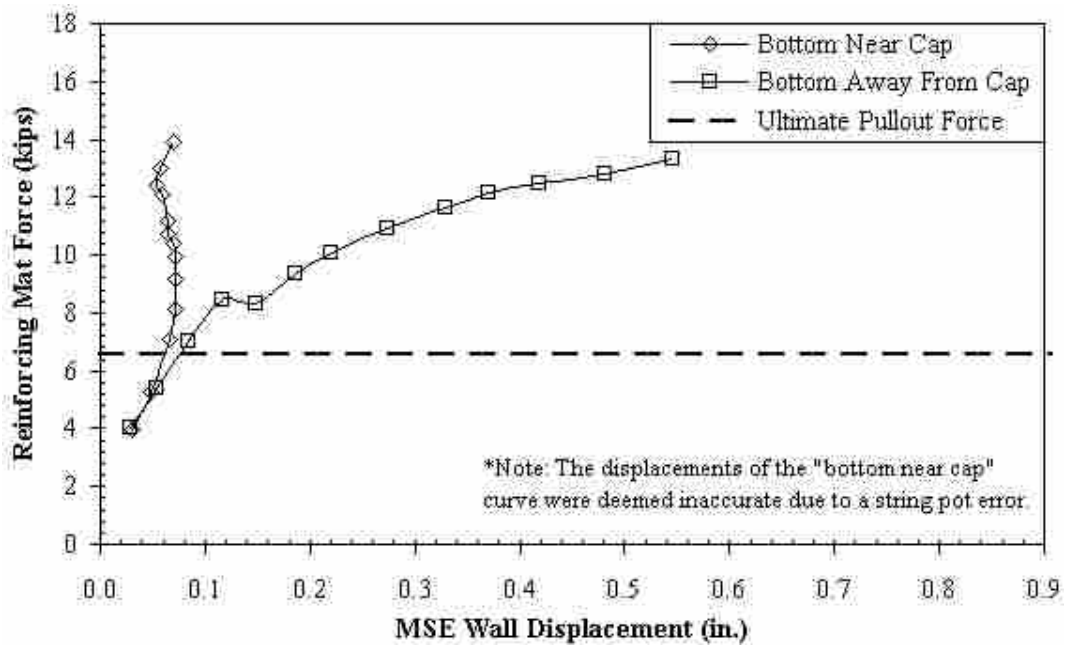

b) Dense MSE Test Bottom Reinforcing Mats

Figure 8.16: Comparison of the Bottom Bar Mar Force Plotted Against MSE Wall Displacement for the Loose and Dense MSE Tests

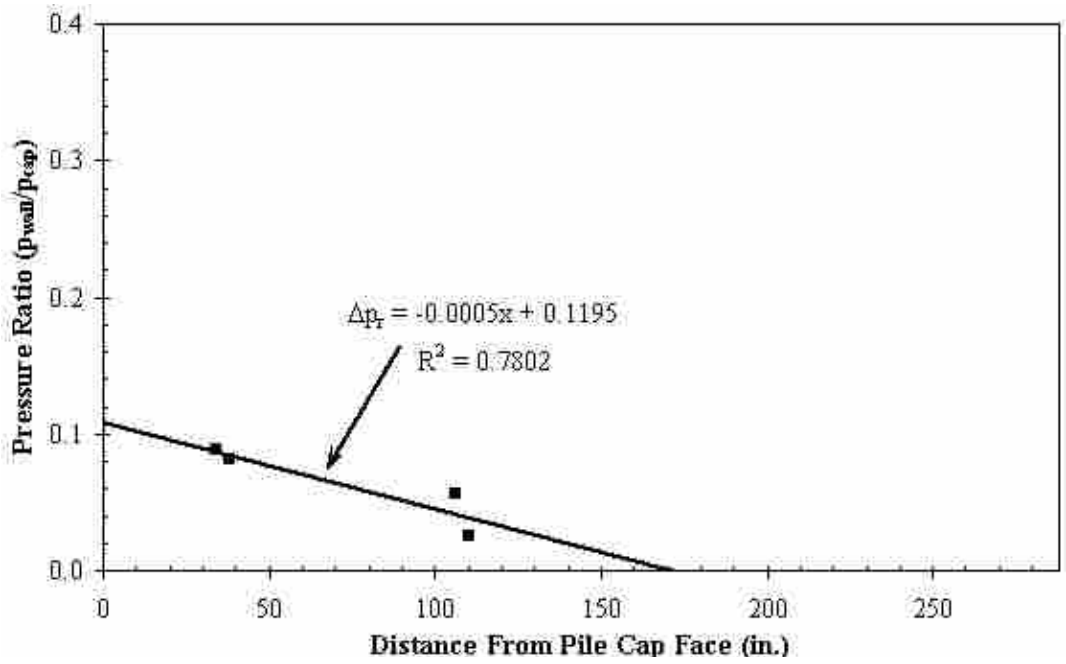

a) Loose Sand MSE Test

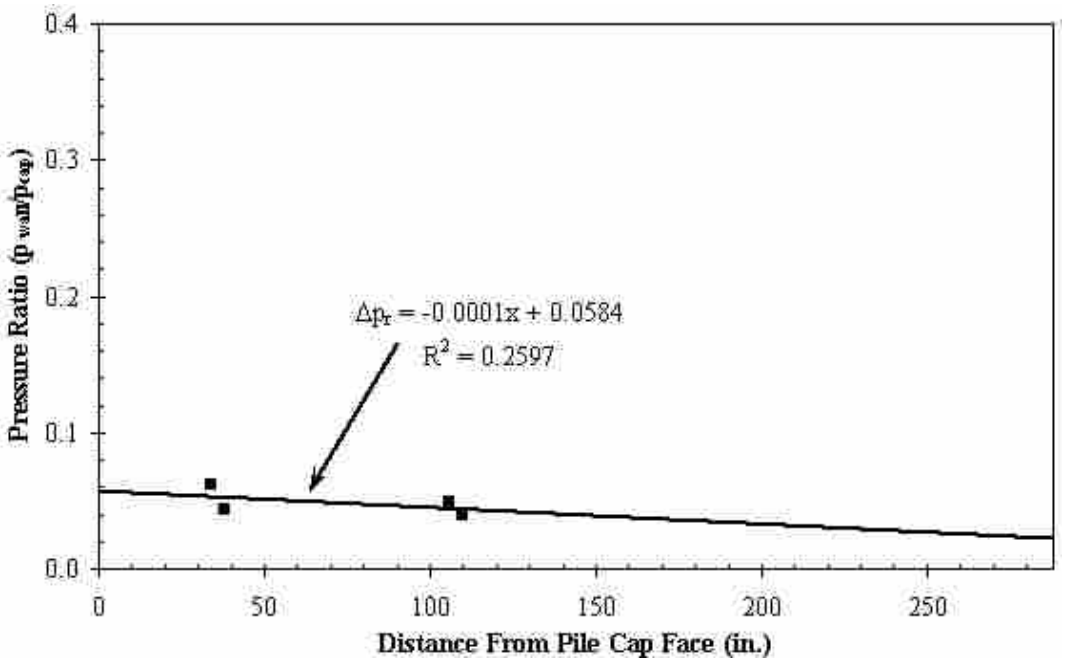

b) Dense Sand MSE Test

Figure 8.17: Comparison of the Reduced Pressure Ratio-Distance Relationship for the Loose and Dense MSE Tests

The pressure ratio-distance correlation trendline equation can be used to determine the pressure placed on the MSE wingwalls at a certain distance from the pile cap face with the known current pressure on the pile cap. This, in turn, aids in the design of MSE wingwalls to predict when pullout of the reinforcement may occur and reduce wingwall deflection depending on how much pressure is being exerted on the pile cap.

To allow for a greater amount of conservatism in the correlation equation, the plots in Figure 8.18 have been determined for the loose and dense MSE tests, which show the trendline of each plot as the mean of the correlation plus one standard deviation with the reduced data set. The recommended pressure ratio-distance equations are shown on the plots and as Equations 8.1 and 8.2:

$$\Delta p_r = -0.0004x + 0.1063 \quad \text{(Loose MSE Test)} \tag{8.1}$$

$$\Delta p_r = -0.0002x + 0.074 \quad \text{(Dense MSE Test)} \tag{8.2}$$

where

Δp_r = pressure ratio between the pressure on the wall and the pressure on the pile cap

x = distance from the pile cap face, in.

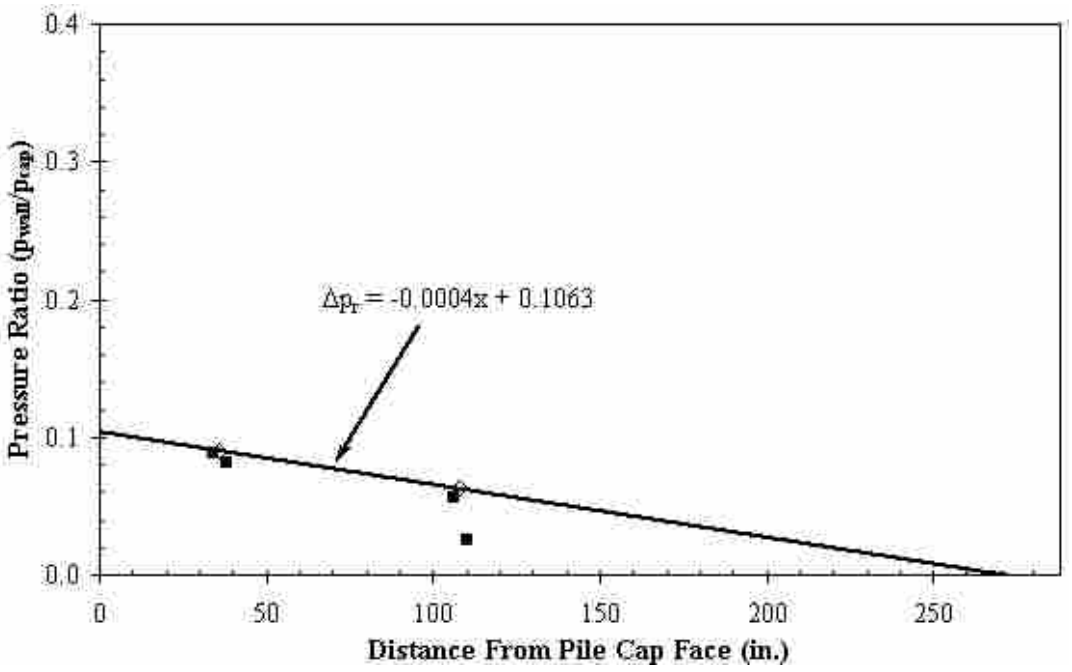

a) Loose Sand MSE Test

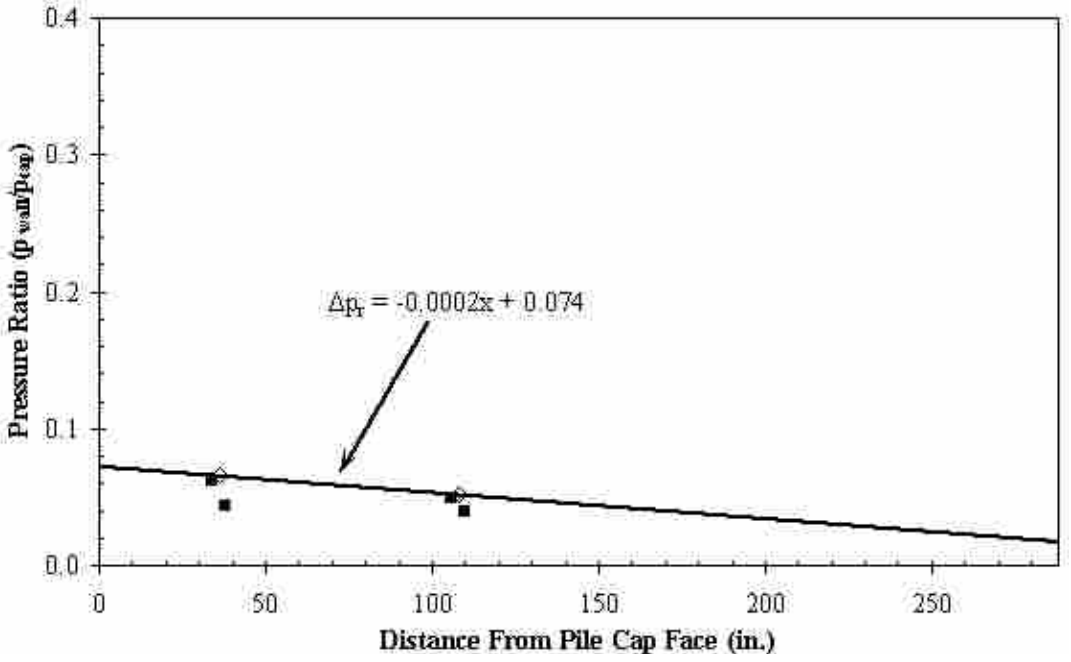

b) Dense Sand MSE Test

Figure 8.18: Conservative Reduced Pressure Ratio-Distance Plots for the Loose and Dense MSE Tests with a Trendline Representing the Mean Plus One Standard Deviation

9 COMPARISON TO CODE- AND COMPUTER-BASED METHODS RESULTS

After the completion of the field tests, the passive load-deflection results compiled from the field tests were compared to the ultimate force and passive load-deflection results generated by the prediction capabilities of three code- and computer-based methods. The code-based method used was that created by Caltrans for seismic design while the computer-based methods included the PYCAP and ABUTMENT programs, which utilize log-spiral and LSH methods of predicting ultimate passive force and load-deflection capacities for abutments. The following sections describe the results of the three methods in comparison to the field data.

9.1 Results Comparison with the Caltrans Seismic Design Method

The Caltrans Seismic Design method was developed from research conducted by Maroney (1995) and Romstad et al. (1996) on large scale abutments and later adopted by Caltrans in the *Caltrans Seismic Design Criteria* Manual. The approach is based on a linear elastic assumption for the backfill material and two generalized values developed from the testing: an initial stiffness (K_i) value of the embankment fill and a maximum passive pressure value found as the ultimate static force developed during testing. The K_i value used in these calculations was 20 kip/in./ft (11.5 kN/mm/m) and the maximum uniform passive pressure value was 5.0 ksf (239 kPa). As noted previously, these values are based on dense compacted backfill material with concrete wingwalls at the sides of the cap.

The ultimate passive force was computed by multiplying the area of the abutment (11 ft x 5.5 ft) by the maximum passive pressure and an abutment height proportionality value of 1.0. This produced an ultimate passive force value of 302.5 kips (1361 kN). The K_i was multiplied by the actual width of the pile cap (11 ft) and the abutment height proportionality value to compute the stiffness of the backfill material and the slope of the design load-displacement curve. This produced an abutment stiffness value of 220 kip/in. (38.5 kN/mm). These values were computed using the actual pile cap width and apply to the three tests with walls. For the loose unconfined (3D) test, the effective pile cap width was used in the calculations to compute higher abutment stiffness and ultimate passive force values. An effective width of about 18 ft (5.49 m) was found by multiplying the actual pile cap width by the 3D correction factor of 1.63.

Figure 9.1 shows the outcome of the Caltrans Seismic Design method in comparison with the measured passive load-displacement curves for the four completed field tests. The loose unconfined (3D) test maximum passive force was over predicted by about 40% (204 kips) using the effective abutment width. However, it should be noted that if the actual abutment width (11 ft) was used in the calculation, the measured passive force would be only 5% (13 kips) lower than the computed value. Unexpectedly, the results also show that the Caltrans method was slightly conservative by about 10% (30 kips) in computing the maximum passive force for the loose slip plane and MSE tests. For the dense sand MSE test, the calculated maximum force value was conservative, underestimating the measured value by about 48% (282 kips).

The calculated backfill stiffness values were also inconsistent with the measured values. The stiffness became considerably flatter than predicted after a deflection of about 0.5 to 0.75 in. (13 to 19 mm) for the loose slip plane and MSE tests. For the dense sand case, the measured stiffness was always greater than predicted.

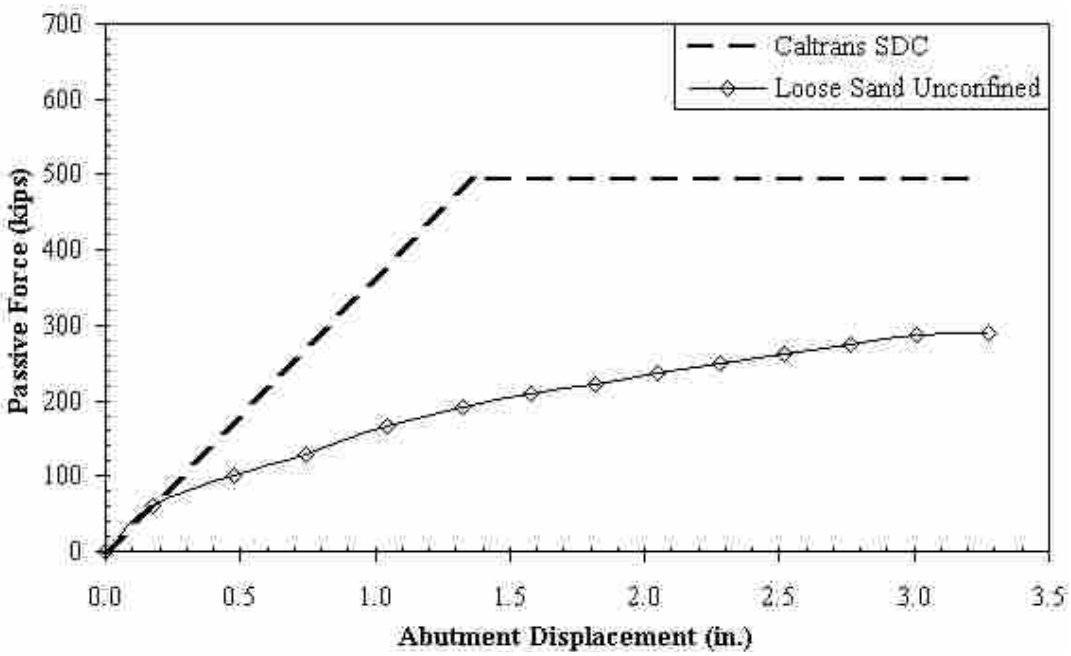

a) Loose Sand Unconfined (3D) Test Caltrans Seismic Design Results

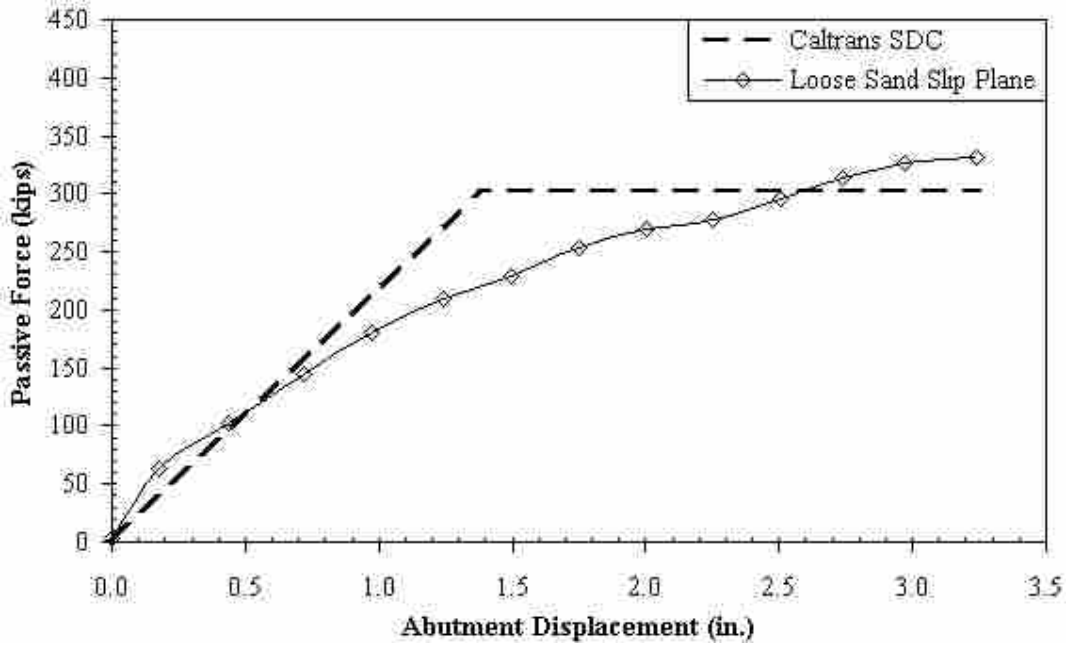

b) Loose Sand Slip Plane (2D) Test Caltrans Seismic Design Results

Figure 9.1: Caltrans Seismic Design Method Passive Force-Displacement Comparisons

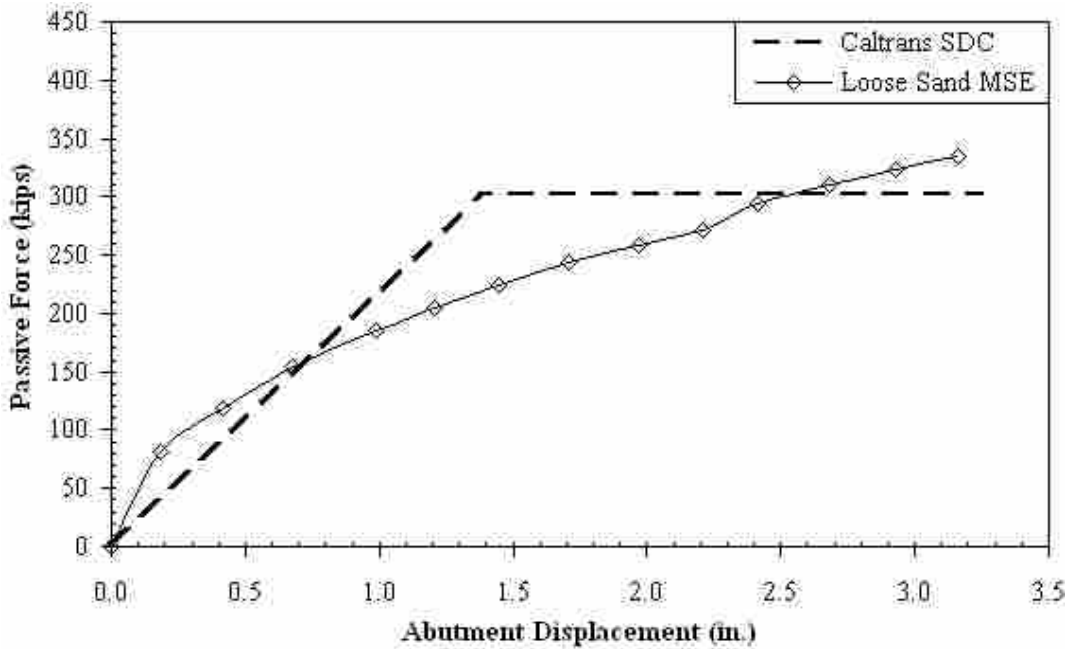

c) Loose Sand MSE Test Caltrans Seismic Design Results

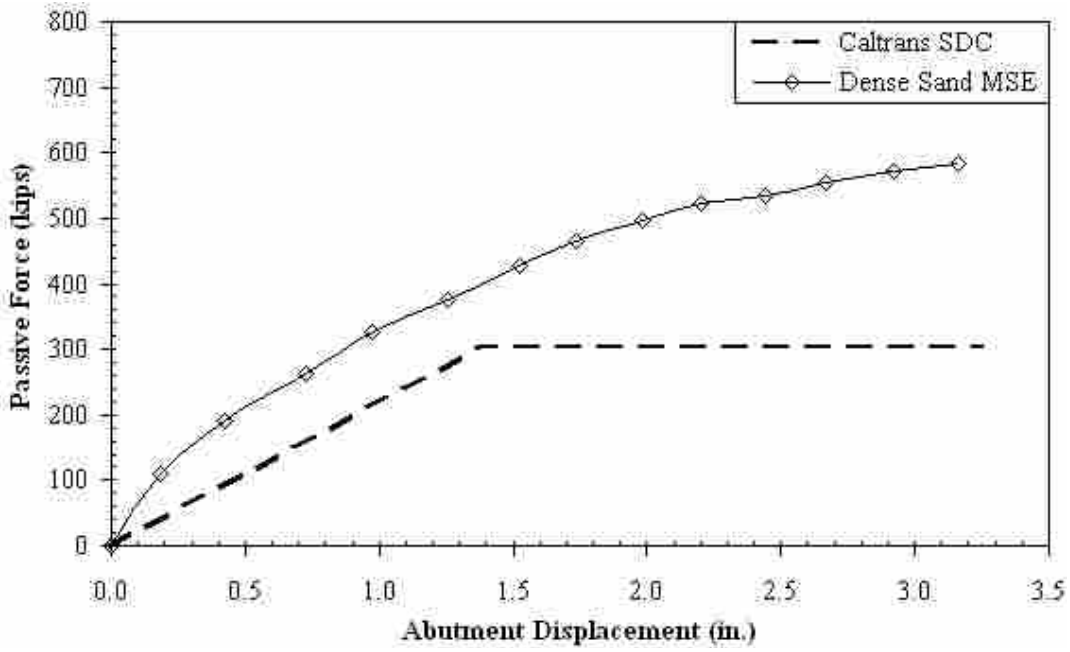

d) Dense Sand MSE Test Caltrans Seismic Design Results

Figure 9.1 (continued): Caltrans Seismic Design Method Passive Force-Displacement Comparison

9.2 Results Comparison with PYCAP

Each of the field tests completed was modeled in PYCAP to see if a similar force-displacement curve could be computed by the program. The results of this attempt are summarized in this section for the loose sand unconfined, loose sand slip plane, loose sand MSE, and dense sand MSE tests. Table 9.1 reports the input parameters used in PYCAP for the four tests. The graphs in Figure 9.2 show the best fit computed PYCAP passive force-displacement curves plotted with the measured curves. For the loose sand unconfined (3D) case, the Brinch Hansen 3D correction factor was applied in the PYCAP computed force-displacement curve because no walls were present during the test. However, the Brinch Hansen 3D correction factor was set equal to 1.0 for the other tests because the shear zone did not extend beyond the edge of the pile cap.

The triaxial friction angle and cohesion values are based on the result of the laboratory testing described in Section 3.4. The unit weights are the moist unit weights based on the average dry unit weight and moisture content measured by the nuclear density tests during construction of the backfills.

PYCAP requires a wall friction angle as an input parameter. The wall friction angle to soil friction angle ratio (δ/ϕ) of 0.75 was used to calculate the appropriate wall friction angle for each test. This value is typically accepted as a good approximation of the δ/ϕ ratio for a sand-concrete interface (Duncan and Mokwa 2001, Potyondy 1961).

As shown in Table 2.1, Duncan and Mokwa (2001) provided ranges for the initial soil modulus (E_i). Of the four tests modeled, only the E_i value used in the loose sand unconfined (3D) model fell outside of the suggested E_i ranges and was much less than the E_i value of the loose sand slip plane and MSE tests. The E_i value used for the loose unconfined case was 210

ksf (10060 kPa). The suggested range for loose (D_r = 40%) compacted material was 400 to 800 ksf (19160 to 38320 kPa). One reason why the E_i value used fell outside of the suggested range is because the D_r of the loose unconfined backfill was 31%, which is lower than the D_r value used to describe loose materials by Duncan and Mokwa. The loose unconfined test was modeled with an E_i value of 400 ksf as a comparison to the best fit value. The result of which showed a much steeper initial slope of the computed passive force-displacement curve.

Table 9.1: PYCAP Input Parameter Summary Table

Input Parameters	Loose Sand Unconfined (3D)	Loose Sand Slip Plane (2D)	Loose Sand MSE	Dense Sand MSE
Cap Width, b (ft)	11.0	11.0	11.0	11.0
Cap Height, H (ft)	5.5	5.5	5.5	5.5
Cohesion, c (psf)	60.0	60.0	60.0	60.0
Soil Friction Angle, ϕ (deg)	36.0	42.0	42.0	47.0
ϕ_{PS}/ϕ_T	1.00	1.17	1.17	1.09
Wall Friction Ratio (δ/ϕ)	0.75	0.75	0.75	0.75
Initial Soil Modulus, E_i (ksf)	210.0	400.0	400.0	680.0
Poisson's Ratio, ν	0.25	0.25	0.25	0.25
Soil Unit Weight, γ_m (pcf)	113.0	118.2	119.5	128.7
Adhesion Factor, α	1.0	1.0	1.0	1.0
Δ_{max}/H	0.049	0.049	0.048	0.048
3D Correction Factor	1.63	1.0	1.0	1.0

For the loose sand slip plane and MSE tests, the E_i was selected as 400 ksf (19160 kPa), which is the low end of the suggested range. The D_r values for these two tests was approximately 40%, which is equal with the D_r value given by Duncan and Mokwa for loose materials.

The dense sand MSE test used an E_i value of 680 ksf (32570 kPa). This value falls in the low end of the suggested range of 600 to 1200 ksf (28740 to 57480 kPa) for dense materials. It

was expected that the stiffness of the dense material would be greater than that of the loose material.

The computed PYCAP curves were able to model the measured force-displacement curves very well for all four tests. The significant aspect of this information is to notice the need to increase the soil friction angle for the tests that confined the backfill by walls. This condition created a situation most like plane strain conditions since 3D pile cap end effects were negated by the walls. Because of the conditions were similar to that of a plane strain situation, the triaxial friction angle (ϕ_T) established from laboratory tests needed to be increased to model accurately the load tests in PYCAP. This same conclusion was reached in the analysis of the additional dense sand tests reported in Bingham (2010).

In Table 9.1, the plane strain to triaxial friction angle ratio (ϕ_{PS}/ϕ_T) is given for each test. For the tests with confined backfills, the triaxial friction angle had to be increased 9 to 17% to produce agreement with the measured force-displacement curves. This increase is consistent with the increase necessary to obtain the plane strain friction angle (ϕ_{PS}) relative to the triaxial friction angle (ϕ_T) as discussed in Section 2.2. The triaxial friction angle (ϕ_T) of a typical sand increased in the ranges of 7 to 17% with a mean of 11% for loose materials and 10 to 18% with a mean of 12% for dense materials when tested under plane strain conditions. Figure 9.3 shows the computed PYCAP passive force-displacement curves utilizing ϕ_T values in comparison with the passive force-displacement curves using ϕ_{PS} and the measured force-displacement curves. The load-deflection curves utilizing ϕ_T produced maximum passive force values approximately 35 to 40% less than those utilizing ϕ_{PS}, thus underestimating the measured curves.

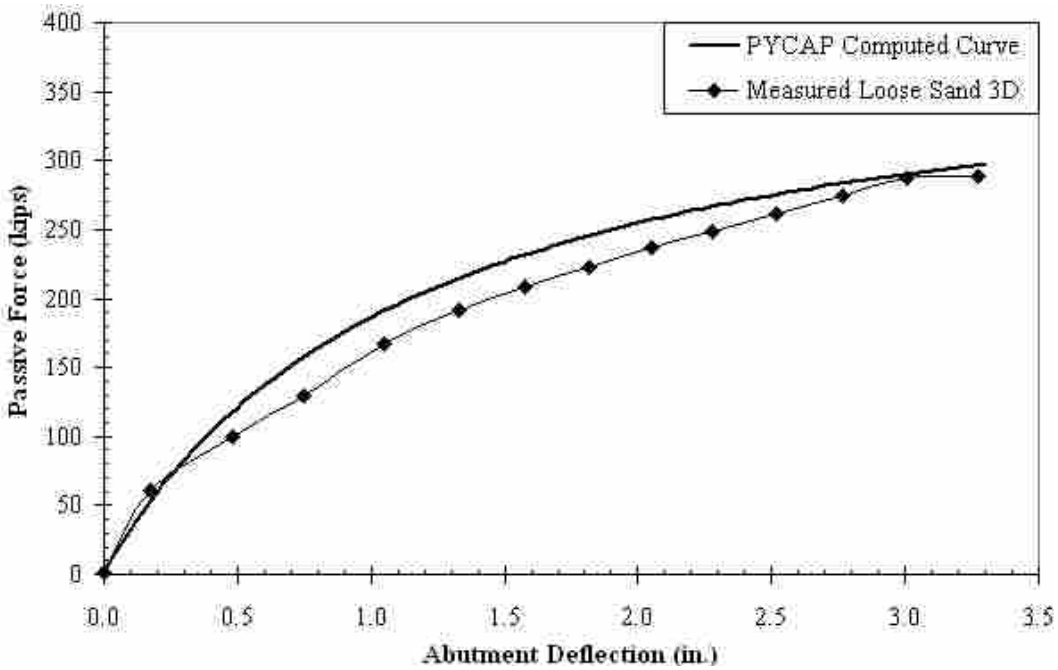

a) Loose Sand Unconfined (3D) Test PYCAP Results

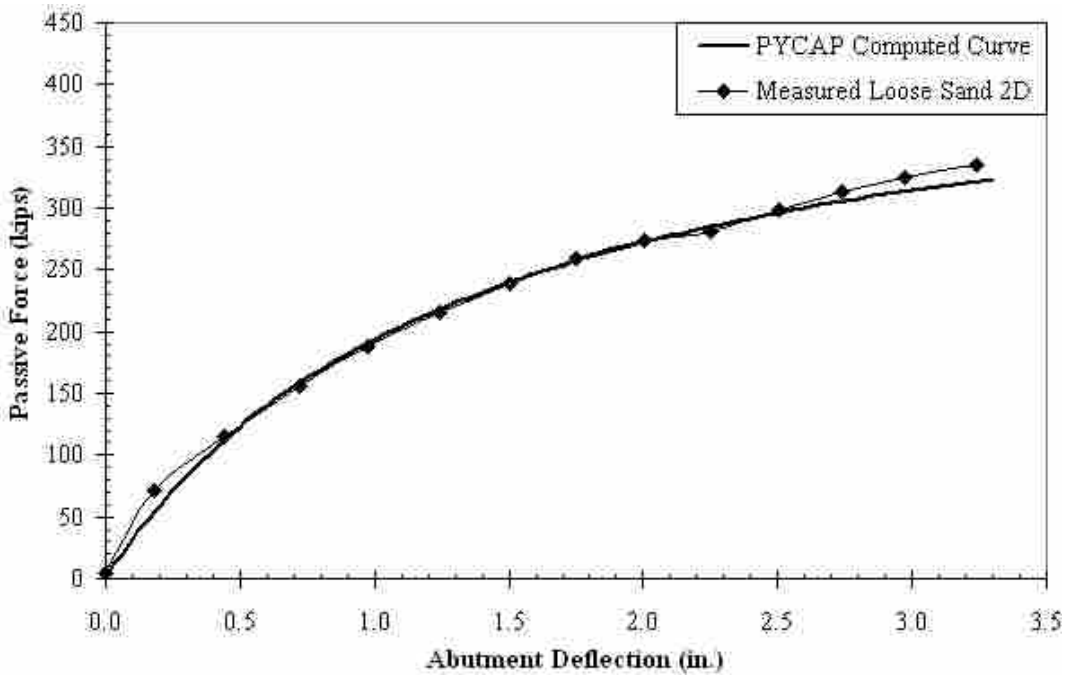

b) Loose Sand Slip Plane (2D) Test PYCAP Results

Figure 9.2: Comparison of PYCAP Best Fit and Measured Load-Displacement Results

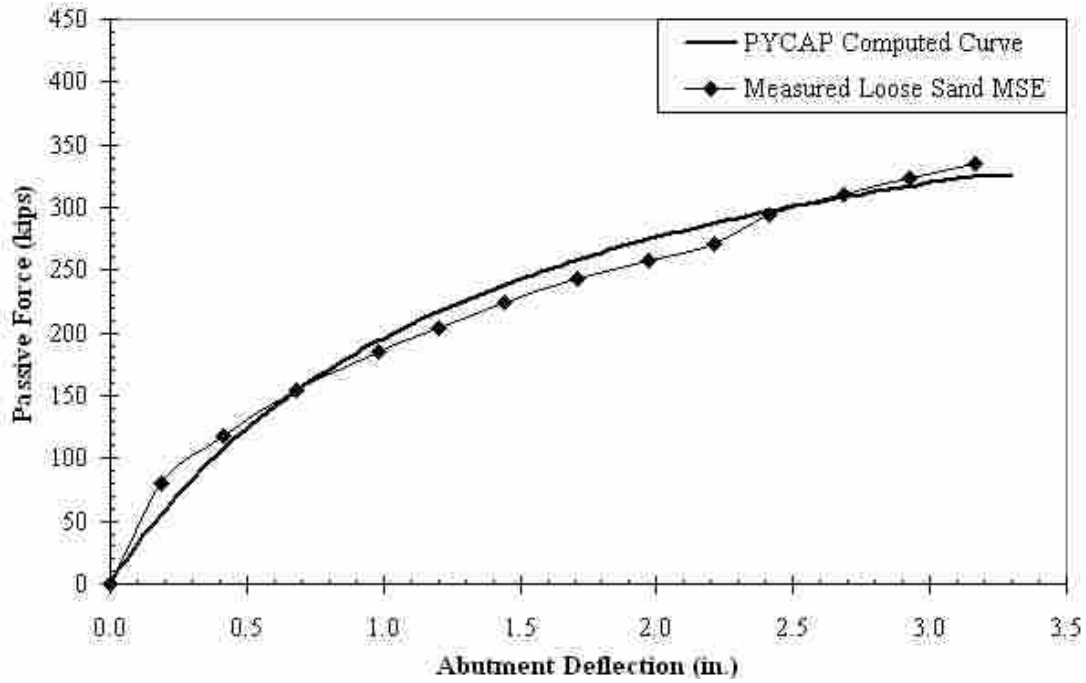

a) Loose Sand MSE Test PYCAP Results

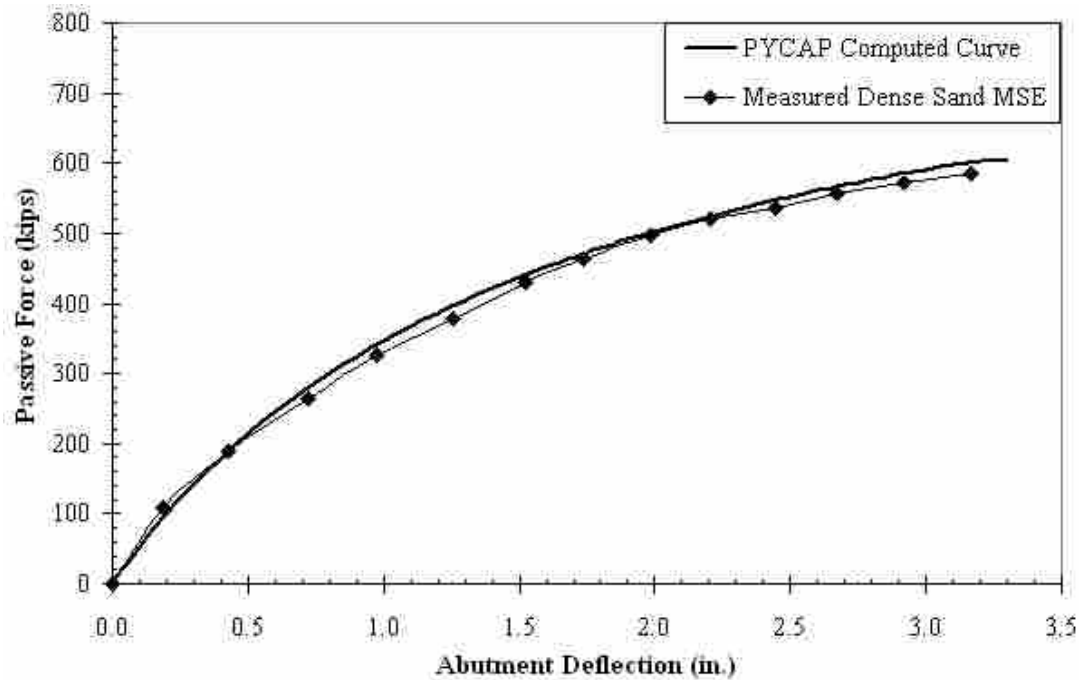

b) Dense Sand MSE Test PYCAP Results

Figure 9.2 (continued): Comparison of PYCAP Best Fit and Measured Load-Displacement Results

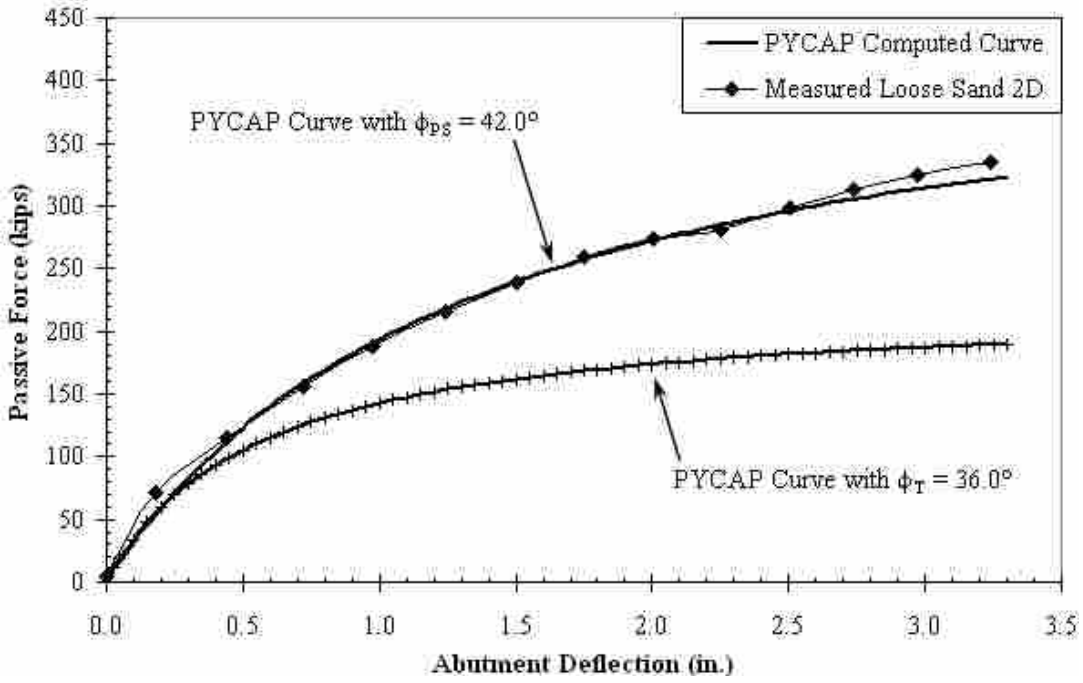

a) Loose Sand Slip Plane (2D) Test

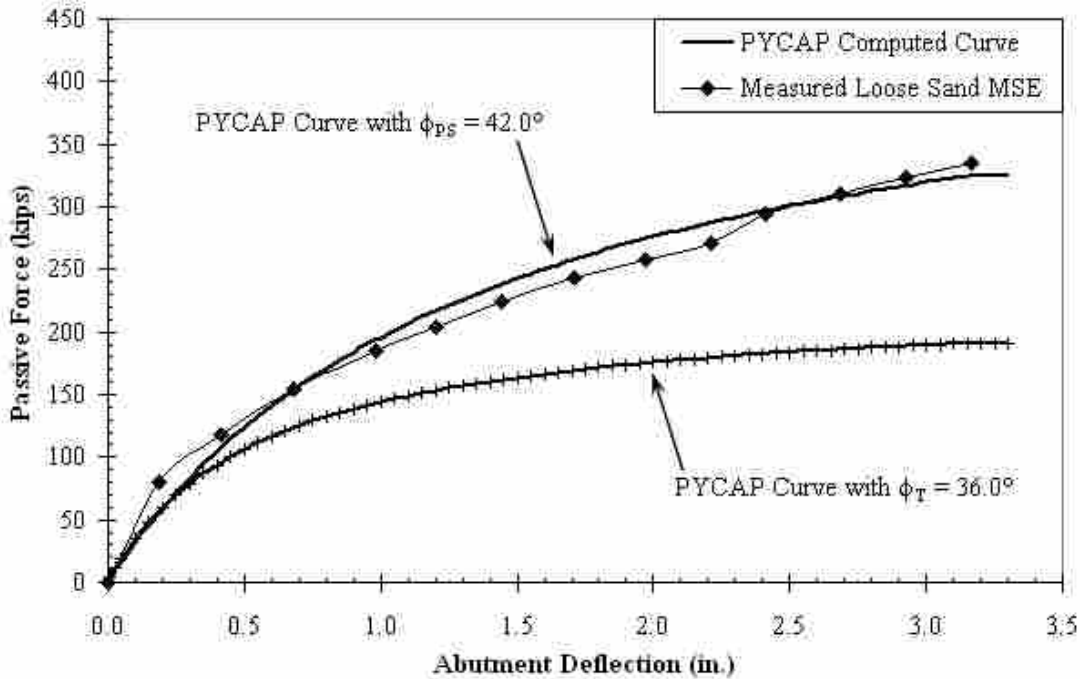

b) Loose Sand MSE Test

Figure 9.3: PYCAP Curve Comparison with Plane Strain and Triaxial Friction Angles

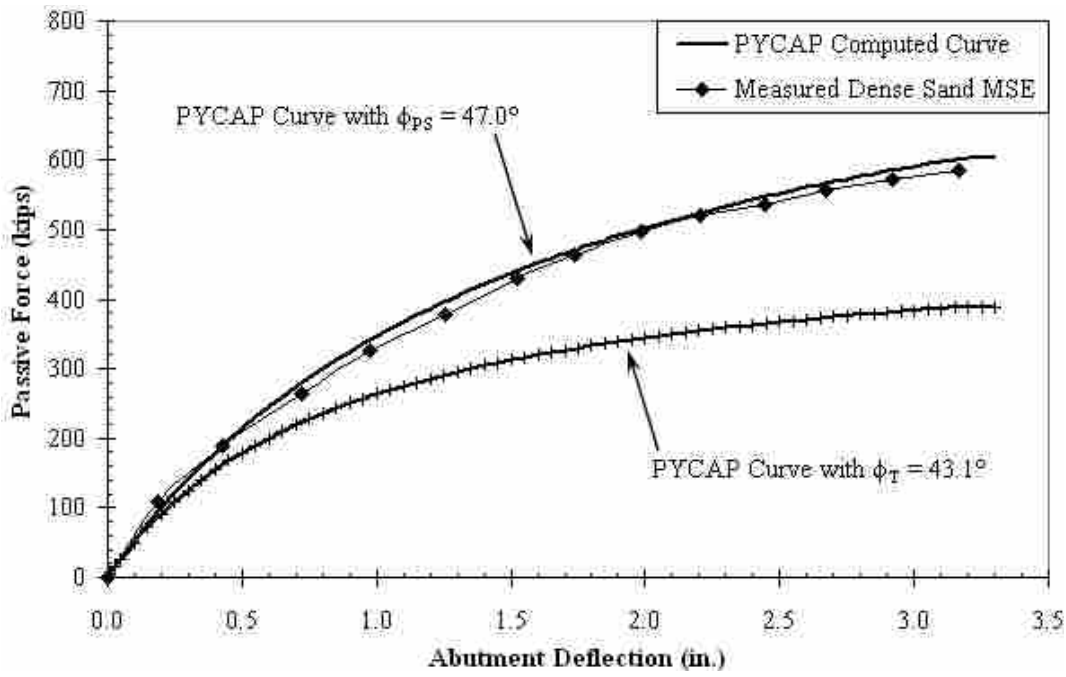

c) Dense Sand MSE Test

Figure 9.3 (continued): PYCAP Curve Comparison with Plane Strain and Triaxial Friction Angles

Also, it should be noted that a small amount of cohesion (60 psf) was used in PYCAP to model the measured passive force-displacement curves despite reporting strength parameters previously with no cohesion. When modeling the loose sand unconfined (3D) test results without the small amount of cohesion, the maximum computed passive force was approximately 13% less than the measured maximum passive force. Thus, when including the cohesion, the friction angle (36.0°) accounted for about 87% of the maximum passive force while the cohesion accounted for about 13% of the maximum passive force. The inclusion of some cohesion was a reasonable way to model the measured passive force-displacement curves. This same cohesion was then used throughout all tests to remain consistent.

Another issue of concern was the difference between the friction angle ratio of the plane strain and triaxial friction angles (ϕ_{PS}/ϕ_T) of the loose and dense tests. The loose confined tests

appeared to have required a 17% increase in ϕ_T while the dense MSE test required only a 9% increase in ϕ_T to accurately model the measured passive force-displacement curves. The high friction angle ratio (ϕ_{PS}/ϕ_T) of the loose tests may be slightly exaggerated because of the difference in relative density between the loose unconfined test and the loose slip plane and MSE tests. The relative density of the loose unconfined test (31%) was approximately 10 percentage points lower than the relative density of the other two loose tests. According to a correlation developed by the U.S. Navy (1982) between relative density and friction angle, an increase in relative density of 10 percentage points for a well-graded sand (SW) would increase the friction angle by approximately 1.5 degrees, from 36.0° to 37.5°. The resulting friction angle ratio (ϕ_{PS}/ϕ_T) between 37.5° and the ϕ_{PS} of 42.0° used in the loose slip plane and MSE tests would be 1.12, which is only a 12% increase in ϕ_T. The 12% percent increase better fits the range of values offered by Kulhawy and Mayne (1990) of the difference between triaxial and plane strain friction angles for loose sands previously presented in Section 2.2.

9.3 Results Comparison with ABUTMENT

The third method used to model the load-deflection curve of each of the field tests was the LSH method incorporated into the ABUTMENT program created by Shamsabadi et al. (2007). The LSH method utilizes the log spiral theory in combination with a modified hyperbolic backfill stress-strain curve to model the load-deflection relationship. In contrast with the PYCAP approach the ultimate passive force is obtained using force equilibrium equations rather than moment equilibrium equations. The results from ABUTMENT are summarized in the following tables and plots for the loose sand unconfined (3D), loose sand slip plane (2D), loose sand MSE, and dense sand MSE tests.

Table 9.2 lists the ABUTMENT input parameters of the best fit curves for the four field tests. The graphs in Figure 9.4 show the best fit passive force-displacement curves generated by ABUTMENT plotted with the measured curves for comparison. Similar to that done in PYCAP, the loose sand unconfined test was modeled using the 3D option in ABUTMENT while the other tests were modeled using the 2D option in ABUTMENT. Also, in an effort to remain as consistent as possible with the common input parameters used in PYCAP and ABUTMENT, only the cohesion values of the backfill differ between the two programs. The cohesion values used in PYCAP were relatively small while those used in ABUTMENT were less than the values used in PYCAP. The stress-strain parameters shown were unique to the ABUTMENT solutions. For every test, the final strain value was kept at a constant value of 0.1.

Table 9.2: ABUTMENT Input Parameter Summary Table

Test Name	Loose Sand Unconfined (3D)	Loose Sand Slip Plane (2D)	Loose Sand MSE (2D)	Dense Sand MSE (2D)
Cap Width, b (ft)	11.0	11.0	11.0	11.0
Cap Height, H (ft)	5.5	5.5	5.5	5.5
Soil Friction Angle, ϕ (deg)	36.0	42.0	42.0	47.0
ϕ_{PS}/ϕ_T	1.00	1.17	1.17	1.09
Wall Friction Ratio (δ/ϕ)	0.75	0.75	0.75	0.75
Soil Cohesion, c (ksf)	0.010	0.013	0.012	0.017
Wall Adhesion (ksf)	0.010	0.013	0.012	0.017
Soil Unit Weight, γ_m (kcf)	0.1130	0.1182	0.1195	0.1287
Poisson's Ratio, ν	0.25	0.25	0.25	0.25
ε_{50}	0.006	0.010	0.009	0.008
Failure Ratio, R_f	0.94	0.90	0.91	0.92

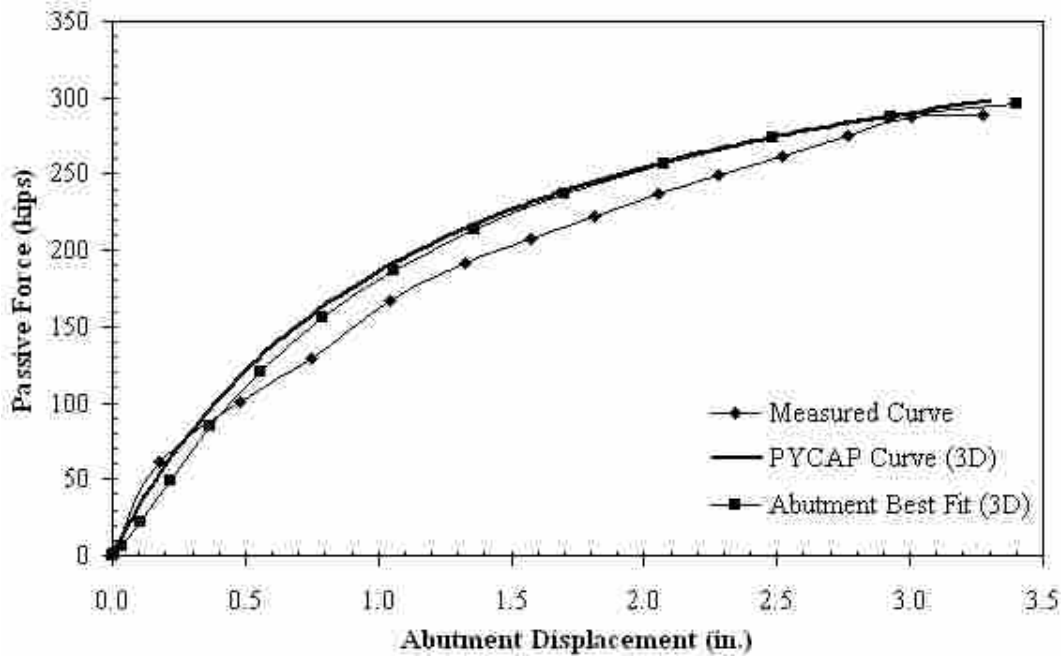

a) Loose Sand Unconfined (3D) Test ABUTMENT Results

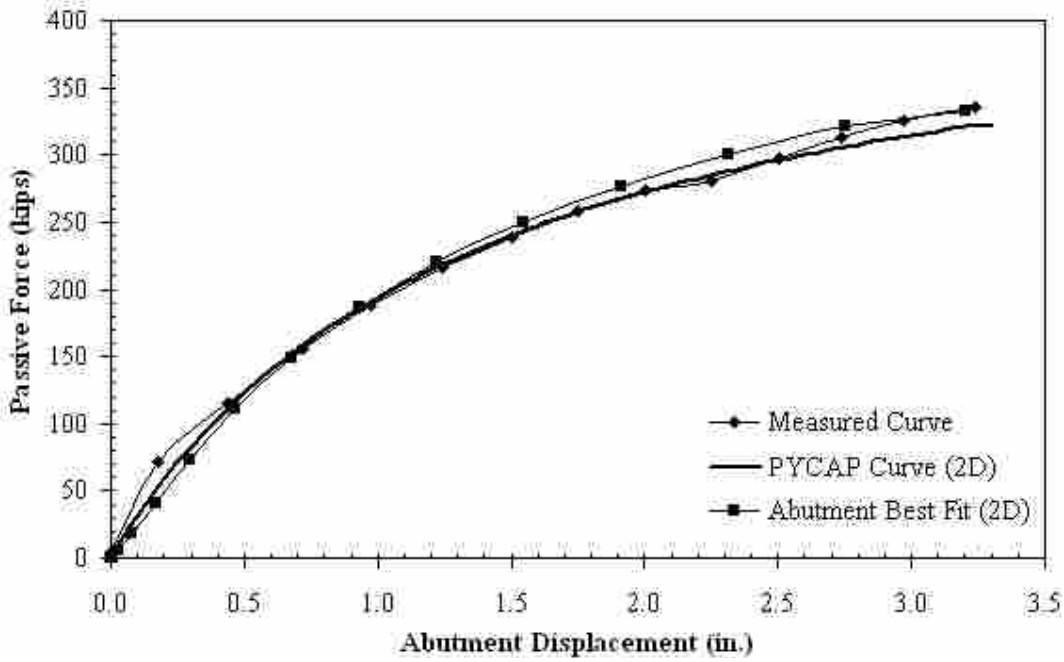

b) Loose Sand Slip Plane (2D) Test ABUTMENT Results

Figure 9.4: Comparison of ABUTMENT Best Fit and Measured Load-Displacement Results

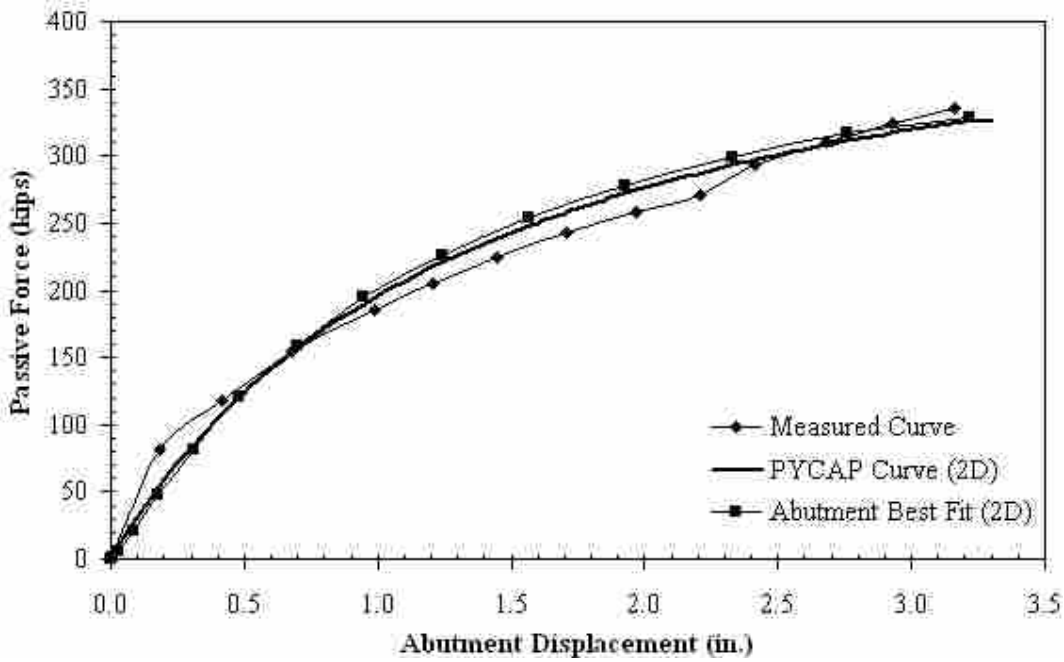

c) Loose Sand MSE Test ABUTMENT Results

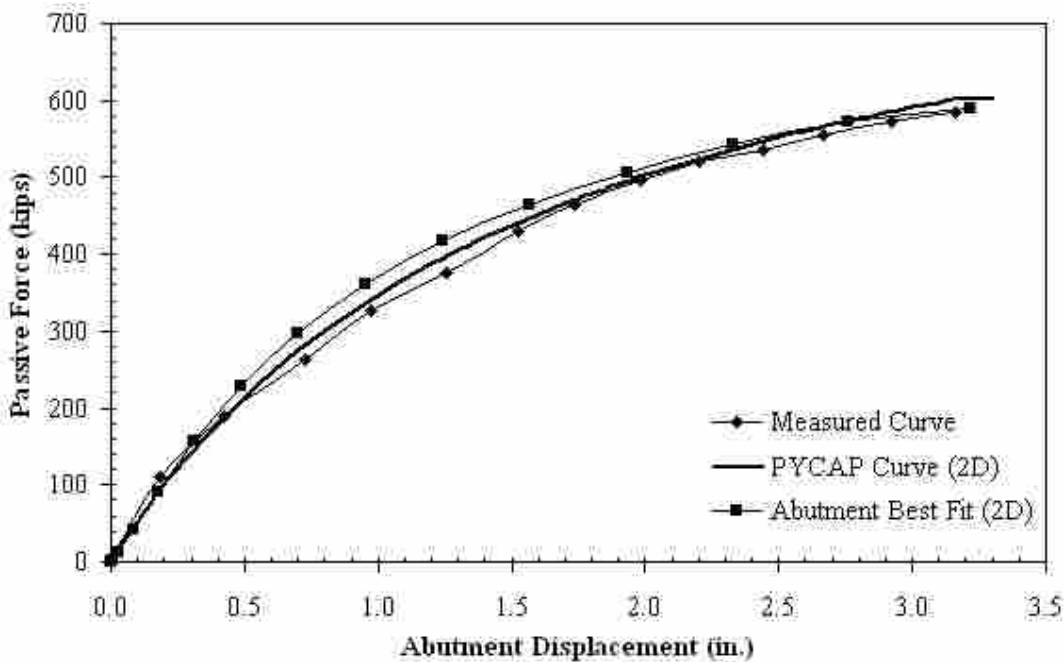

d) Dense Sand MSE Test ABUTMENT Results

Figure 9.4 (continued): Comparison of ABUTMENT Best Fit and Measured Load-Displacement Results

As can be seen in the plots, the ABUTMENT curves model the measured and PYCAP curves successfully for all four tests. Once again these results confirm the idea that it is necessary to use the plane strain friction angles to model the behavior of abutments with MSE wingwalls. The best fit curves, however, had values for ε_{50} which were larger than the recommended values presented by Shamsabadi et al. (2007) for dense sands. The ε_{50} value of 0.006 for the loose sand unconfined test fell just outside the range suggested of 0.002 to 0.005 for clean sands and gravels with a recommended value of 0.0035. The other tests required ε_{50} values that were about 50% greater than the loose sand unconfined test. These results suggest that for sand compacted to about 86% to 88% of the modified Proctor value, the ε_{50} may be in the range of 0.006 to 0.100. The graphs in Figure 9.5 show how the ABUTMENT calculated curves would appear using the recommended value of 0.0035 for ε_{50} for all four tests. With the lower ε_{50}, the initial slope of the load-deflection curve increased in all four instances. This increase leads to computed load-displacement curves which are stiffer than those measured during testing. The three loose sand measured curves give the appearance of being a stiff material within the first two or three pile cap displacements (0.5 to 0.7 in. of displacement) before the curves flatten out and the slopes decrease.

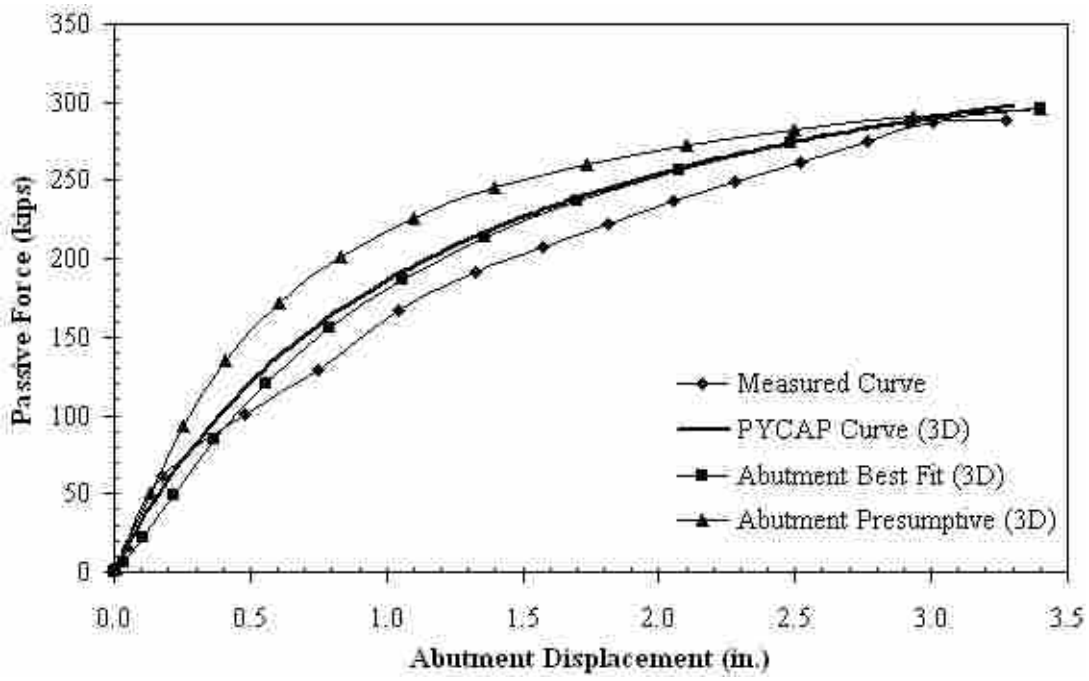

a) Loose Sand Unconfined (3D) Test

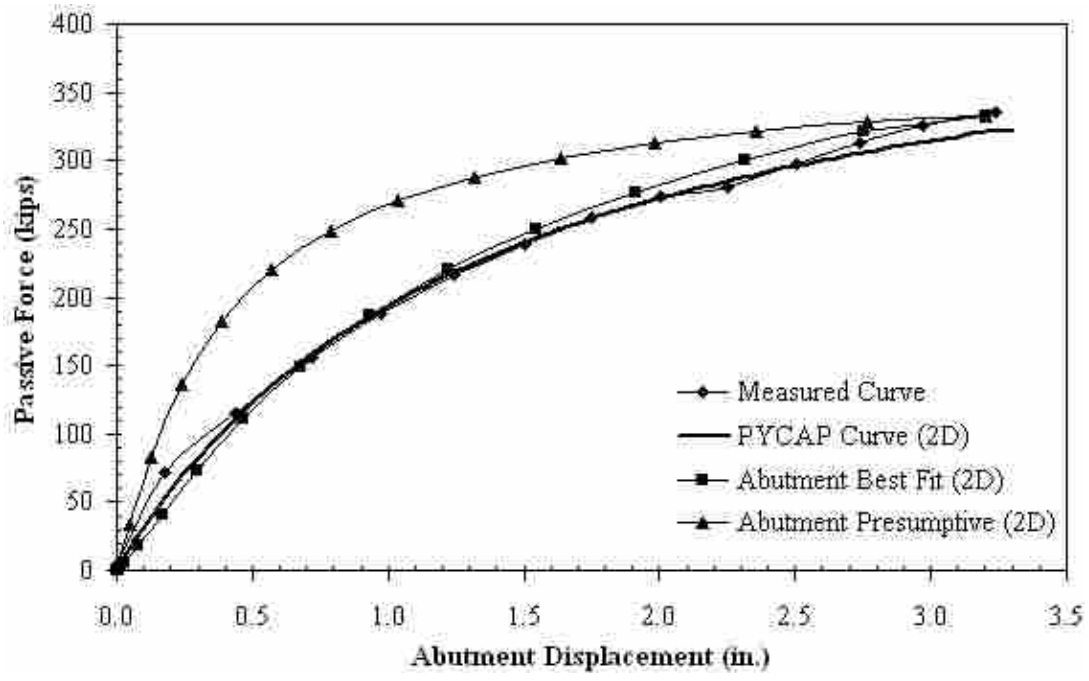

b) Loose Sand Slip Plane (2D) Test

Figure 9.5: ABUTMENT Load-Displacement Curve Comparison with Best Fit and Recommended ε_{50} Values

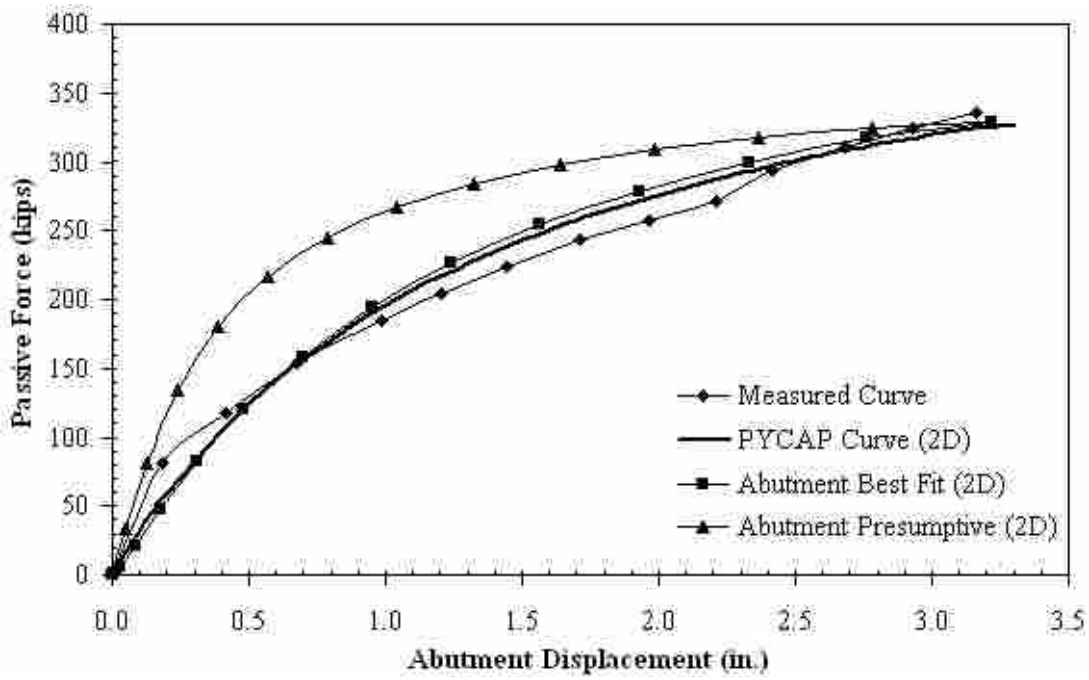

c) Loose Sand MSE Test

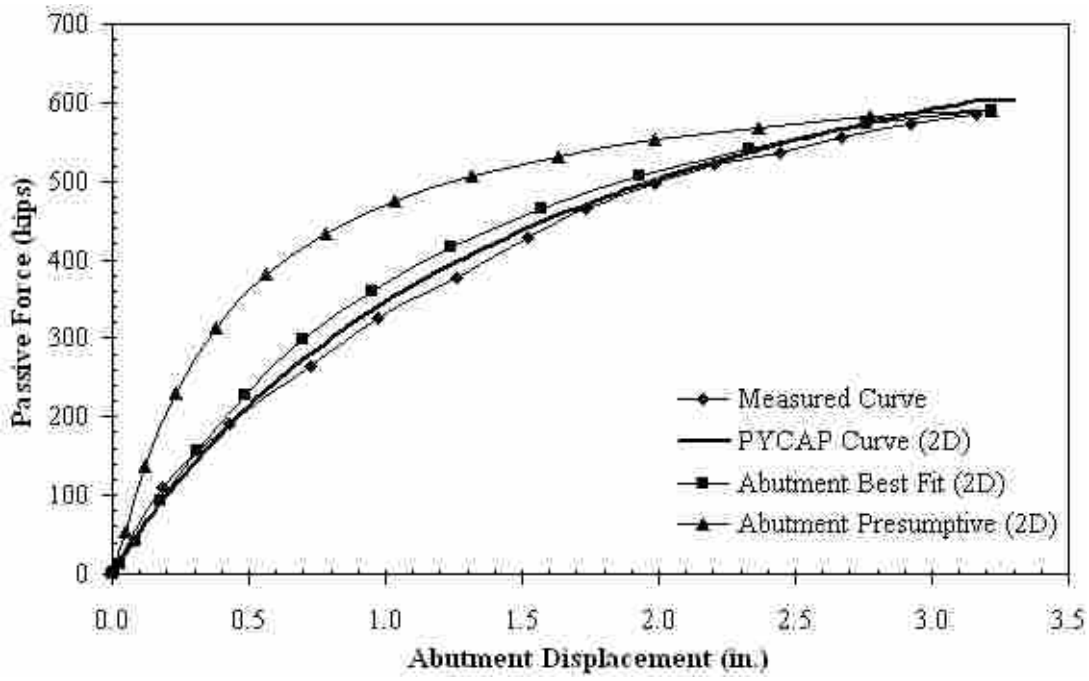

d) Dense Sand MSE Test

Figure 9.5 (continued): ABUTMENT Load-Displacement Curve Comparison with Best Fit and Recommended ε_{50} Values

10 CONCLUSION

This thesis presented results from laterally loaded, large scale pile cap tests with four different backfill conditions: loosely compacted sand with no confinement (3D), loosely compacted sand with side isolation, or slip plane, confinement (2D), loosely compacted sand with MSE wingwall confinement, and densely compacted sand with MSE wingwall confinement. The reinforcement layout of the two MSE wingwall tests was identical. The loosely compacted sand had a relative compaction of 86%, 88%, and 88% of modified Proctor (D_r = 31%, 41%, and 39%) for the loose unconfined, slip plane, and MSE tests, respectively. The densely compacted sand had a relative compaction of 95% of modified Proctor (D_r = 73%) for the dense MSE test. An interpretation and comparison of the results of the loosely compacted tests to the densely compacted tests was also presented. Finally, comparisons were made between measured load-displacement curves and those predicted by available analysis techniques. The following conclusions and recommendations represent a summary of the findings of this work.

1. The passive earth pressure of the backfill material acting on the pile cap increased the lateral load capacity of the pile cap as the relative compaction of the backfill increased. For all tests combined, the maximum passive earth pressure increased by an average of approximately 52% (350 kips) as the relative compaction of the backfill was increased from an average of 87% to 96% of modified Proctor.

2. The maximum passive force of the dense sand MSE test (586 kips) was approximately 43% greater than the maximum passive force of the loose sand MSE test (335 kips) as the relative density (D_r) increased from 39% for the loose test to 73% for the dense test.
3. The maximum transverse MSE wingwall displacement and rotation decreased by approximately 0.2 in. (5 mm) and 0.3 degrees as the backfill compaction level increased between the loose and dense MSE tests.
4. Passive force-displacement curves computed using the Caltrans Seismic Design approach unexpectedly calculated the maximum passive force of the loose sand slip plane and MSE tests relatively well. However, the maximum passive force of the dense sand MSE test was about 48% (282 kips) greater than that computed. Also, the actual backfill stiffness became considerably flatter than predicted after a deflection of about 0.5 to 0.75 in. (13 to 19 mm) for the tests involving loosely compacted sand. For the dense sand case, the measured stiffness was always greater than predicted.
5. Passive force-displacement curves computed using the log spiral method for determining passive earth pressure coefficients including 3D adjustment factors and the triaxial soil friction angle (ϕ_T) showed good agreement with the measured passive force-displacement curves for the loose sand unconfined test.
6. Passive force-displacement curves computed using the log spiral method for determining passive earth pressure coefficients without 3D loading adjustment factors and the triaxial soil friction angle (ϕ_T) underestimated the measured passive force-displacement curves by 30 to 40% for the loose and dense sand slip plane and MSE tests. However, reasonable agreement was readily obtained using plane strain friction

angles (ϕ_{PS}) with the same analysis approach. Analysis of the test results indicates that the plane strain friction angle (ϕ_{PS}) should be used to calculate passive force on abutments with MSE wingwalls. Based on these tests, the plane strain friction angle can be estimated by increasing the triaxial friction angle by 7 to 17% or an average of 11% for loose sands and 10 to 18% or an average of 12% for dense sands as suggested by Kulhawy and Mayne (1990).

7. Passive force-displacement curves computed using the PYCAP provided reasonable agreement with measured curves; however, it was necessary to use minimum initial soil modulus (E_i) values of the ranges suggested by Duncan and Mokwa (2001) for loose and dense sand backfills.
8. Passive force-displacement curves computed using the LSH model provided reasonable agreement with measured curves; however, it was necessary to use ε_{50} values in the 0.006 to 0.010 range for the loose and dense cases. This range fell above the suggested range for dense sands provided by Shamsabadi et al. (2007).
9. The NHI guidelines for estimating the force in steel reinforcing mats for MSE walls was slightly conservative (by 1 to 2 kips or 30 to 40%) for loosely compacted sand backfills. However, this approach became increasingly conservative (by 6 to 8 kips or 2 to 2.5 times) for densely compacted sand backfills.
10. The maximum induced pressure ratio, or the ratio of pressure acting on the MSE walls to the pressure acting on the pile cap, ranged from 0.06 to 0.09 for both the loose and dense MSE tests. This ratio decreased as the distance from the pile cap increased.

11. Induced pressure ratio as a function of distance equations can be used to predict the force exerted on MSE wingwalls knowing the passive earth pressure acting on the pile cap. The MSE wingwall force allows MSE wingwalls to be designed for the appropriate capacity before pullout occurs.
12. Large scale lateral load tests utilizing MSE wingwalls with additional instrumentation along the full length of the wingwalls are recommended with both loose and dense backfills to improve the current correlation level determined for the pressure ratio-displacement relationship from these tests.

REFERENCES

American Association of State Highway and Transportation Officials (AASHTO) (2007). *LRFD Bridge Design Specifications*, 4th Ed., AASHTO, Washington, D.C., Section 3: General Requirements, 68-74

AASHTO (2009). *Guide Specifications for LRFD Seismic Bridge Design*, 1st Ed., AASHTO, Washington, D.C.

Bathurst, R. J., Nernheim, A., Allen, T. M. (2009). "Predicted loads in steel reinforced soil walls using the AASHTO simplified method." *J. Geotech. Geoenviron. Eng.*, 135(2), 177-184.

Bingham, N. G. (2010). "Passive resistance of abutments with MSE wingwalls and densely compacted backfills." M.S. thesis. Dept. of Civil and Environ. Eng., Brigham Young Univ., Provo, UT.

Brinch Hansen, J. (1966). "Resistance of a rectangular anchor slab." *Bull. No. 21*, Danish Geotechnical Institute, Copenhagen, 12-13.

Caltrans (2004). *Seismic Design Criteria*. Caltrans, Sacramento, CA, Section 7: Design, 28-30.

Christensen, D. S. (2006). "Full scale static lateral load test of a 9 pile group in sand." M.S. thesis, Dept. of Civil and Environ. Eng., Brigham Young Univ., Provo, UT.

Cole, R. T., Rollins, K. M. (2006). "Passive earth pressure mobilization during cyclic loading." *J. Geotech. Geoenviron. Eng.*, 132(9), 1154-1164.

Cummins, C. R. (2009). "Behavior of a full-scale pile cap with loosely and densely compacted clean sand backfill under cyclic and dynamic loadings." M.S. thesis, Dept. of Civil and Environ. Eng., Brigham Young Univ., Provo, UT.

Douglas, D. J., Davis, E. H. (1964). "The movement of buried footings due to moment and horizontal load and the movement of anchor plates." *Geotechnique*, London, 14(2), 115-132.

Duncan, J. M., Mokwa, R. L. (2001). "Passive earth pressures: theories and tests." *J. Geotech. Geoenviron. Eng.*, 127(3), 248-257.

Heiner, L., Rollins, K. M., Gerber, T. G. (2008). "Passive force-deflection curves for abutments with MSE confined approach fills." *Proc., 6th National Seismic Conference on Bridges and Highways (6NSC),* Federal Highway Administration (FHWA), Charleston, SC.

Kulhawy, F. H., Mayne, P. W. (1990). *Manual on Estimating Soil Properties for Foundation Design,* Electric Power Research Inst. (EPRI), Palo Alto, CA, Section 4: Strength, 12-14.

Ladd, C. C., Foott, R., Ishihara, K., Schlosser, F., Poulos, H. G. (1977). "Stress-deformation and strength characteristics." *Proc., 9th International Conference on Soil Mechanics and Foundation Eng. (ICSMFE),* ISSMFE, Tokyo, Vol. 2, 421-494.

Lee, K. L., Singh, A. (1971). "Relative Density and Relative Compaction." *J. Soil Mechanics and Foundations Division,* 97(7), 1049-1052.

Maroney, B. (1995). "Large scale bridge abutment tests to determine stiffness and ultimate strength under seismic loading." Ph.D. dissertation, Univ. of Cal., Davis, CA.

Mokwa, R. L., Duncan, J. M., (2001). "Experimental evaluation of lateral-load resistance of pile caps." *J. Geotech. Geoenviron. Eng.,* 127(2), 185-192.

National Highway Institute (NHI), FHWA, (2001). *Mechanically Stabilized Earth Walls and Reinforced Soil Slopes Design and Construction Guidelines*. NHI, FHWA, Washington, D.C.

Peterson, K. T. (1996). "Static and dynamic lateral load testing of a full-scale pile group in clay." M.S. thesis, Dept. of Civil and Environ. Eng., Brigham Young Univ., Provo, UT.

Potyondy, J. G. (1961). "Skin friction between various soils and construction materials." *Geotechnique,* London, 11(1), 339-353.

Rollins, K. M., Cole, R. T. (2006). "Cyclic lateral load behavior of a pile cap and backfill." *J. Geotech. Geoenviron. Eng.,* 132(9), 1143-1153.

Rollins, K. M., Sparks, A., (2002). "Lateral resistance of full-scale pile cap with gravel backfill." *J. Geotech. Geoenviron. Eng.,* 128(9), 711-723.

Romstad, K., Kutter, B., Maroney, B., Vanderbilt E., Griggs, M., Chai, Y. H., (1996). "Longitudinal strength and stiffness behavior of bridge abutments." Dept. of Civil and Environ. Eng., Univ. of Cal., Davis, CA.

Rowe, P. W. (1969). "The relation between the shear strength of sands in triaxial compression, plane strain and direct shear." *Geotechnique,* London, 19(1), 75-86.

Shamsabadi, A., Rollins, K. M., Kapuskar, M. (2007). "Nonlinear soil-abutment-bridge structure interaction for seismic performance-based design." *J. Geotech. Geoenviron. Eng.,* 133(6), 707-720.

Shamsabadi, A., Yan, L. (2008). "Closed-form force-displacement backbone curves for bridge abutment-backfill systems." *Proc., Geotech. Earthquake Eng. and Soil Dynamics (GEESD) IV*, ASCE, Reston, VA, 1-10.

Snyder, J. L. (2004). "Full-scale lateral load tests of a 3x5 pile group in soft clays and silts." M.S. thesis, Dept. of Civil and Environ. Eng., Brigham Young Univ., Provo, UT.

U.S. Navy (1982). *Foundations and Earth Structures Design Manual 7.2*, Dept. of the Navy, Naval Facilities Engineering Command (NAVFAC), Alexandria, VA.